SCUOLA DI DOTTORATO

UNIVERSITÀ DEGLI STUDI DI MILANO-BICOCCA

Department of Biotechnology and Biosciences

PhD program

Converging Technologies for Biomolecular Systems

(TeCSBi)

Ciclo XXXIII

Unconventional purification and labelling strategies of bioreagents for immunodiagnostic assays

Mento Alfredo Registration number: 754183

Tutor: Paola Branduardi

Supervisor: Pier Natale Brusasca

Coordinator: Paola Branduardi

ACCADEMIC YEAR 2019/2020

Index

ABSTRACT

Antigens and antibodies are key reagents for the development of accurate, reproducible and sensible immunodiagnostic assays, which are widely used for the detection of infectious diseases (HIV,HBV, HCV, etc.) and the determination of biological markers (vitamins, hormones, etc.). These bioreagents need to be produced at a high purity degree, in stable formulations and with sufficient reproducibility over time (lot to lot consistency). An aspect often overlooked in the production of these reagents is their cost, which must be low enough to not have a significant impact on the final price of the immunochemical assays. The purification and labeling steps of these bioreagents mainly affect the overall cost of them since costly reagents and instrumentations and complex and time-consuming protocols are used.For all these reasons it is important to seek new purification strategies that allow the development of simpler processes, with less use of reagents and shorter protocol times, and at the end minor costs. Therefore, it is necessary to develop innovative purifications and site-specific labelling protocols. In the first part of this project we exploited the ELP-intein system. This method is based on the combination of two technological tools, the Elastin-like-polypeptides (ELPs) (a physico-chemical tool) and the *MxeGyrA* intein activity (a biochemical tool), belonging to the *cis* intein family. We focused on the purification and labelling of the C33 antigen from Hepatitis C Virus (HCV). The C33 antigen, which is currently used in the Diasorin LIAISON® XL Murex HCV assay for the detection of human antibodies against the Hepatitis C Virus, was purified using a not conventional purification method without chromatographic steps. Moreover, we realized a site-specific biotinylation of C33 antigen at its C-terminus during the purification exploiting the *MxeGyrA* intein biological activity. Two different protocols were developed; both of them brought to the obtainment of a biotinylated C33 antigen with high purity and a comparable immunoreactivity with the one currently used in the Diasorin LIAISON® XL Murex HCV assay. In light of these good results, in the second part of the project, we investigated the possibility to apply the Protein Trans Splicing (PTS) technology to perform site-specific labelling of bioreagents. PTS technology exploits the split intein activity. In particular, in our experiments we used the Cfa split-intein which derives from a mutagenesis process of the natural *Npu* split-intein that significantly improved its kinetic of PTS, thermal stability and tolerance at the chaotropic agents. This new technique allowed us to set up a site-specific labelling protocol for the production of biotinylated bioreagents. Two model protein were used: the same C33 antigen and a recombinant human IgG. Also the use of PTS technique permitted to obtain for both of two proteins a high purity and a comparable performance in the immunoassays. In summary, the ELP-intein system allowed to purify the C33 antigen without chromatographic steps and then to site-specific label the same protein at the C-terminus. Moreover, through the use of the Cfa split-intein system we obtained the site-specific biotinylation of the C33 antigen and the recombinant IgG. A very relevant aspects is that all these proteins are functional in the LIAISON platform. In the future, these protocols could be used for the purification and-or the site-specific labelling of new bioreagents useful for the development of immunodiagnostic assays.

INTRODUCTION

HEPATITES C VIRUS (HCV): STRUCTURE AND PRINCIPAL FEATURES

Hepatitis C virus (HCV) was discovered in 1989 (1). It consists of small virions measuring 55-65 nm in diameter, with a single-stranded RNA genome. A large majority (55% to 85%) of the subjects who acquire HCV infection fail to clear the virus and, in them, the infection becomes persistent (2). A subset of person with chronic HCV infection, defined arbitrarily as persistence of the virus in the person's body beyond 6 months, progress to cirrhosis and liver cancer over the period of several decades: in particular chronic HCV Infection is associated with 25% lifetime risk of developing cirrhosis and a 20% lifetime risk of developing hepatocellular carcinoma (3). These long-term consequences are associated with significant morbidity and mortality.

HCV is a member of the virus family *Flaviviridae*. Its genome is an approximately 9.6 Kb, positive-sense, single stranded RNA (4)that encodes a single polyprotein of about 3000 amino acids. The polypeptide is cleaved by viral and host enzymes to produce at least 10 mature viral proteins, including core E1 and E2 envelope proteins, the p7 ion channel and the non-structural (NS) proteins NS2, NS3, NS4A, NS4B, NS5A and NS5B, as shown in Fig. 1B (5).

The hepatitis C virus particle consists of a lipid membrane envelope that is 55 to 65 nm in diameter.(6) (7) Two viral envelope glycoproteins, E1 and E2, are embedded in the lipid envelope (8).They take part in viral attachment and entry into the cell Within the envelope there is an icosahedral core that is 33 to 40 nm in diameter. Inside the core there is the RNA material of the virus (6) Fig 1A

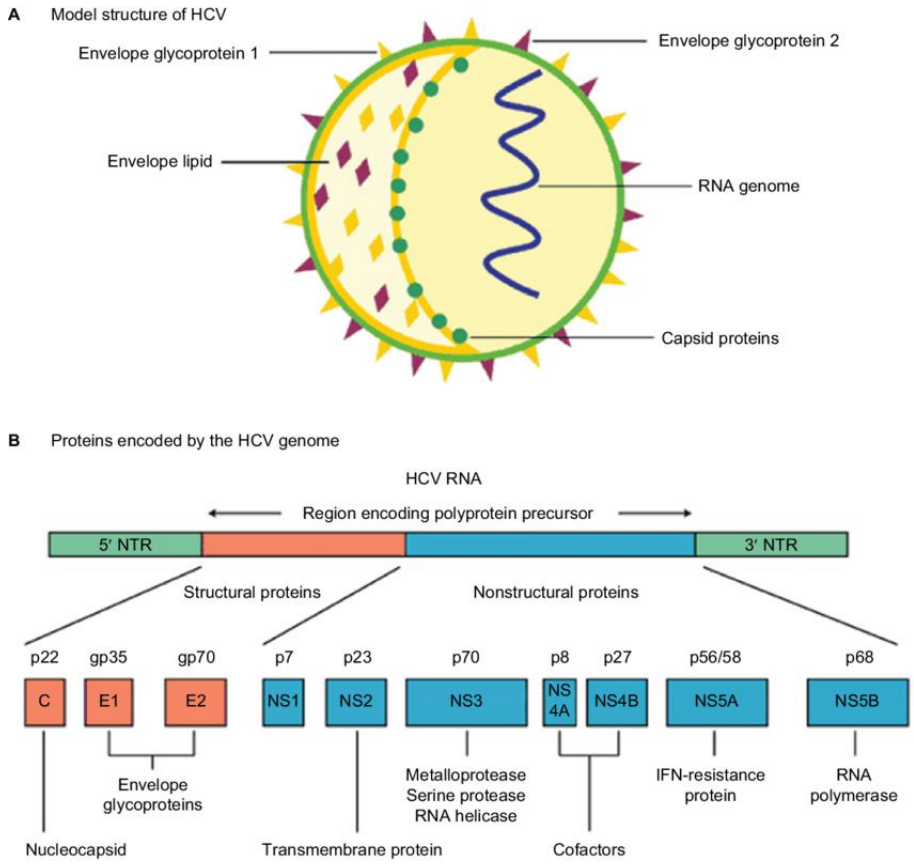

Figure 1 a and b: HCV: model structure and genome organization. Notes: (A) Model structure of HCV(B)(9) Proteins encoded by the HCV genome Abbreviations: HCV, hepatitis C virus; IFN, interferon; NTR, non-translated RNA.

Core

The precursor of the core protein comprises 191 amino acids. Three domains, D1, D2 and D3 of the core protein facilitate comprehensive understanding of the functions of this protein. The N-terminal domain D1 binds to HCV RNA and act as a powerful chaperon. The domain is basic in nature and is involved in RNA dimerization and nucleocapsid formation (10,11). The other two domains, D2 and D3, interact with several glycoprotein, including the viral attachment glycoprotein E1 and E2. These two domains are hydrophobic in nature and also interact with lipid droplets and several host proteins. The mature core protein consists of 177 amino acids (12). Its processing takes place in endoplasmic reticulum (ER), where precursor core protein is cleaved, and a short peptide, which acts as a signal sequence for the E1 glycoprotein, remains in the ER(13,14).

The HCV core protein is an attractive target for drug development because it is the most conserved of all HCV proteins. Its exception level of conservation is uniform across all the HCV genotypes, reflection its essential role in HCV life cycle (15). It is most likely that an inhibitor against this target can effectively be used as a therapeutic agent all the known HCV genotypes.

E1 and E2 glycoproteins

Two envelope glycoproteins, E1 and E2 are encoded by HCV genome. These glycoproteins play and important role in virus entry into hepatocytes, interacting with various cell-surface proteins (16).

P7 protein

HCV P7 is an important protein of 63 amino acids. It is a member of the expanding family of proteins known as viroporins because it forms oligomers and ion channels in the lipid membrane. Physiological studies of the P7 protein have demonstrated that its N-terminal helix is oriented towards channel pores, and it allows the influx of cations through the membrane. In the HCV genome, the genes for these proteins are located at the junction of structural and nonstructural proteins (17,18).

NS2-3 protease and inhibition by peptide

HCV NS2 is an important protein for HCV replication. It modulates the function of various host proteins for the formation of replication complex. It influences the host immune system by affecting apoptosis (19), regulating fat metabolism, altering the expression of various cytokines, arresting the cell cycle, and hampering the cAMP-dependent pathway (20–23).

A peptide derived from NS4A acts as an inhibitor of NS2-3 cleavage (24). The peptide interferes with the proper placement of scissile bound at the junction between NS2 and NS3 in the active site of the protease. Thus, peptides derived from HCV polypeptide may act as an inhibitor of N2-3 cleavage and may be used as therapeutic agents against HCV (25).

NS3

The HCV NS3/4A proteins are membrane-targeted serine protease (25). It has an important role in HCV replication because it cleaves the HCV polyprotein into NS3, NS4A, NS5A and NS5B. In spite of the challenges in the design of NS3 protease inhibitors, it was the first class of direct-acting anti-HCV drugs to be applied clinically (26).The N-terminal portion of NS3 owns a protease domain while its C-terminal part form a three-domain polypeptide that possesses helicase activity (subdomain 1, subdomain 2 and subdomain 3), unwinding dsRNA or DNA. Like other motor proteins, NS3 helicase possesses two domains, one of which appears to rotate upon ATP binding. The two most prominent target sites on NS3

helicase are the ATP and RNA-binding sites. From a biological point of view, due to the co-existence of NS3 protease and helicase activities, it may serve as a useful antiviral target against HCV (27)

NS4A

HCV NS4A is a protein of 54 amino acids whose main function is to act as a cofactor for NS3 protease. The N-terminal part of NS4A has also role in targeting NS3 to the ER (28). Other important function of NS4A involved its role in NS5A phosphorylation. Deletion analysis of NS5A revealed that amino acid residues from 2135 to 2139 were necessary for phosphorylation by NS4A (29)

NS4B

NS4B is a 27-KDa membrane protein. Its main function is its role in the formation of the membranous web for HCV replication, which serves as a scaffold for assembly of the replication complex. It also possesses RNA-binding and NTPase activities in addiction to anti-apoptotic properties. On the basis of known function of NS4B, its inhibitors are broadly classified into two major classes. The first class includes inhibitors that interact directly with HCV RNA, while the other class includes inhibitors that interact with membranes. Most importantly, the drugs of these two separate classes that target individual functions of NS4A are synergic. Recently, it was discovered that NS4A also possesses the ability to hydrolyze ATP, so this function may also be utilized to develop inhibitors against this protein (30).

NS5A

The HCV-NS5A protein is essential for the viral replication, as it is part of membrane-associated replication complex (RC). During HCV replication, a membranous web is formed by membrane vesicles that are partly derived from ER. It is thought that the NS5A protein plays a significant part, but its exact role is this process is still uncertain (31)

NS5B

HCV NS5B is an RNA-dependent RNA polymerase (RdRP). It is also an essential part of HCV replication complex. It initiates and catalyzes RNA synthesis (32). The structure of NS5B resembles a right hand. For ease of understanding its structure is divided into three domains, finger, palm and thumb. The enzyme active site is located inside the palm, which also contains the highly conserved GDD motif (33). It also contains aspartic acid residues that are responsible for binding nucleotides during the process of oligomerization (34). In humans, there is no homolog of NS5B, which has a very important role in viral infectivity (35)and is therefore an important candidate for the development of antiviral compounds. In humans, there is no homolog of NS5B, which has a very important role in viral infectivity (35) and is therefore an important candidate for the development of antiviral compounds.

NS5B inhibitors can be classified into two major groups: nucleoside analogs and non-nucleoside inhibitors (NNIs). Nucleoside analogs act as substitute substrates for NS5B polymerase, while non-nucleoside inhibitors bind to the allosteric region of NS5B. The major problem associated with NNIs is their significantly different activity against various genotypes and even subtypes of HCV (36).

THERAPEUTIC APPROCHES OF HCV INFECTION

Drug treatment for HCV infection first become available in early 1990s. However, the initial treatment, based primarily on interferon or its long-acting congener (pegylated interferon), with or without ribavirin, were limited by low efficacy rates, frequent adverse events leading to discontinuation of treatment, high cost and need for injections. With the launch in 2014 of newer drugs, known as direct-acting anti-viral agents (DAAs), with efficacy rates exceeding 95%, excellent safety record, convenient once-daily regimens, and oral route of administration, treatment of chronic HCV infection has undergone a paradigm change. The only challenge to the use of DAAs worldwide is their high price.

The current most standard treatment for HCV infection includes a protease inhibitor (either telaprevir or boceprevir) along with the PEG-IFN/ribavirin (37). It is chiefly effective against HCV genotype 2 or 3 (38). The treatment duration for genotype 2 and 3 is six months, while for genotype 1 and 4 it may extend up to 12 months (39). There are also side effects associated with therapy, which include pancytopenia, flu-like symptoms, depression, pain in the body, and elevated temperature. These symptoms are most commonly observed and may be the reason for discontinuation of treatment before elimination of the virus has been achieved. In the recent years, researchers have focused on the development of DAA agents, which specifically target HCV replication and posttranslational processing (40).

HCV DIAGNOSIS

HCV infects approximately 170 million people worldwide. The persistence of HCV infection is a major cause of liver cirrhosis and hepatocellular carcinoma (41). HCV infection is often asymptomatic, thus diagnosis relies heavily on clinical laboratory assays, including the serological immunoassays for antibodies to HCV (anti-HCV) or core antigen (HCVcAg) and nucleic acid testing (NAT) for HCV RNA (42).

Since 1989, several iteration of anti-HCV serological assay have been developed with continuously improving of sensitivity to address diagnosis and transfusion demands(43)

The anti-HCV test detects host's humoral immune response to the virus. The appearance of anti-HCV is delayed by a few weeks after infection and may be weak or even non-existent in some persons. On the other hand, HCV RNA, a viral constituent, appears in the blood much earlier, within few days after the virus enters in host. Thus, the period between a person becomes HCV infected (and infectious to others) and the potential for detection of infection (the so-called window period) is longer for anti-HCV antibody test than for HCV RNA. Those who test positive for anti-HCV need additional testing approach for HCV RNA using a NAT to determine whether the HCV infection is current active or has been cleared. This two-step testing approach has several limitations. The anti-HCV tests are cheap, easier to perform and have a widespread availability, however these have a longer window period. The NAT assays have shorter window period, but are costly, and need specialized equipment and manpower, limiting their availability. This had led to a search for alternative screening tests which may efficiently identify new HCV infections at an earlier stage and at low cost. HCV core antigen (HCVcAg) is a viral protein which is released from hepatocytes during assembly of HCV virions. In the recent years, tests for detection of HCVcAg in serum and plasma have been developed and are emerging as affordable point-of-care tests that could replace tests for HCV RNA. A systematic review of published studies on the use of HCVcAg assays showed that these have a high sensitivity and specificity for detection of HCV viremia, in person with HCV RNA concentration exceeding 3000 IU/ml (44,45).

The first commercially available anti-HCV enzyme immunoassay (EIA) used a single HCV recombinant antigen derived from the nonstructural NS4 protein designated c100-3 (46). The sensitivity of this first-generation EIA was low for a high-prevalence population (approximately 80%) and showed a high false-positive rate (up to 70 %) in a low-prevalence blood donor group (47). Therefore, a second-generation EIA was developed and approved for use by Food and Drug Administration (FDA) in 1992 (48). The second-generation EIA, which contained additional HCV antigens from the core (c22-3) and NS3 (c33c) proteins showed increased sensitivity and specificity and shortened the average seroconvertion period from 16 to 10 weeks (47–50). The third-generation EIA, which added a fourth antigen (NS5), showed significant improvement performance, particularly for high-risk

patients (51,52). However, there is a still residual risk due to the seroconvertion period of approximately 56 days, and high false-positive rates were not resolved (53). The Center of Disease Control of and Prevention (CDC) recommended that an anti-HCV screening test positive result be verified by a more specific supplemental assay such as recombinant immunoblot or nucleic acid test (54). To facilitate the use of the supplement assay, the revised guideline included an option for reflex supplement testing based on signal-to-cutoff (s/co) ratios (55). Today, automated chemiluminescent immunoassay (CLIA) analyzers are widely used, particular in high volume clinical laboratories. These instruments offer excellent precision and reliability, high speed throughput, random access, and technical simplicity of full automation. CLIA showed significantly improved specificity, a greater positive predictive value, and a similar sensitivity compared to those EIA, for detectiong anti-HCV antibodies (56,57).

Nowadays, in most HCV immunodiagnostic kits, it's currently used the C33 antigen for the detection of human antibodies against HCV NS3 antigen. The reason of this choice is that the C33 is more immunoreactive than NS3 and this feature is fundamental in HCV immunoassay to obtain a high specificity between antigen and antibody.

Diasorin C33 includes the amino acids from 1188 to 1463 of NS3 of HCV genotype HCV-1, corresponding at subdomain 1 and 2 of its helicase domain and it is produced in *E.coli*. The loss of the protease domain and the helicase subdomain 3 may avoid the cross-reactivity with other targets and a greater exposure of the epitopes recognized by the anti-C33 antibodies present in the human blood samples. This could explain the higher immunoreactivity of C33 than the entire NS3.

In the next sub-chapter is shown the Liaison XL Murex HCV Ab assay where the C33, previously biotinylated, is links at the paramagnetic beats (solid) conjugated with streptavidin.

THE LIAISON® SYSTEM

The Liaison® system is an instrument designed to perform immunometric analyses of biological fluid samples (such as serum or plasma) in a completely automated way (Figure 2). Up to 15 different tests can be performed at once on up to 144 samples in a sequential or random access mode. The output of the analysis is generated through the formation of an immune complex, followed by a chemiluminescent reaction that produces an emission of light.

Figure 2. The Liaison® system.

The instrument is composed of two modules, designed to be both allocated on a single workbench; the first module is a personal computer with touch screen, that hosts the user interface software and all the system data (assay protocols, reagent cartridges database, output of analyses, calibration history, network controls etc.). The second module is the actual analyzer, that performs the analysis from sample loading all the way to the final output for the user. Key components of the analyzer include:

- cuvette loader and stacker: two conveyor belts allow continuous loading of the reaction modules, that are stored on a multilevel rack (7 levels).
- Sample rack slots: in the left-hand part of the instrument, a storage area can hold up to 12 sample racks, each carrying up to 12 samples. A barcode reader allows error-free catalogation of samples.
- Reagent slots: in the right-hand part of the instrument, another storage area can hold up to 15 different reagent cartridge simultaneously. This area is kept at a constant temperature of 15°C for optimal conservation of the reagents, while a stirring device keeps the microbeads always in homogenous suspension. A barcode reader for cartridge identification is present.

- Robot dispense arms: two robotic arms each carrying a dispensing needle. One arm is usually dedicated to dispensing samples, another to dispensing reagents. Each one has a separate washing well to clean the needle after each pipetting.
- Incubator: this area hosts the reaction cuvettes during incubation times, at a constant temperature of 37°C.
- Washing station: through the application of a magnetic field, this part allows retention of the paramagnetic microbeads and removal of the reaction liquids. Any number of washing steps with the desired washing buffer can be set.
- Read area: contains the injection devices of trigger reagents and the photomultiplier tube.

The Liaison® system is based on two key features: the use of paramagnetic microbeads as the solid phase and the generation of signal by means of chemiluminescence. The adoption of microbeads as the solid phase instead of the classic immunoassay supports, as the ELISA microwells gives a clear edge in terms of available reaction surface, which in turn increases the kinetic rates of the antigen-antibody complex formation. Moreover, diffusion of both the analyte and the solid phase in the reaction volume is allowed, while in ELISA system only the analyte can diffuse, decreasing the possibility of the immune complex formation. The microbeads adopted in the Liaison® system (Figure 3) are colloidal particles composed of a ferric oxide core covered by a polystyrene layer formed by spontaneous coalescence of polystyrene linear chains. This structure is in turn coated with another layer composed of polyurethane activated with tosyl-groups. The tosyl-group (4-toluenesulfonyl chloride) can undergo nucleophilic attack, allowing the beads to covalently bind proteins through their available primary amino groups (ε-amino groups of lysines, N-terminal end). The paramagnetic properties of these microbeads allow easy manipulation through the application of a magnetic field. The particles respond to a magnet but are not magnetic themselves and retain no residual magnetism after removal of the magnet.

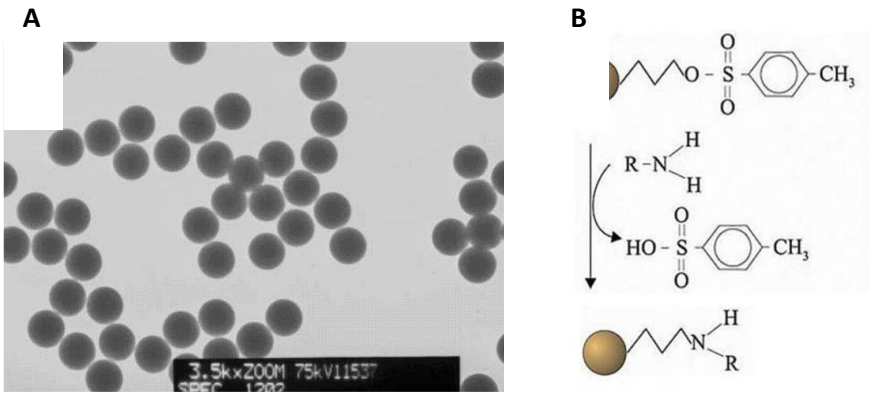

Figure 3. (A) The paramagnetic microbeads used in the Liaison® system.
(B) Chemistry of the covalent binding of amines to the tosyl-activated beads.

The tracer molecule is an antigen or antibody conjugated to a signal generating compound. Chemiluminescent tracers are formed by conjugating the antibody or antigen to a molecule that can generate a photon emission upon addition of certain reagents. The entity of this photon emission is measured with a luminometer, usually equipped with a photomultiplier tube. The chemiluminescent molecule used in the Liaison® system is the luminol derivate ABEI (N-(4-Amino-Butyl)-N-Ethyl-Isoluminol), which is converted to its activated ester to allow conjugation with the antibody or antigen (Figure 4).

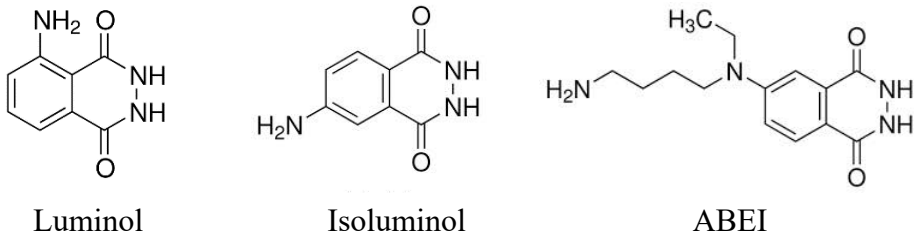

Figure 4. Structure of luminol, isoluminol and ABEI molecules.

In presence of H_2O_2 and a microperoxidase (deuteroferriheme), ABEI achieves an excited state in consequence of a chemical reaction. This excited level decays to the ground level generating energy in form of light (Figure 5). The emission of light is recorded by the photomutiplier tube for an interval of just 3 seconds (called “flash” chemiluminescence) and the signal is integrated over this interval. The final result is expressed in RLUs (Relative Light Units).

Using chemiluminescence is a great improvement over enzymatic signal generation of classic ELISA format assays. Sensitivity is highly increased and a greater dynamic range can be achieved. Lower molecular weight and steric hindrance of ABEI compared to horseradish peroxidase allow conjugation of more signal generating molecules per tracer molecule. Moreover, generation and recording of signal is completed in a very short time (3 seconds), with a sensible throughput increase.

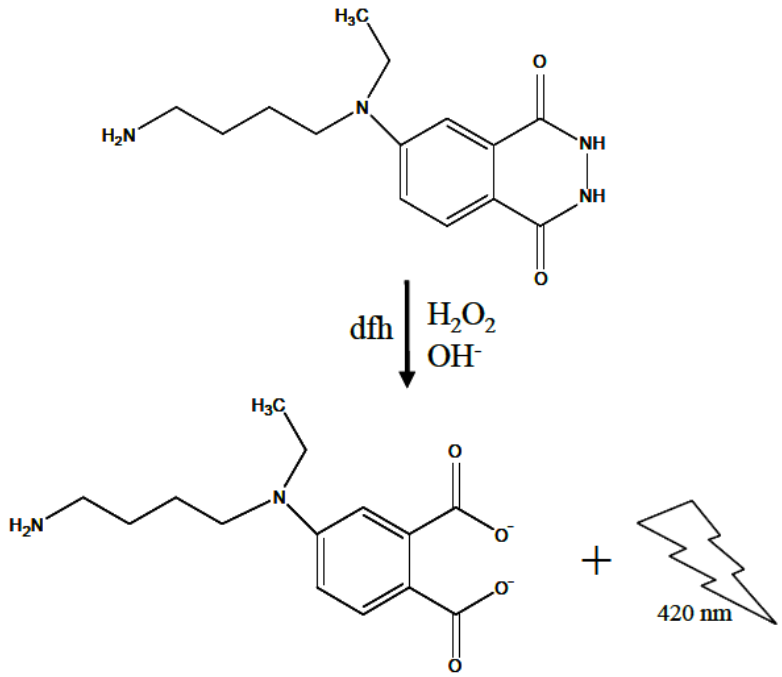

Figure 5. Chemilumiscent reaction of ABEI, H_2O_2 and deuteroferriheme (dfh)

THE LIAISON® XL MUREX HCV Ab ASSAY

The method for qualitative determination of specific IgG to hepatitis C virus (HCV) is an indirect chemiluminescence immunoassay (CLIA). Two recombinant antigens (core and NS4) specific for HCV are used for coating magnetic particles (solid phase), while a third HCV antigen (biotinylated C33) is provided lyophilized, as a separate reagent. During the first incubation, the biotinylated antigen is captured by streptavidin-coated magnetic particles, and HCV antibodies present in calibrator, samples or controls bind to the solid phase through the recombinant HCV antigens. During the second incubation, a mouse monoclonal antibody to human IgG, linked to an isoluminol derivative (isoluminol-antibody conjugate), reacts with human IgG to HCV already bound to the solid phase. After each incubation, the unbound material is removed with a wash cycle. Subsequently, the starter reagents are added and a flash chemiluminescence reaction is thus induced. The light signal, and hence the amount of isoluminol-antibody conjugate, is measured by a photomultiplier as relative light units (RLU) and is indicative of human IgG to HCV presence in calibrator, samples or controls.

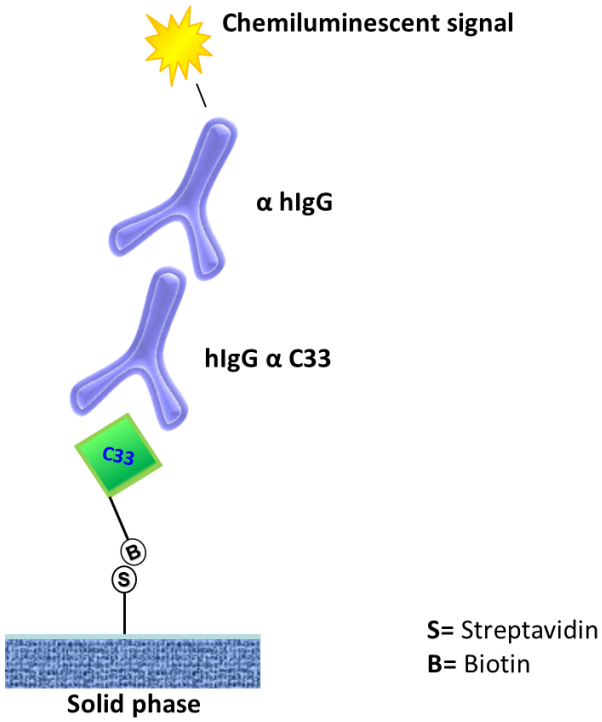

Figure 6: Schematic representation of Liaison XL Murex HCV Ab assay

SITE-SPECIFIC PROTEIN LABELING BY INTEIN MEDIATED PROTEIN LIGATION

The study of protein has taken center stage in biomedical investigation over the past several decades (58). Powerful genetic tools including recombinant protein expression and site-directed mutagenesis (59) have allowed for investigation of particular domains and individual amino acids contribution to the structure and function of complex proteins. Over the past years, unnatural amino acid mutagenesis using non sense suppression and related strategies has expanded the scope of protein study by providing a wide range of new chemical functionality into increasingly large and diverse protein types, addressing many biological challenges (60). Neverthless, in some cases it becomes desirable in protein biochemistry to have even greater chemical precision than provided by genetic methods.

Examples of such cases where the power of chemistry is particularly advantageous in the study of proteins include the analysis of proteins with multiple diverse posttranslational modification, structural studies on segmentally isotopically labeled proteins, or the incorporation of two or more complex chemical probes at particular sites into proteins.

Total synthesis of proteins typically involves generating peptides using solid phase synthesis (SPPS) and ligating such peptides together by chemoselective reactions including the powerful native chemical ligation reaction (NCL). The NCL reaction developed by Kent and colleagues (61) is based on the early work of Wieland (62) and exploits the chemoselective reaction of an N-terminal cysteine (Cys) and a C-terminal thioester of two unprotected peptides. Such chemoselectivity derives from an initial transthioesterification between the thiol of the N-terminal Cys and C-terminal thioester followed by intramolecular aminolysis to afford a stable peptide bound. Total chemical synthesis of proteins has been successfully used to generate small proteins, usually less than 200 aa, but become difficult to execute on larger proteins because of the need for five or more peptide ligation reaction.

A compromise between genetic and chemical approaches to the study of proteins is embodied by protein semisynthesis. Protein semisynthesis refers to the technological merger of recombinant protein expression and chemical modifications, which are often introduced via chemoselective ligation reaction (62). One of the major modalities of protein semisynthesis is intein mediated protein ligation (IPL) or expressed protein ligation (EPL) [7]. The EPL method exploits nature's inteins for generating recombinant proteins with C-terminal thioester, which will further undergo NCL with an N-terminal Cys.

INTEIN (Protein splicing elements)

Inteins were identified 30 years ago, when two groups reported an in-frame insertion in the VMA1 gene, which encodes a vacuolar membrane H+-ATPase of the yeast Saccharomyces cerevisiae. The nucleotide sequence of the VMA1 gene predicts a polypeptide of 1,071 amino acids with a calculated molecular mass of 118 kDa, but the size of the VMA1 protein, as estimated from sodium dodecyl sulfate-polyacrylamide (SDS-PAGE) gels, is only 67 kDa. Furthermore, the N- and C-terminal regions of the deduced sequence were shown to be very similar to the catalytic subunits of vacuolar membrane H+-ATPases of other organisms, while an internal region of 454 amino acid residues displayed no detectable sequence similarity to any known ATPase subunits. Instead, the internal sequence exhibits similarity to an S. cerevisiae endonuclease encoded by the HO gene. The in-frame insertion was found to be present in the mRNA, translated with the Vma1 protein, and excised posttranslationally (63)By analogy to pre-mRNA introns and exons, the segments are called inteins for internal protein sequence, and exteins for external protein sequence, with upstream exteins termed N-exteins and downstream exteins called C-exteins. The post-translational process that excises the internal region from the precursor protein, with subsequent ligation of the N and C-exteins, is termed protein splicing (64).

The products of the protein splicing process are two stable proteins, the mature protein and the intein (Figure 7)

Inteins are now known to be widely expressed and dispersed in nature as they are encoded in genomes of microorganisms from all three domains of life - bacteria, archaea and eukaryotes - and viruses (65), suggesting an ancient evolutionary origin. They exist in proteins with various functions, but proteins involved in DNA metabolism, such as polymerases, helicases, recombinases, topoisomerases and ribonucleotide reductases appear to be the most common functional entities for inteins (66).

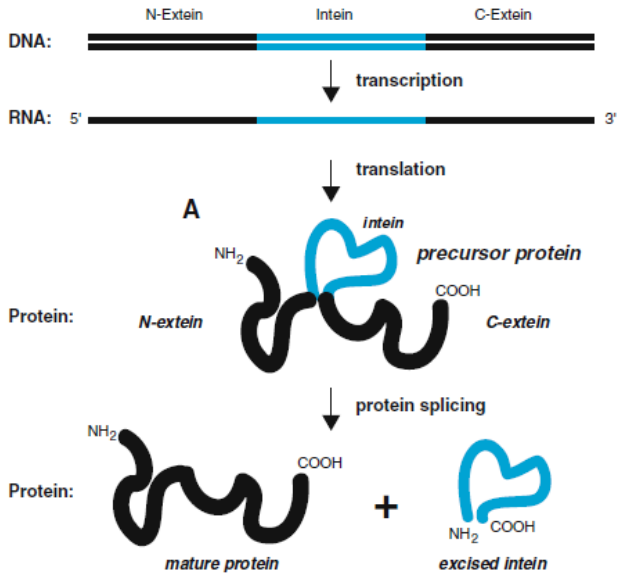

Figure 7 . Protein splicing mechanism.

Structure and types of inteins

Based on their domain structure, inteins are categorized in four classes: full-length inteins, mini-inteins, split-inteins and alanine-inteins (Figure 8).

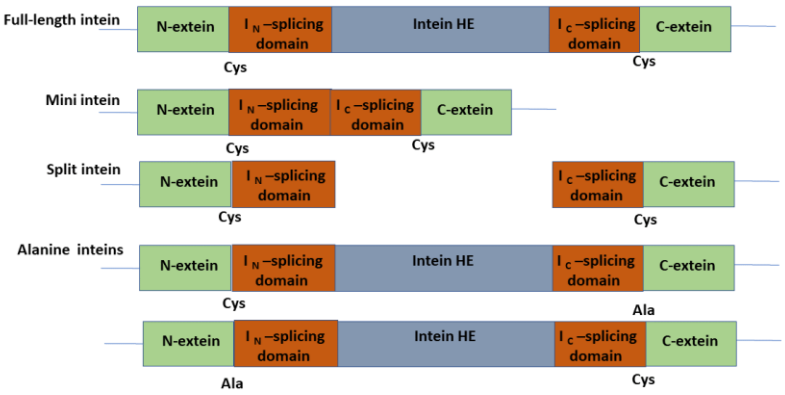

Figure 8. Schematic diagram of host-intein structural domains. Types of inteins. I_N: N-terminal intein fragment; I_C: C-terminal intein fragment; HE: homing endonuclease domain.

Full length inteins

Most inteins are full-length inteins expressed within a single polypeptide chain (cis-splicing inteins). They are bifunctional proteins that include two structural domains - the intein domain responsible for protein splicing out of the precursor polypeptide chain, and a homing endonuclease (HE) domain with a role in DNA-cutting and insertion of the associated mobile genetic element into the precursor protein-coding gene (67–70). The HE domain splits the splicing domain into N and C-terminal splicing domains. Intein sequence alignments revealed important motifs and conserved regions that are mediating the splicing (71). As reported in figure 9, the splicing domain consists of conserved blocks A, B, F and G, while blocks C, D, and E are present in the HE domains. Blocks C and E contain conserved endonuclease active sites with catalytic residues Asp, Glu or Lys (72,73). Several inteins have mutations in these endonuclease active site residues and therefore may not be active endonucleases although the remainder of the motif is present. Blocks A, and B, localize near the N-terminus of the intein, while blocks F and G are located near the C-terminus. Conserved amino acids important for the splicing process (Cys, Ser or Thr) are present both at the intein N-terminus as well as on the C-extein fragment near the intein-extein junction (Figure 9) (71). In addition, a dipeptide His-Asn or His-Gln is present at the intein C-terminus in most full-length inteins.

The mini-inteins

The mini-inteins are typical N- and C-terminal splicing domains that lack the HE domain and have a continuous splicing domain, thus are also cis-splicing inteins.

Split-inteins

In contrast with the mini inteins, the split-inteins are mini-inteins whose N and C-terminal splicing domains are transcribed and translated with different exteins, and are referred to as a trans-splicing inteins. In this case, the fragments associate through a zipper-like interface prior to protein splicing (74).The Split-inteins consist of two short intein segments - the N-terminal intein (IN), and the C-terminal intein (IC). The two fragments reassemble into a complete intein structure similar to full-length inteins through a trans-splicing mechanism (75–77). Based on their conserved residues and mechanism of action, most full-length and split-inteins are classified as class 1 inteins (see below).

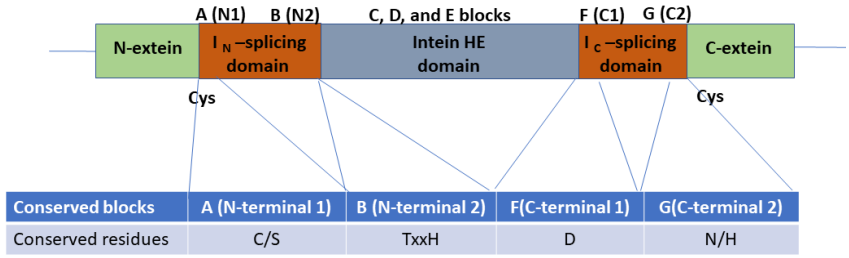

Figure 9. Conserved blocks of the intein splicing domain

Alanine-inteins

Alanine-inteins have an alanine, instead of a cysteine or a serine at the splicing junction (Figure 8). Based on the mechanism of splicing, most alanine-inteins belong to either class 2 or class 3 inteins (see below).

Protein splicing mechanisms

Inteins use the same strategies as classical enzymes to perform catalysis (78). They are single turnover enzymes that splice out during the maturation of their host proteins. Splicing occurs when nucleophilic residues and residues that assist catalysis belonging to the host-intein polypeptide chain are properly aligned as a result of intrachain protein folding. Splicing occurs spontaneously, without the help of any known cofactor, chaperone, or energy source (79).

Standard intein splicing, also known as the splicing mechanism of class 1 inteins, involves the breaking of peptide-bonds at the intein-extein junctions, and the forming of a new peptide bond to connect the separated extein fragments. Class 1 inteins are characterized by motifs and conserved regions that are mediating the splicing (74). The two conserved motifs near the N- and the C-termini of the intein as well as the C-extein fragment near the intein-extein junction contain amino acids important for the splicing process (Figure 9) (74).

The protein splicing mechanism is composed by the following four-steps:

1. The formation of a thio(ester) bond by N-O or N-S shift at the N-terminal splice junction when the side chain of the first residue (either a Cys, a Ser or a Thr) nucleophilically attacks the peptide bond of the immediately upstream residue, which is the end residue of the N-extein.
2. The newly formed (thio)ester is attacked by the side chain of the first residue of the C-extein to free the N-terminal end of the intein, in a trans-(thio)-esterification event. This results in a branched intermediate in which the N-extein and C-extein are attached, albeit not through a peptide bond.
3. The branch is resolved in a next step that involves the last residue of the intein, an asparagine, and its amide nitrogen atom that cleaves apart the peptide bond between the intein and the C-extein. The result is an intein segment with a terminal cyclic imide that is subsequently opened via succinimide hydrolysis.
4. The linked N- and C-exteins undergo a finishing acyl rearrangement reaction that involves the breaking of the thio(ester) bond by an O-N or S-N shift and the creation of a new peptide bond (79) (Figure 10).

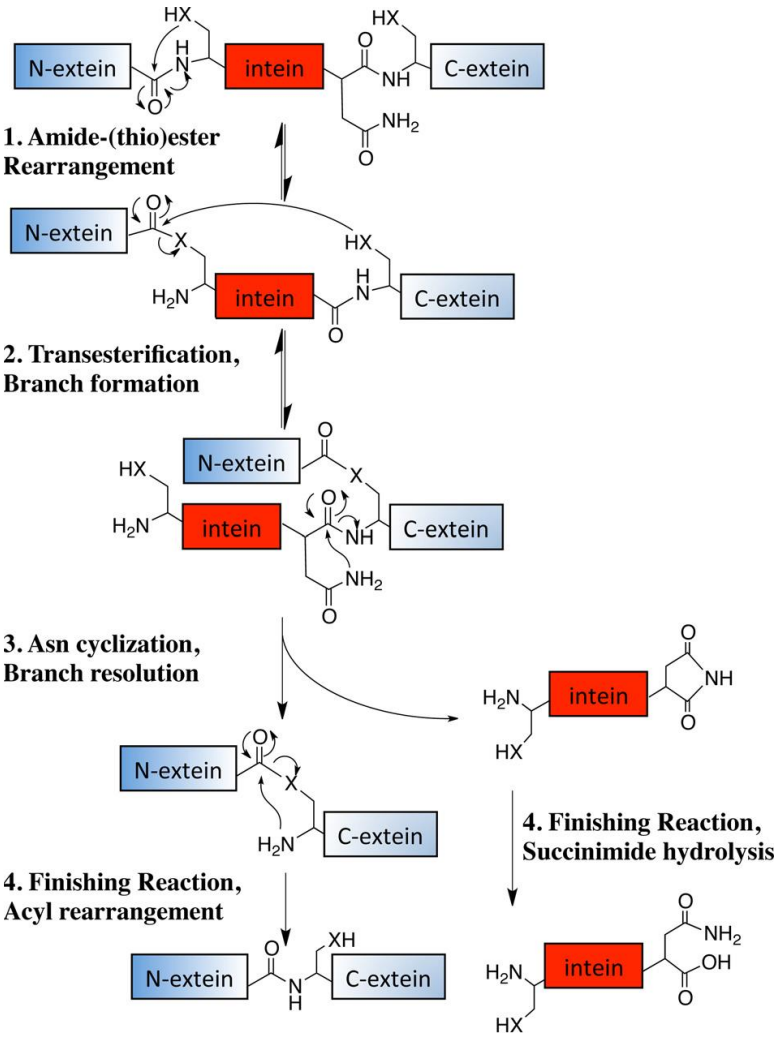

Figure 10. The intein-mediated class 1 protein splicing mechanism

Ser, Thr, Cys and Asn are essential residues that act as nucleophiles in the splicing mechanism of most inteins (as described above; Figure 10). However, inteins have been identified that present variations in the conserved amino acids involved in splicing. Some inteins have an Ala at their N-termini and cannot follow the standard splicing mechanism steps but are able to splice out. Examples of Ala1 inteins are the KlbA and the DnaB families (80,81). These inteins splice by different protein splicing mechanisms. KlbA inteins lack the conserved Ser or Cys at the intein N-terminus and the conserved intein penultimate His has been replaced by a Ser. Under these conditions, the C-extein nucleophile attacks a peptide bond at the N-terminal splice junction rather than a (thio)ester bond, eliminating the need

to form the initial (thio)ester at the N-terminal splice junction. After this first step, the splicing reaction follows the standard steps: branch resolution by Asn cyclization and acyl rearrangement to form a native peptide bond between the ligated exteins (80). Intein that work by this mechanism are classified as class 2 inteins (Figure 11).

DnaB and other inteins classified as class 3 inteins, use a modified mechanism that includes new conserved residues and a second branched intermediate (82–84). The sequence signature of this class of inteins is a noncontiguous Trp-Cys-Thr (WCT) motif and the absence of the standard class 1 N-terminal Cys or Ser nucleophile. A conserved Cys directly attacks the peptide bond at the N-terminal splice site, resulting in the N-extein linked by a thioester to Cys thus forming the class specific branched intermediate. Next, the N-extein is transferred to the side chain of the Ser, Thr, or Cys at the C-terminal splice junction to form the standard branched intermediate (82) (Figure 11).

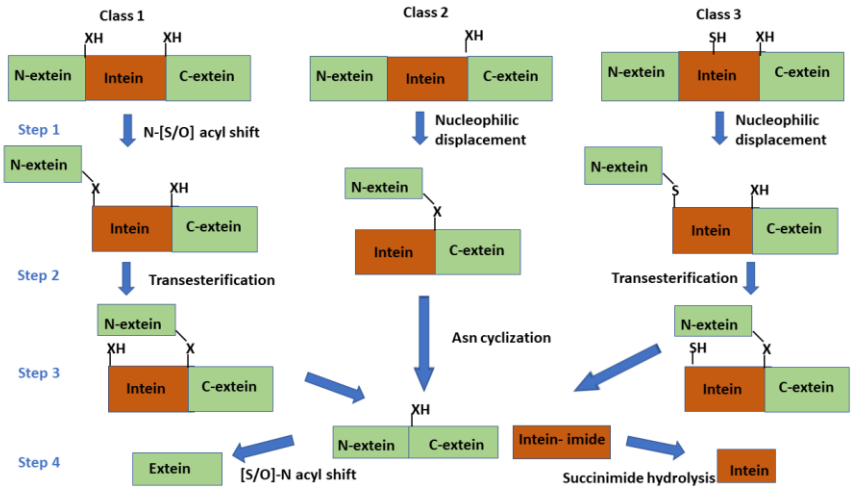

Figure 11. Standard mechanism of intein splicing, characteristic to class 1 inteins (left panel). Conserved splicing motifs at the intein-exteins junctions and main reaction steps are indicated. Variations of the standard splicing mechanism, characteristic to class 2 and class 3 inteins (middle and right panels).

Inteins in Biotechnology

Both cis-splicing and trans-splicing inteins have been used in various biotechnological applications. Natural inteins have been isolated from cells and engineered to create self-splicing proteins for specific functions. For example, the splicing domain is explored for expression and purification of recombinant proteins (85,86), cyclization (87), site-specific modification (88) or labeling of proteins (89,90), post-translational processing, production of selenoproteins, protein regulation by conditional protein splicing, biosensors, or expression of trans-genes (91–93). In addition, the HE domain proved to be a versatile biotechnological tool, as it has been used in various applications that involve genetic manipulation, including gene therapy for monogenic diseases, insect vector control or and development of transgenic crops (94,95). Inteins were also used for in vivo studies, like detecting protein-protein interactions, monitoring protein translocation through cellular organelles (96,97), and even site-specific conjugation of quantum dots (98).

Site-specific cleavage of inteins: a biotechnological application

The scientific success of the identification of the residues directly involved in the breaking and formation of peptide bonds has allowed to understand the way to modulating the protein splicing reaction for various applications. One biotechnological application is the site-specific cleavage of inteins. Inteins mutated at one of the two splice-junctions, at the level of the conserved residues, keeps their ability to self cleave at only the non-mutated splice junctions. These features can be exploited during the purification process.

N-terminus cleavage. Mutation of the Asn residue at the intein C-terminus abolishes steps 3 and 4 of the splicing reaction (Asn cyclization and subsequent cleavage of the peptide bond at the C-terminal junction) and results in N-terminal cleavage (Figure 12). Since step 1 still occurs, the (thio)ester bond can spontaneously hydrolyze, separating the N-extein from the intein/C-extein portion; usually, however, N-terminus cleavage requires the addition/presence of a nucleophilic group (typically thiol group or hydroxylamine) able to perform a transesterification reaction on the -1 carbonyl residue.

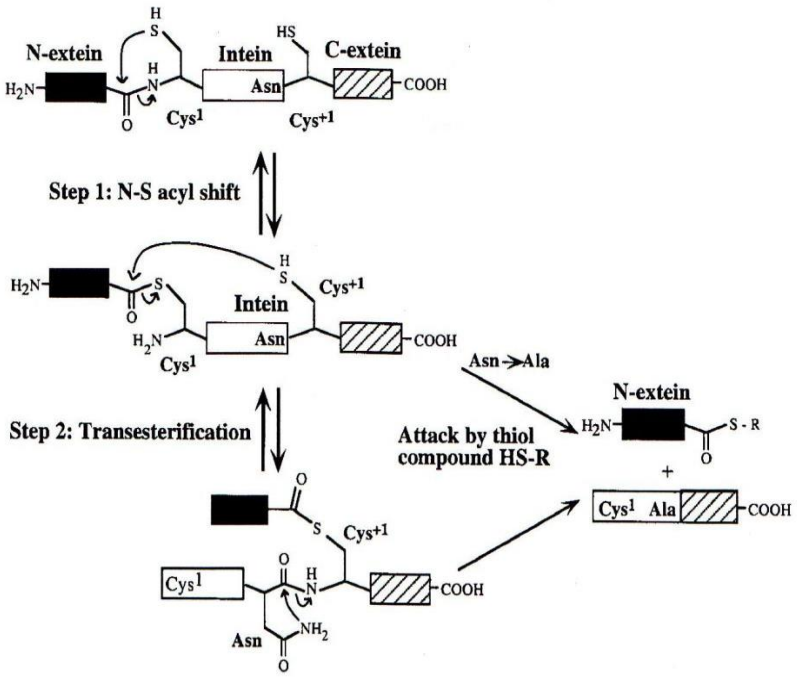

Figure 12. N-terminus cleavage (C-terminus mutation of intein).

C-terminus cleavage. Mutation of the conserved first residue of the intein abolishes steps 1, 2, and 4 of the splicing reaction and leads to C-terminal cleavage (Figure 13). In such a mutated intein, Asn cyclization (step 3) still occurs, to separate the C-extein from the N-extein/intein portion. C–terminal cleavage is usually induced by change in temperature and/or pH conditions.

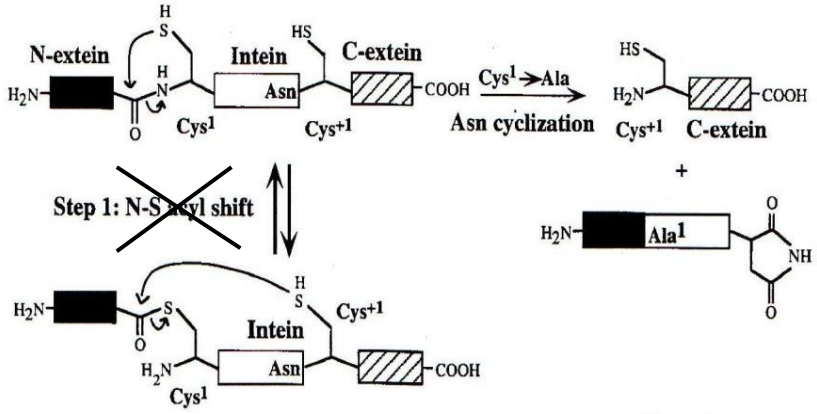

Figure 13. C-terminus cleavage (N-terminus mutation of intein).

Controllable cleavage of modified *cis*-splicing inteins has been adapted for a wide range of useful applications in molecular biology and biotechnology (e.g. IMPACT ™ Kit; a commercial available expression system from New England Biolabs used in proteins purification process).

Most of the inteins used in biotechnology are derived from prokaryotic organisms, or are engineered variants of the first discovered (VMA1 from *Saccharomyces cerevisiae*) (99)

One of the most popular intein employed for the purification of proteins is a 198 aminoacids in-frame insertion in the *gyrA* gene of *Mycobacterium xenopi* (called then *Mxe*GyrA) (99) and it has a molecular weight of 21.3 kDa. Compared to other mycobacterial gyrA inteins, *Mxe*GyrA intein has lost the residues required for endonuclease activity and may thus represent the minimal structure and functional information required for protein splicing. The 198 amino acid *Mycobacterium xenopi* (Mxe) DNA Gyrase subunit A (GyrA) intein has a compact structure composed mainly of β-strands with 2 antiparallel helices and a disordered section in its linker region (100). The C-terminal mutated version of this intein (*Mxe*GyrA N198A; in which the C-terminal asparagine residue was replaced with an

alanine residue) able to perform a thiol-induced cleavage at its N-terminus, is currently exploited in many commercial systems of purification (e.g. IMPACT ™ Kit).

The IMPACT (Intein Mediated Purification with an Affinity Chitin-binding Tag) system is a novel protein purification strategy that utilizes the inducible self-cleavage activity of protein splicing elements (inteins) to separate the target protein from the affinity tag (101). It distinguishes itself from all other purification systems by its ability to purify, in a single chromatographic step, a native recombinant protein without the use of a protease. Each intein tag contains a chitin binding domain (CBD) for the affinity purification of the fusion protein on chitin resin (102–104)The target protein is fused at its C-terminus or N-terminus to a self-cleavable intein tag that contains, in addition to the C-terminus or N-terminus mutated intein sequence, a domain necessary for the purification of the target protein. Induction of on-column cleavage, using thiol reagents such as dithiothreitol (DTT), releases the target protein from the intein tag (Figure 14).

Therefore, these innovative protein purification systems exploit the site-specific inducible self-cleavage activity of inteins to separate in a simple way the target protein from the affinity tag during the purification process.

The vectors included in this kit allow for the fusion of the target protein at its C-terminus (pTXB1) (105) or at its N-terminus (pTYB21) (104) to the intein tag.

In addition, with the use of pTXB1, native recombinant proteins that possess a reactive C-terminal thioester can be isolated for applications, including protein semisynthesis and site-specific labeling through the Intein Mediated Protein Ligation (IPL) (Figure 15).

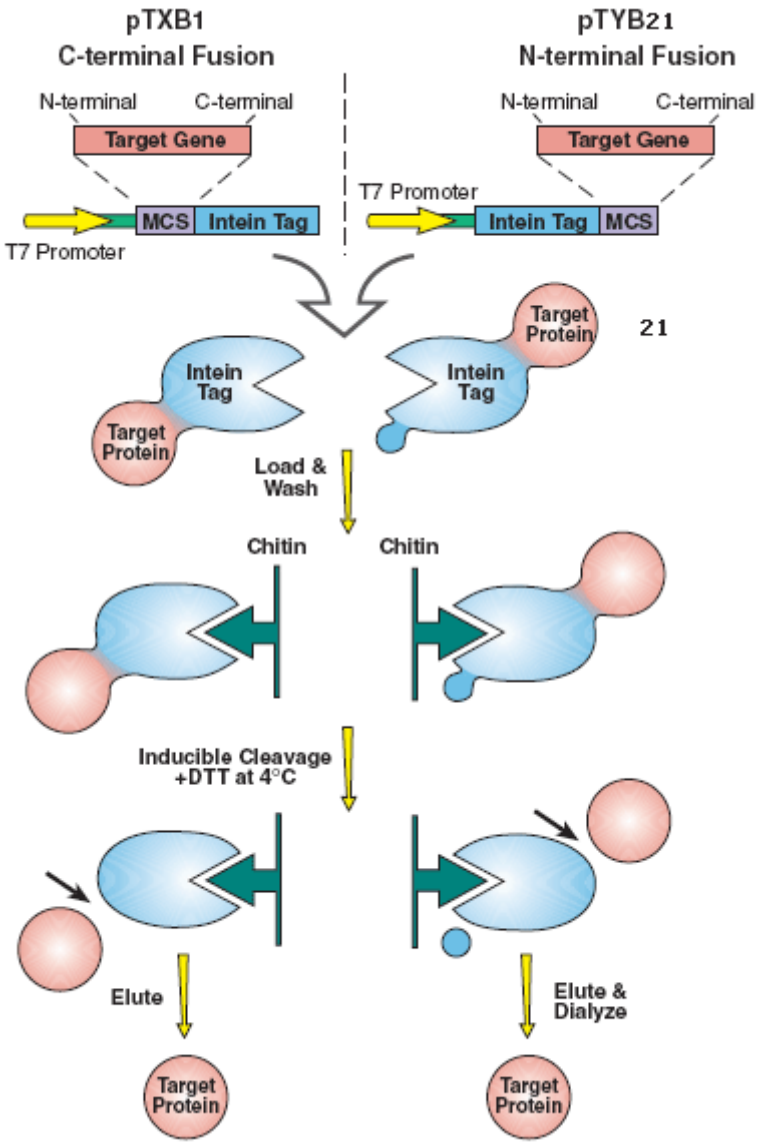

Figure 14. Schematic illustration of an expression/purification system that exploits C-terminus or N-terminus mutation of intein.

EXPRESSED PROTEIN LIGATION: METHOD AND APPLICATIONS

As mentioned before, there are various methods to site specifically label a protein, one of which is intein-mediated protein ligation. Intein mediated protein ligation (IPL) or express protein ligation (ELP) employs an intein, to create a protein possessing a C-terminal thioester that can be ligated to a protein or peptide possessing an N-terminal cysteine to form a native peptide bound. A variety of intein-enabled approaches have broken down the size limitation barrier of traditional chemical methods in protein semisynthesis and has opened new avenues of site-specific labeling of proteins. Unlike some chemical methods of labeling, IPL use a thiol reagent which can be easily removed. Another advantage is that the ligated peptide or protein needs only to contain an N-terminal cysteine and can be synthesized with various non-standard chemical moieties. Furthermore, a peptide as small as two amino acids can be added to your protein of interest, thus reducing possible perturbations to the native structure of the protein.

In order to conduct IPL, the gene encoding a protein of interest is cloned into an expression vector in which the target protein is fused to the N-terminus of a modified intein and a small chitin binding domain (as reported by IMPACT kit described above). Following expression and affinity purification of the three-parts fusion protein from *E.coli*, the intein cleavage is induced with a thiol reagent, such as 2 mercaptoethnesulfonic acid (MESNA), to release the protein of interest. The resulting thioester-tagged protein is mixed with a peptide or protein possessing an amino terminal cysteine and ligation occurs spontaneously to produce a native peptide bound between the two proteins or protein and the peptide (Figure 15). In general, for protein purification 1,4-dithiothreitol (DTT) is used as the intein cleavage reagent, however, the ligation efficiencies were significantly higher when MESNA or thiophenol was used in place of DTT for inducing cleavage. In general, cleavage of a target protein-intein fusion with DTT is more efficient than cleavage with MESNA and is preferred for the purpose of protein isolation in most cases. However, ligation efficiencies using MESNA-tagged paramyosin proteins and peptides are generally higher than those with DTT-tagged proteins, probably due to higher stability and reactivity of a MESNA thioester tag. If the target protein possesses an unfavorable residue at its carboxyl terminus , the insertion of a preferred residue at the cleavage site may improve cleavage and ligation efficiency.

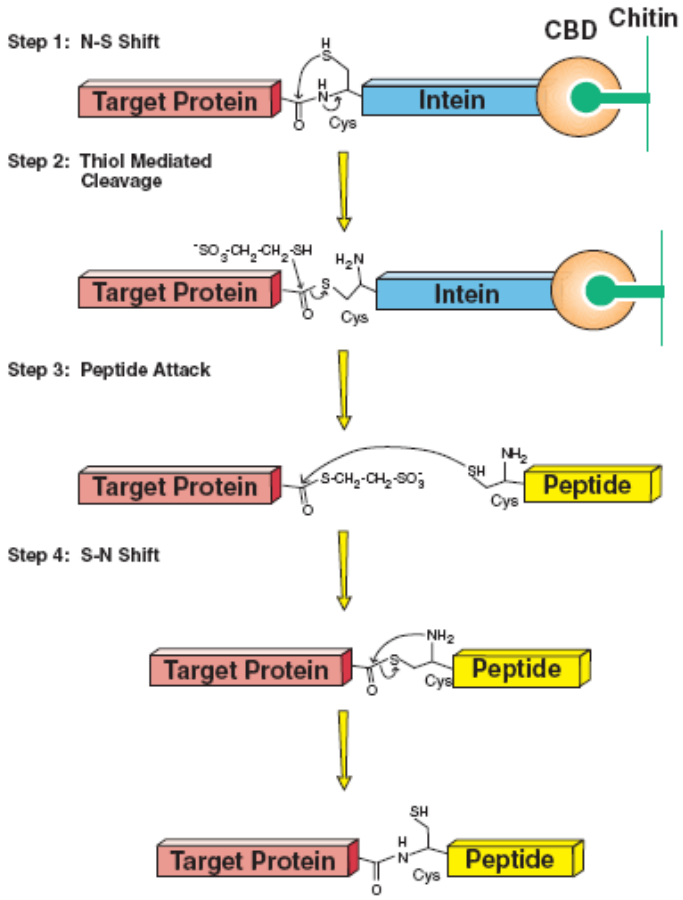

Figure 15. Intein-mediated Protein Ligation (IPL) system

ELASTIN-LIKE-POLYPETIDES AND INVERSE TRANSITION CYCLING (ITC)

A number of systems have been developed to simplify protein purification through the expression of recombinant proteins as function to carrier proteins or peptides(106,107). Examples of commercially available system include maltose binding protein(108), glutathione S-transferase (109), biotin carboxyl carrier protein(110), thioredoxin (111,112), and cellulose binding domain. Similarity, vectors for fusion to short peptide tags such as oligohistidine, S-peptide (113) , and the FLAG peptide are also available. These systems typically allow one-step purification of a recombinant protein from cell extract by affinity chromatography, using an immobilized moderate-affinity ligand specific to the carrier protein. Although it is useful for laboratory-scale purification, affinity chromatography on scale-up can represent a major cost of the protein product at the preparative scale. These limitations of current bioseparation technique, therefore, provide a compelling rationale for the development of more economical and technically simple nonchromatographic methods for the purification of soluble recombinant proteins.

Elastin-like-polypeptides (ELPs) are protein-based biopolymer analog of mammalian elastin (114). The general architecture of an ELP sequence is any number of repeats of the amino acids sequence valine-proline-glycine-X-glycine (VPGXG), where X can be any amino acid except proline (115). In elastin, this guest amino acid is typically valine. What makes this particular sequence of amino acids distinct is that it can reversibly undergo self-assembly in reaction to changes in the local environment factors such as temperature and salinity (114). The amino acid chain typically exists in a random coil conformation in solution, but upon the heating, it undergoes a conformational change, adopting a β- spiral conformation(116). This spiral then self-associate to form aggregates. Upon cooling, it is thought that ELPs prevent to a random coil conformation and regain solubility. The exact environmental condition under which ELPs change their conformation and solubility depend greatly upon the number of repeats of the VPGXG sequence and the side chain chemistry of the amino acid in the guest amino acid position (115) This effectively means that ELPs can be customized to aggregate under very specific conditions and can be employed in a variety of situations. ELPs are being used in a number of applications, including protein purification, environmental sensing, customizable vehicles, and as a method of targeting the delivery of drugs to specific areas (117–120). In addition to their flexibility, the preliminary biocompatibility of ELPs has been favorable and because they are made up of amino acid, there are few concerns about toxic degradation products (121)(Figure 16).

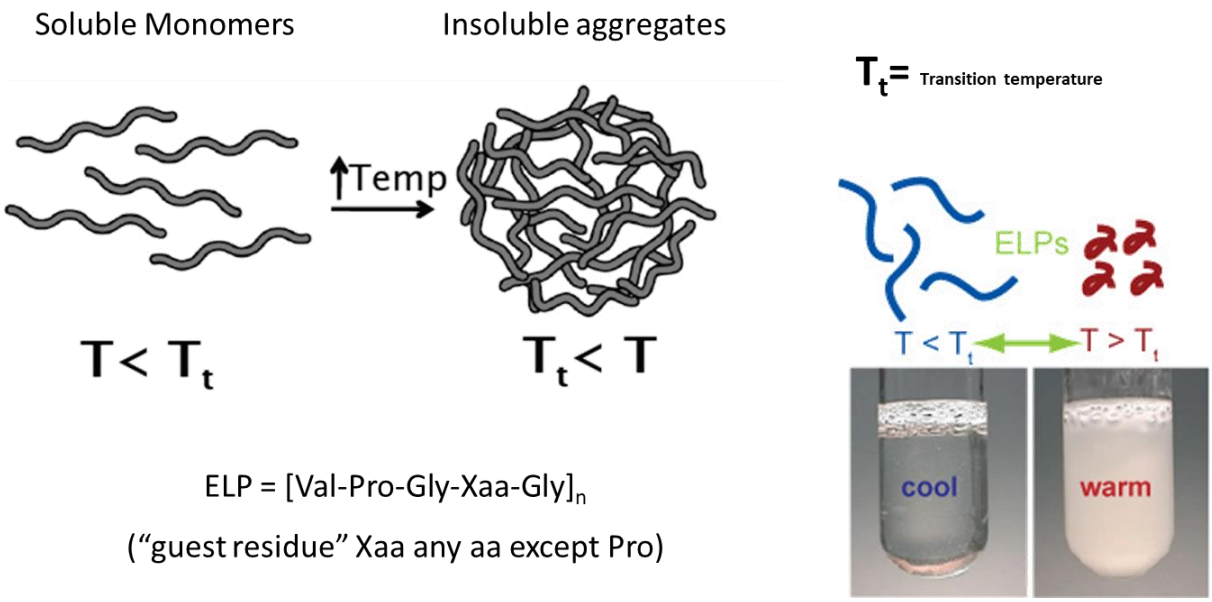

Figure 16. The behavior of Elastin like polypeptides (ELP) depends on its Transition temperature (T_t)

Another advantage of using protein-based polymers such as ELPs is that they can be produced recombinantly by inserting DNA gene encoding an ELP into *Escherichia coli*, using the bacteria as molecular factories. Making these type of molecules using recombinant methods allows for an unprecedented level of control over the final product compared with traditional polymer synthesis and can allow for the straightforward incorporation of various biofunctional moieties, including targeting, cell penetrating, and enzymatically cleavable sequences. The purification of recombinantly produced proteins is typically the largest bottleneck in their production, but with ELPs, their reversible solubility can be exploited to partially simplify purification under the correct condition. This approach is known as inverse temperature cycling (ITC) and was first demonstrated by Meyer and Chilkoti (122). They exploited the inverse phase transition of ELPs to purify the fusion proteins from other soluble *E.coli* soluble proteins using a nonchromatographic separation method for recombinant proteins, which they termed "inverse transition cycling" (ITC). The fundamental principle of ITC is remarkably simple, and shown schematically in the figure 17.

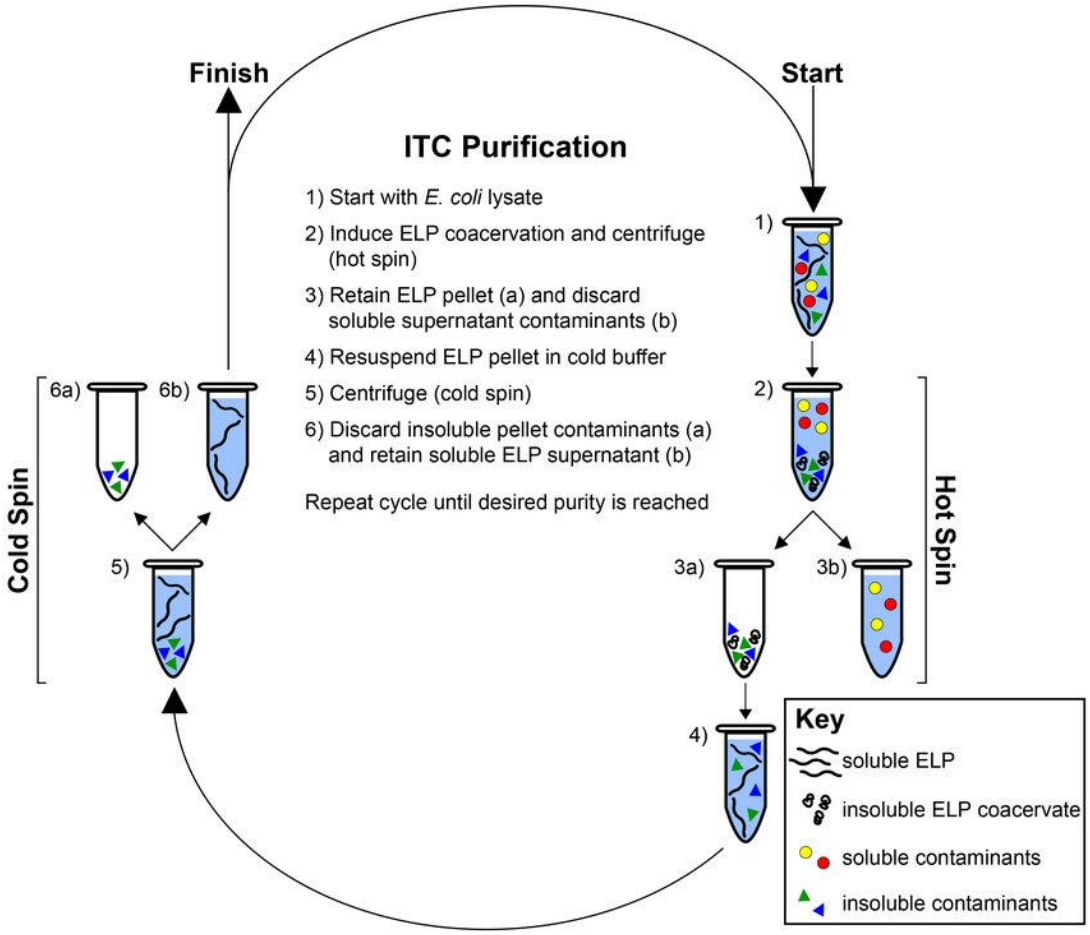

Figure 17. Inverse transition cycling. ELP is purified by means of its lower critical solution temperature (LCST) behavior from both soluble and insoluble contaminants. Starting with the ELP-rich lysate (1) the ELP transition is induced with the addition of heat and/or salt and the ELP is separated by centrifugation (hot spin) (2). The ELP pellet is retained (3a) while the supernatant containing soluble contaminants is discarded (3b). The ELP is resuspended in cold buffer (4) and centrifuged again at 4 °C (cold spin) (5). The pellet containing insoluble contaminants is discarded (6a) while the supernatant containing soluble ELP is retained (6b). Cycles of alternating hot and cold spins are repeated until the desired purity is reached, as determined with SDS-PAGE (123).

The operating principles of ITC involves rendering the ELP fusion protein insoluble in aqueous solution by triggering its inverse transition. This can be accomplished by increasing the solution temperature above the transition temperature (T_t) or alternatively by depressing the T_t below the solution temperature by the addiction of NaCl to the solution. This results in aggregation of the ELP fusion protein, allowing it to be collected by centrifugation. The aggregated fusion protein is then solubilized in buffer at a temperature below the T_t to yield soluble, functionally active, and purified fusion protein. Free target protein can be obtained by site-specific proteolysis at an engineered recognition site, located between the target protein and the ELP tag, followed by another round of ITC to remove cleaved ELP tag.

Inverse transition cycling offers several advantages for purification of recombinant fusion proteins. First, the expense association with chromatographic resins and equipment is eliminated. The potentially low cost and ease of scale-up of this method are likely to prove attractive for large scale purification of proteins (in the grams to kilograms range). Second, the separation and recovery condition are mild, requiring only a modest change in temperature or ionic strength. Third, the method is fast and straightforward, with only a few short centrifugation or filtration steps followed by resolubilization of the purified protein in a buffer of low ionic strength. Fourth, inverse transition cycling can be easily multiplex to purify proteins simultaneously from different cell cultures. Because protein purification is frequently the limiting step in structure/function studies and in screening of proteins in pharmaceutical development, Meyer and Chilkoti (124) believed that the ability to purify simultaneously a large number of proteins by inverse transition purification likely to be extremely useful for laboratory-scale up purification (in micrograms to milligram range) of proteins. Finally, inverse transition purification is independent of a specific expression vector or host and is likely to be extremely useful for eukaryotic expression system because of their ability to overexpress heterologous proteins in a soluble state (125).

In addition to protein purification, a number of different applications for protein-ELP conjugates can be envisioned. Enzyme-ELP fusions could be useful substitutes for immobilized enzymes in industrial biocatalysis, by allowing easy separation of enzyme from product and recycling of the enzyme for the subsequent rounds of biocatalysis. Similarly, fusion of ELPs with engineered antibodies could allow the capture of analyte from biological fluids for immunoassay (126). The use of ELPs conjugated to radionuclides or protein therapeutics for precise targeting for imaging and therapy by targeted hyperthermia is also possible.

Unfortunately, the ITC purification is not applicable to all ELPs. Successfully employing an ITC only purification procedure means the ELP construct and its expression have to meet certain criteria: The ELP must not end up in the insoluble fraction of the cell lysate during the lysis procedure; the ELP must be in its soluble monomer form in the cell lysate; the

phase transition needs to be triggered in the cell lysate under reasonable temperature and salinity conditions; and the protein must be expressed at a concentration high enough for a phase transition to be possible under reasonable conditions but must also be low enough to avoid significant depression of the transition temperature as well as the formation of inclusion bodies. Not all the ELP purification meet these criteria. If ELP is poorly expressed, or if it contains guest amino acid that are significantly more hydrophilic or hydrophobic than those commonly employed in the literature, or shorter than is commonly used, the transition temperature of the ELP construct may be too high or too low for ITC-only approach (127).

ELP-INTEIN SYSTEM

Recently, the study of inteins and in particular the investigation of the site-specific cleavage process of these particular enzymes has made it possible to exploit this system to separate the target proteins from related tags during the purification process (N-terminus cleavage), and therefore to replace the use of proteases overcoming the numerous drawbacks associated with their use

Also in the case of ELP-fusion construct, the insertion of an intein at the right position gives the opportunity to isolate the target protein from the ELP tag avoiding the use of proteases. The combination of these two technological tools, the intein auto-cleavage activity (biochemical tool) and ELP aggregation ad solvation properties (physico-chemical tool), has enabled the development of a highly innovative and efficient purification method. Figure 18 schematically illustrates an example of purification process based on the use of the ELP-intein system. Starting from a construct characterized by the fusion to the C-terminus of the target protein with an intein-ELP tag, where the intein is a C-terminal mutated version (e.g. *Mxe*GrA N198A), a ITC process is carried out as first step to purify the ELP-fusion protein of interest from the other contaminating proteins present in the sample. At the end of the ITC process, the addition of a thiol reagent, such as dithiothreitol (DTT) or MESNA (Sodium 2-mercaptoethanesulfonate), permits the induction of N-terminal intein self-cleavage activity and the consequent release of target protein from the intein-ELP tag.
This new non-chromatographic method, based on the combination of ITC purification process (ELPs tag) with self-cleaving properties of inteins, results in the use of a self–cleavable temperature responsive tag and offers a viable option for protein purification.

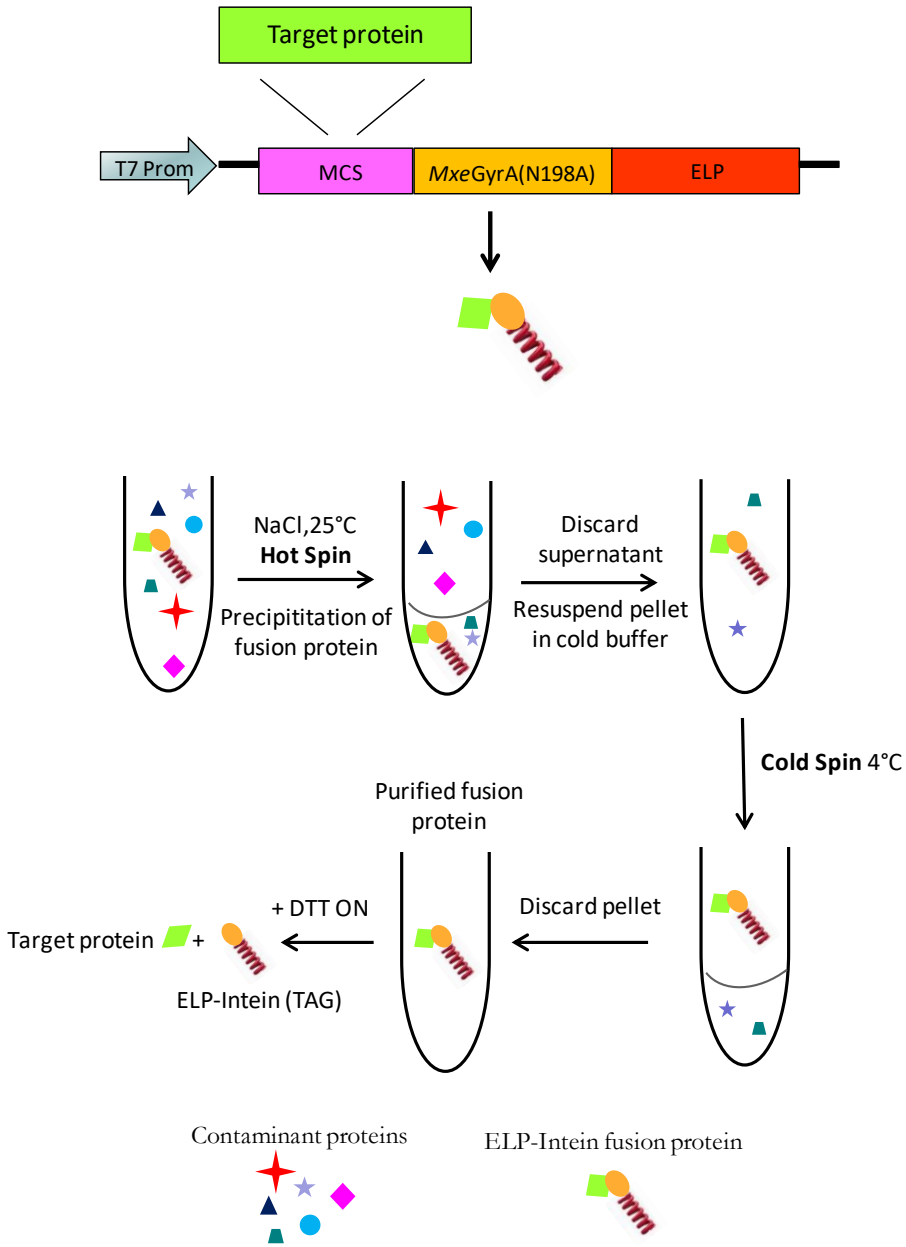

Figure 18 . Schematic representation of protein purification by ELP-Intein system.

SPLIT INTEINS

Split inteins: Main features and advantages

Protein splicing is an intriguing autocatalytic process in which an intervening sequence (intein) excises itself from a precursor protein with concomitant ligation of the flanking protein sequences (extein) (128,129)Inteins can be classified into two types: those with continuous sequences that mediate cis-splicing and the others with split sequences capable of mediating trans-splicing. Both types of inteins have been widely used as tools in protein chemistry and molecular biology. Among the various applications, the trans-splicing inteins appear to be very useful to study protein interactions, as the two protein domains can be expressed separately (130–140).

The inteins are split into separately inactive, short halves. The N-intein (98-123 amino acids) and C-intein (30-36 amino acids) parts have a high affinity for each other and can rapidly self-associate into a compact intein fold (141,142). The split-intein complex has a protein-splicing activity in trans, autocatalytically ligating its flanks into a functional protein (Figure 19).

The principle advantages to the use of split inteins are the following:(1) the intracellular self-cleavage from the tag/fusion protein is very unlikely (2) a good yield of the protein trans-splicing reaction, (3) constant reaction rate, (3) the solubility of the intein fragments, and (4) their tolerance towards different fused ‘‘substrate” exteins (143).

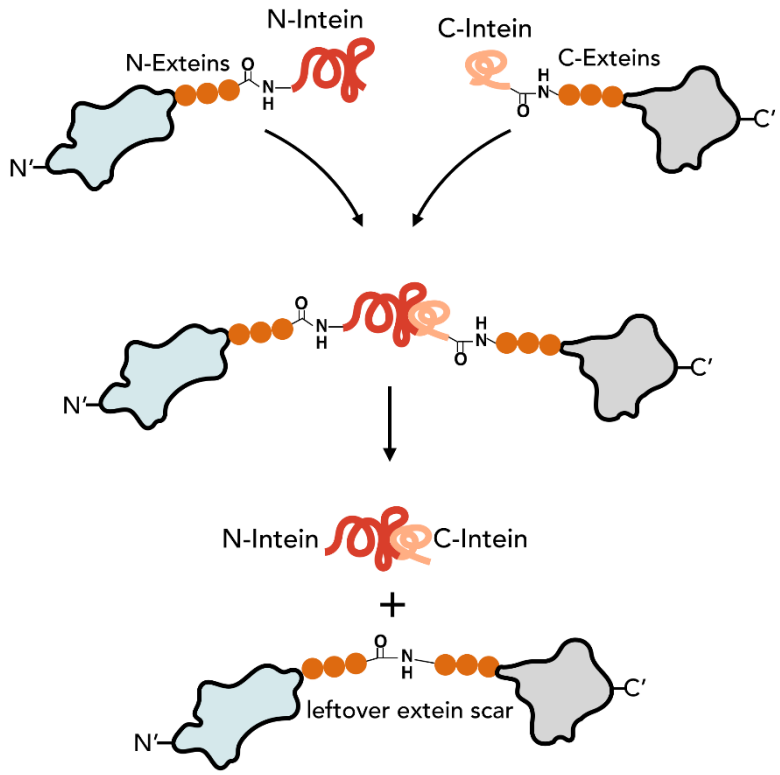

Figure 19 Trans-splicing mechanism reaction by split inteins

Split Inteins contain four blocks of conserved sequences, and several highly conserved residues from these blocks form a catalytic core in the intein structure (Figure 20) (144) These residues are conserved in all inteins and are essential in protein splicing (145,146). A systematic investigation of split inteins showed that residues distant from the catalytic core modulate splicing efficacy (147). These residues, including NGlu89 and CGly19 (where N and C that precede the residue designation refer to the splicing domain concerned), are conserved in the split inteins with high activity, but less so in the low activity inteins (Figure20) (147)

Although conserved residues in the catalytic core are required for protein splicing, residues in the non-catalytic core can modulate intein activity (147)

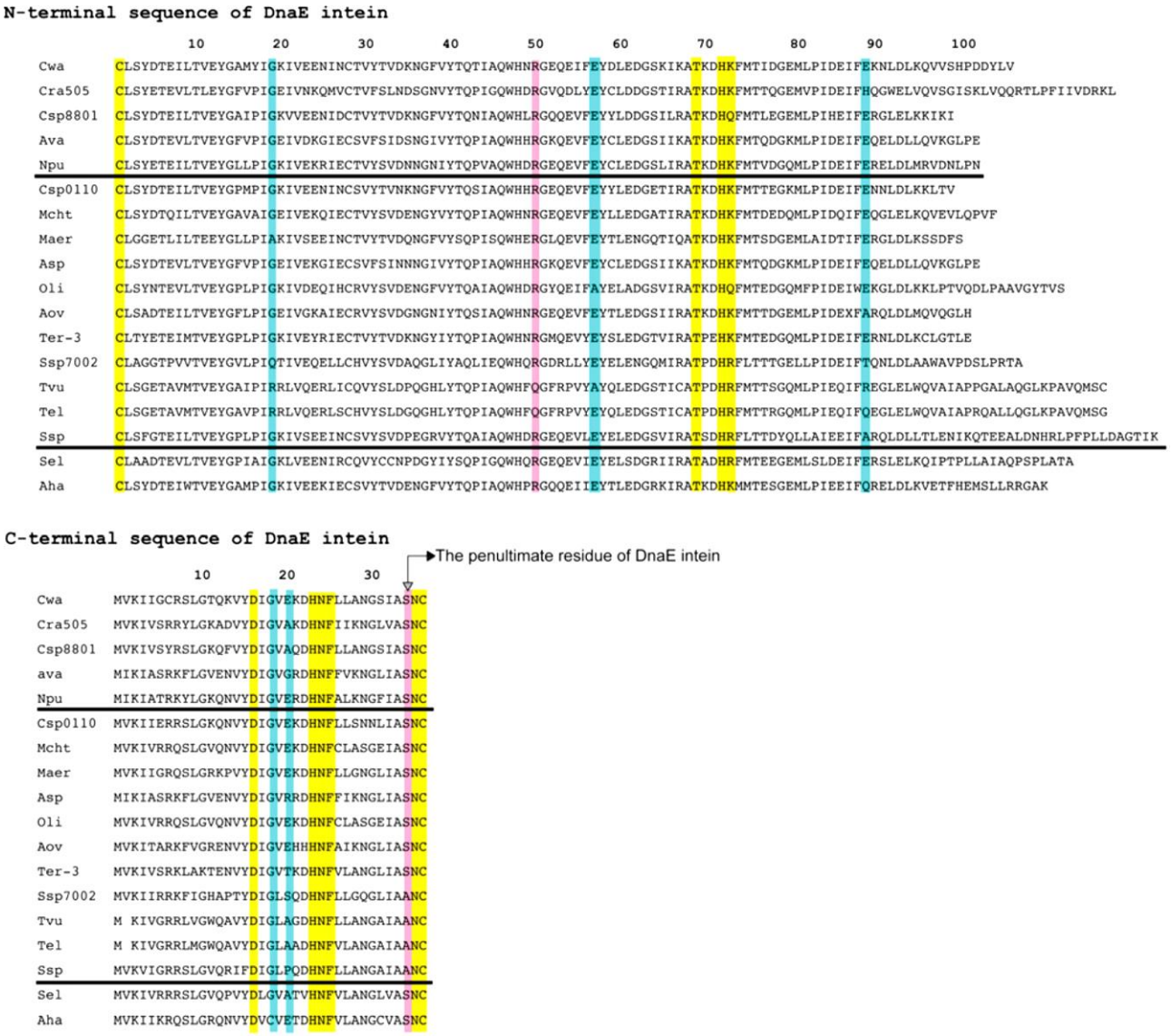

Figure20. Sequence alignment of 18 DnaE split inteins in descending order of in vivo trans-splicing efficiency

The Npu DnaE intein and Ssp DnaE intein compared in the present study are underlined. The residues in the two splicing domains are numbered separately. The highly conserved residues shown in Figure 20 are colored in yellow. The two residues, NArg50 and CSer35, fundamental to modulate the trans splicing reaction, are colored in pink. Residues in cyan are key non-catalytic residues studied in the literature (147) which also modulate the trans-splicing efficiency. The penultimate residue, which is corresponding to a histidine residue in canonical inteins, is indicated by an arrow.

Coulombic forces play an important role in facilitating protein–protein interactions. It has been demonstrated that a strong electrostatic potential between two interacting proteins correlates with a fast rate of association and a strong binding affinity (148)Indeed, this principle has been exploited to enhance the binding properties of engineered protein interfaces (149)Nonetheless, little research has focused on utilizing intermolecular ion pairs to modulate specificity in protein–protein interactions (150–152). Naturally split inteins are a potentially interesting system for engineering electrostatically driven specificity, as the formation of a catalytically competent structure requires the association of two oppositely charged protomers.

Kinetic studies of self-association and splicing rates of split inteins suggest that trans protein splicing is rapid [(6.6 (1.3) × 10^{-5} s^{-1}] and occurs at a low nanomolar affinity. Split inteins were found to interact with a very fast association rate (2.8 × 107 M^{-1} s^{-1}) and a slow dissociation rate (1.2 s^{-1}) (153)

Sequence alignments of naturally split inteins show highly conserved charge segregation, with acidic residues concentrated at specific positions on the N-intein and basic residues conserved on the C-intein (N- and C-terminal protomers) (154) Furthermore, a bioinformatic sequence analysis of the intein family indicates that this charge segregation is significantly more prevalent in naturally split inteins than intact ones. Interestingly, when the conserved charged residues are mapped onto the structure determined by NMR spectrocopy of the wild-type DnaE intein from *Nostoc punctiforme* (NpuWT), many are found to be participating in intermolecular ion pairs and ion triads (155)

Neel H. Shah et (156), proved the role of intermolecular ion clusters for fragment assembly and splicing in the NpuWT split intein both in vivo and in vitro and that electrostatic interactions can engender kinetic control in a complex enzymatic system. Furthermore, these results provide insight into the molecular requirements for efficient and specific protein trans-splicing.

Split intein reaction mechanism

In contrast to the mini and large inteins that mediate cis-splicing reactions, split inteins are responsible for trans-splicing and fusion of protein parts. The trans-splicing reaction can be divided into the following steps (figure 21):

1. N-precursor protein (comprising N-extein and N-intein) and C-precursor protein (containing C-intein and C-extein) first assemble together to form a dimer like structure with a newly formed catalytic core next to the exteins.

2. The tertiary structure of the intein, once correctly formed, facilitates an *N→O/S* acyl rearrangement at its N-terminal serine or cysteine residue. The result is an ester or thioester bond, respectively between the side-chain and the peptide backbone of the N-extein.

3. The two exteins are then linked by trans(thio)esterification involving the N-terminal serine or cysteine residue of the C-extein. The C-terminus of the N-extein is now covalently bound to the N-terminal side-chain of the C-extein, while its backbone still retains its normal peptide bond to the intein.

4. The C-terminal asparagine of the intein undergoes self-cyclisation to form a succinimidyl moiety. The peptide bond between the intein and the extein is thereby broken, resolving the branched intermediate.

5. In a final reaction, an *O/S→N* acyl shift results in the two exteins now being linked by an amide bond, indistinguishable from a ribosome-assembled fusion protein.

   Although the reactions shown in this scheme involve Cys residues at position 1 of both N-intein and C-extein , other residues (Ser and Thr) at these positions are possible (157).

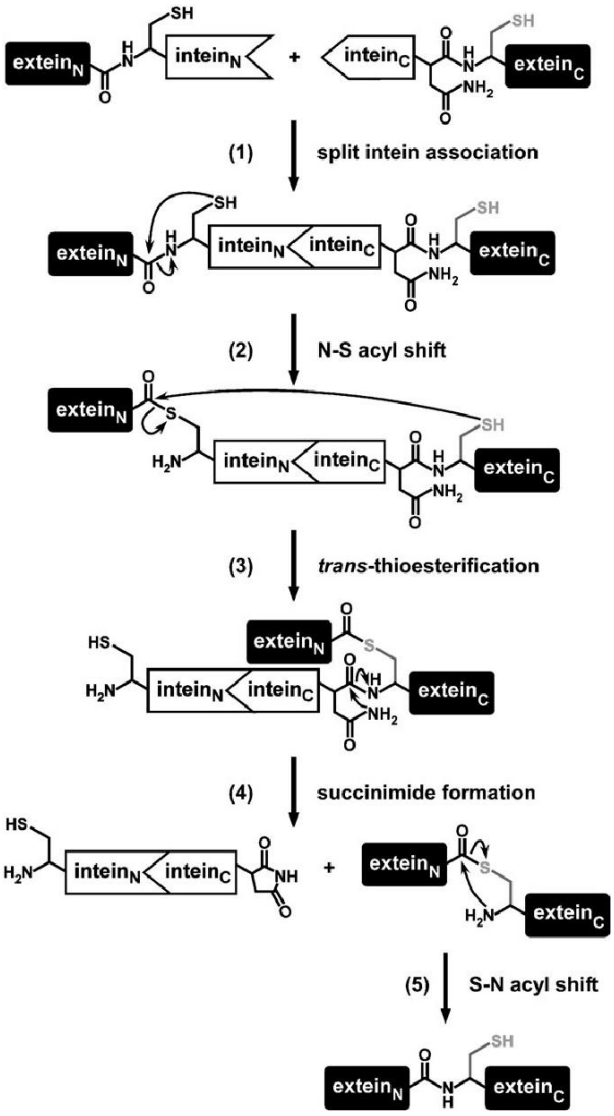

Figure 21. Canonical protein splicing mechanism utilized by split intein

Applications of split inteins

Split inteins have become powerful tools in protein engineering areas. Due to the general promiscuity of split inteins towards extein sequences, one can perform a multitude of protein ligations depending on the purpose of the investigation. (1) Modular proteins can be assembled from precursor fragments if production of the full-length protein is problematic. This has for example been applied to generate full-length phosphoinositide-dependent kinase (PDK) 1 from precursors containing the N-terminal catalytic kinase domain and the C-terminal pleckstrin homology (PH)-domain (158), as well as the signal adaptor protein c-CrkII (159). (2) Single domain globular proteins can be reconstituted from two fragments into a biologically active full-length protein. This reconstitution approach has been the basis for cell-based assays to monitor protein–protein interactions (160) and the spatio-temporal expression of proteins using split reporter proteins, like enhanced green fluorescent protein (161) and luciferase, (162) for the production of environmentally safe transgenic plants by reconstitution of herbicide-resistance proteins from inactive precursor fragments (162,163), for gene therapy, (164) and recently for reconstitution of a β-barrel membrane protein (165). (3) Linear polypeptide chains can be cyclized by inserting the desired protein sequence between a circularly permuted split intein, so that as a result of protein trans splicing, the N- and C-termini of the target protein are joined by a peptide bond (166).

Another interesting application was described in a recent work (167) in which the authors develop a simple, efficient, and potentially low-cost approach called split intein mediated ultrarapid purification (SIRP) for both the purification of the desired tagged protein from *Escherichia coli* lysate and removal of the tag in less than 1 h. The N- and C-fragment of a self-cleaving variant of a naturally split DnaE intein from *Nostoc punctiforme* are genetically fused to the N-terminus of an affinity tag and a protein of interest (POI), respectively. The N-intein/affinity tag is used to functionalize an affinity resin. The high affinity between the N- and C-fragment of DnaE intein enables the POI purified from the lysate via affinity to the resin, and the intein-mediated C-terminal cleavage reaction causes tagless POI to be released into the flow-through (167)

Another paper of Merideth A. Cooper et al., talks about a novel self-cleaving tag technology based on a highly modified split-intein cleaving element. In this system, the N-terminal segment of an engineered split intein is expressed in E. coli and covalently immobilized onto a capture resin, while the smaller C-terminal intein segment is fused to the N-terminus of the desired target protein. During the purification, strong association between the intein segments effectively captures the tagged target onto the capture resin while simultaneously generating a cleaving-competent intein complex. Once the complex is purified by washing the column, intein-mediated cleavage and release of the tagless target is induced with a simple shift in buffer pH from 8.5 to 6.2 (168)

Furthermore, it is possible to combine the two technology of split intein and that of elastin-like -polipetides (ELP) to obtain a purified POI without chromatographic steps (169). Other applications of protein trans splicing include segmental isotopic labeling of proteins for NMR spectroscopy, protein immobilization, and control protein functio (170).

Finally, is important to underline that the split intein technology can be used for the site-specific conjugation of proteins and antibodies (171) and nowadays to realize bispecific IgG antibodies (172)

Of all of the split inteins, two have been studied most extensively: the DnaE intein from Cyanobacterium synechocystis sp. strain PCC6803 (Ssp DnaE intein) and the DnaE intein from Nostoc punctiforme PCC73102 (Npu DnaE intein) (173–175).

DnaE is the catalytic subunit of bacterial DNA polymerase III. In E. coli, DNA polymerase III holoenzyme is the replicative polymerase responsible for the synthesis of the majority of the genome. DnaE (also known as α), in addition to its catalytic role, also serves as an organization protein to hold the 18-protein holoenzyme complex together. Its C-terminal half interacts directly with the τ subunit to form a dimeric polymerase and with the β subunit that forms a sliding clamp on the DNA template, whereas its N-terminal half contains the polymerase active site (176).

The ligation efficiency with Npu DnaE was estimated to be >98% and with a half-time ($t_{1/2}$) of 60 seconds, removing almost all the precursor proteins. This demonstrates the robustness of the trans-splicing by Npu DnaE intein.

The Npu DnaE intein fusion constructs were converted to the splice products in excellent yields from about 55% to 90% depending on the extein sequence and with only minor formation of cleavage side-products (177)

Furthermore, while many split inteins including the Ssp DnaE intein exhibit reduced yields and increased formation of hydrolysis side products at +37 °C compared to temperatures below +30°C (178–180), the splice product yields obtained with the Npu intein were nearly unaffected in the temperature range between +6°C and +37°C with the highest rate observed at +37°C. Sequence comparisons confirm that the conserved non-catalytic residues in the high activity intein are in fact present in the Npu DnaE intein, but are absent from the Ssp DnaE intein (Figure 20)(177).

Qin WU et. al. (181)solved the crystal structure of Npu DnaE intein in the split form. This is the first trans-structure of split inteins. Guided by this structure, they identified two residues, NArg50 and CSer35, which play a significant role in modulating the protein splicing reaction. Sequence comparisons show these residues to be conserved in the DnaE split inteins. The absence of CSer35 in the Ssp DnaE intein might explain its low activity.

Both the Npu DnaE and Ssp DnaE inteins belong to a subfamily of non-canonical inteins characterized by the lack of the highly conserved penultimate histidine (Figure 20). In most inteins, this histidine facilitates cyclization of asparagine in preparation for C-terminal cleavage in the third step of the splicing reaction (182)

The N-terminal part, i.e., DnaEN, seems to determine the trans-splicing efficiency of the split DnaE inteins dominantly, since the replacement of DnaEN but not DnaEC significantly influenced the yield of the reaction. However, Npu DnaE and Ssp DnaE have cross-splicing activity, meaning that one of the N- or C-terminal fragments of both Npu DnaE and Ssp DnaE can be substituted with each other without loss of their protein splicing activity. This indicates that the interaction between DnaEN and DnaEC is not highly specific although Npu DnaEN lacks 21 amino acids at the C-terminus compared with Ssp DnaEN. In contrast to Ssp DnaEN, the trans-splicing with Npu DnaEN can accommodate many amino acid types at the second residue of the C-terminal extein (Phe+2) with no or modest reduction of trans-splicing activity (183)

This tolerance of Npu DnaEN for the substitutions of Phe+2 can widen the application of trans-splicing, because it has often been limited by the inevitable insertion of the native extein sequence at the ligation junction. The mutations of the residue Phe+2 in the C-terminal extein have revealed that aromatic residues and hydrophobic residues seems to be relatively more preferred for protein splicing activity and that hydrophilic side-chains tend to lower the splicing activity significantly (183)

However, all cyanobacterial split inteins are closely inter-related, relative to other inteins, and the residues necessary for the successful interaction between the intein parts are likely to be conserved because of (i) the requirement for compensatory mutations in the two independent loci coding for the intein parts and (ii) the absolute necessity for the replicative DNA polymerase splicing product of the split inteins at every cell generation (184).

Cfa intein

As mentioned before, the high level of conservation within the active sites of Npu and Ssp suggests that differences in distal amino acids account for the disparity in splicing rate between the two. Thus, Adam J. Stevens et al.,(185) focused our attention on “second shell” residues, those directly adjacent to the active site.

The known cross-reactivity of Npu and Ssp intein fragments served as a convenient platform to assess which half of the split intein contributes most significantly to the difference in activity (186) .Both the SspN-NpuC (chimera 1) and NpuN-SspC (chimera 2) chimeras show a decrease in the rates of branch formation and resolution compared to that of native Npu. This indicates that residues on both the N and C-intein fragments of

Npu and Ssp contribute to the difference in their splicing rate. Next, four groups of second shell positions on each of these chimeras were chosen based on their proximity to key catalytic residues, and the corresponding Ssp residues were mutated to those in Npu.

Taken together, the mutagenesis data point highlight the key role that second shell "accelerator" residues play in tuning the activity of split inteins.

The "accelerator" residues found to affect the splicing rate allowed for an activity-guided approach to engineer a consensus DnaE intein. Consensus protein engineering is a tool applied to a homologous set of proteins in order to create a thermostable variant derived from the parent family (187,188). A multiple sequence alignment (MSA) is first generated from homologues of a particular protein, from which the most frequent residue at each position is chosen as the representative in the consensus sequence.

The 73 theoretically fast inteins left in the MSA were then used to generate a consensus fast DnaE intein sequence (Cfa) (Figure 22). The Cfa intein has high sequence similarity to Npu (82%), and the nonidentical residues are spread throughout the 3D structure of the protein.

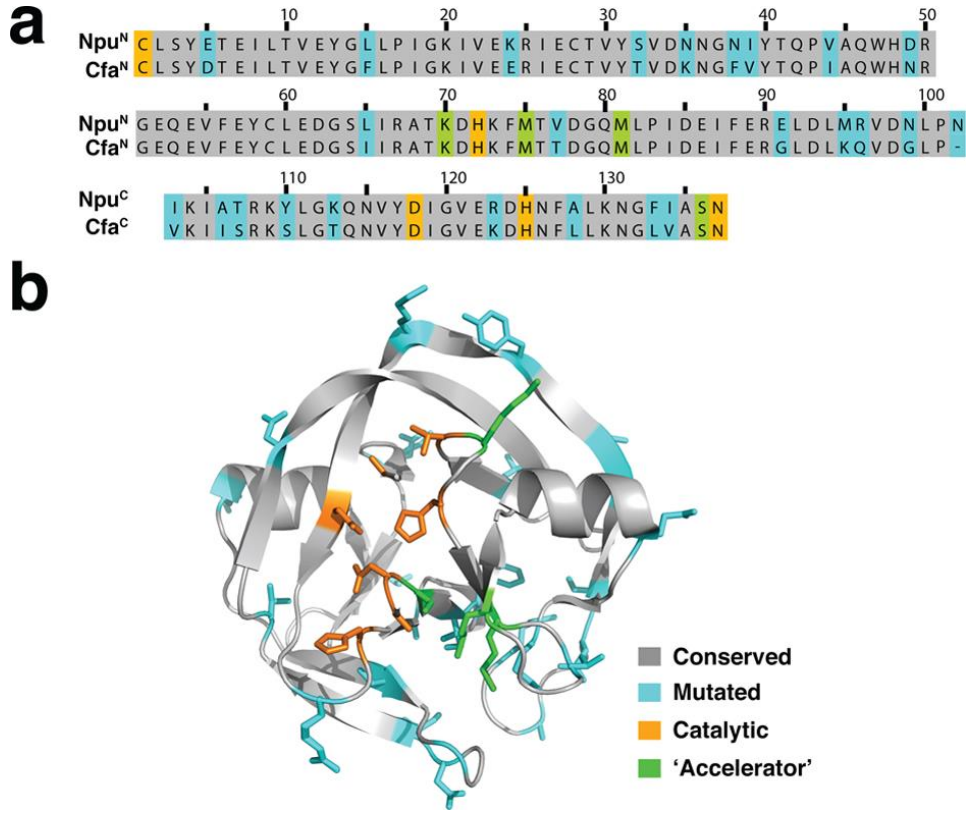

Figure 22. Design of the Cfa split intein.

The Cfa intein splices 2.5 fold faster at +30°C than the Npu ($t_{1/2}$of 20s versus 60 s); it even maintains activity at high temperature (+80°C), albeit with reduced yield of splice product, while Npu is inactive at this temperature. Moreover, the Cfa maintains the splicing activity in presence of high concentration of chaotropic agents, like UREA 8 M and guanidine Hydrochloride (GuHCl) 3 M. This last characteristic is important because applications of protein trans splicing (PTS) typically require fission of a target protein and fusion of the resulting fragments to the appropriate split intein segments (189) and the solubility of these fusion proteins can sometimes be poor.

Fusing a protein of interest to a split intein can result in a marked reduction in cellular expression levels compared to the protein alone (190).This situation is more frequently encountered for fusions to N-inteins than to C-inteins, which is likely due to the larger size of the former and their partially folded state (191). However, model studies in *E.coli* and in mammalian cells revealed a significant increase in soluble protein expression for a Cfa N fusion probably due to improved thermal and chaotropic stability of this intein.

For all these extraordinary features, the Cfa intein could be used for many biotechnological applications.

The first important application of the Cfa intein has been described by Adam J. Stevens et al., in which after the obtainment of the Cfa split intein sequence, they exploited its amazing trans splicing activity to realize an *in vivo* site-specific conjugation at the heavy chains of an anti-Mouse IgG mAb (αDec205).

In particular, they expressed in HEK293 cells a fusion protein between the heavy chains of an anti-mouse IgG antibody and the-N-terminal fragment of Cfa (HC-Cfa^N) and they noted that: the expression levels were comparable with the bacterial expression results relative to other target Cfa^N constructs; the production of HC-Cfa^N fusion was significantly higher than that for the other inteins examined; the secreted levels of mAb-Cfa construct were ~10-fold higher than those for the corresponding Npu-fusion. After these results, starting from the idea that mAb-Cfa retained PTS activity, they thought to perform a site-specific modification on mAb-Cfa with a synthetic peptide by splicing directly in the growth medium following the four-day expression at 37°C with good results.

Finally, to further explore the utility of the Cfa intein in the context of antibody conjugation, they asked whether the PTS system could be used to attach multiple copies of a synthetic cargo to the heavy chain of the mAb. Accordingly, they used semisynthesis to prepare a construct in which the C-terminal half of Cfa (CfaC) was fused to a C-extein containing a dendrimeric scaffold allowing multimeric attachment of cargo, in that case fluorescein. This dendritic cargo was successfully linked to the αDec205 antibody via Cfa-mediated PTS, again performed directly in situ within the cellular growth medium.

These results inspired us to exploit the Cfa intein to produce a recombinant monoclonal IgG antibody anti-interferon gamma (IFNγ) with a site specific biotinylation on its heavy chain. This reagent has been used in a LIAISON immunoassay prototype for the quantification of the IFNγ concentration, replacing the same recombinant monoclonal IgG antibody but randomly biotinylated on lysine residues.

Antibodies have been proved to be useful reagents for the detection and quantification of many types of analytes both *in vitro* and *in vivo* and have, therefore, found wide application in research laboratories and in the diagnostic or pharmaceutical industry. In particular, monoclonal antibodies (mAbs) have long been a potent tool due to their high specificity and affinity for target antigens and have been extensively used as carriers of fluorophores, radioisotopes, cytotoxic agents, and enzymes, yielding conjugates that find utility in therapeutic and diagnostic fields, and in basic research, as well.

In diagnostic field, immunoassays are carried out to detect the presence of a particular antigen or antibody in human body fluids (e.g. blood, urine, saliva); the use of mAbs allows a potentially unlimited supply of identical reagent which can be selected from a number of different clones to have the optimal characteristics for the intended assay. Several approaches have been investigated to improve the sensitivity of immunoassays by manipulation of the detection system. One of the key aspects to improve the sensitivity of an immunodiagnostic assay is the optimization of bioconjugation reactions necessary to label antibodies with a specific probe. The methods employed for making mAb-based conjugates can be classified in two general categories: those that involve the random modification of mAb amino acid residues, and those that are highly regioselective.

Traditionally, conjugation of labeling molecules to an antibody takes place at lysines solvent accessible reactive amino acids. Lysine conjugation results in 0–8 conjugated molecules per antibody, and peptide mapping has determined that conjugation occurs on both the heavy and light chain at ~20 different lysine residues (40 lysines per mAb). The biological and functional properties of these conjugates are often acceptable; however, random modification of mAbs may impair antigen binding and thus the immunoreactivity of antibody (in fact random labeling can take place at the level of the antigen binding site thus affecting the reaction of recognition between antibody and antigen) and leads to conjugate heterogeneity. In the last years, a number of site-specific and selective methods have been described to introduce molecules of interest onto mAbs. The ability to control the location and stoichiometry of conjugation can significantly improve the performance of mAb conjugates in applications such as the immunodiagnostic assays.

In summary, the main advantages to have a site specific labeling, like biotinylation, of antibodies are, (1)to avoid the labeling on the variable regions of the antibodies involve in the binding with the antigen epitopes , (2) to improve the orientation of the antibodies on

the paramagnetic beads used in the immunoassay (3) the high reproducibility of conjugation than the random-methods

The greatest selectivity is obtained using recombinant technologies (192,193). Recently, innovative techniques provide the site-specific conjugation of antibodies through engineered cysteine residues (194), through the incorporation of unnatural amino acids (195). However, selective modification has also been reported for chemically based methods as reductive amination of oxidized mAb carbohydrates (196), photoaffinity labeling of unconventional mAb binding sites (197), and reduction-alkylation of antibody interchain disulfides (198,199). Nowadays, other methods widely exploited to generate site-specific labeling of proteins and antibodies are based on the use of the Sortase A enzyme (200) or the site-specific biotinylation operated by the BirA enzyme (201).

As extensively described in the previous paragraphs, one of the most recent and innovative method, which permits to obtain a site-specific conjugation of antibodies, is through the protein trans splicing. This technology allows to control the PTS reaction conditions (molar excess of reductant, species concentration, temperature, pH, time of reaction, etc.) in order to maximize the reaction yield, and to decide the portion (N- or C-terminus) of the antibody in which we want to introduce the conjugating element.

As model system to explore the PTS as site-specific conjugation method, we selected the monoclonal antibody belonging to the solid phase of a LIAISON® prototype immunoassay for the detection of Interferon gamma (IFNγ).

In particular, we realized a recombinant fusion protein in which the N-terminus of the Cfa split intein was fused at the C-terminus of the heavy chain of the anti-IFNγ IgG antibody previously mentioned. After that, we performed a co-transfection Chinese hamster ovary (CHO) cells using two mammalian plasmids : the first one containing the sequences for the heavy chains of the recombinant anti-IFNγ IgG antibody (included our fusion protein) and the second one having the sequences for the light chains of the same antibody. In this way, we obtained a recombinant anti-IFNγ IgG antibody with the N-terminus-Cfa fragment fused at the C-terminus of its heavy chains in order to use it in the protein trans splicing reaction by Cfa split-intein.

As second reagent involved in PTS reaction, we used a biotinylated synthetic version of the C-terminal portion of the Cfa split intein.

At this point, we mixed these two reagents, to make happen the trans-splicing reaction in a reducing environment and so to achieve our recombinant antibody anti-IFNγ with a site-specific biotinylation at the C-terminal of its heavy chains.

The biotinylated recombinant anti-IFNγ antibody thus obtained was replaced with the current monoclonal antibody used as solid phase for the detection of gamma interferon in the immunoassay prototype.

INFγ: MAIN FEATURES AND ROLES IN IMMUNE SYSTEM

Interferon gamma (IFNγ) is a dimerized soluble cytokine that is the only member of the type II class of interferons (202).The existence of this interferon, which early in its history was known as immune interferon, was described by E. F. Wheelock as a product of human leukocytes stimulated with phytohemagglutinin, and by others as a product of antigen-stimulated lymphocytes (203).It was also shown to be produced in human lymphocytes (204) or tuberculin-sensitized mouse peritoneal lymphocytes using Purified Protein Derivative (PPD) test, developed for tuberculosis (TB) diagnosis; the resulting supernatants were shown to inhibit the growth of vesicular stomatitis virus. Those reports also contained the basic observation underlying the now widely employed interferon gamma release assay used to test for tuberculosis.

The IFNγ, is critical for innate and adaptive immunity against viral, protozoal and some bacterial infections. IFNγ is an important activator of macrophages and inducer of class II major histocompatibility complex (MHC) molecule expression. Aberrant IFNγ expression is associated with a number of autoinflammatory and autoimmune diseases. The importance of IFNγ in the immune system stems in part from its ability to inhibit viral replication directly, and most importantly from its immunostimulatory and immunomodulatory effects. IFNγ is produced predominantly by natural killer (NK) and natural killer T (NKT) cells as part of the innate immune response, and by CD4 Th1 and CD8 cytotoxic T lymphocyte (CTL) effector T cells once antigen-specific immunity develops (205) as part of the adaptive immune response. IFNγ is also produced by non-cytotoxic innate lymphoid cells (ILC), a family of immune cells first discovered in the early 2010s (206)

IFNγ IMMUNOASSAY PROTOTYPE

Our prototype of the IFNγ immunoassay used to determine IFNγ is a direct, sandwich chemiluminescence immunoassay (CLIA). The recombinant and biotinylated IgG anti- IFNγ antibodies coated at the paramagnetic beads (solid phase) functionalized with streptavidin link the IFNγ that later is recognized by monoclonal antibodies to IFNγ (mouse monoclonal) conjugated with a fluorescent dyes called Alexa fluor. Finally, the complex is detected through a mouse monoclonal antibody to Alex fluor (mouse monoclonal) conjugated with the isoluminol derivate molecule ABEI (figure 23). The two mouse monoclonal antibodies (Alexa fluor conjugated anti- IFNγ and the ABEI conjugated anti-Alexa flour) are mixed to constitute the conjugate complex.

During the first incubation, IFNγ present in calibrators, samples or controls will bind to the solid phase and conjugate complex and form a sandwich. During the second incubation, an Assay Buffer is added. It reduces non-specific, sample-related bindings. After each incubation, the unbound material is removed with a wash cycle.

Subsequently, the starter reagents are added and a flash chemiluminescence reaction is thus induced. The light signal, and hence the amount of isoluminol-antibody conjugate, is measured by a photomultiplier as relative light units (RLU) and is indicative of IFNγ concentration present in calibrators, samples or controls.

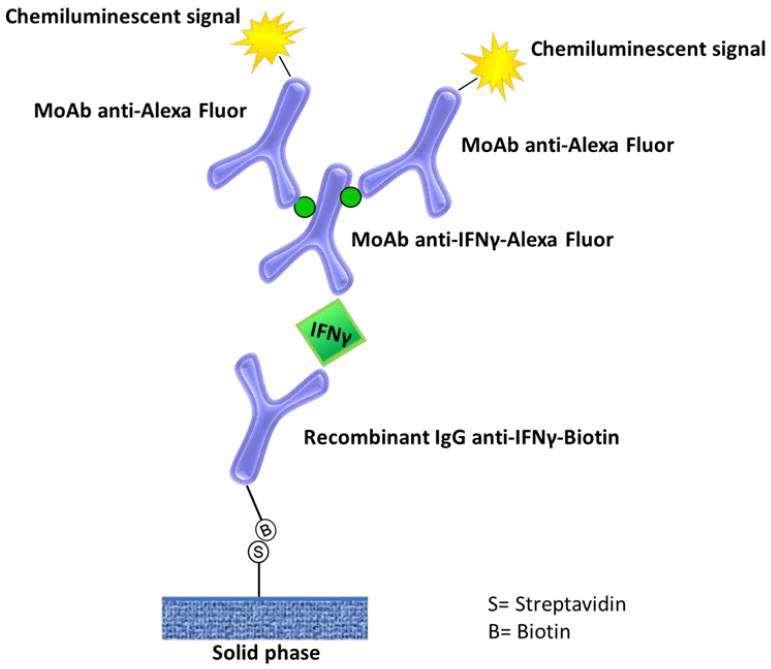

Figure 23: Schematic representation of our prototype of the IFNγ immunoassay

MATERIALS AND METHODS

REAGENTS

Tryptone, peptone were purchased by BD; IPTG was purchased by Inalco; Sodium phosphate, potassium phosphate, ammonium sulphate , EDTA (Ethylenediaminetetraacetic acid), sodium chloride and methanol were purchased by Carlo Erba, Kanamicin, DTT (Dithiothreitol), MESNA (2-mercaptoethanesulfonate Na), urea, Trizma base, SDS (Sodium dodecyl sulphate), glycine, 2-mercaptoethanol, BBF (Bromophenol Blue), DMSO, Hepes, glacial acetic acid, Streptavidin were purchased by Sigma-Aldrich. TFA (tri-fluoroacetic acid), CH3CN (acetonitrile) and Tween20 were purchased by Merck; synthetic C-term-Cfa-Biotin peptide was purchased by Bachem; EZ-link NHS-PEG4-Biotin was purchased by ThermoFisher; Streptavidin was purchased by BIOSPA, Agarose was purchased by IBI scientific; GelRed™ nucleic acid gel stain was purchased by Biotium.

Required materials for the transient production of recombinant IgG anti-IFNγ-N-term-Cfa antibody in ExpiCHO S™:

All the following reagents were provided by ThermoFisher scientific

• ExpiCHO-S™ cells cultured in ExpiCHO™ Expression Medium

• PureLink™ HiPure Plasmid Kit for the plasmid DNA preparation and isolation

• Antibody Expressing Positive Control Vector (100 µL of the 1 mg/mL solution provided in the kit

• ExpiFectamine™ CHO Reagent

• OptiPRO™ SFM complexation medium

• ExpiCHO™ Expression Medium

• Polycarbonate, disposable, sterile Erlenmeyer flasks

• Orbital shaker in a incubator with ≥80% relative humidity and 8% CO2 and temperature ranging from 32-37°C

• Reagents and equipment to determine viable cell density and percent viability

CLONING

- Plasmid extraction was performed with Wizard Plus SV Minipreps kit (Promega).
- DNA purification (from agarose gel and digestions) was performed with Kit Wizard SV Gel and PCR Clean-Up System (Promega).
- *NdeI, NheI, XhoI BglII, SalI,* endonucleases and relative buffers, Quick T4 DNA Ligase and relative buffer were purchased by New England Biolabs (NEB).

A) pET24-MCS-Intein-ELP(KV7F-36) vector

A synthetic gene encoding for the ELP (ELP[KV7F]36) linked to the *Mxe*GyrA gene and a multiple cloning site was purchased by GeneArt (Regensburg, Germany) and cloned via *Nde*I-*Xho*I in pET24a vector (Novagen, Merck Chemicals Ltd) (Figure 24).

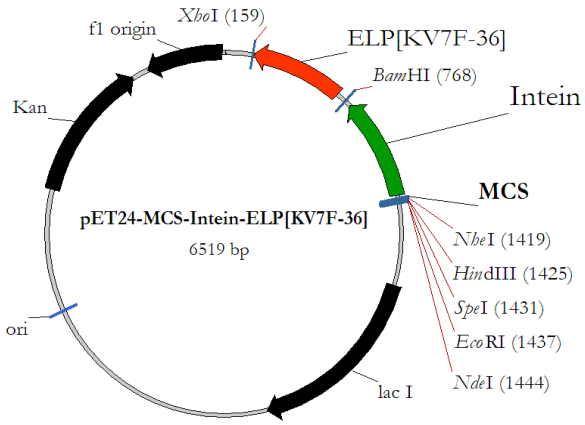

Figure 24. A schematic representation of pET24-MCS-*Mxe*GyrA-ELP[KV7F]36 vector.

The amino acid sequence of the MCS-*Mxe*GyrA- ELP[KV7F]36 protein encoded by pET24-MCS-*Mxe*GyrA-ELP[KV7F]36 vector resulted as shown in Figure 25:

MEFTSKLASGSGMRMCITGDALVALPEGESVRIADIVPGARPNSDNAIDLKVLDRH
GNPVLADRLFHSGEHPVYTVRTVEGLRVTGTANHPLLCLVDVAGVPTLLWKLIDEI
KPGDYAVIQRSAFSVDCAGFARGKPEFAPTTYTVGVPGLVRFLEAHHRDPDAQAIA
DELTDGRFYYAKVASVTDAGVQPVYSLRVDTADHAFITNGFVSHATGGGSGGGSGG
GSGGGSGGGSGGGSGGGSGGGVGVPGKGVPGVGVPGVGVPGVGVPGVGVPGVGVPG
VGVPGFGVPGVGVPGKGVPGVGVPGVGVPGVGVPGVGVPGVGVPGVGVPGFGVPGV
GVPGKGVPGVGVPGVGVPGVGVPGVGVPGVGVPGVGVPGFGVPGVGVPGKGVPGVG
VPGVGVPGVGVPGVGVPGVGVPGVGVPGFGVPG

MCS-Intein (*Mxe*GyrA N198A)-ELP36 (- linkers)

Figure 25. Protein encoded by the pET24-MCS-Intein-ELP] KV7F]36.

B) Cloning of C33 antigen

A synthetic gene encoding for HCV viral nonstructural antigen C33 was purchased by GeneArt and cloned via *Nde*I-*Nhe*I in:
-pET24-MCS-*Mxe*GyrA-ELP(KV7F-36) to obtain pET24-C33-*Mxe*GyrA-ELP(KV7F-36) vector

pET24-C33-*Mxe*GyrA-ELP(KV7F-36) vector encodes for C33-*Mxe*GyrA-ELP36 fusion protein (694 amino acids; 67.93 kDa; Figure 26).

MGVAKAVDFIPVENLETTMRSPVFTDNSSPPVVPQSFQVAHLHAPTGSGKSTKVPAAYA
AQGYKVLVLNPSVAATLGFGAYMSKAHGIDPNIRTGVRTITTGSPITYSTYGKFLADGG
CSGGAYDIIICDECHSTDATSILGIGTVLDQAETAGARLVVLATATPPGSVTVPHPNIE
EVALSTTGEIPFYGKAIPLEVIKGGRHLIFCHSKKKCDELAAKLVALGINAVAYYRGLD
VSVIPTSGDVVVVATDALMTGYTGDFDSVIDCNTCVTQTVDASGSGMRMCITGDALVAL
PEGESVRIADIVPGARPNSDNAIDLKVLDRHGNPVLADRLFHSGEHPVYTVRTVEGLRV
TGTANHPLLCLVDVAGVPTLLWKLIDEIKPGDYAVIQRSAFSVDCAGFARGKPEFAPTT
YTVGVPGLVRFLEAHHRDPDAQAIADELTDGRFYYAKVASVTDAGVQPVYSLRVDTADH
AFITNGFVSHATGGGSGGGSGGGSGGGSGGGSGGGSGGGSGGGVGVPGKGVPGVGVPGV
GVPGVGVPGVGVPGVGVPGVGVPGFGVPGVGVPGKGVPGVGVPGVGVPGVGVPGVGVPG
VGVPGVGVPGFGVPGVGVPGKGVPGVGVPGVGVPGVGVPGVGVPGVGVPGVGVPGFGVP
GVGVPGKGVPGVGVPGVGVPGVGVPGVGVPGVGVPGVGVPGFGVPG

C33-Intein (*Mxe*GyrA N198A)-ELP36 (- linkers)

Figure 26. C33-*Mxe*GyrA-ELP36 sequence.

C) Cloning of NHis-C33-N-term-Cfa antigen

- A synthetic gene encoding for NHis-C33 was purchased by GeneArt and cloned via *Nde*I-*Nhe*I in pET24-MCS-*Mxe*GyrA-ELP(KV7F-36) to obtain the pET24-NHis-C33-*Mxe*GyrA-ELP(KV7F-36) vector
- The pET24-NHis-C33-*Mxe*GyrA-ELP(KV7F-36) was digested via *SalI/XhoI* to excide the *Mxe*GyrA-ELP(KV7F-36) sequence from this vector and to obtain pET24-NHis-C33 vector
- A synthetic gene encoding for N-term-Cfa sequence purchased by GeneArt was digest via *SalI/XhoI* and it was cloned in pET24-NHis-C33 vector to obtain the pET24-NHis-C33-N-term-Cfa vector (Figure 27)

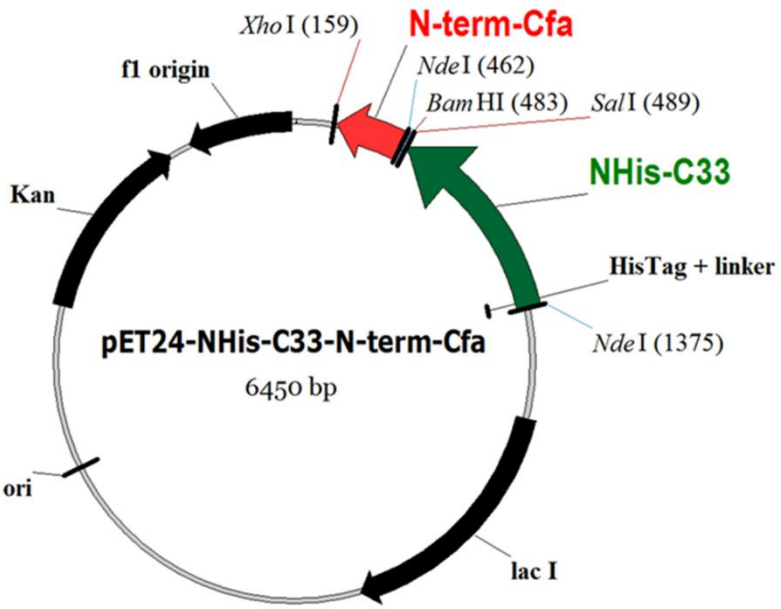

Figure 27. A schematic representation of pET24-NHis-C33-N-term-Cfa vector.

pET24-NHis-C33-N-term-Cfa vector encodes for NHis-C33-N-term-Cfa fusion protein (402 amino acids; 42.67 kDa; Figure 28).

MHHHHHHSSAAASAGGGSASGVAKAVDFIPVENLETTMRSPVFTDNSSPPVVP
QSFQVAHLHAPTGSGKSTKVPAAYAAQGYKVLVLNPSVAATLGFGAYMSKAHG
IDPNIRTGVRTITTGSPITYSTYGKFLADGGCSGGAYDIIICDECHSTDATSI
LGIGTVLDQAETAGARLVVLATATPPGSVTVPHPNIEEVALSTTGEIPFYGKA
IPLEVIKGGRHLIFCHSKKKCDELAAKLVALGINAVAYYRGLDVSVIPTSGDV
VVVATDALMTGYTGDFDSVIDCNTCVTQTVDGSAEYCLSYDTEILTVEYGFLP
IGKIVEERIECTVYTVDKNGFVYTQPIAQWHNRGEQEVFEYCLEDGSIIRATK
DHKFMTTDGQMLPIDEIFERGLDLKQVDGLP

His-tag-C33-N-term-Cfa (- linkers)

Figure 28. His-tag-C33-N-term-Cfa sequence

D) Cloning of C-term-Cfa- *Mxe*GyrA-ELP36

A synthetic gene encoding for C-term-Cfa sequence was purchased by GeneArt and cloned via *Nde*I-*Nhe*I in pET24-MCS-*Mxe*GyrA-ELP(KV7F-36) to obtain pET24-C-term-Cfa-*Mxe*GyrA-ELP(KV7F-36) vector

pET24-C-term-Cfa-*Mxe*GyrA-ELP(KV7F-36) vector encodes for C-term-Cfa-*Mxe*GyrA-ELP36 fusion protein (457 amino acids; 43.52 kDa; Figure 29).

MVKIISRKSLGTQNVYDIGVEKDHNFLLKNGLVASNCFNASGSGMRMCITGDALVALP
EGESVRIADIVPGARPNSDNAIDLKVLDRHGNPVLADRLFHSGEHPVYTVRTVEGLRV
TGTANHPLLCLVDVAGVPTLLWKLIDEIKPGDYAVIQRSAFSVDCAGFARGKPEFAPT
TYTVGVPGLVRFLEAHHRDPDAQAIADELTDGRFYYAKVASVTDAGVQPVYSLRVDTA
DHAFITNGFVSHATGGGSGGGSGGGSGGGSGGGSGGGSGGGSGGGVGVPGKGVPGVGV
PGVGVPGVGVPGVGVPGVGVPGFGVPGVGVPGKGVPGVGVPGVGVPGVGVPGVGVPGV
GVPGVGVPGVGVPGFGVPGVGVPGKGVPGVGVPGVGVPGVGVPGVGVPGVGVPGVGVP
GFGVPGVGVPGKGVPGVGVPGVGVPGVGVPGVGVPGVGVPGVGVPGFGVPG

C-term-Cfa-Intein (*Mxe*GyrA N198A)-ELP36 (- linkers)

Figure 29. C-term-Cfa-Intein (*Mxe*GyrA N198A)-ELP36 sequence.

Cloning strategy to create the Recombinant IgG anti-IFNγ-N-term-Cfa antibody

To obtain the recombinant IgG anti-IFNγ-N-term-Cfa antibody we substituted the constant heavy chain sequence (CH) of this specific antibody anti-IFNγ present in a mammalian expression vector together with its variable heavy chain sequences (VH), with the same constant heavy chain fused at the C-terminal to the N-term-Cfa sequence (CH-N-term-Cfa). In particular, we cloned the CH-N-term-Cfa sequence by NheI/XhoI in the mammalian ~~plasmid~~ expression vector previously deprived of the IgG anti-IFNγ constant heavy chain sequence (CH) to obtain a plasmid having the IgG anti-IFNγ constant heavy chain sequence fused to the C- terminal with the N-term-Cfa sequence(CH-N-term-Cfa ,Figure 30 a).

After that we co-transfected the Expi CHO cells with two mammalian expression vectors: the first one containing the constant heavy chain fused to the N-term-Cfa sequence (Final Expression vector 1, figure 30 a) and the variable heavy chain sequences of the IgG anti-IFNγ antibody and the second one containing the constant and the variable light chain sequences the same antibody (Expression vector 2, figure 30 b).

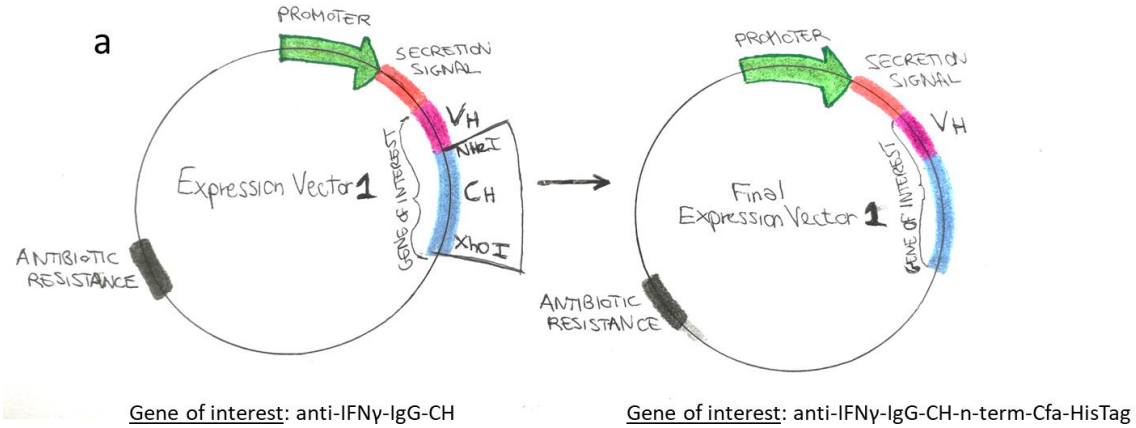

Gene of interest: anti-IFNγ-IgG-CH

Gene of interest: anti-IFNγ-IgG-CH-n-term-Cfa-HisTag

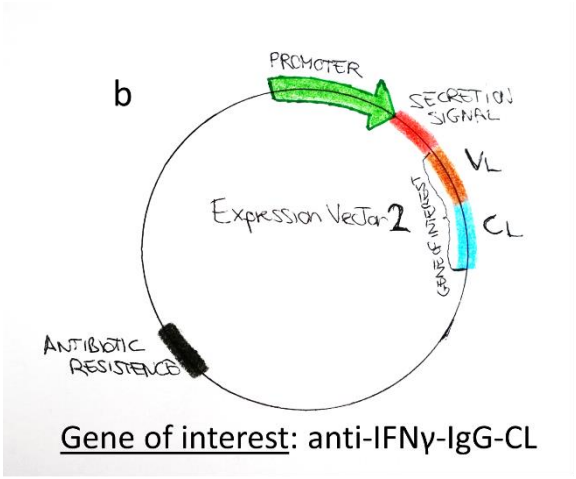

Figure 30. Cloning strategy to obtain the vector coding for anti-IFNγ IgG-CH-N-term-Cfa **(a)** and used for the CHO cell co-transfection with the vector coding for anti-IFNγ IgG-CL-N-term-Cfa sequence **(b)**.

NFMLTQPHSVSESPGKTVTISCTRSSGSIASNYVQWYQQRPGSAPTTVIYEDNERPSG
VPDRFSGSIASPSNSASLTISGLKTEDEADYYCQSYDSSNRAVIFGGGTKLTVLGQPK
AAPSVTLFPPSSEELQANKATLVCLISDFYPGAVTVAWKADSSPVKAGVETTTPSKQS
NNKYAASSYLSLTPEQWKSHRSYSCQVTHEGSTVEKTVAPTECSEVQLVESGGGLVQP
GGSLRLSCAASGFTFSSYAMSWVRQAPGKGLEWVSAISGSGGSTYYADSVKGRFTISR
DNSKNTLYLQMNSLRAEDTAVYYCAKVQWELPDAFDIWGQGTMVTVSSASTKGPSVFP
LAPSSKSTSGGTAALGCLVKDYFPEPVTVSWNSGALTSGVHTFPAVLQSSGLYSLSSV
VTVPSSSLGTQTYICNVNHKPSNTKVDKKVEPKSCDKTHTCPPCPAPELLGGPSVFLF
PPKPKDTLMISRTPEVTCVVVDVSHEDPEVKFNWYVDGVEVHNAKTKPREEQYNSTYR
VVSVLTVLHQDWLNGKEYKCKVSNKALPAPIEKTISKAKGQPREPQVYTLPPSREEMT
KNQVSLTCLVKGFYPSDIAVEWESNGQPENNYKTTPPVLDSDGSFFLYSKLTVDKSRW
QQGNVFSCSVMHEALHNHYTQKSLSLSPGKAEYCLSYDTEILTVEYGFLPIGKIVEER
IECTVYTVDKNGFVYTQPIAQWHNRGEQEVFEYCLEDGSIIRATKDHKFMTTDGQMLP
IDEIFERGLDLKQVDGLPGHHHHHHG

Legend:

VL = Variable Light Chain of recombinant anti-IFNγ IgG antibody

CL = Constant Light Chain of recombinant anti-IFNγ IgG antibody

VH =Variable Heavy Chain of recombinant anti-IFNγ IgG antibody

CH = Constant Heavy Chain of recombinant anti-IFNγ IgG antibody

N-term-Cfa sequence

His tag

Figure 31. Recombinant anti- IFNγ-N-term-Cfa IgG antibody sequence.

STRAINS

E. coli XL1-Blue strain (Stratagene, Agilent Technologies, Santa Clara, USA) was used for mutagenesis and cloning operations and plasmid maintenance.
E. coli BL21(DE3) strain (Novagen, Merck Chemicals Ltd) was used for protein expression.

FERMENTATIONS

Pre-inoculum: few µL of glycerinated BL21(DE3) cells were poured in 50 mL of culture medium (LB, 2xYT) supplemented with antibiotic (kanamycin 30 µg/ml), and left on oscillating device (180 rpm) at 37°C, overnight.
Inoculum: the following day the sample was diluted (1:50 for fermentations performed at 30-37°C or 1:30 for fermentations performed at 15°C).
Bacterial cells, grown in the same medium of pre-inoculum (LB or 2xYT with kanamycin), were induced with 0.03 mM (for fermentations performed at 15-30 and 37°C in 2xYT) or 1 mM IPTG (for fermentations performed at 30-37°C in LB) when the absorbance at 600 nm reached usually a value of 0.6, but in some cases a value of 1.5 (late induction).
For the fermentations performed in Auto-Induction Medium, bacterial cells, grown in 2xYT as medium of pre-inoculum were induced with AIM (Auto Induction Medium) when the absorbance at 600 nm reached usually a value of 0.001.
Protein expression was continued for 3 hours for fermentations at 30-37 °C or for 24 hours for fermentations at 15 °C.

PROTEIN INDUCTION TEST PROTOCOL

Aliquots of a fermentation culture corresponding to 0.6 optical density at 600 nm of wavelength per ml of cellular culture were withdrawn at the moment of protein induction (T0), and at the end of the fermentation. Samples were spun at 10.000xg in a bench top centrifuge and the related bacteria pellets treated with 100 µL of reducing loading buffer at +99ºC for five minutes and then analyzed by SDS-PAGE.

SDS-PAGE GELS

- Precast gel 4-20% Criterion TGX Stain-Free (BIO-RAD) for the SDS-page analysis of the experiments regarding the C33-*MxeGyrA*-ELP36 and the recombinant IgG anti-IFNγ antibody
- Precast gel 16,5% Criterion Tris-Tricine/Peptide, 1.0 mm (BIO-RAD) for the SDS-page analysis of the experiments regarding the Cfa split-intein reaction tests (site specific biotinylation of the C33 antigen).

Proteins Standard: Precision Plus Protein All Blue Standard+Unstained (BIO-RAD)

Electrophoresis condition:
250 Volts for 33 minutes for Precast gel 4-20% Criterion TGX Stain-Free while 125 Volts for 120 minutes for Precast gel 16,5% Criterion Tris-Tricine/Peptide, 1.0 mm, using the power supplier power supplier Power-Pac HC from BIO-RAD.

Staining solution: Coomassie blue G250 3 g/Liter, Methanol 50 % (v/v), Acetic acid 10 (v/v).
Destaining solution: Methanol 20 % (v/v), Acetic acid 10 (v/v).

For stain-free gels we visualized the proteins by Chemidoc XRS+ (BIO-RAD)

Tris/Glycine/SDS (TGS) running buffer composition (diluted 1:10, BIO-RAD):

Compound	**Concentration**
Tris base	25 mM
Glycine	192 mm
SDS	0.1 (w/v)

Reducing loading buffer for precasted gel 4-20% Criterion TGX Stain-Free:

Compound	**Concentration**
Tris base	125mM (pH 6.8)
Glycerol	22 % (v/v)
β-OH	2.5 % (v/v)
SDS	2.5 % (w/v)
Bromophenol Blue	0.0025 (w/v)
Pyronin	0.0025 (w/v)

Reducing loading buffer for precast gel Criterion Precast Gel 16,5% Tris-Tricine/Peptide:

Compound	**Concentration**
Tris-HCl	200mM (pH 6.8)
Glycerol	40 % (v/v)
β-OH	2.5 % (v/v)
SDS	2 % (w/v)
Coomassie blue G250	0,04 % (v/v)

Non-reducing loading buffer:

Compound	**Concentration**
Tris base	125mM (pH 6.8)
Glycerol	22 % (v/v)
SDS	2.5 % (w/v)
Bromophenol Blue	0.0025 (w/v)
Pyronin	0.0025 (w/v)

WESTERN BLOT PROTOCOL

After electrophoresis separation on a polyacrylamide gel, protein bands were transferred to a nitrocellulose membrane (BIO-RAD) using the Trans-Blot Turbo Transfer system from BIO-RAD.
Transfer conditions:

Amperage (A): 2.5 *time*: 7 min

Membrane: Trans-blot Turbo TM (Biorad)

For the detection of NHis-C33-Biotin after the Cfa split-intein reaction test we used the following protocol:

HRP-Streptavidin	Product	Buffer	Dilution	Incubation time (min)	Temp. (°C)	Agitation (rpm)
Blocking		PBS-BSA 0.5%	-	60	RT	60
Immuno-staining	HRP-streptavidin 0,5 mg/ml Cat:405210 Lot:B232497	PBS-BSA 0.5%	1:5000	60	RT	60
Washing		PBS-Tween20 0.1%	-	3x1' + 3x5'	RT	60
Development	ECL Clarity Biorad (*code product*: 170-5061; *batch*: 102031024)	-	-	1	RT	-

For the detection of recombinant IgG anti IFNγ-N-term-Cfa after the transient production in ExpiCHO -S™ Cells, Chinese hamster ovary (CHO) cells we used the following protocol:

Primary Antibody Immunostaining:

Anti-human IgG	Product	Buffer	Dilution	Incubation time (min)	Temp. (°C)
Blocking		PBS-BSA 0.5%	-	90	RT
Primary Antibody	Goat anti-human IgG (H+L) (Jackson, Cat.no: 109-005-088)	PBS-BSA 0.5%	1:100	60	RT
Washing	-	PBS-Tween20 0.1%	-	10x3	RT

Secondary Antibody Immunostaining:

Secondary Antibody	Donkey Anti-Goat IgG H&L (HRP) (AbCam, Cat.no: ab97110)	PBS-BSA 0.5%	1:5000	1	RT
Washing	-	PBS-Tween20 0.1%	-	10x3	RT
Development	ECL Clarity Biorad (code product 170-5061; batch 102031024)	-	-	1	RT

SOLUBILITY TEST PROTOCOL

At the end of fermentation, 15 mL of the cell culture were centrifuged (2000xg at 4°C). Then, the following working scheme was performed:

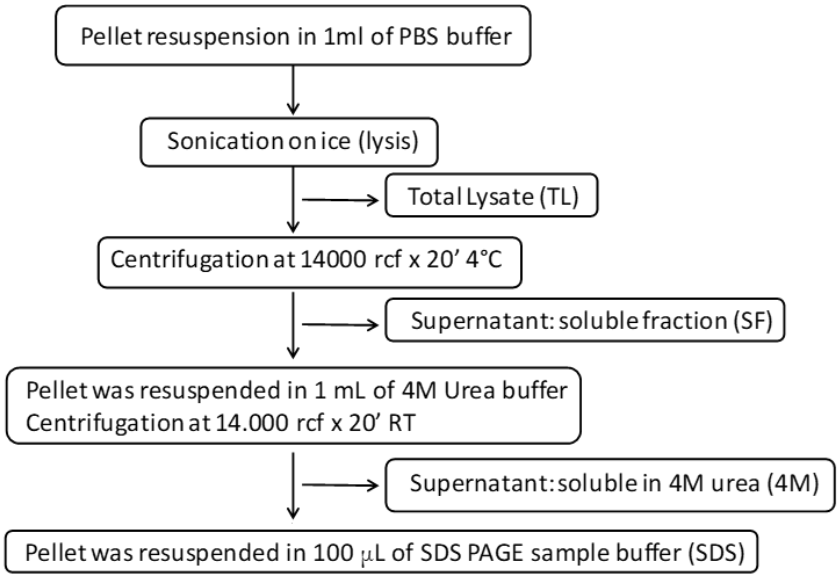

50 µL of each collected fraction (TL; SF; 4M) were treated with 50 µL of reducing loading buffer (1:1) at +99ºC for five minutes and then analyzed by SDS-PAGE. The SDS sample was directly boiled at +99ºC for five minutes and then analyzed by SDS-PAGE.

PRECIPITATION TEST PROTOCOL

At the end of solubility test, the C33-*MxeGyrA*-ELP36 and the C-term-Cfa- *MxeGyrA*-ELP36 proteins underwent to the precipitation test characterized by the following steps:

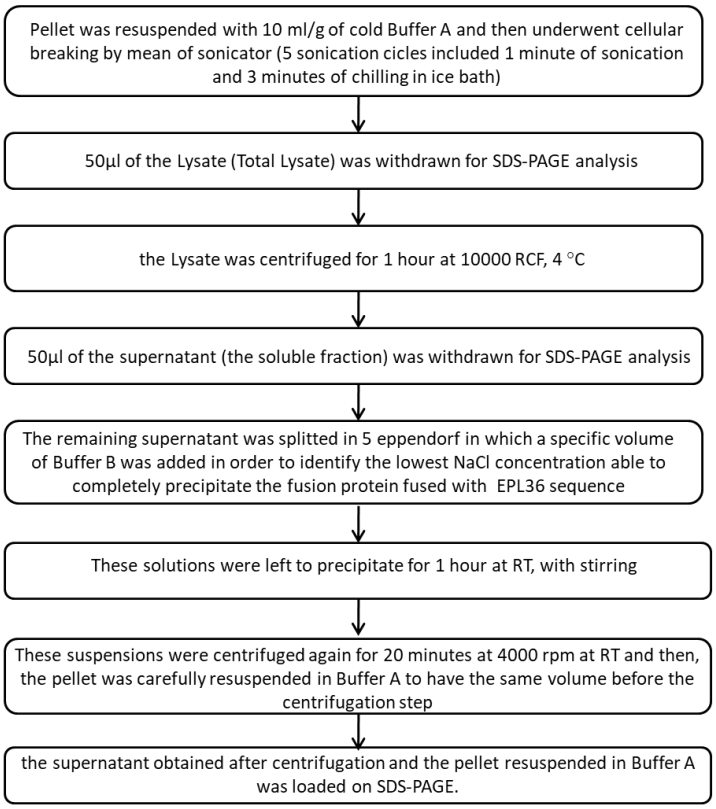

Buffer	Composition
Buffer A	50 mM Na_2HP0_4*$2H_20$; 5 mM EDTA pH 8
Buffer B	5M NaCl

Table 1. List of buffers used in the precipitation test of C33-*Mxe*GyrA-ELP36/C-term-Cfa-*Mxe*GyrA-ELP36.

C33-*Mxe*GyrA-ELP36 purification protocol for the subsequent EPL reaction (C-terminal site-specific biotinylation)

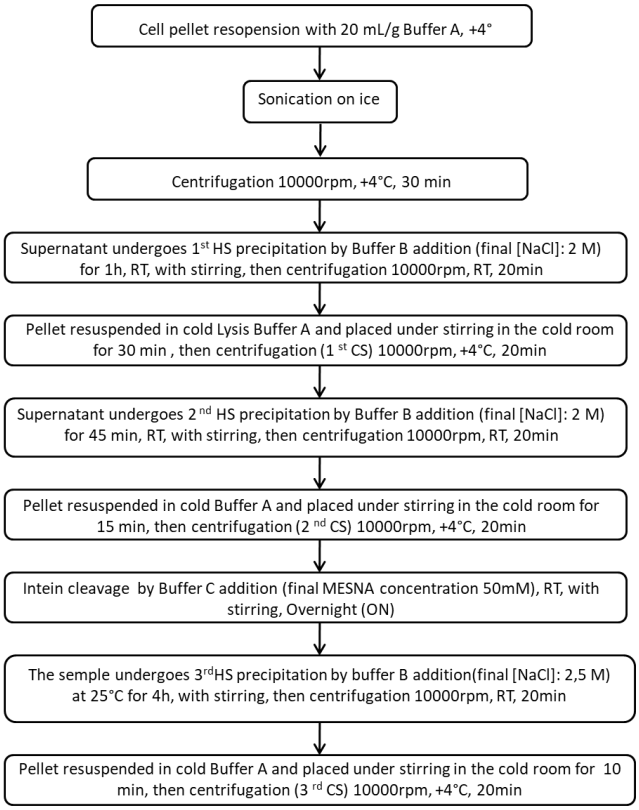

Figure 32. C33-thioester purification scheme from C33-*Mxe*GyrA-ELP36 for the subsequent EPL reaction (C-terminal site-specific biotinylation of C33 antigen).

Buffer	Composition
A	50 mM Na_2HP0_4*$2H_20$; 5 mM EDTA pH 8
B	NaCl 5M
C	MESNA 1,5 M

Table 2. List of buffers used in purification protocol of C33-*Mxe*GyrA-ELP36 to obtain C33-thioester for the subsequent EPL reaction.

The supernatant after the 3rd HS underwent a concentration (10x) and buffer exchange in Buffer A (5x10mL) to reduce the NaCl concentration by mean of an Amicon Ultra-15 (10 KDa) device, Millipore

THIOLYSIS REACTION WITH MESNA: C33-THIOESTER FORMATION

For the cleavage of C33 from *Mxe*GyrA-ELP36 tag and the simultaneous formation of thioester, MESNA (stock solution 1,5 M in water) was added to the sample at a final concentration of 50mM, at the end of ITC process. The reaction was carried out in phosphate buffer (see below) at room temperature and reaction time course was followed by SDS-page analysis: the C33 thioesterification reaction went to completion in 4 hours but the reaction was performed overnight (ON) for experimental timing.

Phosphate buffer: 50mM Na2HPO4*2H2O; 5mM EDTA; pH 8.

BIOTINYLATION OF C33 ANTIGEN THROUGH EXPRESSED PROTEIN LIGATION TECHNIQUE
The EPL reaction between C33-thioester (stock solution 1 mg/ml in phosphate buffer) and (Cys)-GGEK-(Lys-Biotin) peptide (stock solution 8 mg/ml in phosphate buffer) was carried out in phosphate buffer, overnight, at room temperature, in presence of 8 fold molar excesses of peptide.

C33-thioester MW: 29513,45 Da; (Cys)-GGEK-(Lys-Biotin) peptide MW: 874 Da; C33-Biotin (product) MW: 30447,45 Da.
Phosphate buffer: 50mM Na2HPO4*2H2O; 5mM EDTA; pH 8.

C33-Biotin purification protocol

Procedure

After biotinylation reaction through EPL (Expressed Protein Ligation) with (Cys)-GGEK-(Lys-Biotin) peptide, the sample was loaded onto the column HiLoad 26/ 600 Superdex 200 pg (1 CV = 318.6 mL). This column was equilibrated with PBS buffer. Protein elution was achieved by an isocratic gradient of the same buffer at a flow rate of 2.5 mL/min.

Chromatographic conditions:

- Column: HiLoad 26/600 Superdex 200 pg; CV=120.6 mL (GE)
- Flow rate: 2.5 mL/min
- Wavelengths: 260/280 nm
- Gradient: isocratic in PBS buffer

SDS-PAGE retardation assay protocol

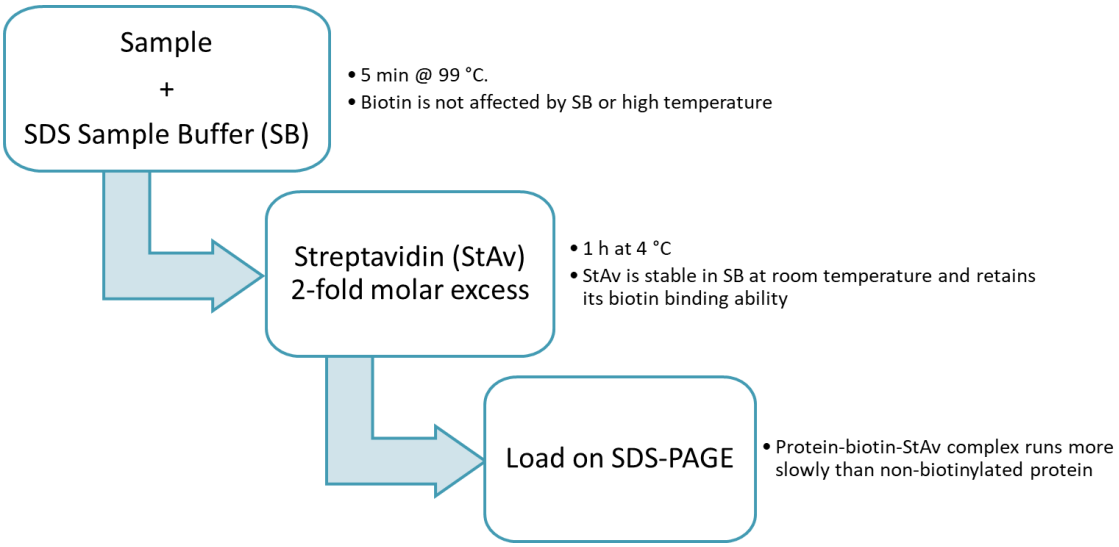

Figure 33. Scheme of the main steps to perform the SDS PAGE retardation assay

This technique is based on the interaction between biotin and streptavidin: if the target protein is conjugated with one or more molecules of biotin, after the addition of the streptavidin in that sample, complexes biotin-streptavidin will form an then we will observe onto SDS-page gel a band shift of the biotinylated protein at higher molecular weight compared to a non-biotinylated protein that will show on SDS-page gel a band according to its own expected molecular weight. Therefore, by the retardation assay we can verify whether a target protein is biotinylated and also we can understand the efficiency of the biotinylation reaction. This last datum is detectable loading the sample containing the biotinylated protein before and after the StAv addition and comparing the band intensity relative to the own molecular weight of the non- biotinylated target protein in each of the two samples. We performed the retardation assay for all the lots of biotinylated C33 obtained.

LIAISON® XL MUREX HCV Ab

This immunoassay uses chemiluminescence immunoassay (CLIA) technology for the qualitative determination of specific antibodies to hepatitis C virus (anti-HCV) in human serum or plasma samples. LIAISON® XL MUREX HCV Ab assay employs HCV polypeptides able to recognize antibodies directed to HCV. The polypeptides correspond to highly antigenic determinants of both the structural and non-structural regions of HCV.

Reagents and relative concentrations:

- Solid phase: 0,1% of paramagnetic particle (PMP) with streptavidin (StAv) + Diasorin-C33-biotin at 5µg/ml diluted in assay buffer+ 0,3% tosyl beads coated with the antigens p22 (0,025 mg/mL) and NS4 (0,1 µg/mL)
- Tracer: anti-human IgG functionalized with chemiluminescent molecule (70ng/ml)
- Samples detected:
    1) Panel of human HCV negative blood samples
    2) Panel of human HCV positive blood samples

In the specific case, we replaced our biotinylated C33 to the Diasorin C33-biotin maintaining the setting and the other reagents of the LIAISON XL Murex HCV Ab assay in order to evaluate and compare only the immunoreactivity of the two biotinylated antigens.

Assay protocol:

The method for qualitative determination of specific IgG to hepatitis C virus (HCV) is an indirect chemiluminescence immunoassay (CLIA). Two recombinant antigens (p22 and NS4) specific for HCV are used for coating tosyl magnetic particles (solid phase), while a third HCV antigen (biotinylated C33) is captured by streptavidin-coated magnetic particles (PMP StAv). During the first incubation the HCV antibodies present in calibrator, samples or controls bind to the solid phase through the recombinant HCV antigens. During the second incubation, a mouse monoclonal antibody to human IgG, linked to an isoluminol derivative (isoluminol-antibody conjugate, tracer), reacts with IgG to HCV already bound to the solid phase. After each incubation, the unbound material is removed with a wash cycle. Subsequently, the starter reagents are added and a flash chemiluminescence reaction is thus induced. The light signal, and hence the amount of isoluminol-antibody conjugate, is measured by a photomultiplier as relative light units (RLU) and is indicative of IgG to HCV presence in calibrator, samples or controls.

C33-*Mxe*GyrA-ELP36 purification protocol that includes the simultaneous cleavage of the fusion protein and site-specific biotinylation of C33-thioester by EPL reaction

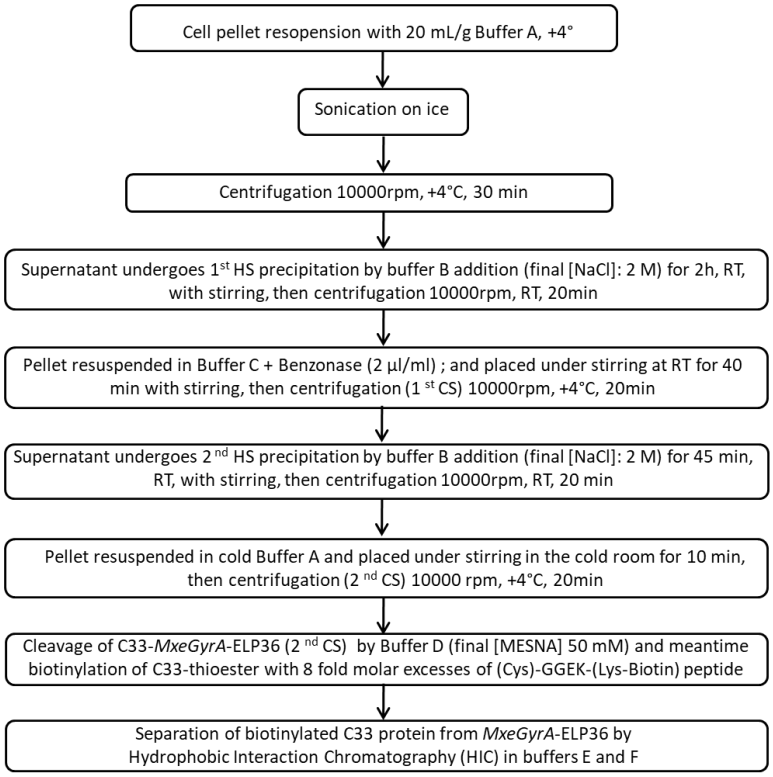

Figure 34. Biotinylated C33 purification scheme characterized by the simultaneous cleavage of C33-*MxeGyrA*-ELP36 with MESNA and biotinylation of C33-thioester by EPL reaction (C-terminal site-specific biotinylation of C33 antigen).

Buffer	Composition
A	50 mM Na_2HP0_4*$2H_20$; 5 mM EDTA pH 8
B	NaCl 5M
C	Trisma BASE 20 mM; $MgCl_2$ 2 mM; pH 8
D	MESNA 1M
E	800 mM Ammonium sulphate $(NH_4)_2$ S04; 50 mM Na_2HP0_4*$2H_20$; 5 mM EDTA; pH 7,6
F	50 mM Na_2HP0_4*$2H_20$; 5 mM EDTA; pH 7,6

Table 3. List of buffers used in purification protocol of biotinylated C33 through the simultaneous cleavage of C33-*Mxe*GyrA-ELP36 with MESNA and site-specific biotinylation of C33-thioester by EPL reaction.

HIC chromatography

We performed a HIC scouting in order to select the best chromatographic conditions to separate the biotinylated C33 form the *Mxe*GyrA-ELP36.

In particular, we tested some hydrophobic resins, concentrations of ammonium sulphate and elution methods shown in the tables below.

A)

Hydrophobic resin	[Starting Ammonium sulphate] mM	Elution method
Hitrap Phenyl HP	500	Linear gradient from 0% to 100 of Elution Buffer
Hitrap Butyl-S-FF	500	Linear gradient from 0% to 100 of Elution Buffer
Hitrap Octyl-FF	500	Linear gradient from 0% to 100 of Elution Buffer

B)

Hydrophobic resin	[Starting Ammonium sulphate] mM	Elution method
Hitrap Butyl-S-FF	700	Linear gradient from 0% to 100 of Elution Buffer
Hitrap Butyl-S-FF	800	Linear gradient from 0% to 100 of Elution Buffer
Hitrap Butyl-S-FF	900	Linear gradient from 0% to 100 of Elution Buffer

C)

Hydrophobic resin	[Starting Ammonium sulphate] mM	Elution method
Hitrap Butyl-S-FF	800	Steps gradient (30%-60% of elution buffer)
Hitrap Butyl-S-FF	800	Steps gradient (35%-60% of elution buffer)
Hitrap Butyl-S-FF	800	Steps gradient (40%-60% of elution buffer)

Binding Buffer: Ammonium sulphate 700, 800, or 900 mM, mM $Na_2HP0_4*2H_20$; 5 mM EDTA; pH 7,6
Elution Buffer: $Na_2HP0_4*2H_20$; 5 mM EDTA; pH 7,6

Table 4 A, B and C. Conditions tested in the HIC scouting: Table A (Different Hydrophobic resins), Table B (Different Ammonium sulphate concentrations) and Table C (Different elution methods). The final chosen HIC condition is highlighted by a red rectangle (Table C).

Hydrophobic Interaction Chromatography (HIC) to separate the biotinylated C33 from the *Mxe*GyrA-ELP36 tag

Procedure

After the simultaneous cleavage with MESNA and site-specific biotinylation through EPL (Expressed Protein Ligation) with (Cys)-GGEK-(Lys-Biotin) peptide, we brought the biotinylated C33 in 800 mM ammonium sulphate from a 2.5 M stock solution. This initial dilution step is necessary to promote a partial unfolding of the proteins present in the sample (exposure of hydrophobic regions) and thus promote their interaction onto the resin. After that, the sample was loaded onto the column Hitrap Butyl-S-FF (1 CV = 5 mL). This column was equilibrated with binding buffer and the unbound sample was washed out flowing the same buffer. Protein elution was achieved by a steps gradient of 30%-60% of elution buffer.

Ammonium sulphate stock solution: Ammonium sulphate 2.5 M, Phosphate dibasic dehydrate 50 mM, EDTA 5 mM, pH 7.6

Chromatographic conditions

- Column: HiTrap Butyl-S-FF CV=5 mL (GE)
- Flow rate: 2 mL/min (load, wash and elution)
- Wavelengths: 260/280 nm
- Gradient: steps gradient (30% of elution buffer in 4 CVs + 60% of elution buffer in 4 CVs)

NHis-C33-N-term-Cfa purification protocol

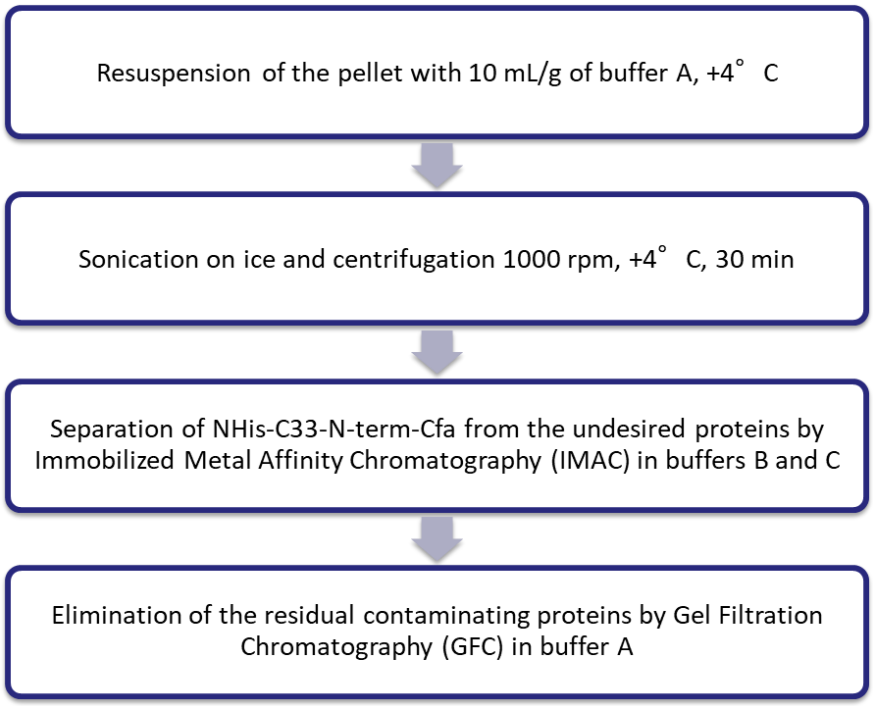

Figure 35. Purification scheme of NHis-C33-N-term-Cfa through two chromatographic steps: IMAC and GFC

Buffer	Composition
A	25 mM $Na_2HP0_4*2H_20$, pH 8
B	25 mM $Na_2HP0_4*2H_20$; 200 mM NaCl; pH 8
C	25 mM $Na_2HP0_4*2H_20$; 500 mM Imidazole; 200 mM NaCl; pH 8

Table 5. List of buffers used in purification protocol of NHis-C33-N-term-Cfa by IMAC and GFC

IMAC conditions:

The IMAC column (ZetaCell Ni-NTA) was previously activated with Ni^{2+} ($NiCl_2$ 0.1 M) and equilibrated with buffer B.

- Column: ZetaCell Ni-NTA CV=10 mL
- Flow rate: 2 mL/min
- Wavelengths: 260/280 nm
- Washing: 10 CVs
- Gradient: from 0% to 100% of Buffer C in 5.5 CVs

GFC conditions:

- Column: HiLoad 26/600 Superdex 200 pg; CV=318.6 mL (GE)
- Flow rate: 2.5 mL/min
- Wavelengths: 260/280 nm
- Gradient: isocratic in buffer A

C-term-Cfa-*Mxe*GyrA-ELP36 purification protocol that includes the simultaneous cleavage of the fusion protein and the site-specific biotinylation of C33-thioester by EPL reaction

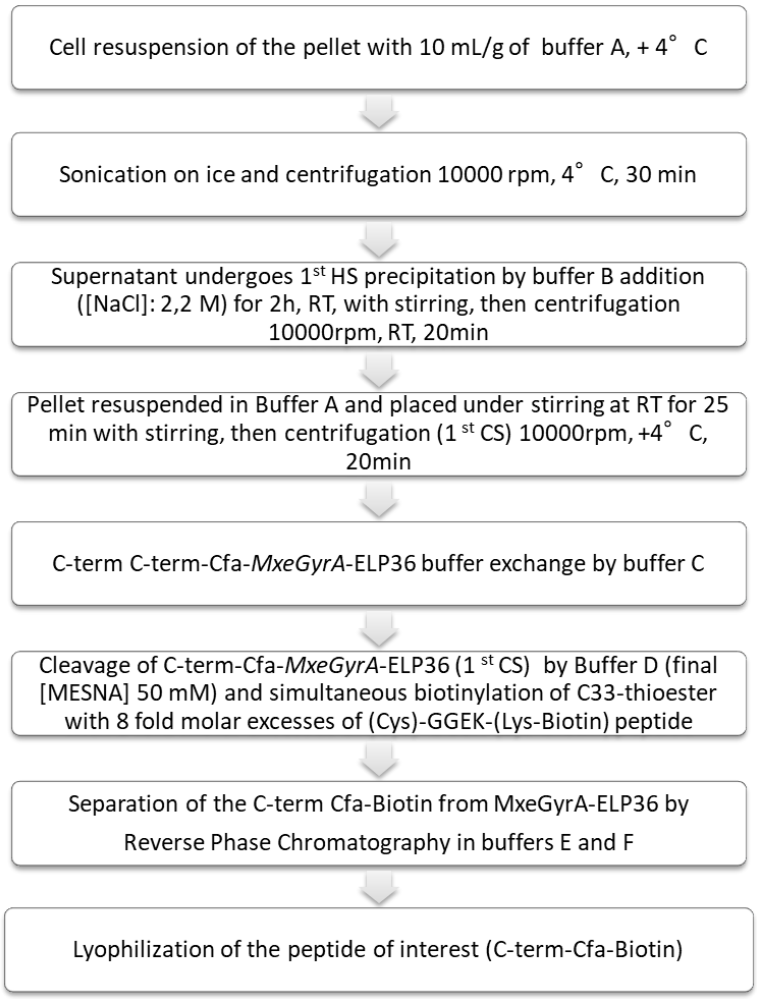

Figure 36. C-term-Cfa-Biotin purification scheme characterized by the simultaneous cleavage of C-term-Cfa-*MxeGyrA*-ELP36 with MESNA and biotinylation of C33-thioester by EPL reaction (C-terminal site-specific biotinylation of C-term-Cfa peptide)

Buffer	Composition
A	100 mM Trizma-BASE¸15 mM NaCl; 1,5 mM MgCl2; pH 7,6
B	NaCl 5M
C	50 mM Na_2HP0_4*$2H_20$; 5 mM EDTA; 300 mM NaCl; 1500 mM UREA; pH 8
D	MESNA 1,5 M
E	H2O, Trifluoroacetic acid 0.1% (v/v)
F	CH3CN, Trifluoroacetic acid 0.1% (v/v)

Table 6. List of buffers used in C-term-Cfa-Biotin purification protocol

RPC (Reversed Phase Chromatography) chromatographic conditions:

The sample was diluted 1:1 with H_2O/TFA 0,2% (v/v) buffer and loaded onto a 15RPC source column (1 CV) = 6.667 mL. This column had just been equilibrated with buffer E.

- Column: Source15RPC 15µm 8.5x100mm; CV=6.7 mL (GE)
- Flow rate: 2.5 mL/min
- Wavelength: 214 nm
- Sample loading and washing: 90% buffer E, 10% buffer F
- Gradient: 10-60% buffer F in 12 CVs

Cfa split intein reaction test between NHis-C33-N-term-Cfa and C-term-Cfa-Biotin

1) Overnight dialysis of the NHis-C33-N-term-Cfa in splicing buffer (with or without 4M UREA) and quantification of the sample with the spectrophotometer
2) Resuspension of the lyophilic C-term-Cfa-Biotin in splicing buffer (with or without 4M UREA) and quantification with the spectrophotometer
3) Dilution of the two species at the desired concentration in splicing buffer, addition of 2 mM of the reducing agent TCEP to both and incubation for 30 min at 25°C under stirring
4) Mixing of NHis-C33-N-term-Cfa and C-term-Cfa-Biotin equal volumes, then incubation at the selected temperature under stirring
5) Monitor of the reaction for 24 hours taking at different time points (T0', T30', T1h, T2h and T overnight) a sample (50 µl) for SDS-page analysis

Splicing Buffer*:* Phosphate dibasic dihydrate ($Na_2HPO_42H_2O$) 100 mM, NaCl 150 mM, EDTA 1 mM, TCEP 2 mM, pH 7.2

Splicing Buffer 4M UREA*:* Phosphate dibasic dihydrate ($Na_2HPO_42H_2O$) 100 mM, NaCl 150 mM, EDTA 1 mM, TCEP 2 mM, urea 4 M, pH 7.2

In the tables below are reported the different conditions of Cfa split intein reaction test (Table 7) performed in order to obtain the best conversion yield in the final product (NHis-C33-Biotin).

A)

Test	Constructs	Concentration (mg/ml) Molarity (µM)	Molar ratio C-term-Cfa/ N-term-Cfa	Temperature	Buffer
A	NHis-C33-N-term-Cfa	0,2 mg/ml 9,4 µM	8,3X	+25°C	Splicing Buffer
	Synthetic C-term-Cfa-Biotin	0,2 mg/ml 78 µM			
B	NHis-C33-N-term-Cfa	0,2 mg/ml 9,4 µM	16,6 X	+25°C	Splicing Buffer
	Synthetic C-term-Cfa-Biotin	0,4 mg/ml 156 µM			
C	NHis-C33-N-term-Cfa	0,2 mg/ml 9,4 µM	16,6 X	+25°C	Splicing Buffer 4M UREA
	Synthetic C-term-Cfa-Biotin	0,4 mg/ml 156 µM			
D	NHis-C33-N-term-Cfa	0,2 mg/ml 9,4 µM	16,6 X	+30°C	Splicing Buffer 4M UREA
	Synthetic C-term-Cfa-Biotin	0,4 mg/ml 156 µM			

B)

Test	Constructs	Concentration (mg/ml) Molarity (µM)	Molar ratio C-term-Cfa/ N-term-Cfa	Temperature	Buffer
E	NHis-C33-N-term-Cfa	0,2 mg/ml 9,4 µM	16,6 X	+25°C	Splicing Buffer 4M UREA
	Recombinant C-term-Cfa-Biotin	0,4 mg/ml 156 µM			
F	NHis-C33-N-term-Cfa	0,2 mg/ml 9,4 µM	16,6 X	+25°C	Splicing Buffer 4M UREA
	Synthetic C-term-Cfa-Biotin	0,4 mg/ml 156 µM			

Table 7 A and B. Tested conditions for the protein trans splicing reaction by Cfa-split-intein between NHis-C33-N-term-Cfa and C-term-Cfa-Biotin

The best final chosen condition is highlighted by a red rectangle (Condition C).

Purification process of NHis-C33-Biotin

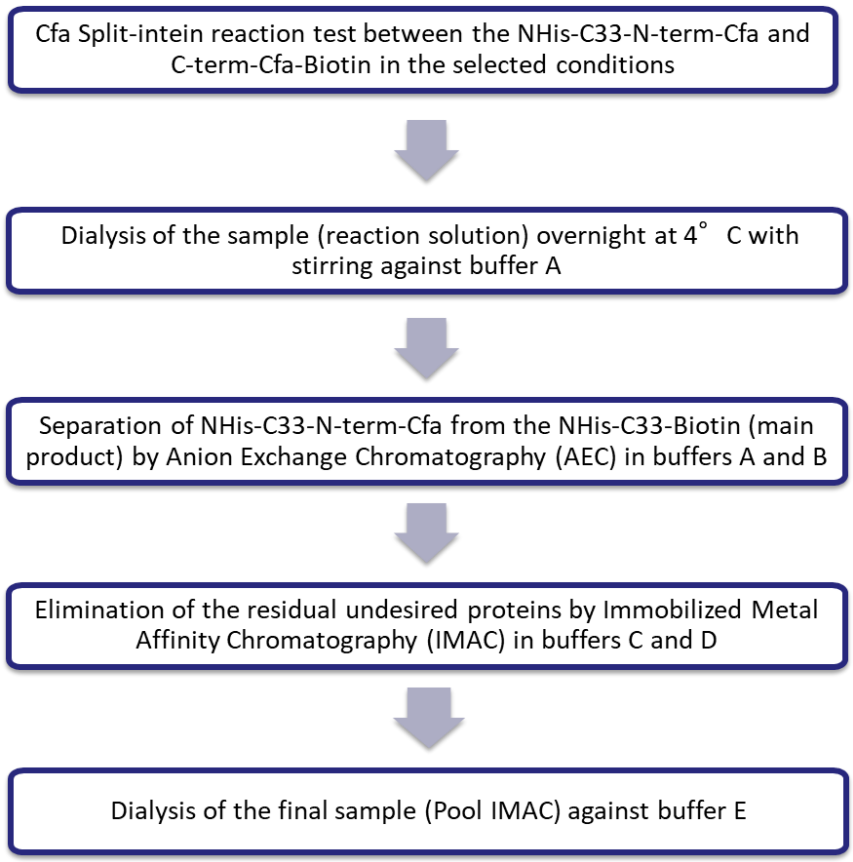

Figure 37. Purification scheme of NHis-C33-Biotin by two chromatographic steps: AEC and IMAC.

Buffer	Composition
A	20 mM $Na_2HP0_4*2H_20$; pH 7,5
B	20 mM $Na_2HP0_4*2H_20$; 1M NaCl; 1 mM EDTA pH 7,5
C	25 mM $Na_2HP0_4*2H_20$; 200 mM NaCl; pH 8
D	25 mM $Na_2HP0_4*2H_20$; 500 mM Imidazole; 200 mM NaCl; pH 8
E	25 mM $Na_2HP0_4*2H_20$; 200 mM NaCl; pH 8

Table 8. List of buffers used in NHis-C33-Biotin purification protocol

AEC (Anion Exchange Chromatography) chromatographic conditions:

- Column: Foresight Nuvia Q; CV=1 mL (Bio-Rad)
- Flow rate: 0,5 mL/min (Load); 1 mL/min (Wash and Elution)
- Wavelengths: 260/280 nm
- Loading and washing buffer: buffer A
- Washing: 5 CVs
- Gradient: 1,8% of Buffer B in 15 CVs, 8,5% of Buffer B in 10 CVs and linear gradient from 8,5% to 100% of Buffer B in 15 CVs

IMAC (Immobilized Metal Affinity Chromatography) Chromatographic conditions:

The IMAC column Mini Chrom Fractogel Chelat (M) (1ml) was previously activated with Ni^{2+} ($NiCl_2$ 0.1 M) and equilibrated with buffer C.

- Column: Mini Chrom Fractogel Chelat (M) (1ml) CV=1mL (Merckmillipore)
- Flow rate: 1 mL/min (load, wash and elution)
- Wavelengths: 260/280 nm
- Washing: 10 CVs in buffer C
- Gradient: from 0% to 100% of Buffer D in 7 CVs

Purification process of recombinant IgG anti-IFNγ-N-term-Cfa antibody

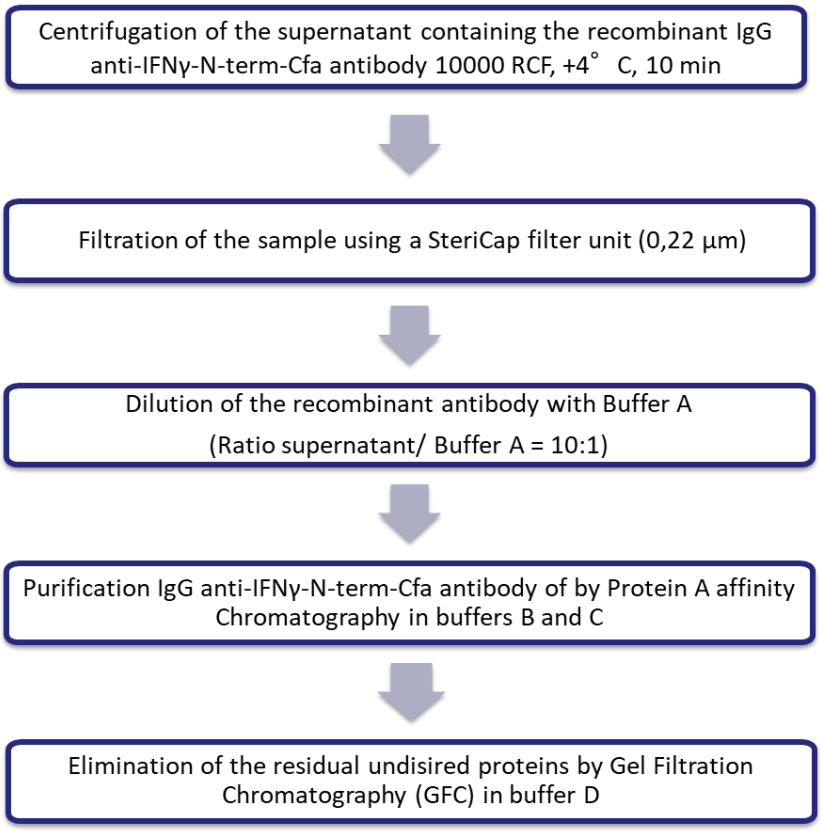

Figure 38. Purification scheme of the recombinant IgG anti-IFNγ-N-term-Cfa by two chromatographic steps: Protein A and GFC.

Buffer	Composition
A	500 mM Tris; 3 M NaCl; pH 8,6
B	50 mM Tris; 300 mM NaCl; pH 8,6
C	100 mM Citric acid monohydrate ($C_6H_8O_7$* H_2O); pH 3
D	100 mM Na_2HP0_4*$2H_20$; 150mM NaCl; 1 mM EDTA pH 7,2

Table 9. List of buffers used in recombinant IgG anti-IFNγ-N-term-Cfa purification protocol

Protein A affinity Chromatography conditions:

The Protein A column HiTrap Fibro PrismA 2X0,4 ml) Pre-Packed Column (total column volume of 0,8 mL) was previously equilibrated with buffer B.

- Column: HiTrap Fibro PrismA 2X0,4 ml Pre-Packed Column CV=0,8 mL (cytiva)
- Flow rate: 3 mL/min (loading), 5 mL/min (wash and elution)
- Wavelengths: 260/280 nm
- Washing: 10 CVs in buffer B
- Gradient: Single step with 100% of buffer C for 10 CVs

Gel Filtration Chromatography (GFC) chromatographic conditions:

- Column: HiLoad 16/600 Superdex 200 pg; CV=120.6 mL (GE)
- Flow rate: 1.3 mL/min
- Wavelengths: 260/280 nm
- Gradient: isocratic in buffer D

Cfa split intein reaction test between recombinant IgG anti-IFNγ-N-term-Cfa antibody and C-term-Cfa-Biotin

1) Spectrophotometric quantification of the recombinant IgG anti-IFNγ-N-term-Cfa, stored in splicing buffer
2) Resuspension of the lyophilic C-term-Cfa-Biotin (Recombinant or Synthetic) in splicing buffer (with or without 2M UREA) at the concentration of 0,75 mg/mL
3) Dilution of the two species at the desired concentration in splicing buffer, addition of 2 mM of the reducing agent TCEP to both and incubation for 30 min at 25°C under stirring
4) Mixing of recombinant IgG anti-IFNγ-N-term-Cfa and C-term-Cfa-Biotin equal volumes then incubation at the selected temperature under stirring
5) Monitor of the reaction overnight taking at different time points (T0', T30', T1h, T2h, T3h, T5,5h and T overnight) a sample (30 µl) for SDS-page analysis

Splicing Buffer*:* Phosphate dibasic dihydrate ($Na_2HPO_42H_2O$) 100 mM, NaCl 150 mM, EDTA 1 mM, TCEP 2 mM, pH 7.2

Splicing Buffer 2M UREA*:* Phosphate dibasic dihydrate ($Na_2HPO_42H_2O$) 100 mM, NaCl 150 mM, EDTA 1 mM, TCEP 2 mM, urea 2 M, pH 7.2

In the tables below are reported the different conditions of Cfa split intein reaction test (Table 10) performed in order to obtain the best conversion yield in the final product (recombinant IgG anti-IFNγ-Biotin)

Test	**Constructs**	**Concentration (mg/ml) Molarity (µM)**	**Molar ratio C-term-cfa/ N-term-Cfa**	**Temperature**	**Buffer**
A	Recombinant IgG anti-IFNγ-N-term-Cfa	2,55 mg/ml 15 µM	10X	25°C	Splicing Buffer
	C-term-Cfa-Biotin	0,75 mg/ml 150 µM			
B	Recombinant IgG anti-IFNγ-N-term-Cfa	2,55 mg/ml 15 µM	20X	25°C	Splicing Buffer
	C-term-Cfa-Biotin	1,5 mg/ml 300 µM			
C	Recombinant IgG anti-IFNγ-N-term-Cfa	2,55 mg/ml 15 µM	10X	25°C	Splicing Buffer 2M UREA
	C-term-Cfa-Biotin	0,75 mg/ml 150 µM			

Table10 A and B. Tested conditions for the protein trans splicing reaction by Cfa-split-intein between Recombinant IgG anti-IFNγ-N-term-Cfa and C-term-Cfa-Biotin

The best final chosen condition is highlighted by a red rectangle (Condition A).

Purification process of recombinant IgG anti-IFNγ-Biotin by Gel Filtration Chromatography (GFC)

Gel Filtration Chromatography (GFC) chromatographic conditions:

- Column: HiLoad 16/600 Superdex 200 pg; CV=120.6 mL (GE)
- Flow rate: 1.3 mL/min
- Wavelengths: 260/280 nm
- Gradient: isocratic in PBS buffer

Transfection protocol of ExpiCHO S cells™ (ThermoFisher scientific) using the plasmids containing the heavy chains (CH) and the light chains (CL) of the recombinant IgG anti-IFNγ-N-term-Cfa antibody, respectively

Number of cells required: 1.2×10^9

Culture volume to transfect: 200 mL

1. Subculture and expand ExpiCHO-S™ cells until the cells reach a density of approximately 4×10^6 –6×10^6 viable cells/mL.

Day –1: Split cells

2. On the day prior to transfection (Day –1), split the ExpiCHO-S™ culture from Step 1 to a final density of 3×10^6 –4×10^6 viable cells/mL and allow the cells to grow overnight.

Day 0: Transfect cells

3. On the next day (Day 0), determine viable cell density and percent viability. The cells should have reached a density of approximately 7×10^6 – 10×10^6 viable cells/mL. Viability should be 95–99% to proceed with transfection.

4. Dilute the cells from Step 2 to a final density of 6×10^6 viable cells/mL with fresh ExpiCHO™ Expression Medium, pre-warmed to 37°C. Swirl the flasks gently to mix the cells (125 rpm, 37°C, 8 % CO2).

Note: Discard the remaining cells; do not re-use high density cells for routine subculturing.

5. Prepare ExpiFectamine™ CHO/plasmid DNA complexes using cold reagents (4°C), as described below. It is not necessary to keep reagents on ice during complexation. Simply remove reagents from refrigeration and commence with DNA complexation.

Note: Total plasmid DNA in the range of 0.5–1.0 µg per mL of culture volume to be transfected is appropriate for most proteins.

a) Gently invert the ExpiFectamine™ CHO Reagent bottle 4–5 times to mix.

b) Dilute plasmid DNA with cold OptiPRO™ medium. Mix by swirling the tube and/or by inversion.

c) Dilute ExpiFectamine™ CHO Reagent with OptiPRO™ medium. Mix by swirling the tube and/or by inversion or gentel pipetting 2–3 times.

Note: Dilute the ExpiFectamine™ CHO reagent with cold OptiPRO™medium just prior to addition to the diluted DNA. Holding diluted ExpiFectamine™ CHO reagent for longer than 5 minutes before addition to diluted plasmid DNA can lead to reduced protein titers.

d) Add the diluted ExpiFectamine™ CHO Reagent to diluted DNA. Mix by swirling the tube or by inversion.

6. Incubate ExpiFectamine™ CHO/plasmid DNA complexes (from Step 5d) at room temperature for 1–5 minutes, and then slowly transfer the solution to the shaker flask from Step 4, swirling the flask gently during addition.

7. Incubate the cells in a 37° C incubator with a humidified atmosphere of 8% CO2 in air on an orbital shaker (125 rpm).

Day 1: Add ExpiFectamine™ CHO Enhancer and ExpiCHO™ Feed

At day 1st the eGFP cells (transfection D) were counted to estabilish transfection efficiency

8. On the day after transfection (Day 1, 18–22 hours post-transfection), perform the addition of 1,2 mL ExpiFectamine™ CHO Enhancer and 48 mL ExpiCHO™ Feed to the flask (High Titer Protocol), gently swirling the flask during addition. Transfer the flask to a 32°C incubator with a humidified atmosphere of 5% CO2 in air with shaking (125 rpm).

Note: It is not necessary to pre-warm the ExpiFectamine™ CHO Enhancer or the ExpiCHO™ Feed prior to addition to flasks.

Note: ExpiFectamine™ CHO Enhancer and ExpiCHO™ Feed may be premixed together immediately prior to adding to flasks.

Day 5:

9. Optimal time to harvest protein will depend on the specific properties of the protein being expressed and usually is after 10-12 days post-transfection.

Transient transfection	Ratio CL:CH	Constructs	MIX DNA	MIX ExpiFectamine	Final Volume
A-B-C	1:1	Recombinant IgG anti-IFNγ-N-term-Cfa antibody _CL	56,6 ug (56,6 ul)	640 ul ExpiFectamine	16 mL
		Recombinant IgG anti-IFNγ-N-term-Cfa antibody _CH	63,4 ug (63,4 ul)		
		OptiPRO medium	mL	7,4 mL	
D	-	eGFP	15 ug (15 ul)	80 ul	2 mL
		OptiPRO medium	985 ul	920 ul	

Table 11. Volumes of the transfection reagents and constructs used for the production of the recombinant IgG anti-IFNγ-N-term-Cfa antibody **(A-B-C)** and for the transfection control by using an expression vector containing eGFP

As reported in table, we performed three transient production of recombinant IgG anti-IFNγ-N-term-Cfa antibody (total volume= 260 mL) (Transfection A, B and C).

The supernatants were harvested at day 9 from transfection based on the data of cell viability and cell growth collected. The aim was to preserve the protein quality.

Cells were centrifuged at 220 rpm for 5 minutes, +4°C and supernatant was stored at -80°C.

LIAISON® IFNγ immunoassay prototype

The LIAISON® IFNγ immunoassay prototype is a direct test (antibody sandwich) that uses chemiluminescent immunoassay (CLIA) technology for the detection of interferon-γ (IFNγ) in human serum or plasma samples the use of recombinant IgGs anti-IFNγ. In particular, the immunoassay is characterized by a sandwich format in which a first biotinylated recombinant anti- IFNγ antibody is used as a capture binder on solid phase (streptavidinated beads), while a second anti- IFNγ antibody, linked to isoluminol-derivative is used as chemiluminescent tracer.

By the use of this prototype of IFNγ immunoassay we wanted to compare the immunoreactivity of our recombinant IgG anti- IFNγ-Biotin characterized by a site-specific biotinylation obtained through the Cfa split intein reaction and the same IgG anti-IFNγ antibody that was biotinylated on the ammine group of the Lysine residues by a NHS-PEG-Biotin reactive (standard random biotinylation).

Coating protocol (off-line):

Since, our recombinant anti- IFNγ antibody of solid phase biotinylated in a site specific way through the trans-slicing reaction contained a mix of biotinylated and non- biotinylated recombinat IgG anti- IFNγ, as a first step, it was necessary to execute a coating of this reagent on the paramagnetic beads conjugated with streptavidin (solid phase) and a subsequent washing step to eliminate from the solution the non- biotinylated IgG anti-IFNγ antibody, unable to link the solid phase.

In this specific case the M-280 Streptavidin-coupled Dynabeads® microparticles were used as solid phase at a final concentration of 0.25%. The recombinant IgG anti-IFNγ-biotin antibodies having a site specific biotinylation or a classical biotinylation were diluted at a final concentrations of 500 ng/ml in assay buffer, they were coated at Streptavidin-beats and used in the first incubation of the assay protocol described below.

Reagents and relative concentrations:

- Solid phase: 0,25% M-280 Streptavidin-coupled Dynabeads®+ recombinant IgG anti-IFNγ-biotin biotinylated in a site-specific way or by a classical biotinylation) at 500 ng/ml
- Tracers:
    1) MoAb anti human- IFNγ conjugated with Alexa Fluor 488 at 3,75 µg/mL
    2) MoAb anti-Alexa Fluor functionalized with chemiluminescent molecule at 7,5 µg/mL
- Sample detected: Standard curve with increasing concentration of INFγ diluted in PBS/BSA 0,1 %

Assay protocol:

In the first incubation of the immunoassay for the detection of IFNγ (antibodies sandwich), the recombinant IgG anti- IFNγ-Biotin coated at the paramagnetic beats was able to link the IFNγ present in the IFNγ standard curve, samples, calibrators or controls, after this first capture step, the IFNγ was recognized by a second anti-IFNγ conjugated with a fluorescent dye called Alexa fluor. Finally, the complex was detected through an anti-Alex fluor antibody, functionalized with an isoluminol derivative (isoluminol-antibody conjugate). During the second incubation, the assay buffer was added. It reduced non-specific, sample-related bindings. After each incubation, the unbound material is removed with a wash cycle.

The light signal emitted by the chemiluminescent molecule (isoluminol derivative) was measured by a photomultiplier as relative light units (RLU) and is indicative of IFNγ concentration present in the IFNγ standard curve, calibrators, samples or controls.

We chose to use two antibodies as tracers (the first one conjugated with an Alexa-Fluor dye detected by the second one conjugated with a chemiluminescent molecule emitting the signal) because this system allow a RLU signal amplification resulting in an increase of the INFγ immunoassay prototype sensitivity.

RESULTS

NON-CHROMATOGRAPHIC PURIFICATION PROCESS AND SITE SPECIFIC LABELLING OF C33 ANTIGEN

As previously described, we wanted to explore an innovative purification method without chromatographic steps, exploiting the Elastin Like Polypeptides (ELP) and the Intein auto cleavage activity for the production of the C33 antigen. After that, we wanted to perform its site-specific biotinylation by the express protein ligation technique in order to use the biotinylated C33 in the HCV immunoassay.

In this chapter we will talk about the downstream and labeling process of our antigen and the final characterization of the biotinylated C33 obtained through this unconventional protocol.

INDUCTION TESTS of C33-*Mxe*GyrA-ELP36

The fusion protein C33-*MxeGyrA*-ELP36 was expressed in BL21 (DE3) *E. coli* strain, in different fermentation media, at various temperatures, and OD of induction for the purpose of identifying the best expression condition in which to produce our target protein (Table 12) The SDS-page analysis showed that the protein had a good expression level in all performed conditions (Figure 39, red circles, C33-*MxeGyrA*-ELP36 expected molecular weight 67,9 KDa).

Fermentation	Vector	Medium	Temperature	Induction	Harvest time	[IPTG]
A	pET24-C33-*MxeGyrA*-ELP36	LB	+30°C	0,6 OD	3 hours	1mM
B	pET24-C33-*MxeGyrA*-ELP36	LB	+37°C	0,6 OD	3 hours	1mM
C	pET24-C33-*MxeGyrA*-ELP36	LB	+37°C	1,5 OD	3 hours	1mM
D	pET24-C33-*MxeGyrA*-ELP36	2xYT	+37°C	0,6 OD	3 hours	0,03 mM
E	pET24-C33-*MxeGyrA*-ELP36	2xYT	+15°C	0,6 OD	3 hours	0,03 mM

Table 12. Different fermentation conditions used for C33-*Mxe*GyrA-ELP fusion protein expression.

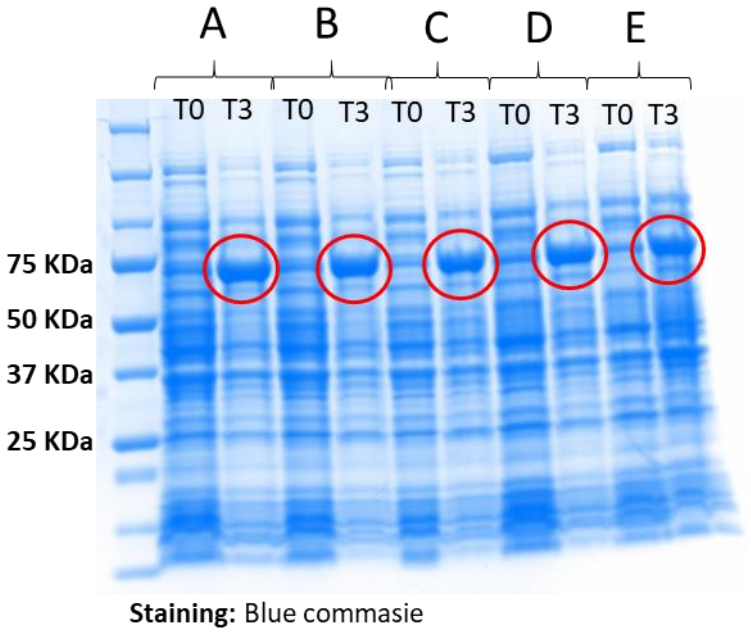

Figure 39. SDS-PAGE analysis showing the induction test of BL21(DE3) pET24-C33-*Mxe*GyrA-ELP36, fermented in different media and at various temperatures: see table 12 for experimental conditions. Red circles indicate C33-*Mxe*GyrA-ELP36 target protein.

In order to choose the best condition among those listed above in terms of fusion protein expression levels, we performed a densitometric analysis of the bands related to the induction test (Figure 40). If we analyze the C33-*MxeGyrA*-ELP36 bands' volume, considering the same OD (Optical Density of bacterial culture) loaded onto gel (0,6 OD), the fermentation performed in LB at +30°C (fermentation A) seemed to produce higher quantity of C33-*MxeGyrA*-ELP36 protein than the others one (see the histogram below).

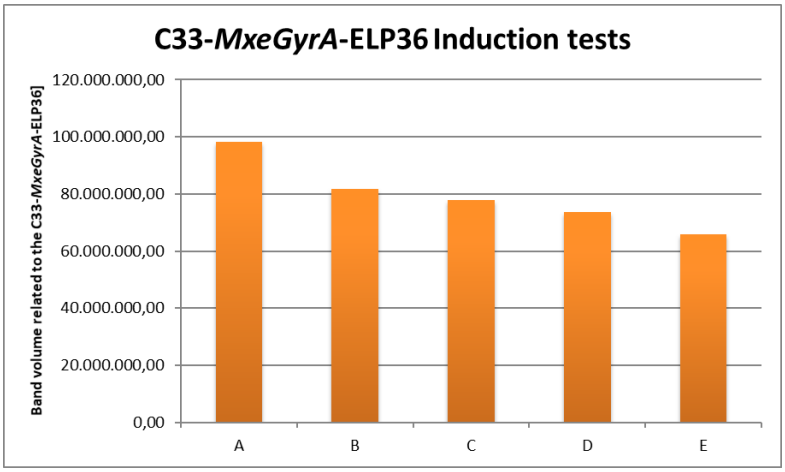

Figure 40. Histogram showing the bands' volume of C33-*Mxe*GyrA-ELP36, obtained from different fermentation conditions, considering the same optical density of bacterial culture (0,6 OD) loaded onto gel (induction test).

We have further investigated the possibility to produce the C33-*MxeGyrA*-ELP36 in the Auto Induction Medium (AIM). We performed two fermentations at different temperatures (Table 13) in this medium, to compare the expression levels of our fusion protein in these conditions with the best one previously obtained (LB a +30°C). The SDS-page analysis indicated that we obtained a very low expression level during the fermentation in AIM at +15°C (fermentation B, red circle), while we reached a good expression of our protein in the same medium at +37°C (fermentation A, red circle). However, the target protein expression level in this last condition (AIM at +37°C) was lower than that one in LB at +30°C, considering the same 0,6 OD loaded onto gel (figure 41).

Fermentation	Vector	Medium	Temperature	Induction	Harvest time	[IPTG]
A	pET24-C33-*MxeGyrA*-ELP36	AIM	+37°C	-	24 hours	-
B	pET24-C33-*MxeGyrA*-ELP36	AIM	+15°C	-	24 hours	-
C	pET24-C33-*MxeGyrA*-ELP36	LB	+30°C	0,6	3 hours	1 mM

Table 13. Further fermentation conditions used for C33-*Mxe*GyrA-ELP fusion protein expression

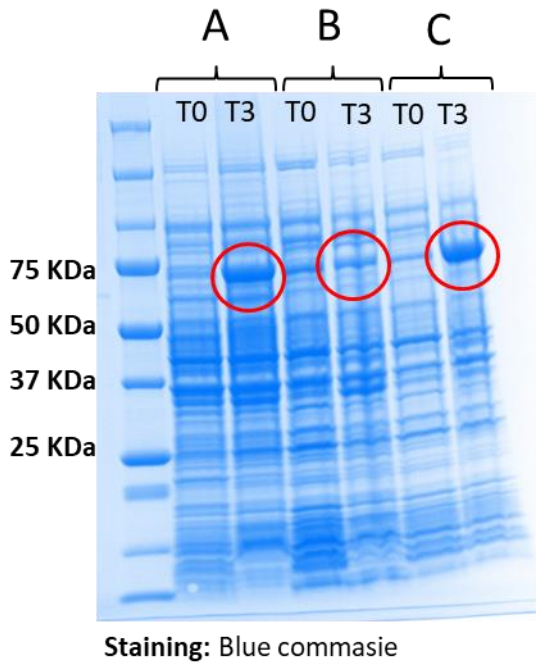

Figure 41. SDS-PAGE analysis showing the induction test of BL21(DE3) pET24-C33-*Mxe*GyrA-ELP36, fermented in AIM medium at +37°C and +15°C, and in LB medium at +30°C (see table 13 for experimental conditions). Red circles indicate the time of the harvest of the C33-*Mxe*GyrA-ELP36 target protein for each fermentation.

At this point, we analyzed another important parameter for confirming the best fermentation condition: the solubility of the target protein.

For this aim, we evaluated the solubility of our protein in all fermentation conditions previously tested.

SOLUBILITY TEST of C33-*Mxe*GyrA-ELP36

From the SDS-page analysis of the solubility test it was clear that the C33-*MxeGyrA*-ELP36 protein was mainly soluble in all the conditions that we had considered (Figure 42, red circles). In particular, a high percentage of soluble protein was present in the conditions A, B and E.

Moreover, we observed that during the fermentations in LB at +37°C with induction at 1,5 OD (C) and in 2xYT at +37°C (D) were produced a little percentage of insoluble proteins that we hypothesized to be an insoluble fraction of the C33-*MxeGyrA*-ELP36 (Figure 41, green circles).

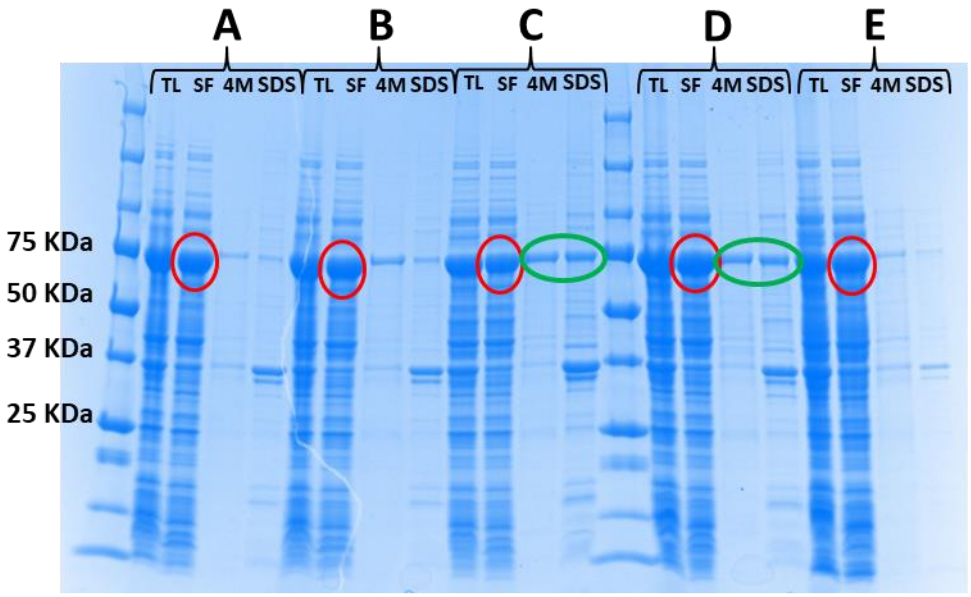

Figure 42. SDS-PAGE analysis showing the solubility test of BL21 (DE3) pET24-C33-*Mxe*GyrA-ELP36, fermented in the conditions reported in tables 12 and 13. Red circles indicate the C33-*Mxe*GyrA-ELP36 present in soluble fractions while green circles indicate the C33-*Mxe*GyrA-ELP36 present in insoluble fractions.

Following these results, we analyzed various parameters including the composition of the medium (complexity of components and costs), the fermentation time, the expression level and the solubility of our fusion protein; after these considerations we established that the best condition to produce the C33-*Mxe*GyrA-ELP36 was in LB medium at +30°C with IPTG induction at 0,6 OD (Fermentation A).

After finding the best condition for the fermentation of the C33-*MxeGyrA*-ELP36–fusion protein, we started to work on the setting of the purification process.

To exploit the characteristics of Elastin Like Polypeptides (ELPs) during the purification process through the Inverse Transition Cycle (ITC), described in the introduction, the first parameter to be evaluated was the NaCl concentration in which we observed the precipitation of our fusion protein at +25°C.

PRECIPITATION TESTS OF C33-*MxeGyrA*-ELP36

After the resuspension of the bacteria wet pellets (derived from the fermentations in LB at +30°C) in a phosphate buffer, the sonication and centrifugation of the samples, we add to the supernatants a specific volume of NaCl stock solution to obtain samples with an increasing concentration of NaCl, comprising from 0,5M to 2,5M (Table 14). After that, we left to precipitate the supernatant containing our target protein at room temperature (RT) with stirring for 1 hour. Finally, we centrifuged at +25°C and loaded onto gel an aliquot of supernatants and an aliquot of pellets resuspended in SDS-PAGE sample buffer (see details in materials and methods).

	NaCl 0,5 M	NaCl 1 M	NaCl 1,5 M	NaCl 2 M	NaCl 2,5 M
Supernatant (ml)	1,3	2	2	2	2
NaCl 5M (ml)	0,144	0,5	0,857	1,33	2
Final Volume (ml)	1,444	2,5	2,857	3,33	4

Table 14. Volumes and NaCl concentration used for the first precipitation test of the C33-*Mxe*GyrA-ELP fusion protein

The SDS-PAGE analysis of this test showed that the C33-*MxeGyrA*-ELP36 protein at NaCl concentrations of 0,5-1 and 1,5 M was mainly present in the supernatant, while at NaCl concentrations of 2 and 2,5 M it was almost completely precipitated and therefore presents in the pellet (Figure 43, red circles).

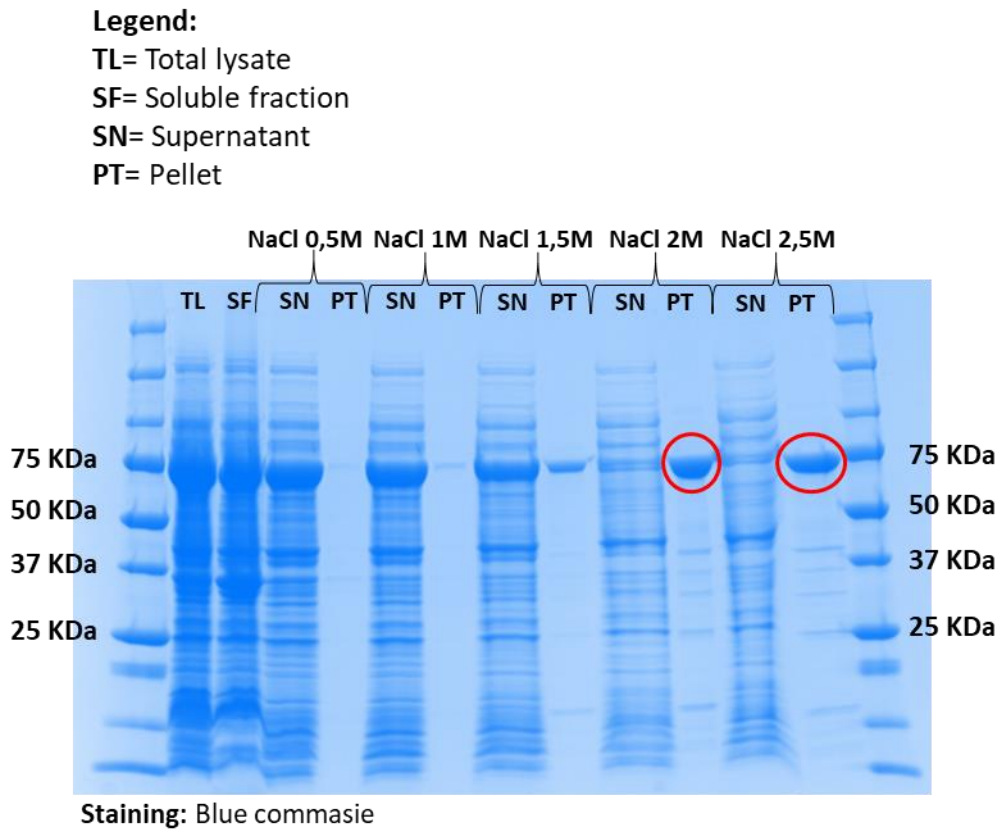

Figure 43. SDS-PAGE analysis showing the first precipitation test of BL21 (DE3) pET24-C33-*Mxe*GyrA-ELP36, fermented in LB at 30°C in which we tested the precipitation level of our fusion protein at different NaCl concentrations. Red circles indicate the C33-*Mxe*GyrA-ELP36 precipitated and then presents in the pellet.

To better understand the best NaCl concentration to use for the precipitation of our target protein in the ITC process we thought to perform another precipitation test in a more selective range of NaCl concentrations, from 1,5M to 2M (Table 15 and figure 44).

	NaCl 1,5 M	NaCl 1,6 M	NaCl 1,7 M	NaCl 1,8 M	NaCl 1,9 M
Supernatant (ml)	2	2	2	2	1,7
NaCl 5M (ml)	0,857	0,941	1,03	1,125	1,048
Final Volume (ml)	2,857	2,941	3,03	3,125	3,1

Table 15. Volumes and NaCl concentration used for the second precipitation test of the C33-*Mxe*GyrA-ELP fusion protein

The SDS-PAGE analysis showed that the C33-*MxeGyrA*-ELP36 at the concentration of NaCl among 1,5M and 1,8M was mainly present in the supernatant, while at the concentration of NaCl 1,9M it was almost completely precipitated and thus presented in the pellet (red circle). Analyzing the results obtained from these two precipitation tests we could conclude that the ideal concentration of NaCl in which to perform the fusion protein precipitation during the ITC was 2M. Also at NaCl concentration higher than 2M our fusion protein was almost totally in the pellet, but increasing the salt concentration we could promote the precipitation of other proteins or contaminants.

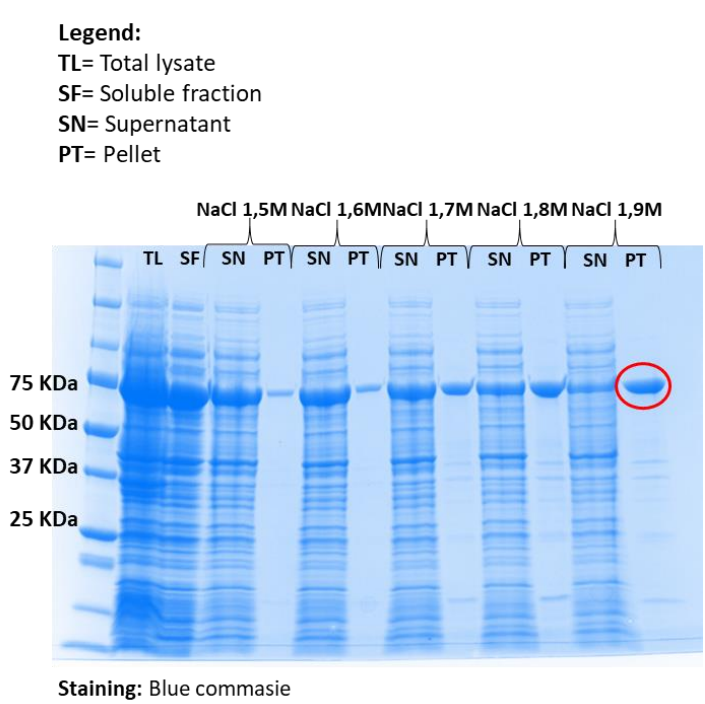

Figure 44. SDS-PAGE analysis showing the second precipitation test of BL21 (DE3) pET24-C33-*Mxe*GyrA-ELP36, fermented in LB at 30°C in which we tested the precipitation level of our fusion protein in a narrower range of NaCl concentration than the previous one. Red circle indicates the C33-*Mxe*GyrA-ELP36 precipitated and then presents in the pellet.

PURIFICATION PROCESS AND SITE-SPECIFIC BIOTINYLATION OF C33 ANTIGEN

The purification process of the C33 antigen currently performed in our company includes several chromatographic steps that require many days of work and in which, inevitably, there is a considerable loss of target protein. These drawbacks affect the yield, the production and productivity of the C33 antigen downstream process. Furthermore, since a biotinylated version of C33 protein is used in the current Liaison HCV IgG assay, it is necessary to realize the antigen biotinylation after the purification process. The current biotinylation procedure of C33 antigen consists in the random conjugation of Maleimide-PEG-Biotin molecules on the side chain of cysteine residues present in the antigen polypeptide sequence. This labelling process is characterized by low efficiency, because is a complex procedure that requires several reaction steps, because it is random and therefore not controllable and leads to conjugate heterogeneity. Moreover, it is performed after the purification process and then it entails other working days.

For all these reasons we tried to improve the C33 purification process developing a not conventional purification method easier and faster than that currently used in HCV immunoassay and, especially, without chromatographic steps. Moreover, we thought to realize a site-specific biotinylation of our antigen directly linked to the purification process to optimize the experimental time (productivity), to have a controllable reaction and to increase the performance of the C33 antigen in the HCV immunodiagnostic assay.

PURIFICATION PROCESS OF C33 ANTIGEN

Once established the precipitation conditions of our fusion protein, we thought to purify the C33 antigen exploiting the two technological tools present in our construct: the intein-autocleavage activity and the Elastin-Like-Polypeptides (ELP). For this purpose, we combined these technologies developing a new non-chromatographic purification process Figure 46.

Initially, we performed two repeated rounds of ITC (details reported in materials and methods section). This method allows to drastically remove, after several precipitation and solvation steps of ELP fusion protein followed by centrifugation at different temperatures, the contaminants from the C33-*MxeGyrA*-ELP36 and to obtain a purified fusion protein. After that, we promoted the release of C33 target protein from the *MxeGyrA*-ELP36 (tag) triggering the intein *MxeGyrA* autocleavage activity through a reducing agent called MESNA. The success of the tag cleavage was reached because in our construct we had a C-terminal mutation in the intein splicing junction (Asn->Ala) and then only the N-terminus cleavage was possible (Figure 45).

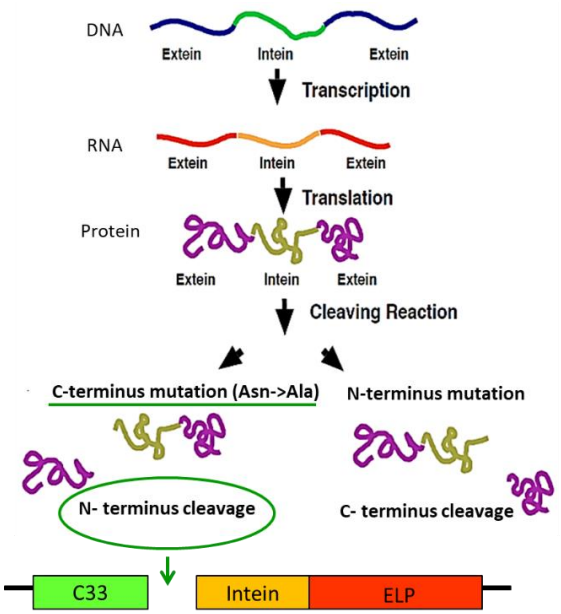

Figure 45. Result of the C33-*MxeGyrA*-ELP36 cleavage with MESNA considering the C-terminal mutation in the splicing junction of our construct

It's fundamental underline that the cleavage with MESNA generated a C33 antigen with a C-terminal thioester end that was indispensable for its site-specific-biotinylation. Finally, we performed the third round of ITC to separate the tag from the C33-thioester.

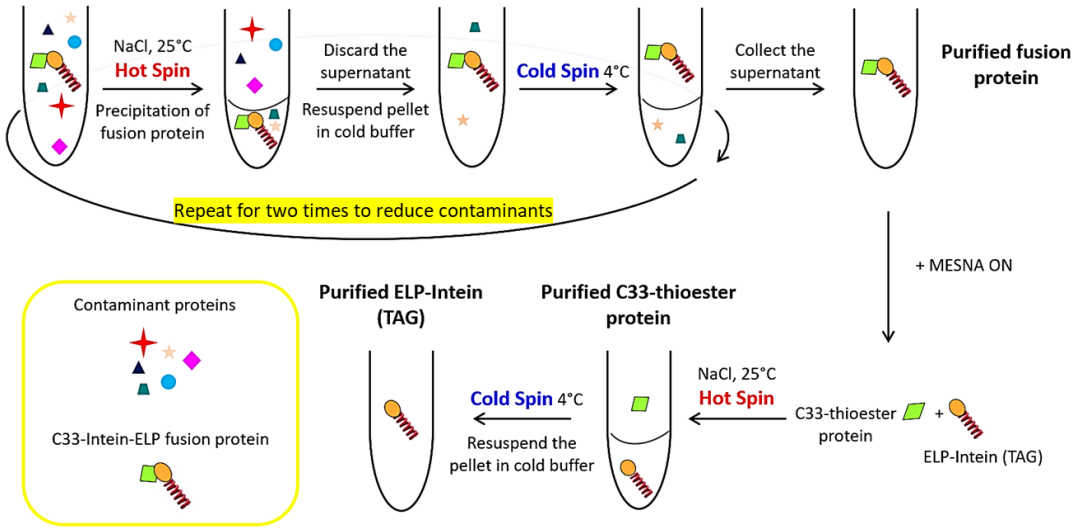

Figure 46. Schematic representation of the purification process of C33 antigen. It consists in two rounds ITC, the cleavage of the C33-*Mxe*GyrA-ELP36 fusion protein with MESNA and another round ITC (the third one) to separate our target protein (C33-thioester) from the tag (*MxeGyrA*-ELP36).

The SDS-PAGE analyzing the ITC process described above is shown in Figure 47. HS (Hot Spin) lanes represent the supernatants obtained after precipitation process and centrifugation at +25°C; in these lanes the ELP-fusion target protein is therefore not present. CS (Cold Spin) lanes represent the supernatants obtained after resuspension process and centrifugation at +4°C; in these fractions the ELP-fusion protein is present. After the first precipitation-solvation round (1CS lane), the C33-*Mxe*GyrA-ELP36 target protein reached a good purity grade which was further increased by a second precipitation-resuspension cycle (2CS lane). MESNA cleavage lane indicates the sample after cleavage with MESNA. As clearly shown in the SDS-PAGE analysis, the cleavage reaction occurred successfully (both cleavage products, C33 antigen and *Mxe*GyrA-ELP36 tag, are visible) and only a small amount of the entire precursor protein (C33-*Mxe*GyrA-ELP36) remains. Moreover, the really interesting result is present on the lane of 3HS (underline by the green rectangle and arrow, Figure 47) where we can observe only the band of C33-thioester. This is a very important result for us because, after the third round ITC, we successfully separated the *MxeGyrA*-ELP36 tag from target protein achieving a C33-thioester antigen with high purity and, for the first time in our laboratory, we managed to get a purified protein without chromatographic steps.

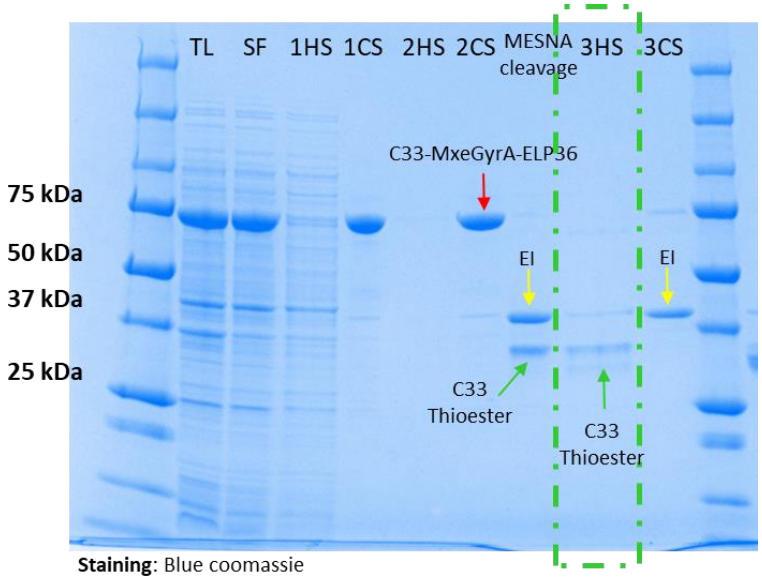

TL: Total Lysate
SF: Soluble fraction
1HS: 1° hot spin
1CS: 1° cold spin
2HS: 2° hot spin
2CS: 1° cold spin
3HS: 3° hot spin
3CS: 3° cold spin
EI: MxeGyrA-ELP36

Figure 47. SDS page analysis of an entire purification process of C33 antigen through ELP-Intein system. The C33-*Mxe*GyrA-ELP36 fusion protein is indicated by the red arrow, the EI tag by the yellow arrow and the C33-thioester by the green arrow.

SITE-SPECIFIC BIOTINYLATION OF C33-THIOESTER

After the C33 antigen purification, the next step was its site-specific biotinylation exploiting the C-terminal thioester end on the antigen obtained thanks to the tag cleavage with MESNA. We performed this conjugation through the Express Protein Ligation method (EPL) widely described in the introduction. In particular, as reported in Figure 48, we decided to link a biotinylated peptide having a free thiol group of a cysteine residue at its N-terminal to our purified C33 having a thioester end at its C-terminal, in reducing environment. The specific interaction between the thiol group on the biotinylated peptide and the thioester end on the C33 antigen leads to the peptide bond formation and to obtain a biotinylated C33.

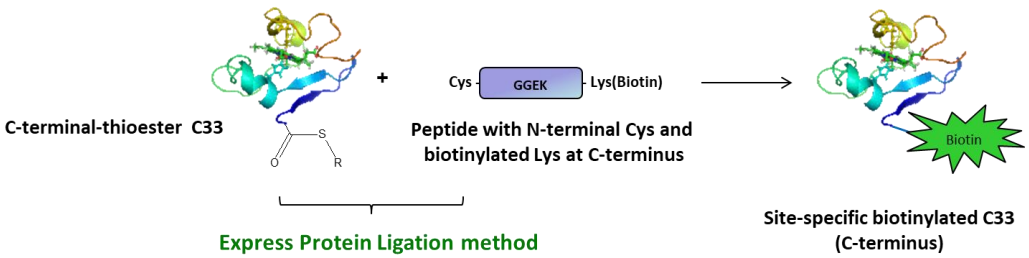

Figure 48. Site-specific biotinylation of C33-thioester antigen through the Express Protein Ligation method (EPL).

GEL FILTRATION CHROMATOGRAPHY OF BIOTINYLADED C33

After the Site-specific biotinylation of C33, we performed a Gel filtration Chromatography step (GFC) to separate the biotinylated peptide, used in molar excess to favor the conjugation reaction of our antigen, from the biotinylated C33.

The GFC chromatogram in figure 49 shows a unique peak (highlighted in green) corresponding to the biotinylated C33 and a high 260 nm signal at higher retention volumes that represents the biotinylated peptide in excess.

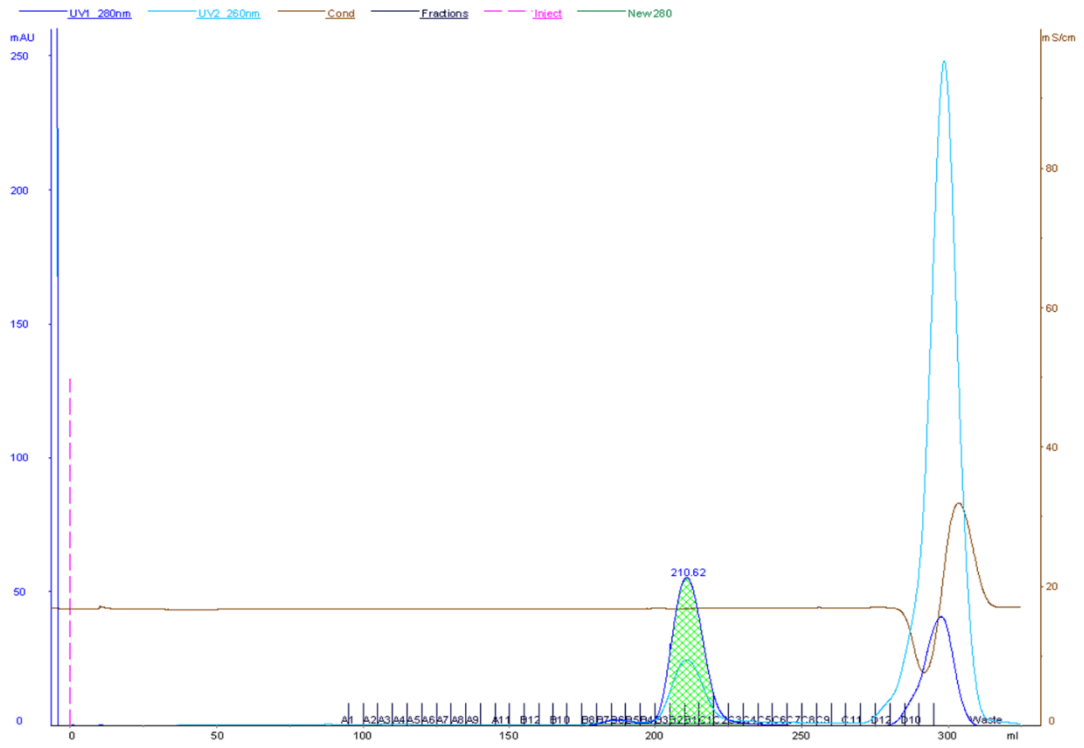

Figure 49. The chromatogram of biotinylated C33 obtained later Gel filtration chromatography (GFC).

To verify the reproducibility of our innovative purification process followed by the site-specific biotinylation of C33 antigen, we realized three lots of biotinylated C33 starting from a fermentation volume of 1000 ml. The results indicated that the new purification method and the site-specific biotinylation are efficient and reproducible because we obtained a similar yield, production and productivity of biotinylated C33 antigen in all three lots (Table 16)

	Concentration (mg/ml)	Wet pellet (gr)	Quantity (mg)	Fermentation volume (ml)	Yield (mg/gr)	Production (mg/l)	Productivity (mg/l/h)
Lot 1	0,542	6	20,32	1000	3,4	20,32	0,28
Lot 2	0,552	5,2	19,31	1000	3,7	19,31	0,27
Lot 3	0,401	4,9	16,03	1000	3,3	16,03	0,22

Table 16. Final experimental data obtained from three different lots of biotinylated C33.

RETARDATION ASSAY OF BIOTINYLATED C33

To verify if our antigen was really biotinylated and also to know the biotinylation efficiency, we performed a simple experiment called retardation assay. This technique, described in detail in materials and methods, is based on the interaction between biotin and streptavidin. To allow a clear interpretation of the results derived from this biotinylation test it's important to remember that: if the target protein is conjugated with one or more molecules of biotin, after the addition of the streptavidin in that sample, complexes biotin-streptavidin will form an then we will observe onto SDS-page gel a band shift of the biotinylated protein at higher molecular weight compared to a non-biotinylated protein that will show on SDS-page gel a band according to its own expected molecular weight.

The SDS-PAGE analysis shows the comparison among a non-biotinylated C33 protein, the C33-Atag (negative control), the biotinylated C33 currently used in our HCV immunodiagnostic assay, the Diasorin C33-biotin (positive control) and our three lots of biotinylated C33 obtained through the non-chromatographic purification process followed by the site-specific biotinylation (lot 1, lot 2 and lot 3). Every sample was loaded two times, with and without the addition of streptavidin in order to appreciate on the SDS-PAGE gel the band shift at high molecular weight in the biotinylated sample. Observing the results of the retardation assay on SDS-PAGE gel we noted that:

- as expected, after the addition of streptavidin, the C33-Atag sample did not form complexes at high molecular weights and we could observe the presence of the same band corresponding to the correct molecular weight of this protein (~30 kDa) in both of the two lanes. This datum indicated that the C33-Atag was not biotinylated.

- In opposite to the previous situation, the Diasorin C33-biotin partially interacted with the streptavidin because complexes at high molecular weights were formed after the addition of streptavidin. In this case, we observed the same band at ~37 kda of the Diasorin C33-biotin in both of the two lanes, even if it is slightly less intense after the streptavidin addition. For this reason, we deduced that about only half of the Diasorin C33-Biotin was biotinylated.

Our three lots of biotinylated C33 formed complexes at high molecular weight after the streptavidin addition and, for the first time, we observed the complete disappearance of the band that represented the biotinylated C33. Based on these results, we can say that the biotinylation of our three lots occurred with an efficiency close to 100 %.

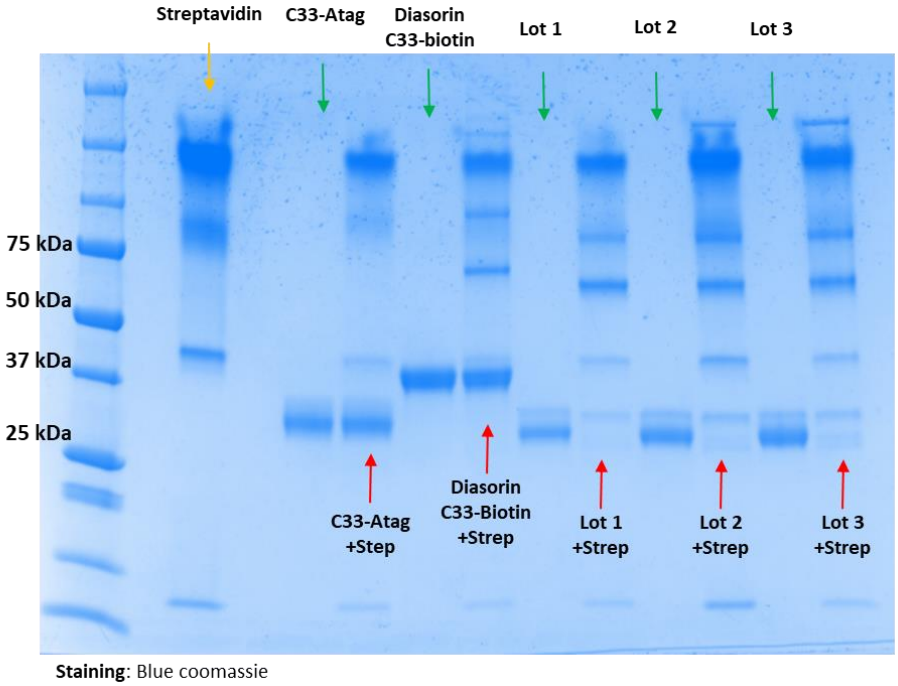

Figure 50. Retardation assay of our three different lots of biotinylated C33 compared with C33-Atag (negative control) and with Diasorin C33-biotin (positive control). The yellow arrow indicates the streptavidin, the green arrows the samples without streptavidin and the red arrows the samples with streptavidin.

IMMUNOREACTIVITY TEST OF BIOTYNILATED C33

Finally, we wanted to verify the immunoreactivity of our three lots of biotinylated C33 comparing them with the Diasorin C33-biotin currently used in the Diasorin HCV immunodiagnostic assay.

In the LIAISON XL Murex HCV Ab assay, illustrated below, the biotinylated C33 is linked to the paramagnetic beads (solid phase) previously functionalized with streptavidin.

When a human HCV positive blood sample, which contains antibodies against the C33, is incubated with the paramagnetic beats, its antibodies bind the biotinylated C33. After this incubation, the complex is recognized trough an anti-human IgG conjugated with a chemiluminescent molecule. The emitted signal is detected by the instrument and expressed in Relative Light Unit (RLU). The RLU values obtained, correlate with the different level of infectivity of positive samples.

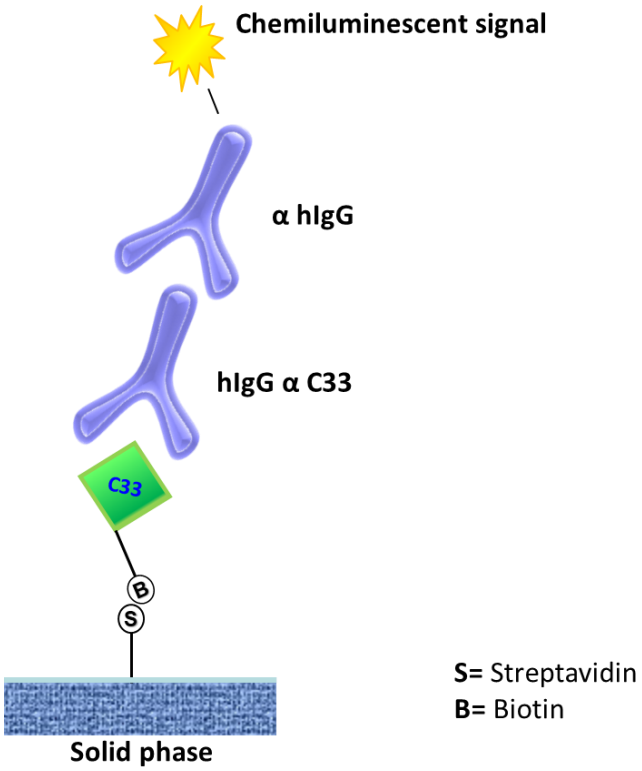

Figure 51. Schematic representation of LIAISON XL Murex HCV Ab assay.

In particular, during this experiment we replaced our biotinylated C33 to the Diasorin C33-biotin maintaining the setting and the other reagents of the LIAISON XL Murex HCV Ab assay in order to compare only the immunoreactivity of the two biotinylated antigens.

For the purpose to prove the immunoreactivity of the biotinylated C33, we test our antigen in the LIAISON XL Murex HCV Ab assay on a panel of human HCV negative samples and on a panel of human HCV positive samples in comparison to the biotinylated C33 currently used. It's important to underline that each experiment was analyzed in triplicate in order to confirm the data reproducibility.

The panel of the human HCV negative blood samples, present in Figure 52, showed that the RLU signals resulted comparable using in the HCV immunoassay the Diasorin C33-biotin or our three lots of biotinylated C33. These data demonstrate the negativity of the samples tested.

The histogram about the panel of the human HCV positive blood samples (Figure 53) displayed comparable RLU signal, higher than the cut-off previously set, both coating in solid phase the Diasorin C33-biotin and our three lots of biotinylated C33. These results indicate the positivity of all the samples tested and a similar immunoreactivity among the Diasorin C33-biotin and our three lots of biotinylated C33.

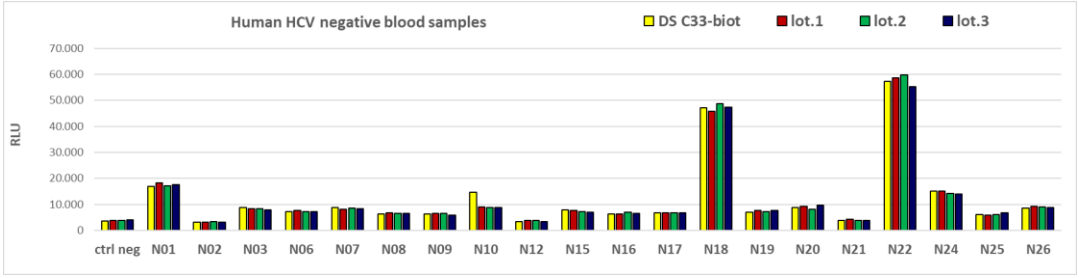

Figure 52. Histogram about the panel of human HCV negative blood samples tested in the LIAISON XL Murex HCV Ab assay.

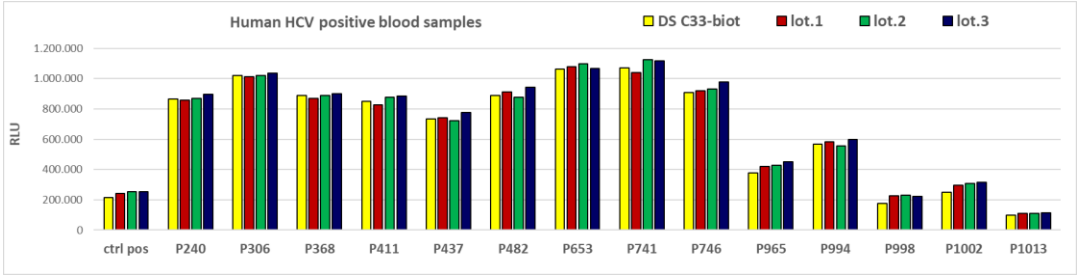

.

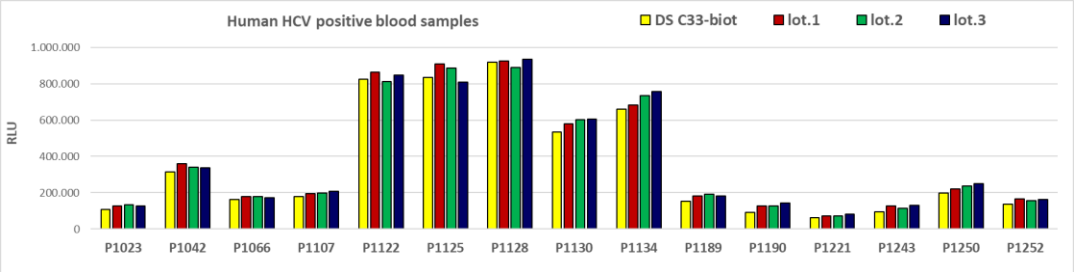

Figure 53. Histograms of the panel of human HCV positive blood samples analyzed in the LIAISON XL Murex HCV Ab assay.

SENSITIVITY TEST OF BIOTINYLATED C33 WITH A LOWER CONCENTRATION THAN THE CURRENTLY USED IN LIAISON XL Murex HCV Ab ASSAY

Since the Diasorin C33-biotin is currently used in the HCV immunoassay at the concentration of 5 µg/ml but the retardation assay demonstrated that only half of this antigen is biotinylated, this fact determines that a remarkable portion of C33 is not able to bind the paramagnetic beads and therefore it is removed during the wash step of the solid phase preparation. For this reason we thought to performed an experiment in which we compared the immunoassay sensitivity by using the Diasorin C33-biotin and our three biotinylated C33, that appeared totally biotinylated from the retardation assay results, at a lower concentration (3 µg/ml) compared to that currently used (5 µg/ml). In this way, we wanted to verify if our antigen could be used at a lower concentration than the standard value keeping a good sensitivity on the entire panel of human HCV positive blood samples, in particular in the C33 prevalent ones.

As in previously experiment, we performed the HCV immunoassay on a wide panel of human HCV negative and positive blood samples (Tables 17 a and b) and also in this case, we achieved the experiment in triplicate to confirm the data reproducibility.

The results derived from this experiment indicated that our biotinylated C33 could be really used in the LIAISON XL Murex HCV Ab assay at 3 µg/ml because the human HCV positive blood samples, C33 prevalent (in bold, table) maintain an index, calculated as RLU signal/cut-off, significantly higher by using our biotinylated antigen than the current Diasorin C33-biotin, (Table b). Therefore, by these very interesting data we demonstrated the more sensitivity of our biotinylated C33 than the Diasorin C33-biotin.

			Index	Index
	Diasorin C33-Biotin	**Lot 3**	**Diasorin C33-Biotin**	**Lot 3**
id	**RLU**	**RLU**	**RLU signal /Cut-off**	**RLU signal /Cut-off**
ctrl neg	2.950	2.428	0,03	0,03
N01	16.127	15.978	0,19	0,19
N02	6.093	4.333	0,07	0,05
N03	11.747	10.145	0,14	0,12
N06	11.506	9.553	0,13	0,11
N07	4.821	3.731	0,06	0,04
N08	10.181	6.362	0,12	0,07
N09	10.031	8.723	0,12	0,10
N10	9.022	7.210	0,10	0,08
N12	8.602	8.360	0,10	0,10
N15	3.372	2.927	0,04	0,03
N16	7.759	6.674	0,09	0,08
N17	11.124	8.986	0,13	0,10
N18	12.016	9.349	0,14	0,11
N19	5.886	5.422	0,07	0,06
N20	6.754	4.816	0,08	0,06
N21	13.285	8.410	0,15	0,10
N22	52.930	50.125	0,62	0,58
N24	9.396	8.995	0,11	0,10
N25	74.756	66.448	0,87	0,77
N26	16.425	15.991	0,19	0,19
Cut-Off	**86.000**	**86.000**		

Table 17a. Panel of human HCV negative blood samples selected for HCV immunoassay using the biotinylated C33 at 3 µg/ml.

			Index	Index
	Diasorin C33-Biotin	**Lot 3**	**Diasorin C33-Biotin**	**Lot 3**
id	**RLU**	**RLU**	**RLU signal /Cut-off**	**RLU signal /Cut-off**
ctrl pos	***193.494***	***286.908***	***2,2***	***3,3***
P240	932.450	973.052	10,8	11,3
P306	1.124.193	1.154.800	13,1	13,4
P368	958.434	957.016	11,1	11,1
P411	951.636	988.383	11,1	11,5
P437	872.014	831.303	10,1	9,7
P482	948.011	986.010	11,0	11,5
P653	1.162.484	1.265.050	13,5	14,7
P741	1.140.327	1.264.751	13,3	14,7
P746	992.233	1.031.688	11,5	12,0
P965	***354.911***	***497.352***	***4,1***	***5,8***
P994	***606.856***	***614.142***	***7,1***	***7,1***
P998	***167.884***	***263.292***	***2,0***	***3,1***
P1002	***246.338***	***327.893***	***2,9***	***3,8***
P1013	***93.944***	***114.375***	***1,1***	***1,3***
P1023	***96.093***	***122.425***	***1,1***	***1,4***
P1042	339.477	320.875	3,9	3,7
P1066	***162.463***	***202.231***	***1,9***	***2,4***
P1107	***159.066***	***222.429***	***1,8***	***2,6***
P1122	821.270	741.994	9,5	8,6
P1125	983.412	1.012.423	11,4	11,8
P1128	989.267	1.026.245	11,5	11,9
P1130	580.195	611.656	6,7	7,1
P1134	688.867	752.444	8,0	8,7
P1189	***134.464***	***211.916***	***1,6***	***2,5***
P1190	***100.728***	***148.324***	***1,2***	***1,7***
P1243	***102.367***	***150.652***	***1,2***	***1,8***
P1250	***158.568***	***276.206***	***1,8***	***3,2***
P1252	***129.623***	***195.954***	***1,5***	***2,3***

Table 17b. Panel of Human HCV positive blood samples selected for HCV immunoassay using the biotinylated C33 at 3 µg/ml.

To sum up the results achieved until now, we can say that:

- we developed an innovative purification process for the C33 antigen without chromatographic steps through which we obtained a C33-thioester with high purity.
- We realized a site-specific biotinylation of C33-thioester and we verified the very high efficiency of this reaction through the retardation assay.
- We demonstrate that our three lots of biotinylated C33 had an immunoreactivity comparable to the Diasorin C33-biotin in the LIAISON Murex HCV Ab assay.
- Our biotinylated C33 could be use at a lower concentration than the current one in the HCV immunoassay maintaining a good sensitivity.

SHORT PURIFICATION AND LABELLING PROTOCOL OF C33 ANTIGEN

OPTIMIZATION OF C33 PURIFICATION PROCESS

Our next aim was to further optimize the non-chromatographic purification process of C33 antigen described in the previous paragraphs; in particular we tried to improve the productivity of the purification method decreasing the working days needed to get the biotinylated C33.

To achieve our goal, we developed a new purification process in which we executed two rounds of ITC, as it was already done in our previous protocol, to drastically reduce the contaminants and therefore to obtain a C33-*MxeGyrA*-ELP36 target protein with a high purity degree.

After that, we decided to perform the cleavage with MESNA and the site-specific biotinylation of C33 simultaneously: MESNA and the biotinylated peptide were added to the sample simultaneously and the reaction was performed overnight at room temperature with stirring.

Finally, in order to separate the biotinylated C33 from the *MxeGyrA*-ELP36 (tag), we thought to exploit the different hydrophobicity of the two species performing a Hydrophobic Interaction Chromatography (HIC). The coupling of cleavage and site-specific biotinylation reactions followed by HIC would allow us to obtain the biotinylated C33 a day earlier than our previous purification process.

To understand which was the most suitable hydrophobic resin for the separation of the biotinylated C33 from the *MxeGyrA*-ELP36, we realized a scouting of hydrophobic resins with different characteristics (Table 18).

At the beginning, we explored different resins but we maintained constant the other chromatographic conditions.

Hydrophobic resin	**[Starting Ammonium sulphate] mM**	**Elution method**
Hitrap Phenyl HP	500	Linear gradient from 0 to 100 % of elution buffer
Hitrap Butyl-S-FF	500	Linear gradient from 0 to 100 % of elution buffer
Hitrap Octyl-FF	500	Linear gradient f from 0 to 100 % of elution buffer

Table 18. HIC conditions to separate C33 antigen from the *MxeGyrA*-ELP36 tag: first scouting on different HIC resins

While the Phenyl HP resin was not able at all to separate the C33 antigen from the *MxeGyrA*-ELP36 tag, both Hitrap Butyl-S-FF and Hitrap Octyl-FF resins were able to discriminate the two species: both resins showed in the chromatographic profiles two low resolved peaks; the SDS-page analysis showed that while in the first peak was mainly present the biotinylated C33, in the second peak was mainly present the *MxeGyrA*-ELP36.

Since the use of the Hitrap Butyl-S-FF resin showed a better separation of the two species than the Hitrap Octyl-FF resin, we selected the Hitrap Butyl-S-FF resin to continue our optimization.

In figure 54 are shown the chromatographic profile and the SDS-page analysis of the HIC performed by the Hitrap Butyl-S-FF resin with an ammonium sulphate concentration of 500 mM and an elution through a linear gradient.

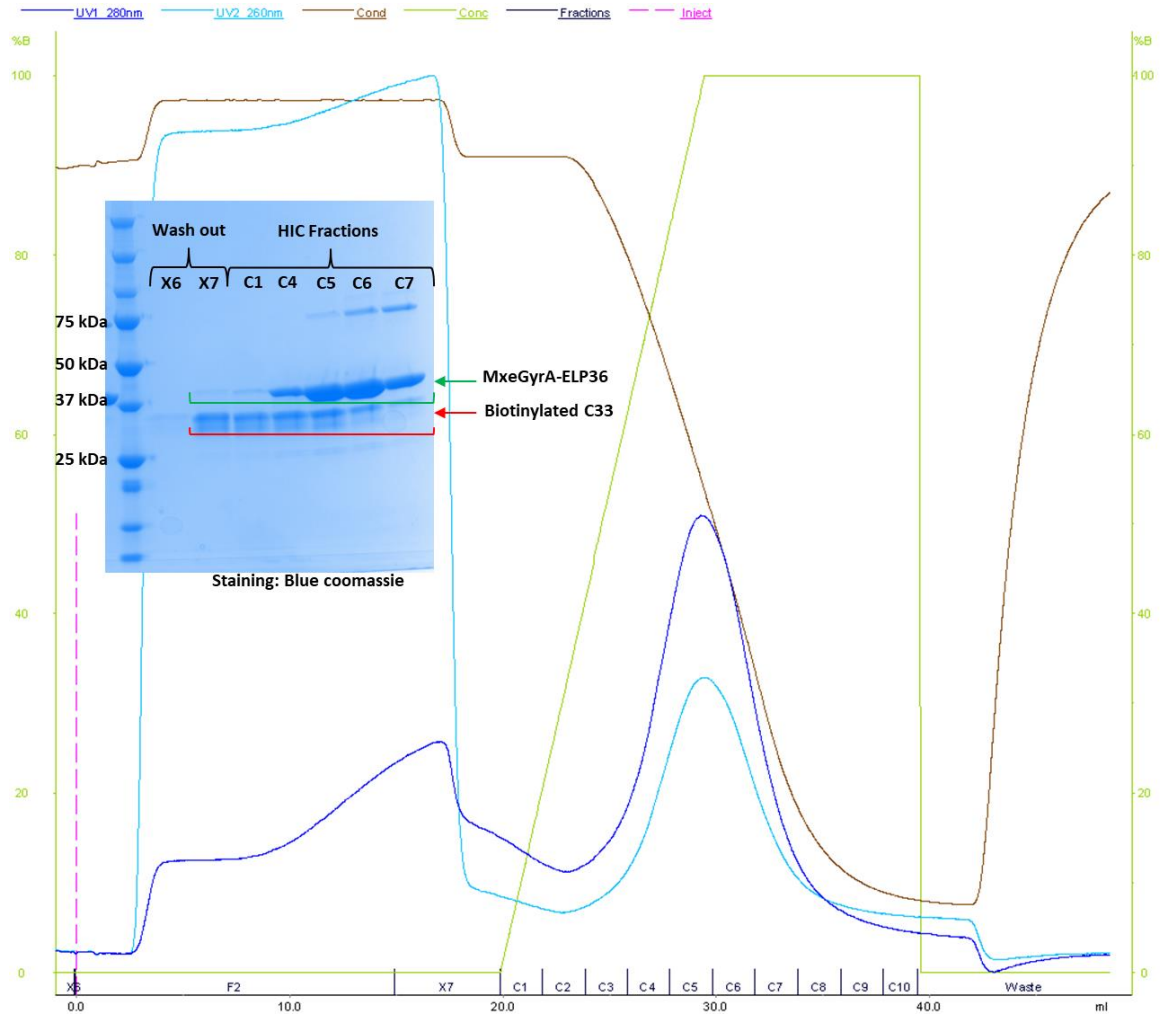

Figure 54. Chromatogram and relative SDS-PAGE analysis of HIC performed with the Hitrap Butyl-S-FF resin, at 500 mM of ammonium sulfate and by a linear gradient elution.

In order to further optimize the separation of the two proteins by HIC, we thought to change the ammonium sulphate concentration. The variation of this parameter should allow a different interaction of the biotinylated C33 and the *MxeGyrA*-ELP36 tag onto the hydrophobic resin and it should lead to a better separation than the previous experiments. The concentration of Ammonium sulphate tested are reported in the table 19 below.

Hydrophobic resin	**[Starting Ammonium sulphate] mM**	**Elution method**
Hitrap Butyl-S-FF	700	Linear gradient from 0 to 100% of elution buffer
Hitrap Butyl-S-FF	800	Linear gradient from 0 to 100% of elution buffer
Hitrap Butyl-S-FF	900	Linear gradient from 0 to 100% of elution buffer

Table 19. HIC conditions to separate C33 antigen from the *MxeGyrA*-ELP36 tag: second scouting with different ammonium sulfate concentrations

The HIC performed with an ammonium sulphate concentration of 800 mM and an elution through a linear gradient resulted to be the best condition for the separation of the biotinylated C33 from the *MxeGyrA*-ELP36 (Figure 55). In particular, the chromatographic profile showed two peaks with a better resolution than the other conditions analyzed until now. SDS-page analysis confirmed that the condition with ammonium sulphate concentration of 800 mM permitted to obtain the better separation of the two species.

In Figure 55 are shown the chromatographic profile and the SDS-page analysis of the HIC performed by the Hitrap Butyl-S-FF resin with an ammonium sulphate concentration of 800 mM and an elution through a linear gradient.

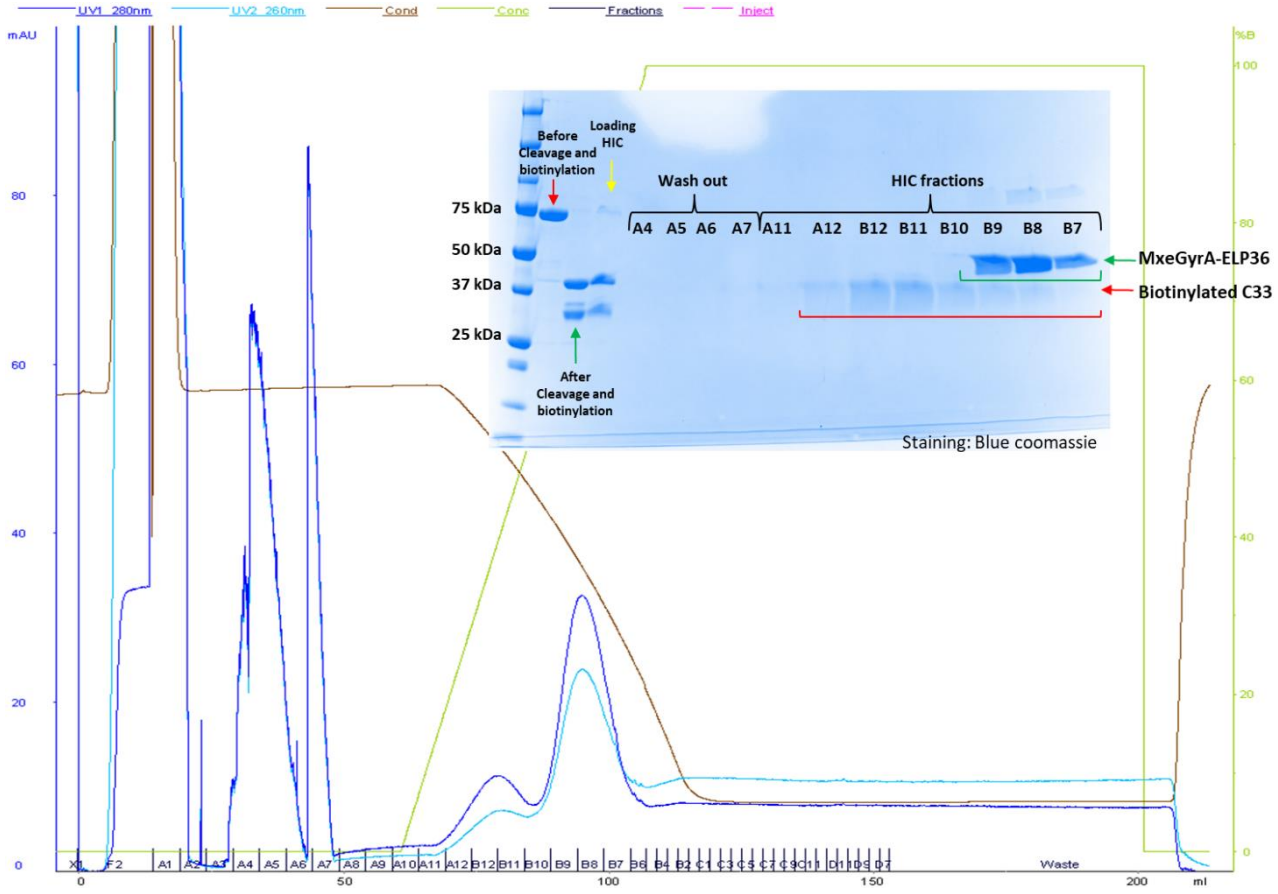

Figure 55. Chromatogram and relative SDS-PAGE analysis of HIC performed with the Hitrap Butyl-S-FF resin, at 800 mM of ammonium sulfate and by a linear gradient elution.

After the selection of the hydrophobic resin and the optimization of the ammonium sulphate concentration, we wanted to try to further improve the separation of the two species, and the resolution of the chromatographic peaks.

To reach this result, we thought to modify the HIC elution method testing different step-gradients instead of a simple linear gradient (Table 20).

Hydrophobic resin	**[Starting Ammonium sulphate] mM**	**Elution method**
Hitrap Butyl-S-FF	800	Steps gradient (30%-60% of elution buffer)
Hitrap Butyl-S-FF	800	Steps gradient (35%-60% of elution buffer)
Hitrap Butyl-S-FF	800	Steps gradient (40%-60% of elution buffer)

Table 20. HIC conditions to separate C33 antigen from the *MxeGyrA*-ELP36 tag: third scouting with different elution steps gradient

We achieved a very good result performing the HIC with the following two steps elution: 30%-60% of elution buffer. During the first step (30%) we eluted the biotinylated C33 while in the second step (60%) we eluted the tag. This steps gradient elution compared to the other steps gradient elution and compared to the linear gradient elution allowed us to obtain a very good resolution with an excellent peaks separation.

Therefore, after several tests and optimizations (scouting of different resins, ammonium sulfate concentrations and elution methods), we defined the final HIC conditions to have the best separation between the biotinylated C33 and the *MxeGyrA*-ELP36 tag and to reach a good yield and purity of our target protein.

In summary, the best selected conditions of the HIC step were: the use of a Butyl-S-FF resin with an ammonium sulphate concentration of 800 mM and a steps gradient 30%-60% (of elution buffer).

The chromatographic profiles (total profile and magnification) obtained from the optimized HIC and the relative SDS-page analysis are showed below.

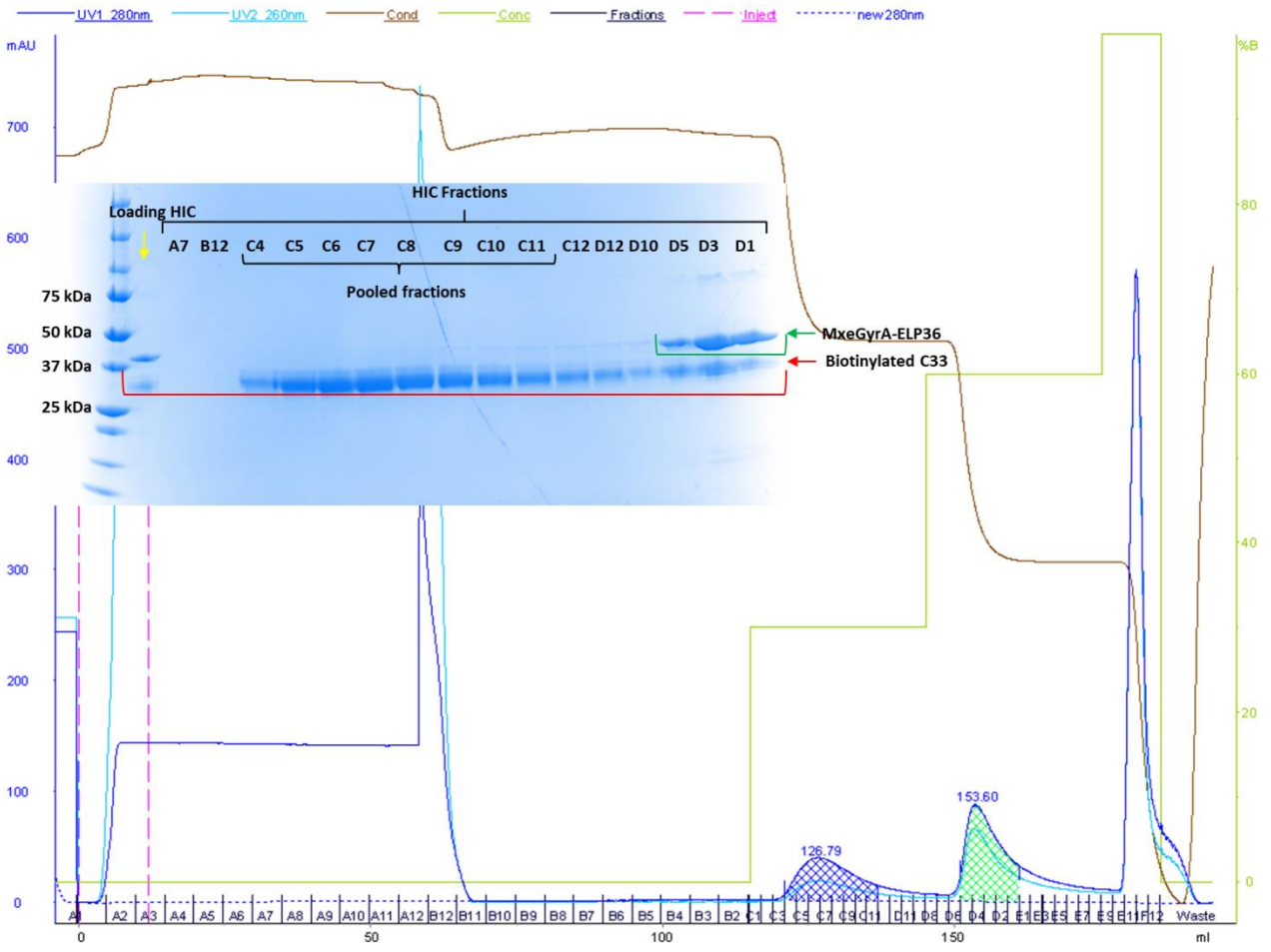

Figure 56. Chromatogram (total profile) and relative SDS-PAGE analysis of optimized HIC with Hitrap Butyl-S-FF resin, at 800 mM of ammonium sulfate and by a steps gradient elution (30-60% of elution buffer).

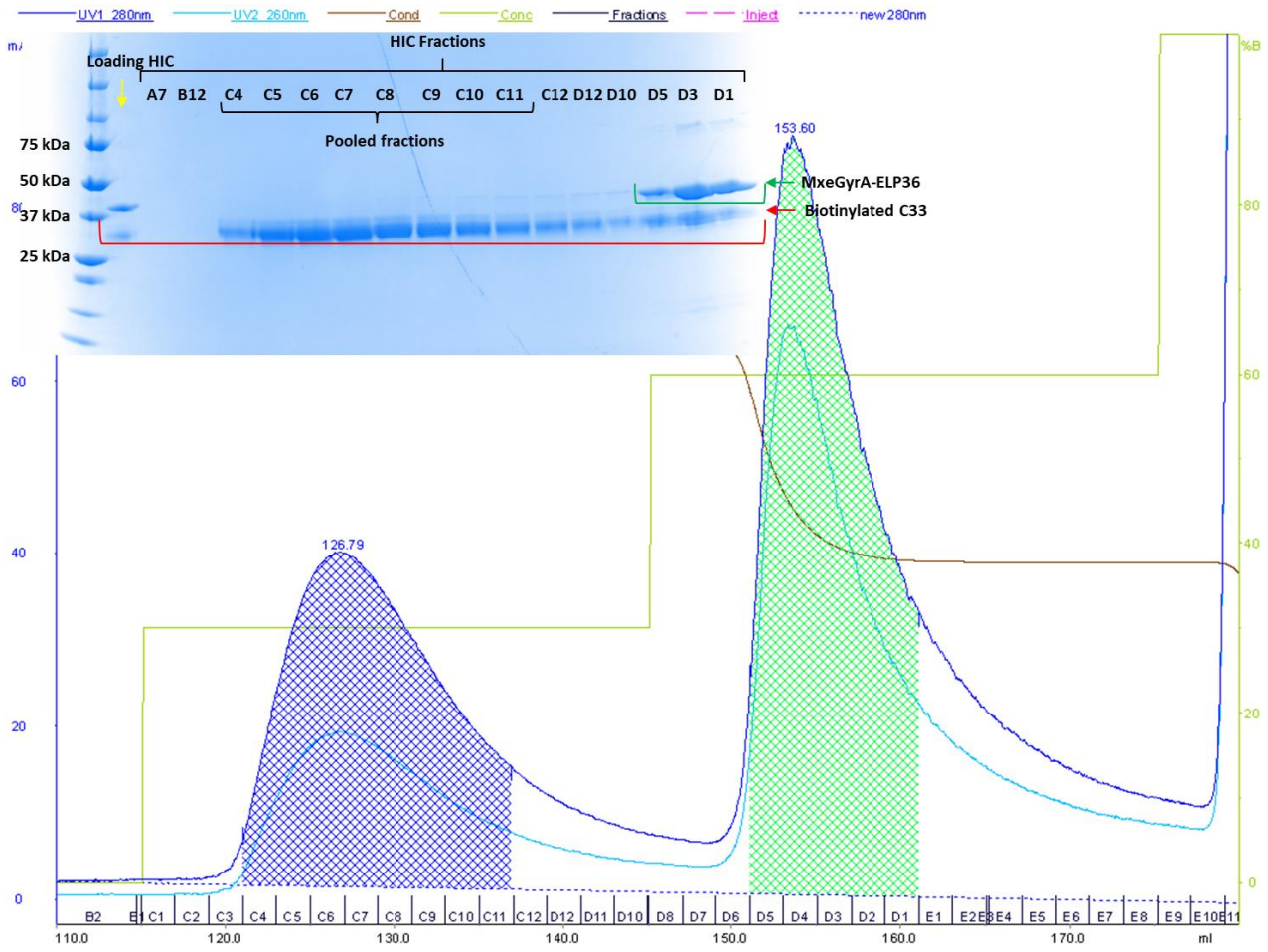

Figure 57. Chromatogram (magnification) of optimized HIC and relative SDS-PAGE analysis of optimized HIC with Hitrap Butyl-S-FF resin, at 800 mM of ammonium sulfate and by a steps gradient elution (30-60% of elution buffer).

To sum up, after the two round ITC and the simultaneous cleavage with MESNA and site-specific biotinylation of our C33, we decided to perform the HIC by using the conditions described in detail above to eluted separately the biotinylated C33 from the *MxeGyrA*-ELP36 and to obtain a final protein target with high purity.

Also in this case, to check the reproducibility of this new purification process and the simultaneous site-specific biotinylation of C33 antigen, we realized three lots of biotinylated C33 starting from ~ 4 gr of wet pellet, derived from a fermentation volume of 1000 ml. Results indicated that the new purification method and the site-specific biotinylation were efficient and reproducible because we obtained a similar yield, production and productivity of biotinylated C33 antigen in all three lots (Table 21).

	Concentration (mg/ml)	**Wet pellet (gr)**	**Quantity (mg)**	**Fermentation volume (ml)**	**Yield (mg/gr)**	**Production (mg/l)**	**Productivity (mg/l/h)**
Lot 1	0,315	4	7,56	1000	1,9	7,56	0,16
Lot 2	0,236	4,1	7,68	1000	1,9	7,68	0,16
Lot 3	0,206	4,5	7,02	1000	1,6	7,02	0,15

Table 21. Final experimental data relative to three different lots of biotinylated C33 obtained with the new purification process.

To conclude, we can say that we developed a purification process shorter than the previous one through which we managed to get the cleavage from the tag and the site-specific biotinylation of C33 in the same purification step, with a gain in terms of time. In addition, we obtained an excellent separation of the biotinylated C33 from the *MxeGyrA*-ELP36 tag by performing a HIC and by optimizing the relative chromatographic conditions. The final result is the achieving of our biotinylated target protein with a good purity. However, we reached a yield, production and especially productivity lower than the non-chromatographic purification method previously developed.

RETARDATION ASSAY OF BIOTINYLATED C33

To verify if our antigen was really biotinylated and also to know its percentage of biotinylation we performed the retardation assay.

The SDS page analysis shows the comparison among a non-biotinylated C33, the C33-Atag (negative control), the Diasorin C33-biotin currently used in LIAISON XL Murex HCV Ab assay (positive control) and our three lots of biotinylated C33 obtained through the new purification process coupled with the antigen site-specific biotinylation (lot 1, lot 2 and lot 3). Every sample was loaded two times, with and without the addition of streptavidin in order to appreciate on the SDS-page gel the band shift at high molecular weight in the biotinylated sample.

The results showed that, as in the previous retardation assay, the C33-Atag was not biotinylated and the Diasorin-C33-biotin resulted biotinylated with an efficiency of about 50%. Also in this test, in all our three lots the C33 antigen biotinylation efficiency was approximately of 100%.

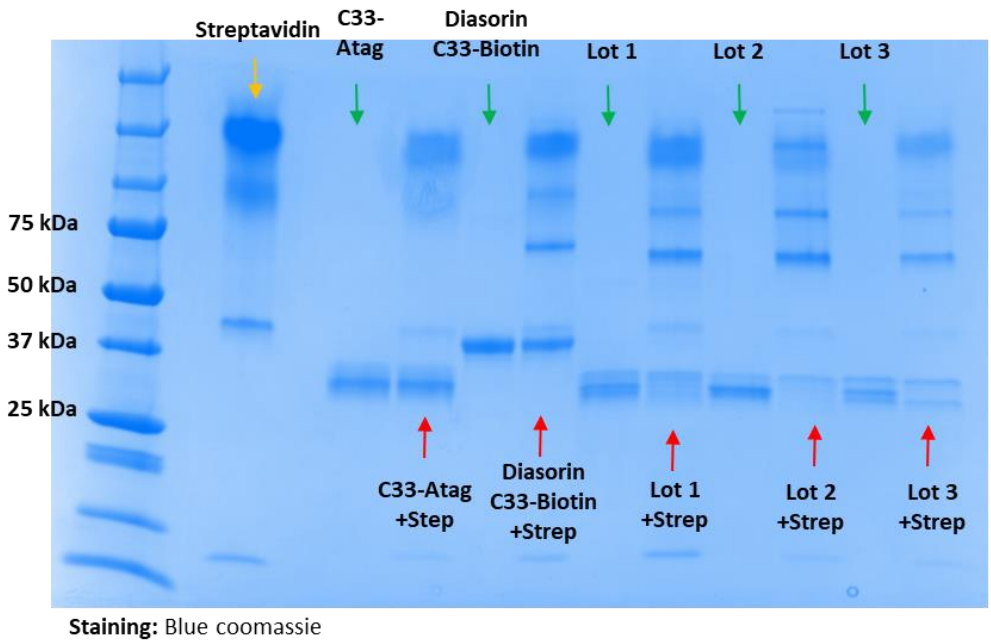

Figure 58. Retardation assay of our three different lots of biotinylated C33 obtained with the second downstream process compared with C33-Atag (negative control) and with Diasorin C33-biotin (positive control). The yellow arrow indicates the streptavidin, the green arrows the samples without streptavidin and the red arrows the samples with streptavidin.

IMMUNOREACTIVITY TEST OF BIOTYNILATED C33

Also for these three lots, we verified their immunoreactivity comparing them with the Diasorin C33-biotin currently used in the LIAISON XL Murex HCV Ab assay.

To verify the immunoreactivity of the biotinylated C33, we performed the HCV immunoassay on a panel of human HCV negative samples and on panel of human HCV positive samples. It's important to underline that each experiment was realized in triplicate in order to confirm the data reproducibility.

The panel of the human HCV negative blood samples, present in Figure 59, showed that the RLU signals result comparable using in the HCV immunoassay the Diasorin C33-biotin or our three lots of biotinylated C33 (Figure 59).

The histogram about the panel of the human HCV positive blood samples (Figure 60) displayed comparable RLU signal, higher than the cut-off previously set, both coating in solid phase the Diasorin C33-biotin and the three lots of biotinylated C33. These results indicated similar immunoreactivity among the Diasorin C33-biotin an our three lots of biotinylated C33 obtained from this new purification.

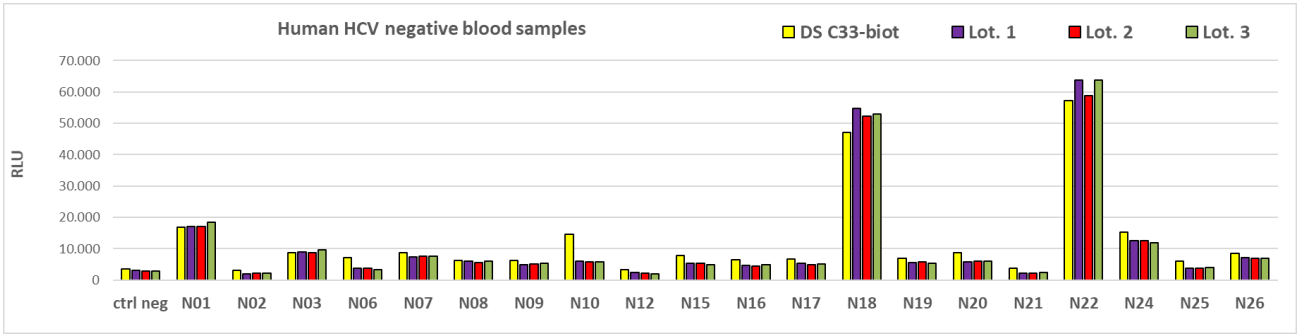

Figure 59. Histogram about the panel of human HCV negative blood samples tested in the LIAISON XL Murex HCV Ab assay

Figure 60. Histograms of the panel of human HCV positive blood samples analyzed in the LIAISON XL Murex HCV Ab assay

Therefore, as the previous process, also this new purification method allow us to obtain a biotinylated C33 antigen that has a good performance in the LIAISON XL Murex HCV Ab assay and a comparable immunoreactivity of the antigen currently used.

SITE SPECIFIC BIOTINYLATION OF C33 THROUGH THE PROTEIN TRANS SPLICING

As described in the introduction chapter, the use of the split-inteins has several biotechnological applications and many advantages than the *cis*-inteins. The most relevant characteristics of the split intein are (1) they very unlikely undergo to intracellular self-cleavage (2) the kinetics of the protein trans-splicing reactions are usually faster than those with *cis*-inteins, (3) the possibility to express separately two portions of the same protein to enhance its low solubility when it is expressed as a whole protein and (4) the site-specific labeling or other modifications of proteins and antibodies.

For these reasons, we decided to explore this new technology to realize the site specific biotinylation of the C33 antigen. In particular, we found in literature a paper about the Cfa split intein, derived from several mutations of the cyanobacteria *Nostoc punctiforme* (Npu) split-intein and characterized by rapid protein trans-splicing, unprecedented thermal and chaotropic stability. Following the discovery of these advantageous features, we chose this split-intein to perform our experiments.

Therefore, we created two constructs having respectively the N-terminal portion of the Cfa split intein and the C-terminal fragment of the Cfa split intein (Figure 61).

In particular, the first construct is characterized by the fusion of C33 sequence with the Cfa-N-terminal portion. At the N-terminal of C33 is present a His-Tag necessary for the purification of this first fusion protein. In the second construct, the C-terminal portion of Cfa is fused with the *MxeGyrA*-ELP36 tag; we exploited this tag to purify and to perform the site-specific biotinylation of this second construct, as extensively described in the previous sections.

We purified them separately and then we have set up the reaction between the two constructs to trigger the recognition of the two-intein portions and to promote the consequent protein trans-splicing mechanism.

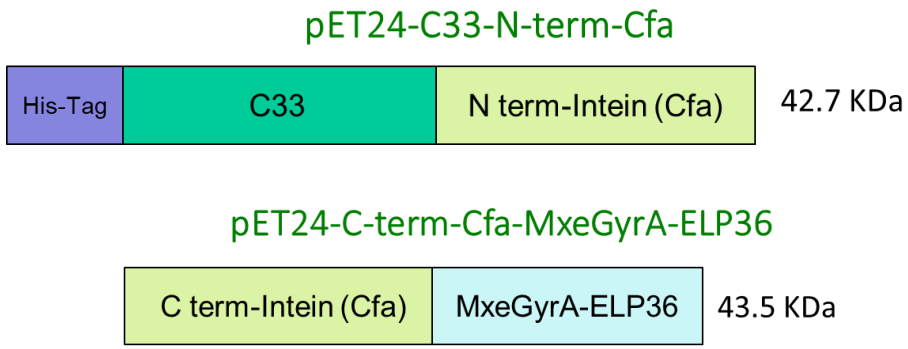

Figure 61. Schematic representation of the two constructs used for the site-specific biotinylation of C33 antigen through trans splicing reaction.

INDUCTION TESTS OF pET24-NHI-C33- N-TERM-CFA AND pET24-C-TERM-CFA-MxeGyrA-ELP36

We explored different fermentation conditions in which to produce the pET24-NHis-C33-N-term-Cfa and pET24-C-term-Cfa-MxeGyrA-ELP36 constructs (Table 22) and then we performed the induction tests to choose the best ones.

Also in this case, we expressed the two constructs in BL21 (DE3) *E. coli* strain.

Fermentation	Constructs	Medium	Temperature	Induction	Harvest time	[IPTG]
A	pET24-NHis-C33-N-term-Cfa	LB	+37°C	0,6 OD	3 hours	1 mM
	pET24-C-term-Cfa--*MxeGyrA*-ELP36	LB	+37°C	0,6 OD	3 hours	1 mM
B	pET24-NHis-C33-N-term-Cfa	LB	+30°C	0,6 OD	3 hours	1 mM
	pET24-C-term-Cfa--*MxeGyrA*-ELP36	LB	+30°C	0,6 OD	3 hours	1 mM
C	pET24-NHis-C33-N-term-Cfa	LB	+37°C	1,5 OD	3 hours	1 mM
	pET24-C-term-Cfa--*MxeGyrA*-ELP36	LB	+37°C	1,5 OD	3 hours	1 mM
D	pET24-NHis-C33-N-term-Cfa	2xYT	+37°C	0,6 OD	3 hours	0,03 mM
	pET24-C-term-Cfa--*MxeGyrA*-ELP36	2xYT	+37°C	0,6 OD	3 hours	0,03 mM
E	pET24-NHis-C33-N-term-Cfa	2xYT	+30°C	0,6 OD	3 hours	1 mM
	pET24-C-term-Cfa--*MxeGyrA*-ELP36	2xYT	+30°C	0,6 OD	3 hours	1 mM
F	pET24-NHis-C33-N-term-Cfa	AIM	+37°C	0,001 OD	24 hours	-
	pET24-C-term-Cfa--*MxeGyrA*-ELP36	AIM	+37°C	0,001 OD	24 hours	-

Table 22. Fermentation conditions used for the pET24-NHis-C33- N-term-Cfa and pET24-C-term-Cfa-MxeGyrA-ELP36 fusion proteins expression.

We expressed our two constructs in six different fermentation conditions but the SDS-page analysis below (Figure 62 and 63) showed that only in three of these ones we had a good expression of both NHis-C33- N-term-Cfa and C-term-Cfa-MxeGyrA-ELP36 fusion proteins (fermentations A, C and D). In particular, the best fermentation condition seemed to be that performed in LB at 37°C with induction at 0,6 OD (condition A) and for this reason we verified the solubility of the two proteins in this selected condition by the solubility test.

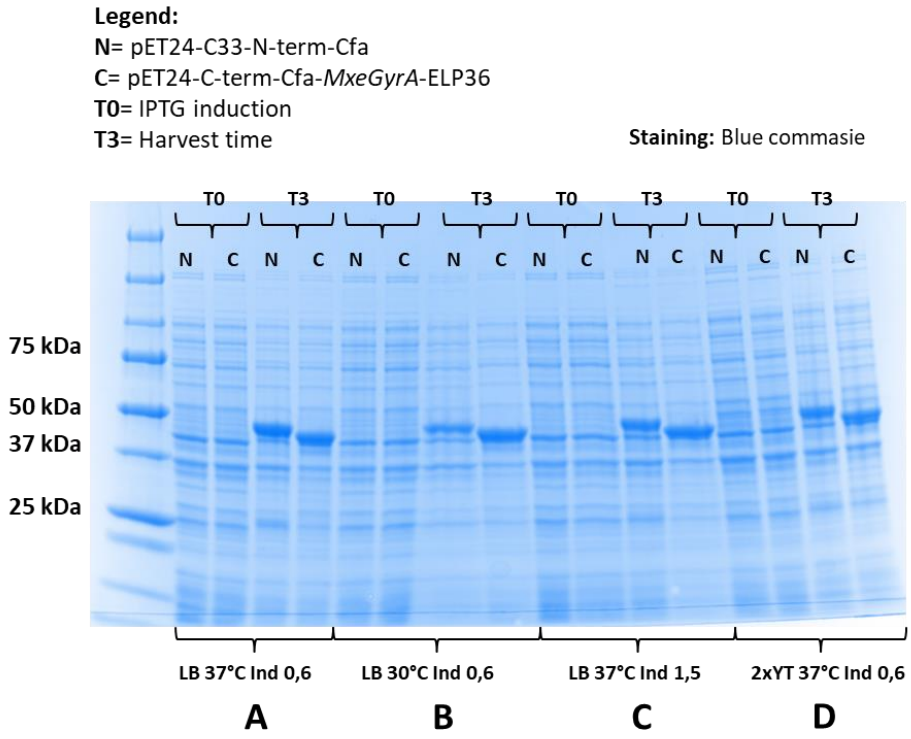

Figure 62. SDS-PAGE analysis showing the induction test of BL21(DE3) pET24-NHis-C33-N-term-Cfa and BL21(DE3) pET24-C-term-Cfa-*Mxe*GyrA-ELP36, fermented in different media and at various temperatures: conditions A,B,C and D (see table 22).

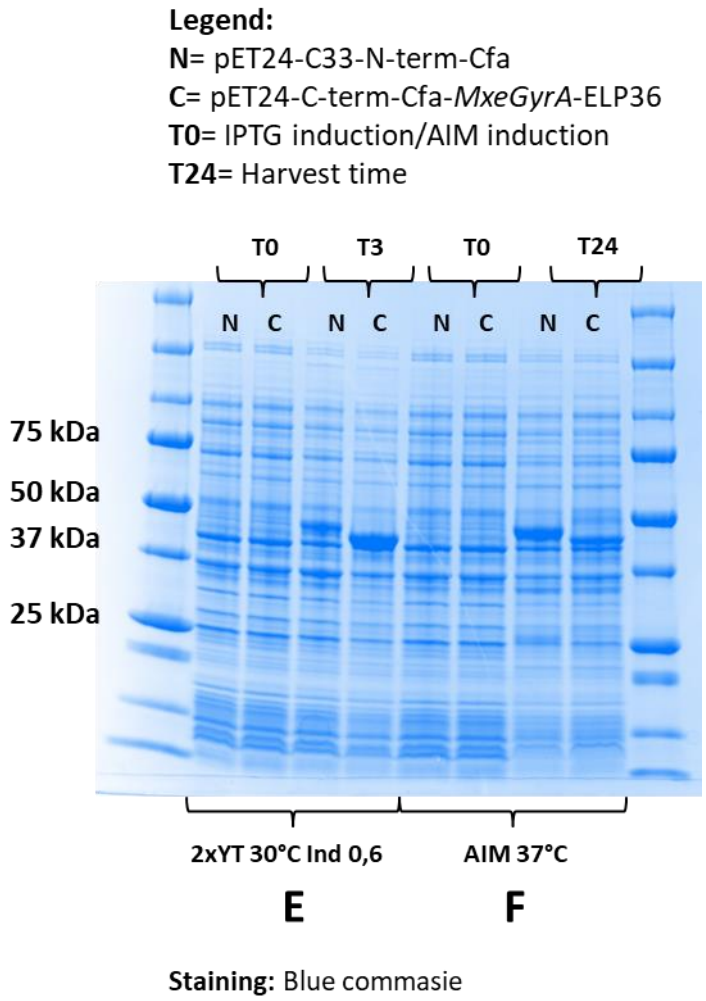

Figure 63. SDS-PAGE analysis showing the induction tests of BL21(DE3) pET24-C33-NHis-N-term-Cfa and BL21(DE3) pET24-C-term-Cfa-*Mxe*GyrA-ELP36, fermented in 2xYT medium at 30°C and in AIM at 37°C (conditions E and F ,see table 22).

SOLUBILITY TEST OF pET24-NHIS-C33-N-TERM-CFA AND pET24-C-TERM-CFA-MxeGyrA-ELP36

The SDS-page analysis of the solubility test (Figure 64) showed that the NHis-C33-N-term-Cfa protein was mainly soluble in the conditions that we tested (red circles) while a relevant portion of the C-term-Cfa-MxeGyrA-ELP36 was present in the insoluble fraction (IF, green circles). To found a better condition for the solubility of the C-term-Cfa-MxeGyrA-ELP36, we performed a second solubility test, only for this construct, in the other conditions in which we observed a good expression levels for the C-term-Cfa-MxeGyrA-ELP36 (conditions B and E of induction test).

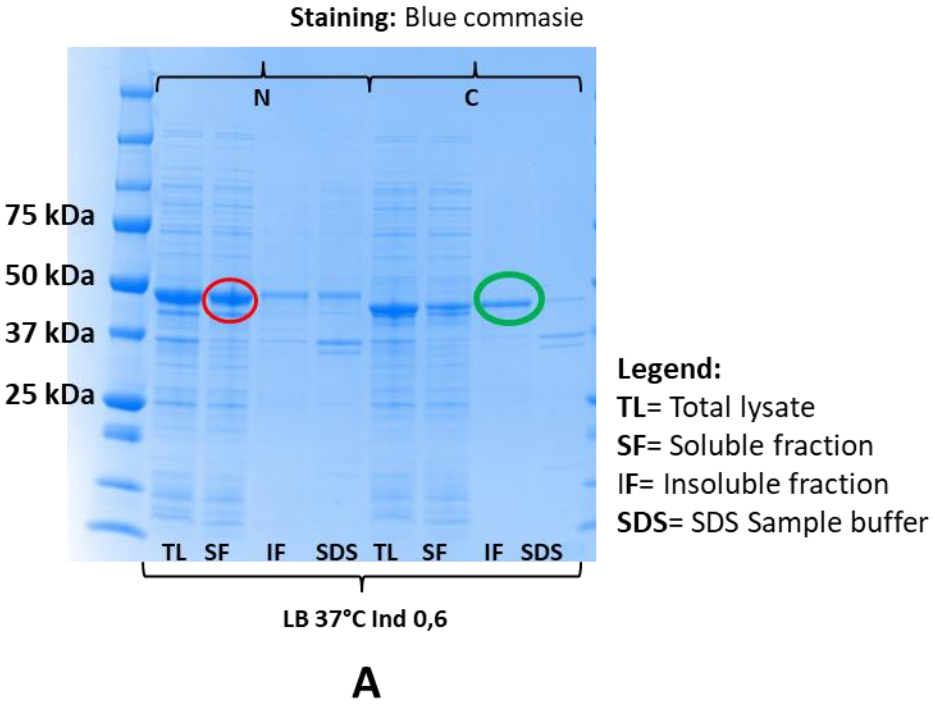

Figure 64. SDS-PAGE analysis showing the solubility test of the NHis-C33-N-term-Cfa and the C-term-Cfa-*Mxe*GyrA-ELP36, fermented in LB at 37°C with induction at 0,6 OD (condition A). Red circle indicates the NHis-C33-N-term-Cfa soluble fraction while green circle indicates C-term-Cfa-*Mxe*GyrA-ELP36 insoluble fractions.

The SDS-page analysis about this second solubility test (Figure 65) showed that the C-Term-Cfa-MxeGyrA-ELP36 protein was mainly soluble both in LB and 2xYT medium at +30° C (red circles) but the best one was the condition B in which there was a lower portion of insoluble protein than in the condition E (IF and SDS, green circles).

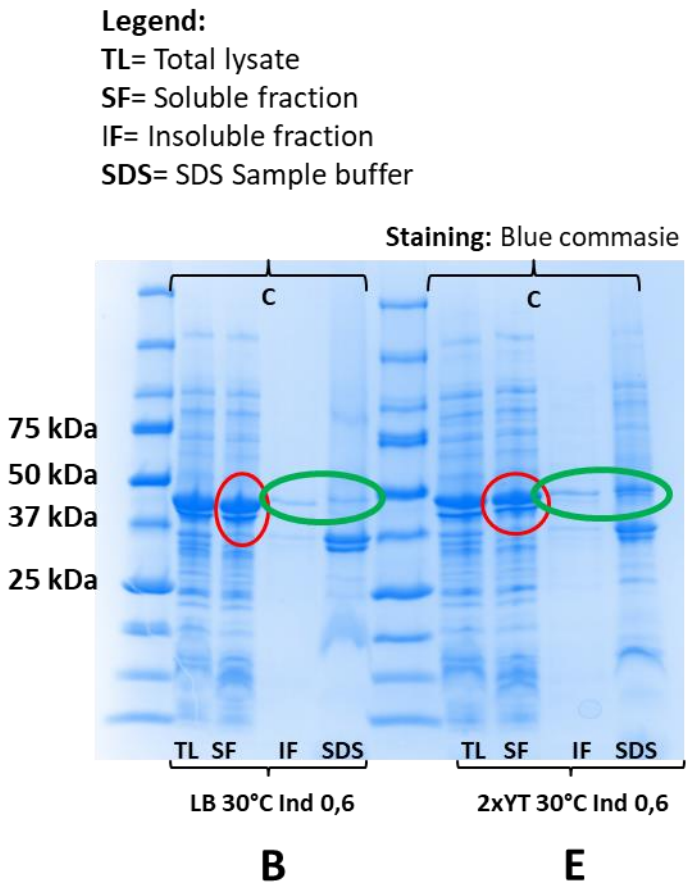

Figure 65. SDS-PAGE analysis showing the second solubility test of the C-term-Cfa-*Mxe*GyrA-ELP36 fermented in LB at +30°C and 2xYT at +30°C with induction at 0,6 OD. Red circles indicate the C-term-Cfa-*Mxe*GyrA-ELP36 present in soluble fraction while green circles indicate the construct present in insoluble fractions.

On the basis of the data obtained from the induction and solubility tests we decided to perform the production of the two fusion proteins in the following conditions:

- LB at 37°C with induction at 0,6 OD for the C33-N-term-Cfa, condition A
- LB at 30°C with induction at 0,6 OD for the C-term-Cfa-*Mxe*GyrA-ELP36, condition B

PURIFICATION PROCESS OF NHIS-C33-N-TERM-CFA

We decided to purify the NHis-C33-N-term-Cfa construct through an Immobilized Metal affinity Chromatography (IMAC), exploiting the His-tag at the N-terminal of the polypeptide sequence, followed by a Gel Filtration Chromatography (GFC) as further polishing step (for more details relative to IMAC and GFC steps see materials and methods section).

The chromatogram profile and the relative SDS-page analysis here below (Figure 66) show the IMAC of the NHis-C33-N-term-Cfa. Eluted fractions of purified NHis-C33-N-term-Cfa were pooled together as shown in the chromatogram (underline in green) and on the SDS-page gel (red rectangle).

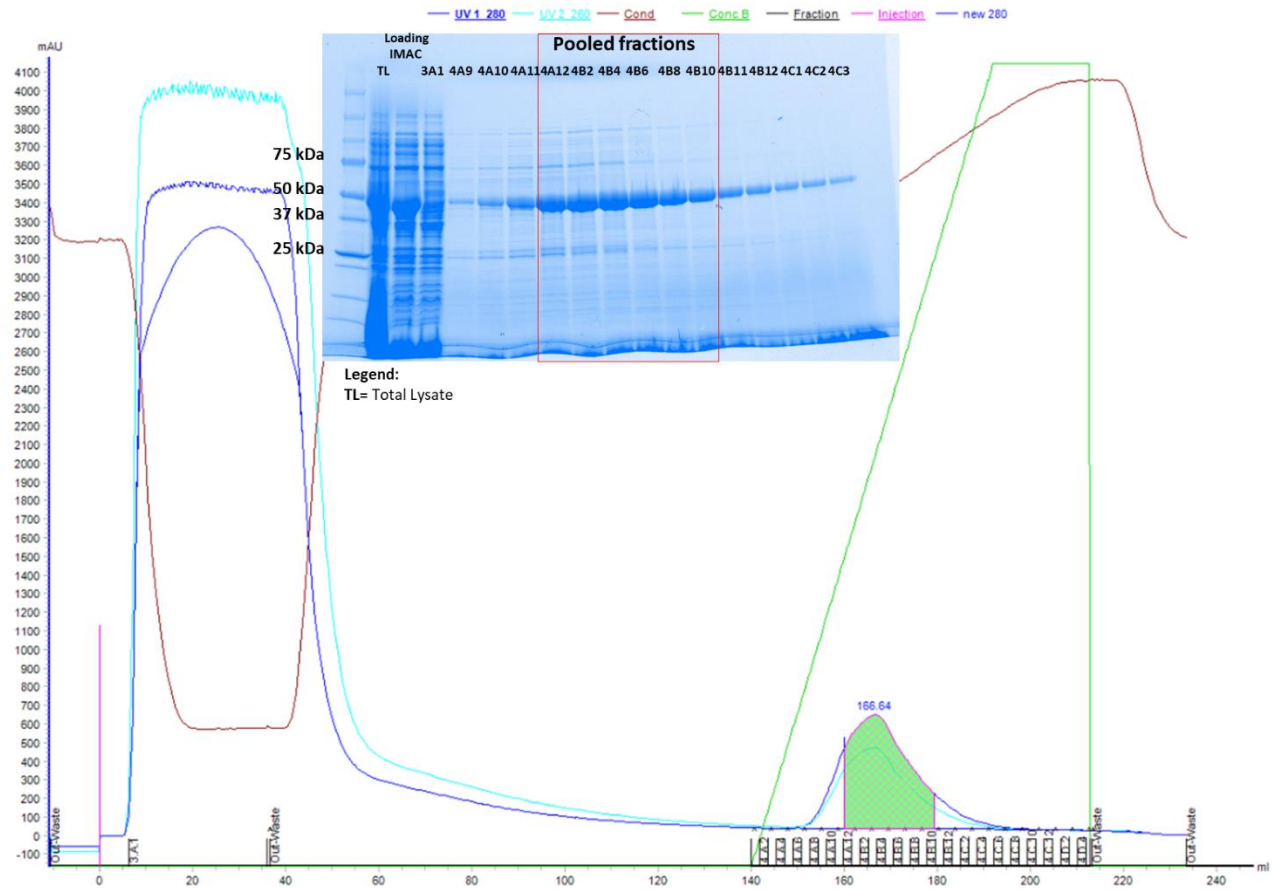

Figure 66. Chromatogram obtained from the IMAC of the NHis-C33-N-term-Cfa construct and relative SDS-page analysis.

After this step, the resulting IMAC pool was loaded on a gel filtration column to further increase the purity of our target protein.

The chromatogram profile and relative SDS-page analysis (Figure 67) show the GFC of the NHis-C33-N-term. Eluted fractions of the purified NHis-C33-N-term-Cfa were pooled together as shown in the chromatogram (underline in blue) and on the SDS-page gel (red rectangle).

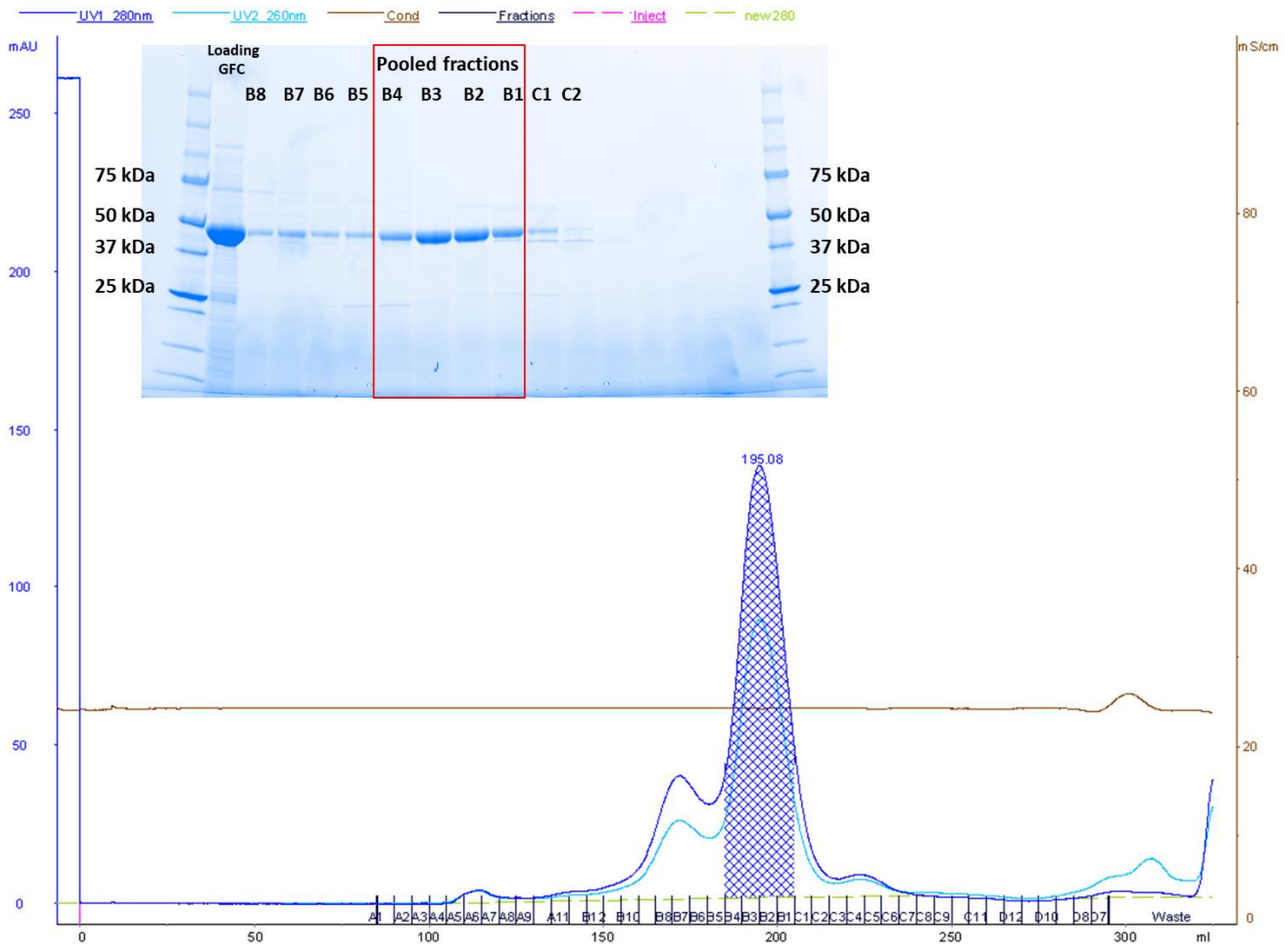

Figure 67. GFC profile of the NHis-C33-N-term-Cfa construct and relative SDS-page analysis.

Summarizing, this purification scheme (IMAC and GFC) allowed us to obtain NHis-C33-N-term-Cfa with good purity degree and yield.

We performed this purification process in triplicate: the data regarding the three purifications are showed in the table below.

	Concentration (mg /ml)	**Wet pellet (gr)**	**Quantity (mg)**	**Fermentation volume (ml)**	**Yield (mg/gr)**	**Production (mg/l)**	**Productivity (mg/l/h)**
Lot 1	1,45	3,7	26,03	1000	7	26,03	0,54
Lot 2	1,15	4	45,95	1000	11,5	45,95	0,98
Lot 3	1,15	4,53	36,25	1000	8,1	36,25	0,76

Table 23. Experimental data regarding the purification process of the three lots of C33-N-term-Cfa

PRECIPITATION TEST OF C-TERM-CFA-MxeGyrA-ELP36

To exploit the ELP technology during the purification process of the C-Term-Cfa-MxeGyrA-ELP36 protein by the ITC process, we had to identify the right NaCl concentration in which to precipitate our fusion protein; for this purpose, we performed a precipitation test, as described in a previous paragraph.

We tested different NaCl concentrations in a range between 0,5 M and 2,5 M, as reported in the table below.

	NaCl 0,5 M	NaCl 1 M	NaCl 1,5 M	NaCl 2 M	NaCl 2,5 M
Supernatant (ml)	0,7	1	2	2	2
NaCl 5M(ml)	0,0777	0,25	0,857	1,33	2
Final Volume (ml)	0,777	1,25	2,857	3,33	4

Table 24. Volumes and NaCl concentrations used for the precipitation test of the C-term-Cfa-*Mxe*GyrA-ELP fusion protein.

The SDS-PAGE analysis showed that the C-term-Cfa-*MxeGyrA*-ELP36 protein at NaCl concentrations of 0,5-1 and 1,5 M was mainly present in the supernatant, while at NaCl concentrations of 2 and 2,5 M it was almost completely precipitated and therefore presents in the pellet (Figure 68, red circles). For this reason we chose the NaCl concentrations of 2 M because by using a higher salt concentrations (> 2,0 M) we could promote the precipitation of other contaminant proteins.

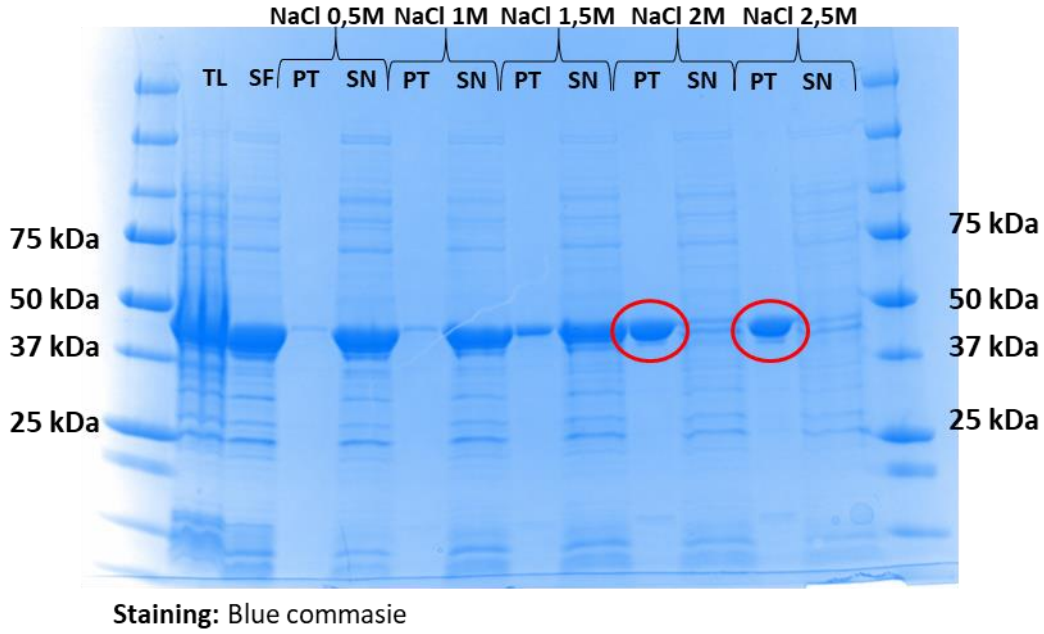

Figure 68. SDS-PAGE analysis showing the precipitation test of C-term-Cfa-*Mxe*GyrA-ELP36, fermented in LB at +30°C in which we tested the precipitation level of our fusion protein at different NaCl concentrations. Red circles indicate the C-term-Cfa-*Mxe*GyrA-ELP36 precipitated and then presents in the pellet.

PURIFICATION PROCESS OF C-TERM-CFA-*MxeGyrA*-ELP36 AND SITE-SPECIFIC BIOTINYLATION OF C-TERM-CFA

Once obtained the purified NHis-C33-N-term-Cfa, we need to purify the C-term-Cfa-*MxeGyrA*-ELP36 and to perform the subsequent biotinylation of the C-term-Cfa in order to set up the split intein reaction test.

For the purification of the C-term-Cfa-*MxeGyrA*-ELP36 and the following site-specific biotinylation of C-term-Cfa, we thought to exploit the first purification protocol developed for the production of the biotinylated C33 antigen since this new fusion protein owns the same tag (see dedicated paragraph). The process for obtaining the biotinylated C33 included two rounds ITC, the cleavage of the *MxeGyrA*-ELP36 from the target protein with MESNA, the third round ITC to separate the tag from the protein of interest and finally the site-specific biotinylation through the express protein ligation technique.

We tried to apply the same method also for the C-term-Cfa-*MxeGyrA*-ELP36 purification but unfortunately, we found some problems and bottlenecks in different steps and, consequently, we made some observations as showed in figure 69, in particular:

- we had problems in the resuspension of the pellet obtained after the 1st CS in the phosphate /EDTA buffer at pH 8.
- We observed that the second ITC round was not necessary since the contaminants were almost completely eliminated after the 1st ITC round.
- During the third ITC round we were unable to separate C-term-Cfa from the *MxeGyrA*-ELP36. Therefore, it was not possible to perform the site-specific biotinylation of the C-term-Cfa-thioester with a biotinylated Cys-peptide (the same used for the C33 biotinylation) and the following GFC purification step.

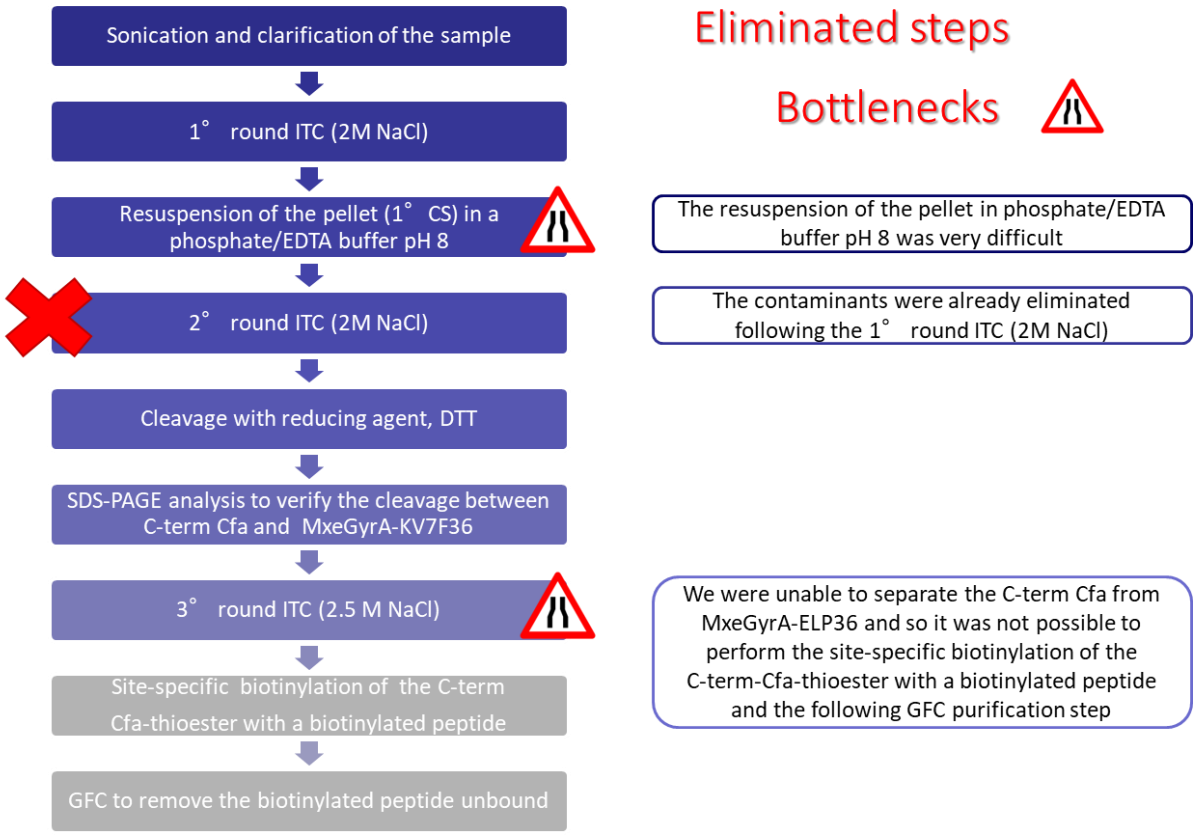

Figure 69. Problems, bottlenecks and observations related to the purification of the C-term-Cfa-*MxeGyrA*-ELP36.

For these reasons, we optimized the purification process described above and we obtained a final satisfactory experiment procedure to produce the C-term-Cfa-Biotin, as reported in the scheme below, figure 70 In details:

- the resuspension of the pellet after the 1st CS in Tris buffer instead of the phosphate/EDTA buffer improved the pellet solubility.
- The removal of the second round ITC simplified the process and allowed us to save working time.
- The simultaneous cleavage with MESNA and site-specific biotinylation (as done in the second process developed for the C33 antigen) was also important to have a shorter process time.
- Since the third round ITC did not allow the separation of the C-term-Cfa from the *MxeGyrA*-ELP36, we thought to exploit the Reverse Phase Chromatography (RPC) to separate our biotinylated peptide from the tag. We selected the RPC technique to obtain a purified C-term-Cfa-Biotin because it is currently the more appropriate and used chromatographic technique for the purification of peptides.

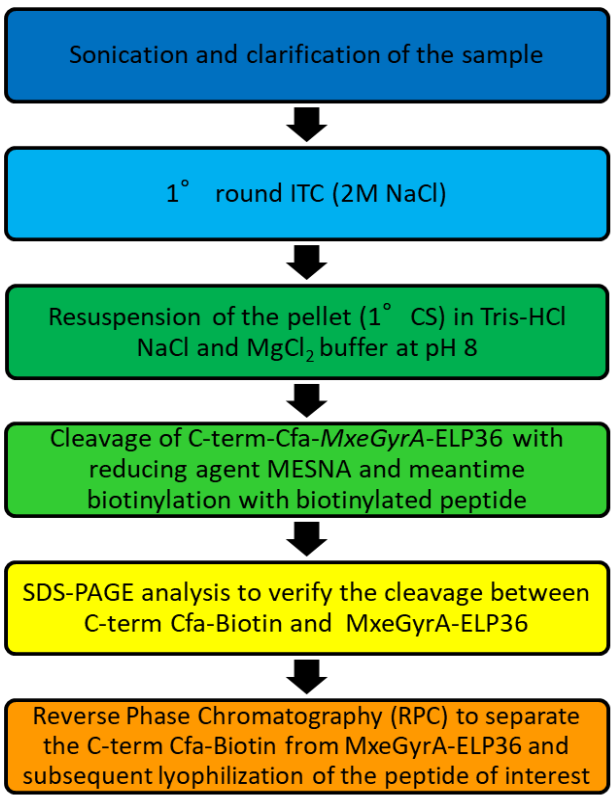

Figure 70. Final purification process for the production of the C-term-Cfa-Biotin protein.

Figure 71 shows the SDS page analysis of the C-term-Cfa-*MxeGyrA*-ELP36 purification through the ITC process and the kinetics of the cleavage with MESNA.

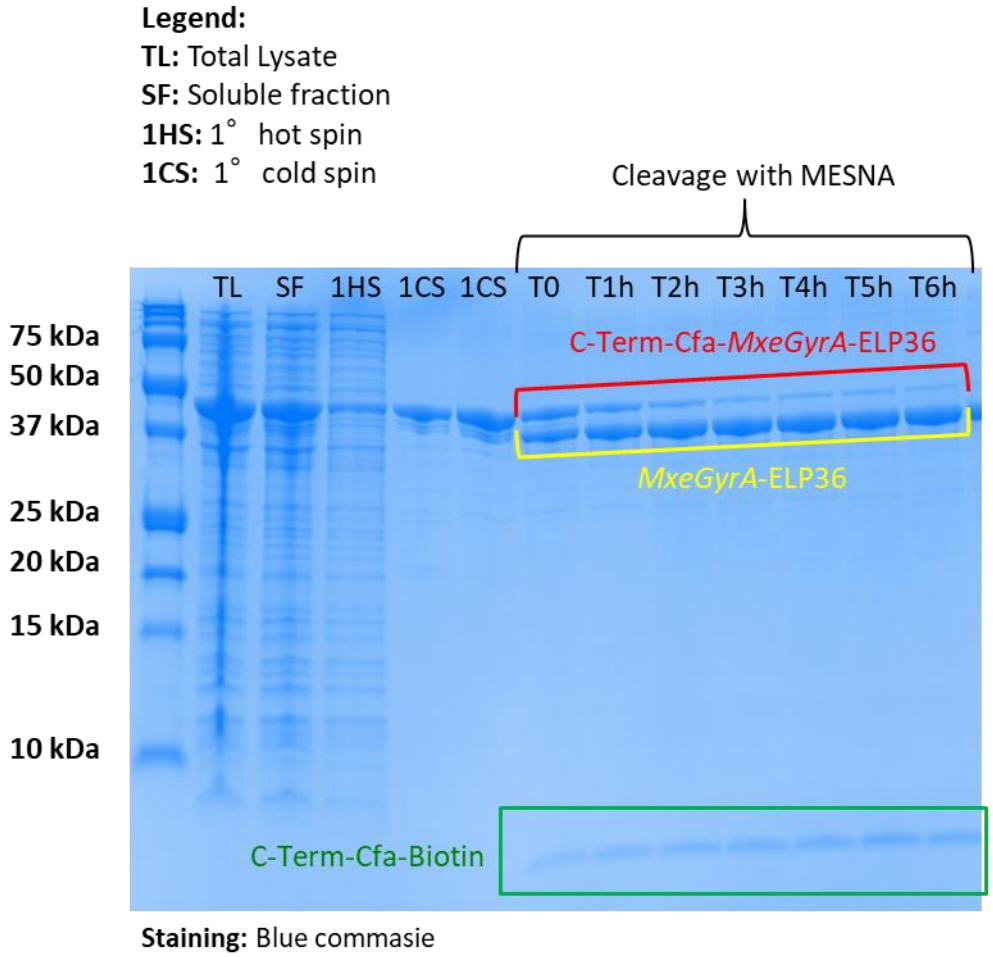

Figure 71. SDS-page analysis showing the purification of C-term-Cfa-*MxeGyrA*-ELP36 and the site-specific-biotinylation of C-term-Cfa.

The SDS-page gel shows that the cleavage of *MxeGyrA*-ELP36 from the C-term-Cfa-thioester of the target peptide were fast: since T0 we observed the presence of the main product (C-term-Cfa-Biotin) and we noted the completion of the reactions after 6 h.

As mentioned before, after the purification of C-term-Cfa-*MxeGyrA*-ELP36, the cleavage with MESNA and the site-specific biotinylation of the C-term-Cfa we performed a Reverse Phase Chromatography (RPC) to separate our biotinylated peptide from the *MxeGyrA*-ELP36 (for more details relative to RPC, see materials and method section).

The RPC chromatographic profile (Figure 72) recorded at 214 nm of wavelength showed two peaks at different retention volumes. The first peak eluted was demonstrated to correspond to the C-term-Cfa-Biotin (main product) while the second one corresponded to the tag. We pooled the fractions relative to the first peak (C-term-Cfa-Biotin) and we lyophilized the final sample.

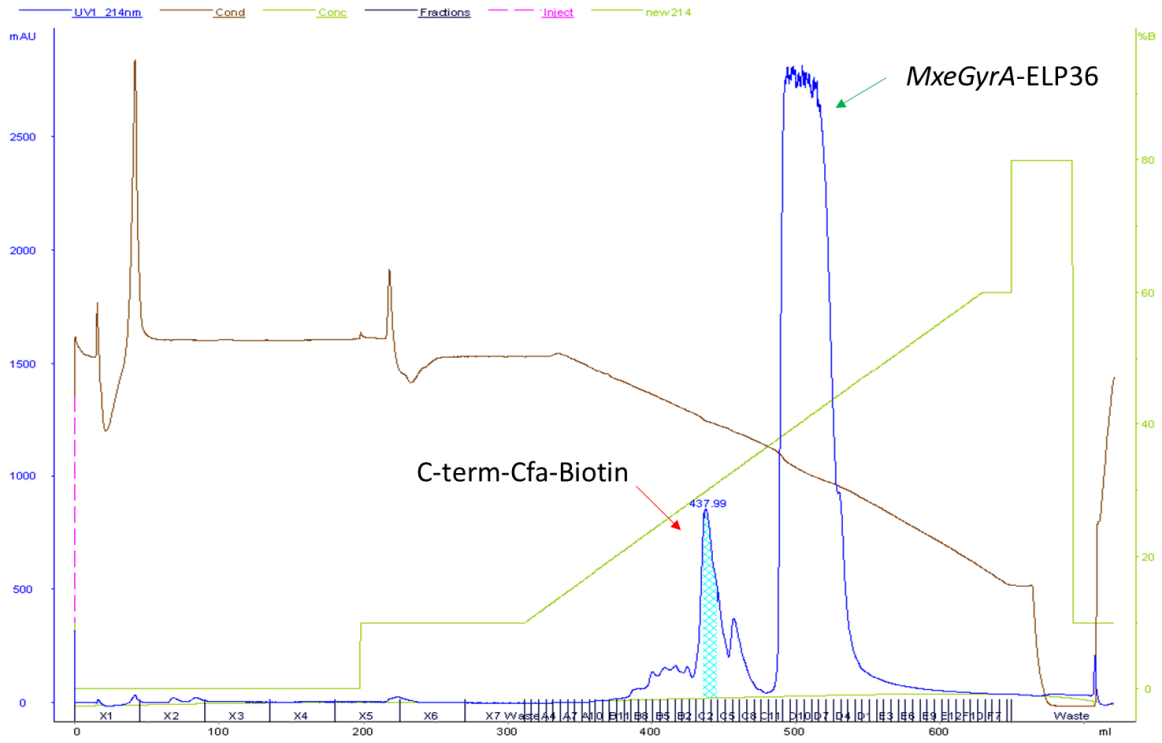

Figure 72. Chromatogram profile of the RPC to separate the C-term-Cfa-Biotin from *MxeGyrA*-ELP36.

Despite many difficulties encountered during this experimental procedure we managed to get 4.4 mg of lyophilized C-term-Cfa-Biotin starting from 3,5 gr of wet bacteria pellet obtained by 1000 ml of fermentation in LB at +30°C.

Since the yield of the final purification process for C-term-Cfa-Biotin was quite low and therefore it was difficult to obtain sufficient material to continue the studies, we decided to explore the trans splicing reaction conditions by reacting the NHis-C33-N-term-Cfa internally produced to a synthetic C-term-Cfa-Biotin peptide. Once the best reaction conditions were established, we compared the trans-splicing activity of our recombinant C-term-Cfa-Biotin peptide against that of the analogous synthetic peptide (see next paragraph).

CFA SPLIT-INTEIN REACTION TESTS

After the purification of the NHis-C33-C-term-Cfa and the production of C-term-Cfa-biotin we have set up the split intein reaction test to obtain the site-specific biotinylation of NHis-C33 through the Cfa protein trans splicing activity.

Starting from the literature information (185), we performed the Cfa split intein test in different conditions (Table 25), in order to obtain the best conversion yield in the final product (NHis-C33-biotin).

At the beginning, due to the low yield obtained for the recombinant C-term-Cfa-biotin production, we used a synthetic C-term-Cfa-biotin peptide for the setting of Cfa split intein reaction conditions.

Test	Constructs	Concentration (mg/ml) Molarity (µM)	Molar ratio C-term-Cfa/ N-term-Cfa	Temperature	Buffer
A	NHis-C33-N-term-Cfa	0,2 mg/ml 9,4 µM	8,3X	+25°C	Splicing Buffer
	Synthetic C-term-Cfa-Biotin	0,2 mg/ml 78 µM			
B	NHis-C33-N-term-Cfa	0,2 mg/ml 9,4 µM	16,6 X	+25°C	Splicing Buffer
	Synthetic C-term-Cfa-Biotin	0,4 mg/ml 156 µM			
C	NHis-C33-N-term-Cfa	0,2 mg/ml 9,4 µM	16,6 X	+25°C	Splicing Buffer 4M UREA
	Synthetic C-term-Cfa-Biotin	0,4 mg/ml 156 µM			
D	NHis-C33-N-term-Cfa	0,2 mg/ml 9,4 µM	16,6 X	+30°C	Splicing Buffer 4M UREA
	Synthetic C-term-Cfa-Biotin	0,4 mg/ml 156 µM			

Splicing Buffer*:* Phosphate dibasic dihydrate ($Na_2HPO_42H_2O$) 100 mM, NaCl 150 mM, EDTA 1 mM, 2 mM TCEP, pH 7.2

Splicing Buffer 4M UREA*:* Phosphate dibasic dihydrate ($Na_2HPO_42H_2O$) 100 mM, NaCl 150 mM, EDTA 1 mM, 2 mM TCEP, 4M UREA, pH 7.2

Table 25. Selected conditions to carry out the protein trans splicing reaction by Cfa-split-intein.

For the Cfa-Split intein reaction test we mixed the recombinant NHis-C33-N-term-Cfa and the synthetic C-term-Cfa-biotin, at the desired concentration, and then we incubated the reaction mix at the selected temperature with stirring. We followed the kinetic of the

reaction for several hours taking at different time points (T0, T30', T1h, T2h and T overnight (TON)) a sample for the SDS-page analysis.

All the reaction tests were performed in a reducing environment, in particular in presence of the reducing agent TCEP at the concentration of 2mM.

As reported in literature (185), the protein trans splicing by split intein is very fast but unfortunately the reaction does not reach the complete conversion of the initial species into the final product. For this reason, at the end of the reaction, in addition to our main product and the other secondary reaction products, also a portion of the two starting reagents that had not reacted was still present (Figure 73).

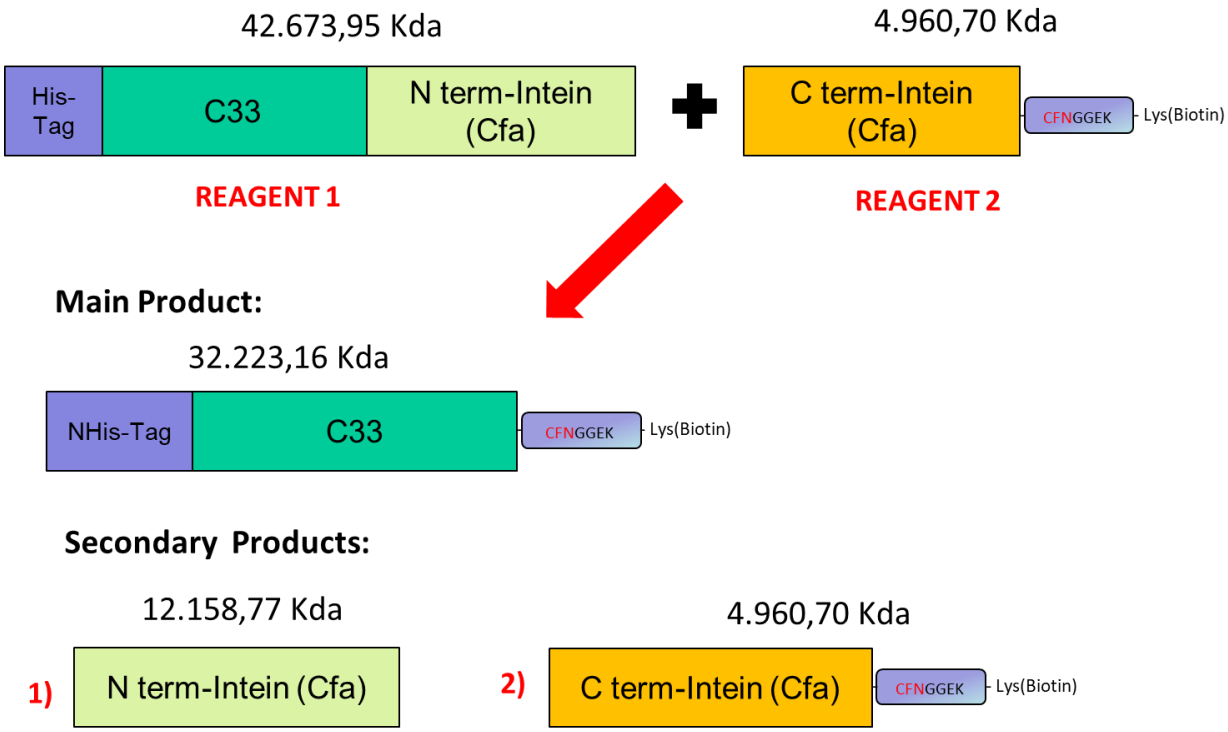

Figure 73. Scheme of the Cfa-split-intein reaction test between NHis-C33-N-term-Cfa and C-term-Cfa-Biotin and the different species obtained from this reaction.

The SDS-page analysis reported below shows the comparison among the first three conditions (A, B, C; see table above) in which we performed the Cfa-split-intein reaction test. In the first one we used the two initial reagents at the same concentration (test A); in the second one we tried to promote the reaction yield by adding a concentration 2x of C-

term-Cfa-biotin than the NHis-C33-N-term-Cfa (Test B); in the third one we performed the split-intein reaction in a splicing buffer containing UREA at a final concentration of 4M (Test C). The purpose in the use of this chaotropic reagent was to get a relaxed proteins structure in order to favor the interaction between the two Cfa-split intein fragments and therefore to reach a higher conversion yield in the NHis-C33-biotin final product than the previous conditions. It's important to say that at this UREA concentration the two proteins did not undergo to denaturation.

As shown in the SDS-PAGE analysis (Figure 74), the increase of C-term-Cfa-biotin concentration had a positive effect on the kinetic of reaction because the condition B brought to a higher conversion yield than the condition A. The addition of UREA (condition C) further improved the production yield of NHis-C33-biotin than the condition B.

On the basis of these results we can say that we obtained the best conversion yield in the main product during the Test C. Observing the SDS-page gel, we supposed that ~60% of the starting NHis-C33-N-term-Cfa was converted in the NHis-C33-biotin (final product).

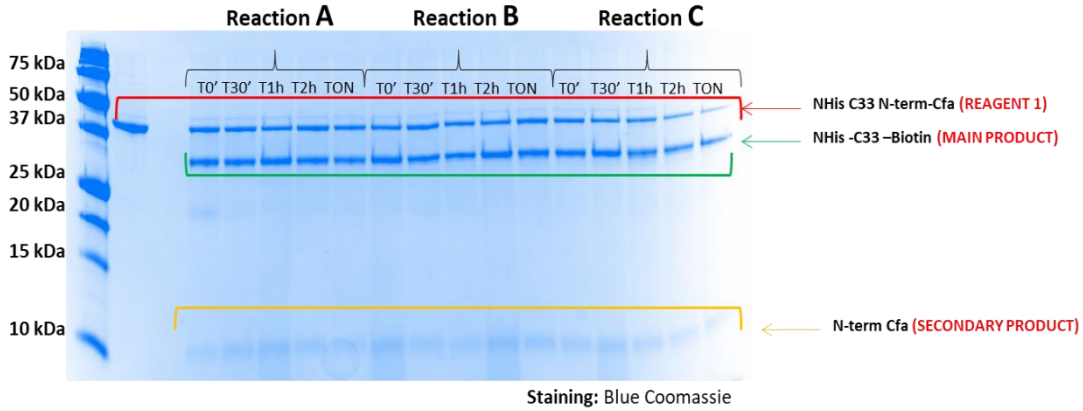

Figure 74. SDS-page showing the comparison among kinetics of Cfa split-intein reaction performed with three different reaction setting.

After that, we wanted to investigate if the increase of the temperature could further improve the reaction yield. We therefore decided to compare the best condition (test C) obtained in the previous Cfa-split-intein reaction tests, which were performed at +25 °C, with another one performed in the same condition but at +30 °C (Test D).

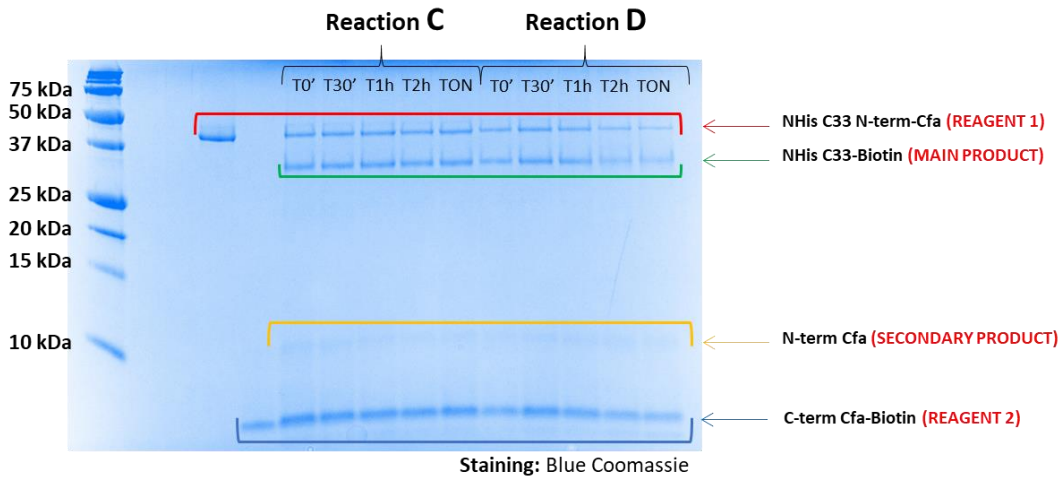

The SDS-page analysis (Figure 75) showed the same conversion yield in both of the two conditions tested and so we thought to choose the condition C (+25°C) and to exclude the condition D performed at higher temperature (+30°C) in order to avoid any thermal stress for our C33 antigen.

Figure 75. SDS-page showing the comparison between the kinetics of Cfa split-intein reactions performed at two different temperature, +25°C and +30°C.

All the explored conditions underlined that the protein trans splicing reaction was very fast: from T0 we observed the conversion of NHis-C33-N-term-Cfa into the main product and we noticed the completion of the reaction after 1-2h.

At this point, we performed two Cfa-split-intein reactions exploiting the best reaction conditions selected from previous tests, but in the first one, we used our recombinant C-term-Cfa-biotin obtained by the express protein ligation, and in the second one the synthetic C-term-Cfa-biotin peptide already used in the previous tests (Table 26). The aim of this last test was to compare the efficacy of protein trans splicing activity of our recombinant C-term-Cfa-biotin compared to that of synthetic origin.

Test	Constructs	Concentration (mg/ml) Molarity (µM)	Molar ratio C-term-Cfa/ N-term-Cfa	Temperature	Buffer
E	NHis-C33-N-term-Cfa	0,2 mg/ml 9,4 µM	16,6 X	+25°C	Splicing Buffer 4M UREA
	Recombinant C-term-Cfa-Biotin	0,4 mg/ml 156 µM			
F	NHis-C33-N-term-Cfa	0,2 mg/ml 9,4 µM	16,6 X	+25°C	Splicing Buffer 4M UREA
	Synthetic C-term-Cfa-Biotin	0,4 mg/ml 156 µM			

Table 26. Selected conditions to carry out the protein trans splicing by Cfa-split-intein

The SDS-page analysis indicated that using the two different biotinylated C-term-Cfa-biotin (recombinant vs synthetic) for the protein trans splicing reaction, we reached the same conversion yield in the main product (about ~80%). Therefore, we demonstrated that recombinant C-term-Cfa-biotin had a performance completely comparable to that of synthetic C-term-Cfa-biotin in the Cfa-split-intein reaction test.

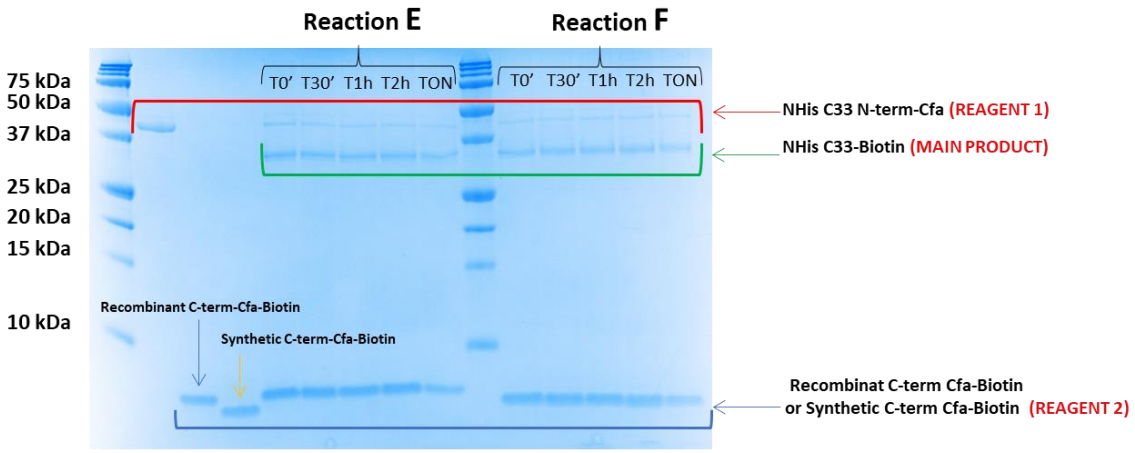

Staining: Blue Coomassie

Figure 76. SDS-page showing the kinetics of Cfa split-intein reaction performed with the recombinant C-term-Cfa and the relative synthetic version.

WESTERN BLOT ANALYSIS OF THE CFA SPLIT-INTEIN REACTION TESTS

To verify the site-specific biotinylation of the NHis-C33 obtained by the last two Cfa-split intein reaction tests (E-F; see table above), we decided to perform a western blot analysis by using a Streptavidin-HRP as probe (see materials and methods section for more details).

The results of the western blot (Figure 77) showed that in both of the two reactions the NHis-C33 was biotinylated because we observed the signal at the level of the main product using the Streptavidin-HRP for the detection.

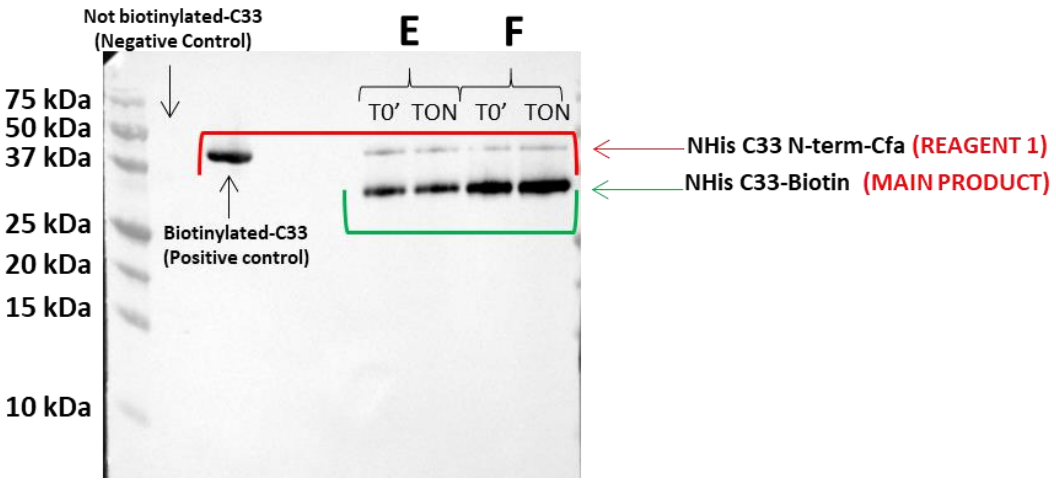

Figure 77. Western blot showing the site-specific-biotinylation of NHis-C33 after the Cfa split-intein reactions performed with two different C-term-Cfa-Biotin, recombinant (E) and Synthetic (F).

In summary, the best conditions in which we decided to perform the Cfa split intein reation were:

- The molar ratio between C-term-Cfa-biotin and NHis-C33-N-term-Cfa was set at 17 to 1 respectively, which means that the concentration of C-term-Cfa-biotin was double that of the NHis-C33-N-term-Cfa (different molecular weights).
- Splicing buffer with 4 M UREA.
- Temperature of +25°C with stirring and in presence of 2mM TCEP.
- Reaction time of an hour and thirty minutes because, from the previous kinetic experiments, we demonstrated that after this time frame we reached the maximum conversion yield in the NHis-C33-biotin final product.

PURIFICATION PROCESS OF NHIS-C33-BIOTIN

After the optimization of the Cfa split-intein trans splicing reaction, we obtained a good conversion yield of the starting reagents (NHis-C33-N-term-Cfa and C-term Cfa-biotin) in the main product (NHis-C33-biotin), but unluckily the protein trans splicing reaction didn't reach the total efficiency. For this reason, after the reaction, we needed to develop a purification process to remove the two starting reagents that didn't react and the secondary products from the main product, the biotinylated NHis-C33. For a better comprehension, we illustrated again the details of the reaction scheme and the expected products in the figure 78 below.

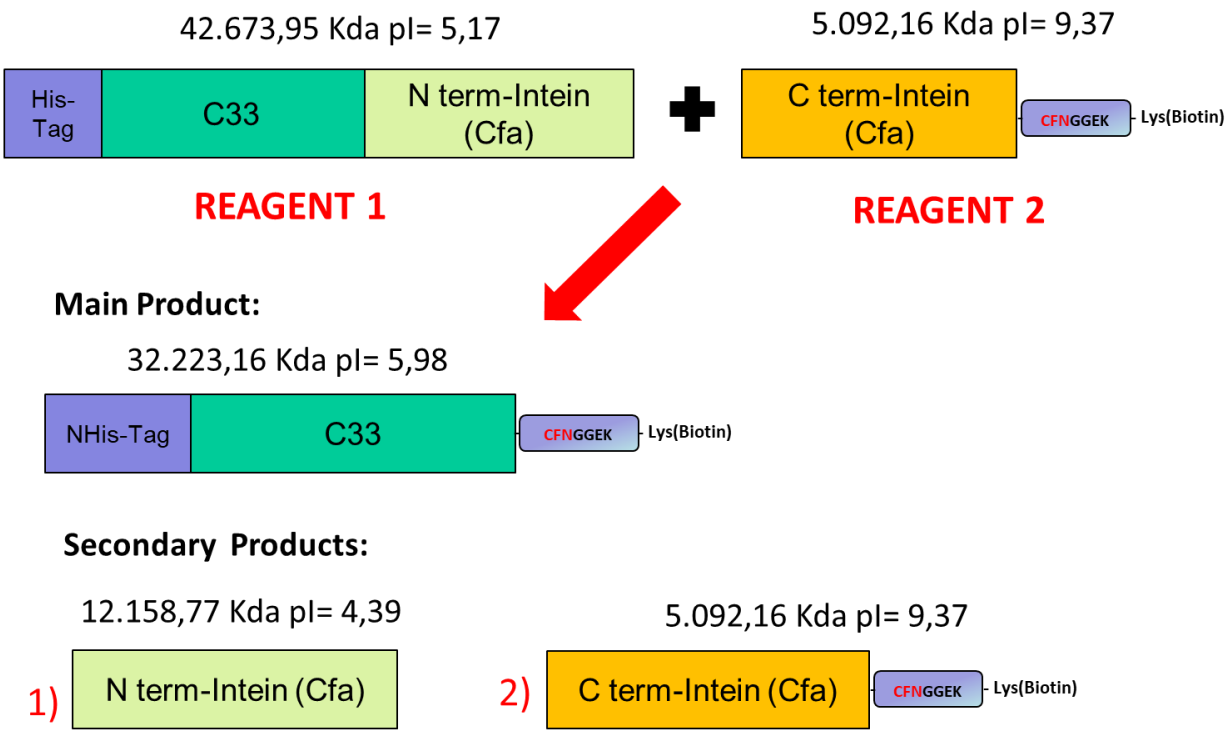

Figure 78. Cfa split-intein reaction scheme with the characteristics of all the species involved in the reaction.

At the beginning, we thought to purify the NHis-C33-biotin final product from the NHis-C33-N-term-Cfa initial reagent performing a Hydrophobic Interaction Chromatography followed by an IMAC to eliminate the other undesired species. We decided to perform the HIC as first step, exploiting the higher hydrophobicity of the NHis-C33-N-term-Cfa than the NHis-C33-biotin, but we were not successful because we obtained a chromatographic profile with a unique peak comprising the two proteins that we wanted to separate and the other undesired species (data not shown).

Based on this result, we tried to separate the two NHis-C33-N-term-Cfa and the NHis-C33-biotin proteins by Anion Exchange Chromatography (AEC).

As show in the figure above, the fusion protein NHis-C33-N-term-Cfa has an isoelectric point slightly lower than the NHis-C33-biotin, but the large number of acid residues in the N-term-Cfa sequence bring to a different charges distribution in the protein structure of two species. This characteristic should allow a different interaction on the anion exchange resin between the two proteins and therefore lead to a different elution during chromatography.

As first test, we performed the AEC at pH 7,5 with a NaCl linear gradient from 0 to 1 M during the elution step, with the aim to understand if this chromatographic method was suitable for our purposes. The chromatographic profile showed that, as expected, the C-term-Cfa-biotin was eluted in the flow-through fraction due to its high pI (figure 79), while the main elution peak contained both NHis-C33-N-term-Cfa and NHis-C33-biotin. However, it is necessary to specify that there was a different distribution of the two species during the linear elution gradient: while the NHis-C33-biotin (principal product) linked less strongly the AEC resin and consequently eluted in the first part of the peak, the NHis-C33-N-term-Cfa (reagent 1) interacted more strongly with the AEC resin and therefore was mainly present in the second portion of the peak (Figure 79).

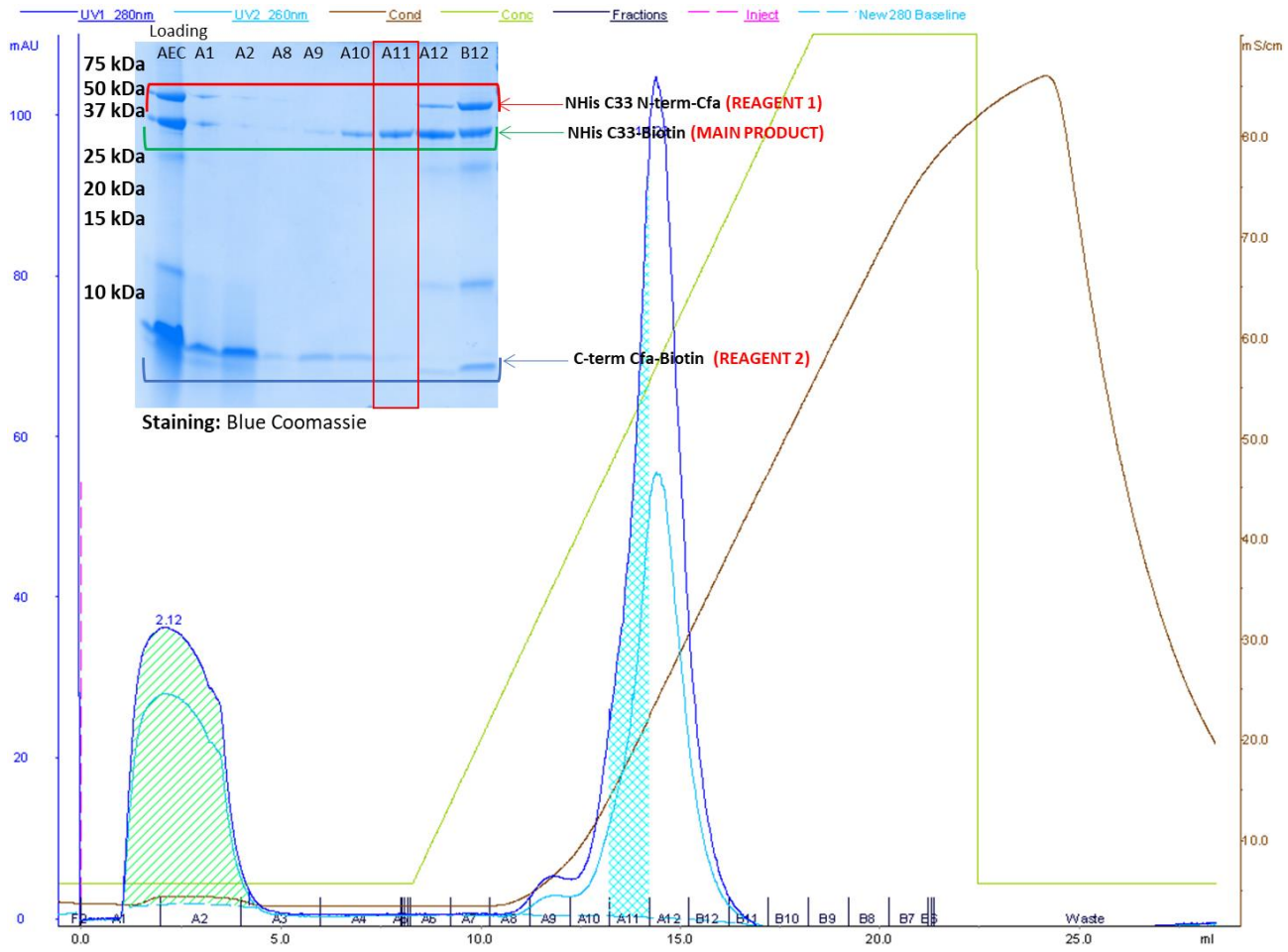

Figure 79. Chromatogram and SDS-page analysis relative to the first AEC purification of NHis-C33-biotin target protein. The fractions containing the C-term-Cfa-biotin are highlight in green on the chromatogram, while the fraction containing the NHis-C33-biotin are indicated by red rectangle onto SDS-page gel and underline in light blue on the chromatogram.

These data showed the potentiality of this chromatographic technique for the separation of our biotinylated antigen from the NHis-C33-N-term-Cfa; for this reason we tried to optimized the NaCl gradient during the AEC elution in order to obtain a better chromatographic resolution and separation of the two proteins than the first AEC test.

After a thorough study, which required several experiments, we were able to find the best elution conditions for the separation of NHis-C33-N-term-Cfa and NHis-C33-biotin proteins. These conditions are summarized in Table 27.

For more details relative to the final conditions of Anion Exchange chromatography see materials and methods section.

Constructs	**Concentration (mg/ml)** **Molarity (µM)**	**Molar ratio** **C-term-Cfa/** **N-term-Cfa**	**AEC** **Column**	**Elution method**
NHis-C33-N-term-Cfa	1 mg/ml 23,4 µM	17,2X	Foresight Nuvia Q	Steps gradient 1,8 % - 8,5% + linear gradient 8,5%-100% of elution buffer
Synthetic C-term-Cfa-Biotin	2 mg/ml 403 µM			

Table 27. Conditions of Cfa split-intein reaction and selected elution method for the AEC

The chromatogram and the SDS-page analysis of the optimized AEC method confirmed that there was in the flow-through fractions mainly the C-term-Cfa-biotin and that there was in the first half of the principle peak only our target protein (NHis-C33-biotin). Only a little portion of NHis-C33-biotin eluted in the second half of the peak together with the other undesired species (NHis-C33-N-term-Cfa, N-term-Cfa and C-term-Cfa-biotin). Therefore, we pooled the fractions (indicated by a red rectangle on SDS-page and underline in pink on the chromatogram) in which there was mainly our target protein (Figure 80).

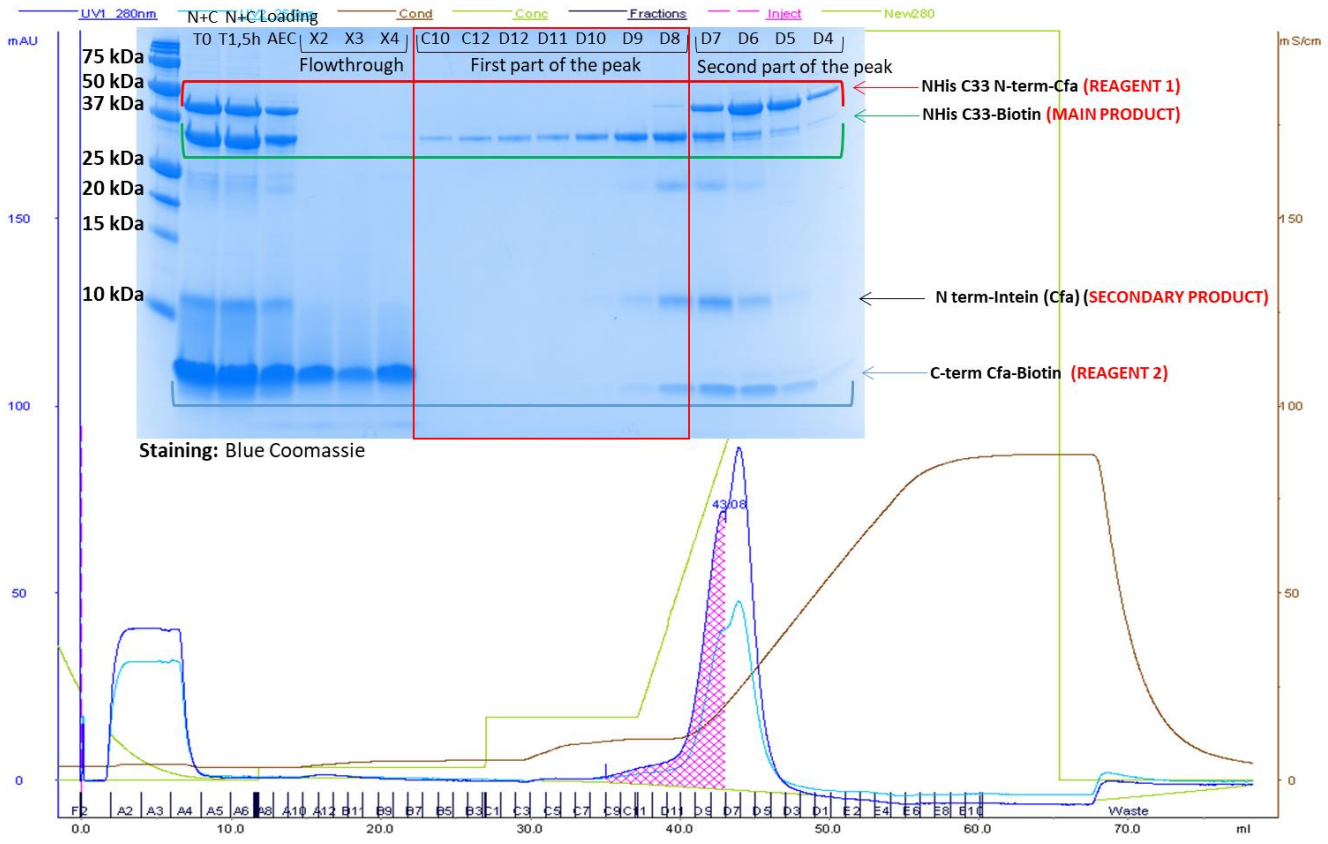

Figure 80. Chromatogram and SDS-page analysis relative to the purification of NHis-C33-biotin target protein by AEC. The pooled fractions are indicated by red rectangle and underline in pink on the chromatogram.

After that, the AEC pool was loaded on an IMAC column (metal chelate affinity chromatography) through which we wanted to further purify the NHis-C33-biotin from the residual undesired proteins (for more details relative to the IMAC conditions see materials and methods section).

The chromatogram and the SDS-page analysis about the IMAC showed that in the flow-through (X1 fraction) there was mainly the residual N-term-Cfa and others slight contaminations. As expected, our NHis-C33-biotin was in the principal peak. Finally, we pooled the more concentrated fractions (red rectangle onto SDS-page and highlighted in pink on the chromatogram, Figure 81).

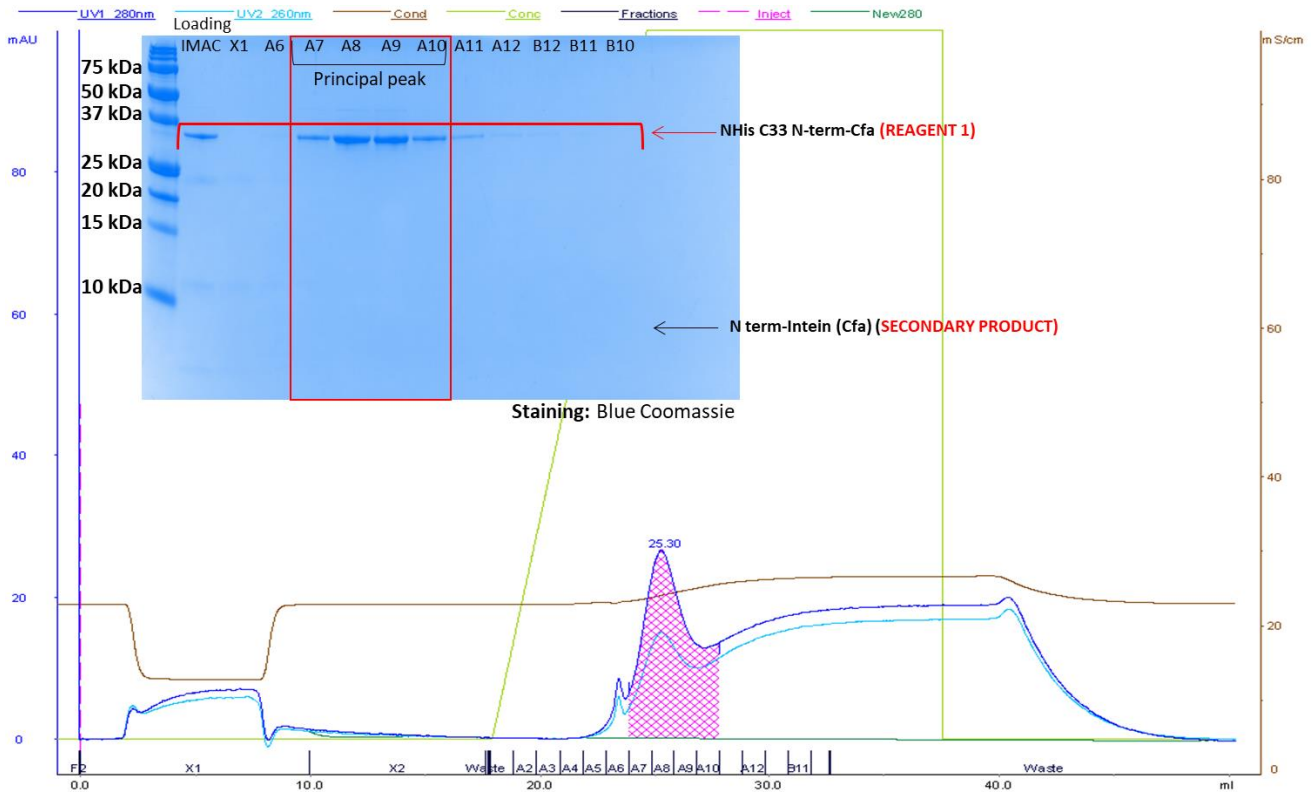

Figure 81. Chromatogram and SDS-page analysis relative to the purification of NHis-C33-biotin target protein by IMAC. The pooled fractions (final sample) are indicated by red rectangle and underline in pink on the chromatogram.

To verify the reproducibility of the site-specific biotinylation of NHis-C33 by protein trans splicing (PTS) and its purification process, we performed three replicates of the Cfa split-intein reaction starting from the same quantity of NHis-C33-N-term-Cfa and C-term-Cfa-biotin and then we purified the NHis-C33-biotin product through the combination of AEC and IMAC techniques. The results demonstrated the robustness of both the site-specific biotinylation by Cfa split-intein reaction and the purification method of the biotinylated antigen, since we obtained comparable quantity of NHis-C33-biotin from three different lots (Table 28).

Lot	NHis-C33-N-term-Cfa (mg)	C-term-Cfa-Biotin(mg)	NHis-C33-Biotin (mg)
1	7,5	15	2,78
2	7,5	15	2,17
3	7,5	15	2,34

Table 28. Three different lots of NHis-C33-Biotin obtained through Cfa split intein reaction followed by AEC and IMAC purifications. In the first and in the second column are shown respectively the mgs of the NHis-C33-N-term-Cfa and the C-term-Cfa-biotin used to perform the protein trans splicing reactions. In the third column the mgs of the main product (NHis-C33-biotin) obtained.

RETARDATION ASSAY OF NHIS-C33-BIOTIN

Once we had obtained the biotinylated antigen we wanted to check the efficiency of the site specific biotinylation by protein trans splicing and therefore we performed the retardation assay (see material and method for more informations).

The SDS page analysis showed the comparison among a non-biotinylated C33, the C33-Atag (negative control), the Diasorin C33-biotin currently used in LIAISON XL Murex HCV Ab assay (positive control) and our three lots of NHis-C33-biotin obtained through the protein trans splicing and subsequent AEC and IMAC purifications (lot 1, lot 2 and lot 3, respectively). Every sample was loaded two times, with and without the addition of streptavidin in order to appreciate on the SDS-page gel the band shift at high molecular weight of the biotinylated NHis-C33 protein.

The results showed that, as in the previous retardation assay, the C33-Atag was not biotinylated and the Diasorin-C33-biotin resulted biotinylated with an efficiency of about 50%. Also in this test, in all our three lots the NHis-C33 antigen biotinylation efficiency was approximately of 100%.

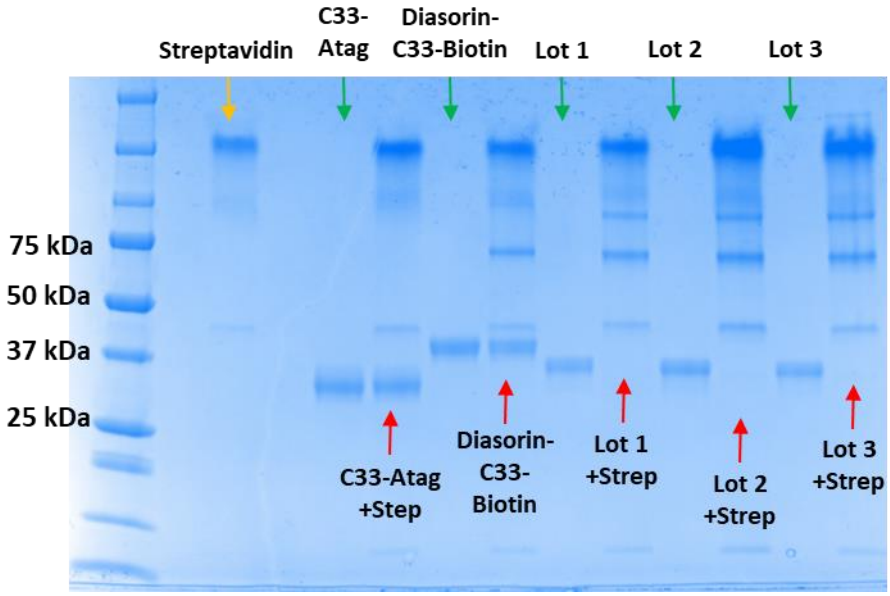

Figure 82. Retardation assay of three different lots of NHis-C33-biotin obtained by protein trans splicing and subsequent AEC and IMAC purification, compared with C33-Atag (negative control) and with Diasorin C33-biotin (positive control). The yellow arrow indicates the streptavidin, the green arrows the samples without streptavidin and the red arrows the samples with streptavidin.

IMMUNOREACTIVITY OF NHIS-C33-BIOTIN

Also for these three lots we verified their immunoreactivity comparing them with the Diasorin C33-biotin currently used in the LIAISON XL Murex HCV Ab assay.

In particular, we replaced our biotinylated C33 with the Diasorin C33-biotin maintaining the setting and the other reagents of the LIAISON XL Murex HCV Ab assay in order to compare only the immunoreactivity of the two biotinylated antigens.

To check the immunoreactivity of the NHis-C33-biotin, we performed the HCV immunoassay on a panel of human HCV negative samples and on panel of human HCV positive samples. It's important to highlight that each experiment was realized in triplicate in order to confirm the data reproducibility.

The panel of the human HCV negative blood samples, presented in figure 83, showed that the RLU signals result comparable using in the HCV immunoassay the Diasorin C33-biotin or our three lots of NHis-C33-Biotin.

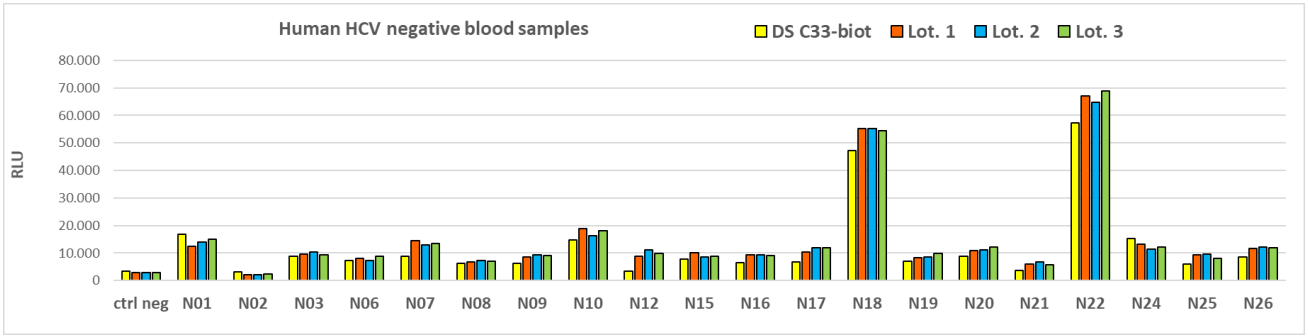

Figure 83. Histogram about the panel of human HCV negative blood samples tested in the LIAISON XL Murex HCV Ab assay.

The histogram about the panel of the human HCV positive blood samples (Figure 84) displayed comparable RLU signal. These results indicated a similar immunoreactivity among the Diasorin C33-biotin an our three lots of NHis-C33-biotin obtained by protein trans splicing followed by AEC and IMAC purifications.

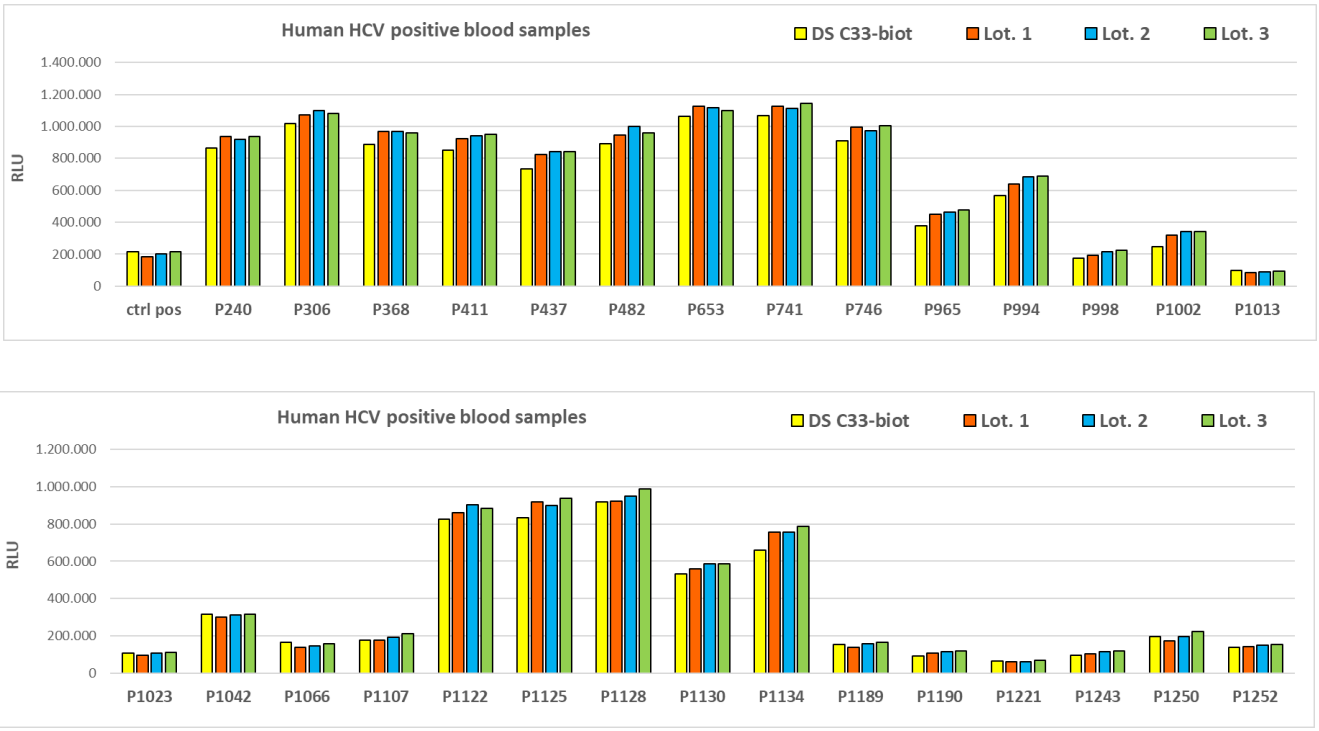

Figure 84. Histograms of the panel of human HCV positive blood samples analyzed in the LIAISON XL Murex HCV Ab assay

To conclude, we proved the potentiality and efficiency of the protein trans splicing by Cfa split-intein to perform the site-specific biotinylation of the C33 antigen and also we developed an efficient method for its purification after the split-inteins reaction.

Finally, we demonstrated that all the three lots of NHis-C33-Biotin were characterized by an immunoreactivity comparable to that of the Diasorin-C33-biotin in the LIAISON XL Murex HCV Ab assay.

A BIOTECHNOLOGICAL APPLICATION OF PROTEIN TRANS SPLICING: SITE-SPECIFIC BIOTINYLATION OF A RECOMBINANT IgG ANTI-IFNγ ANTIBODY

In the previous paragraph, we demonstrated that the site-specific biotinylation of C33 antigen by protein trans splicing was a reproducible and controllable process that led to obtain a biotinylated protein with a good immunoreactivity in LIAISON XL Murex HCV Ab assay. For these reasons, we decided to exploit the wide potentiality of the PTS technique by the use of Cfa split-intein to execute a site-specific biotinylation of a recombinant IgG anti-IFNγ antibody. After that, the aim was that to verify if the immunoreactivity of the site-specific biotinylated antibody in an immunoassay for the detection of INFγ, could be higher than the same antibody biotinylated on the ammine group of the Lysine residues (classical random biotinylation). In details, we realized a recombinant IgG anti-IFNγ antibody having the N-term-Cfa-His tag sequence fused to the C-terminal of its heavy chains. In this way we exploited the N-term-Cfa sequence fused to the C-terminus of the heavy chains of the anti-IFNγ antibody to perform a trans splicing reaction with the synthetic C-term-Cfa-biotin peptide (the same used for the site specific biotinylation of C33 antigen; as described in details in the previous paragraph). As result of the protein trans splicing reaction we wanted to obtain the recombinant IgG anti-IFNγ antibody biotinylated in a site-specific way at the C-terminal (Figure 85).

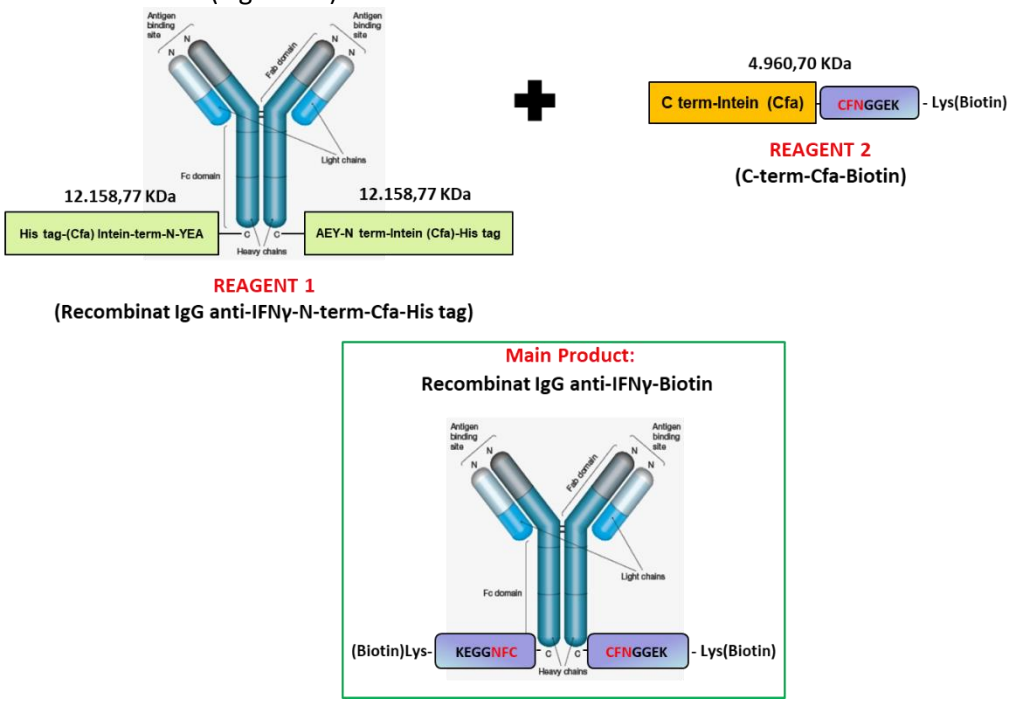

Figure 85. Cfa Split-intein reaction between the recombinant IgG anti-IFNγ-N-term-Cfa antibody and C-term-Cfa-biotin peptide to obtain the recombinant IgG anti-IFNγ-biotin (Main product).

EXPRESSION OF RECOMBINAT. IgG anti-IFNγ-N-TERM-CFA

The recombinant IgG anti-IFNγ antibody carrying the N-term-Cfa was expressed exploiting the Expi CHO expression system. This technology is based on the transient transfection of Chinese Hamster Ovary cells (CHO). In particular, the CHO cells were co-transfected using two plasmids with a ratio of 1:1: the first plasmid codified for the light chain of the recombinant IgG anti-IFNγ antibody and the second one contained the sequence expressing the heavy chain of the same antibody fused at its C-terminal with the N-term-Cfa sequence (see Materials and Methods section for more details).

Supernatants were collected at day 9 from transfection based on the collected cell viability and cell growth data (data not shown). The goal was to preserve the quality of the proteins.

A supernatant sample was collected each cell culture day to follow transient production. Samples were analyzed through SDS-PAGE and western blot (WB) analysis to characterize the final product.
The SDS page and western blot analysis in reducing condition (Figure 86 A and B) highlighted that the expression of the IgG antibody increased during the days of manufacture (from day 5 to 9, lanes 1 to 5, red arrow). As, expected, the band corresponding to the heavy chain carrying the extra sequence N-term-Cfa was higher than those of the controls. The controls were the same recombinant IgG anti-IFNγ antibody without the N-term-Cfa (lane 6, green arrow) and a commercial recombinant IgG (lane 7, green arrow).

The western blot was developed with a polyclonal anti-human IgG that binds both heavy and light chain, with high specificity for k light chain (see Materials and Methos section for more details). This primary antibody allowed us to underline the difference between the specific and intense detection of a k light chain (lane 7) and the less specific and mild one of a λ light chain (from lane 1 to 6) confirming that our antibody is characterized by the λ light chain.

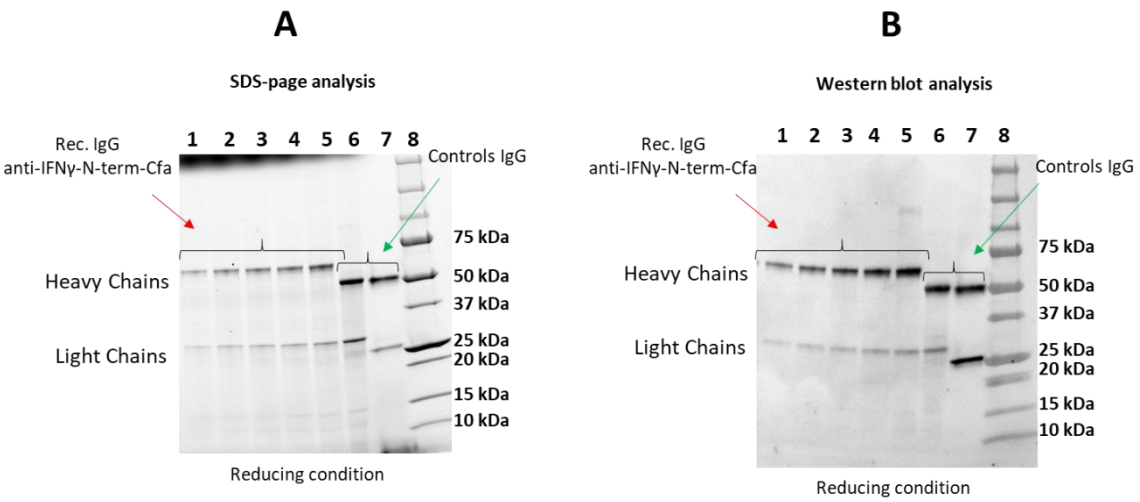

Figure 86 A and B. SDS-page and western blot analysis in reducing conditions about the recombinant IgG anti-IFNγ-N-term-Cfa antibody transient production in Expi-CHO cells. From lane 1 to 5 is shown respectively the antibody expression from day 5 to day 9 (red arrow), in the lane 6 and 7 are reported respectively the recombinant IgG anti-IFNγ antibody without the N-term-Cfa and a commercial recombinant IgG (controls, green arrow).

The SDS page and western blot analysis in non reducing conditions (Figure 87 A e B) showed the bands of our antibody at the molecular weight that corresponds to a folded full IgG, as the controls. However, the shift to higher molecular weight of the not reduced antibody carrying the N-term-Cfa (lanes 1 to 5, red arrow) was observed compared to the controls (recombinant IgG anti-IFNγ antibody without the N-term-Cfa and a commercial recombinant IgG, lanes 6 and 7, respectively, green arrow). A typical three bands pattern of IgG antibody in non-reducing conditions was recognized in our samples and in the controls (light blue parenthesis, figure 87 B). Moreover, no degradation products were present.

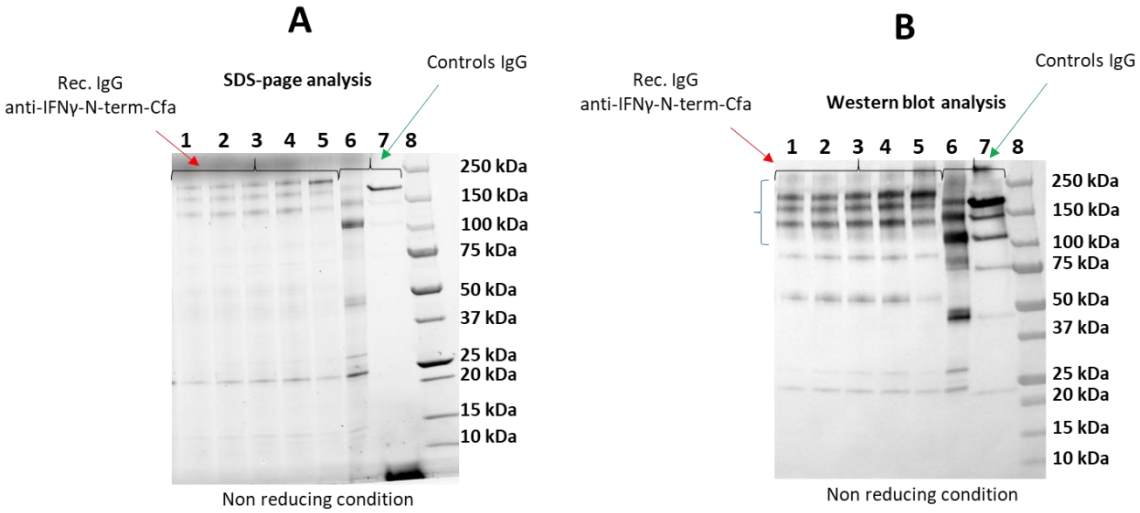

Figure 87 A and B. SDS-page and western blot analysis in non reducing conditions about the recombinant IgG anti-IFNγ-N-term-Cfa antibody transient production in Expi-CHO cells. From lane 1 to 5 is shown respectively the antibody expression from day 5 to day 9 (red arrow), in the lane 6 and 7 are reported respectively the recombinant IgG anti-IFNγ antibody without the N-term-Cfa and a commercial recombinant IgG (controls, green arrow). The light blue parenthesis indicates the typical three bands pattern of IgG antibody.

PURIFICATION PROCESS OF RECOMBINANT IgG anti-IFNγ-N-TERM-CFA ANTIBODY

At the beginning, the harvested supernatant containing our recombinant IgG anti-IFNγ-N-term-Cfa was clarified by centrifugation and then by filtration (0,22 µm) to remove eventual cells debris and aggregates.

After that, we purified the antibody through two chromatographic steps: Protein A affinity chromatography followed by Gel Filtration Chromatography (GFC).

The figure 88 below shows the chromatographic profile and relative SDS-page analysis obtained with the protein A purification (see Materials and Methods section for more details).

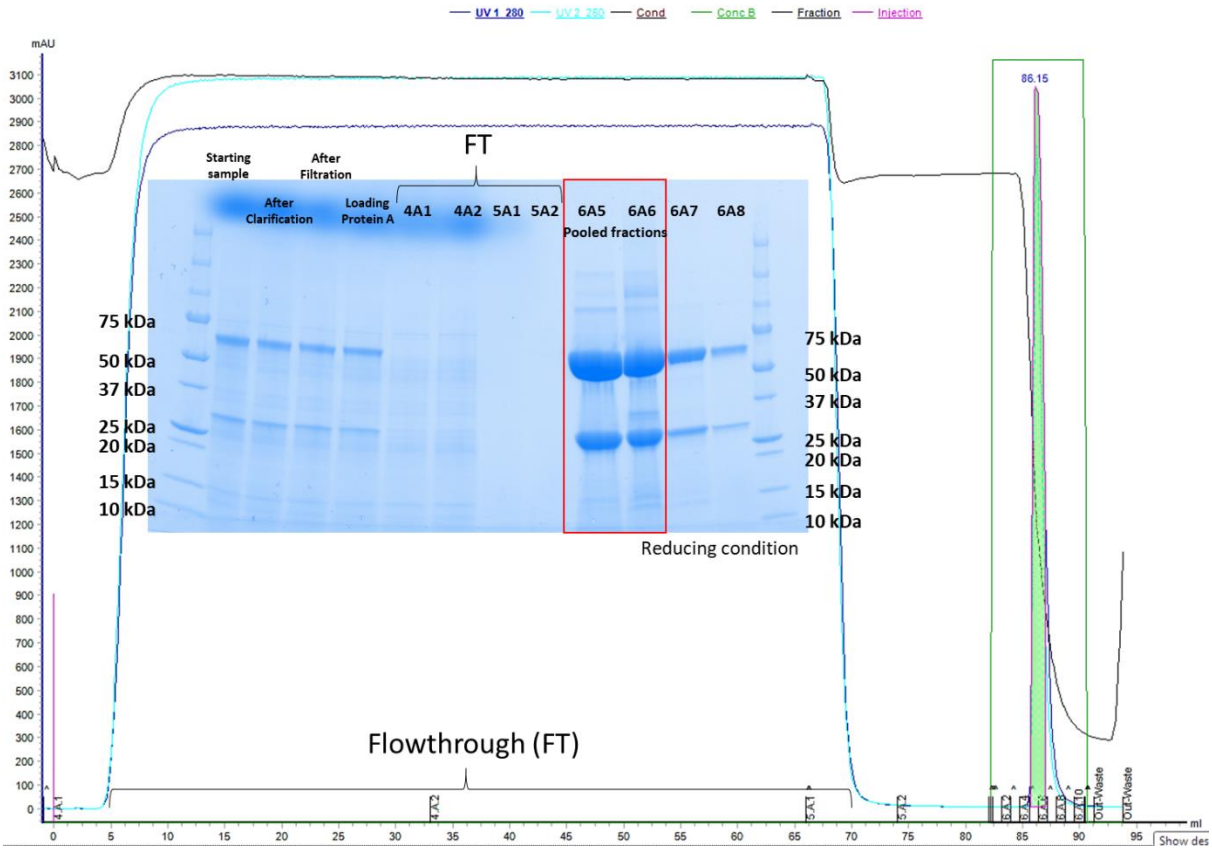

Figure 88. Chromatographic profile and SDS-page analysis relative to the protein A purification of the recombinant IgG anti-INFγ-N-term-Cfa antibody. We pooled the fractions underline in green on chromatogram and by the red rectangle onto SDS-page gel.

The Protein A pool was loaded onto a gel filtration column to perform a final polishing step of the recombinant antibody.

The chromatographic profile and the SDS-page analysis of the GFC purification are displayed below in the figure 89. The main peak eluted was the monomeric form of purified recombinant IgG anti-IFNγ-N-term-Cfa with high degree of purity and represented the GFC pool (final sample).The fractions relative to the minor peaks eluted at lower retention volumes (higher molecular weights) contained the aggregate forms of our recombinant antibody and for this reason, they were discarded.

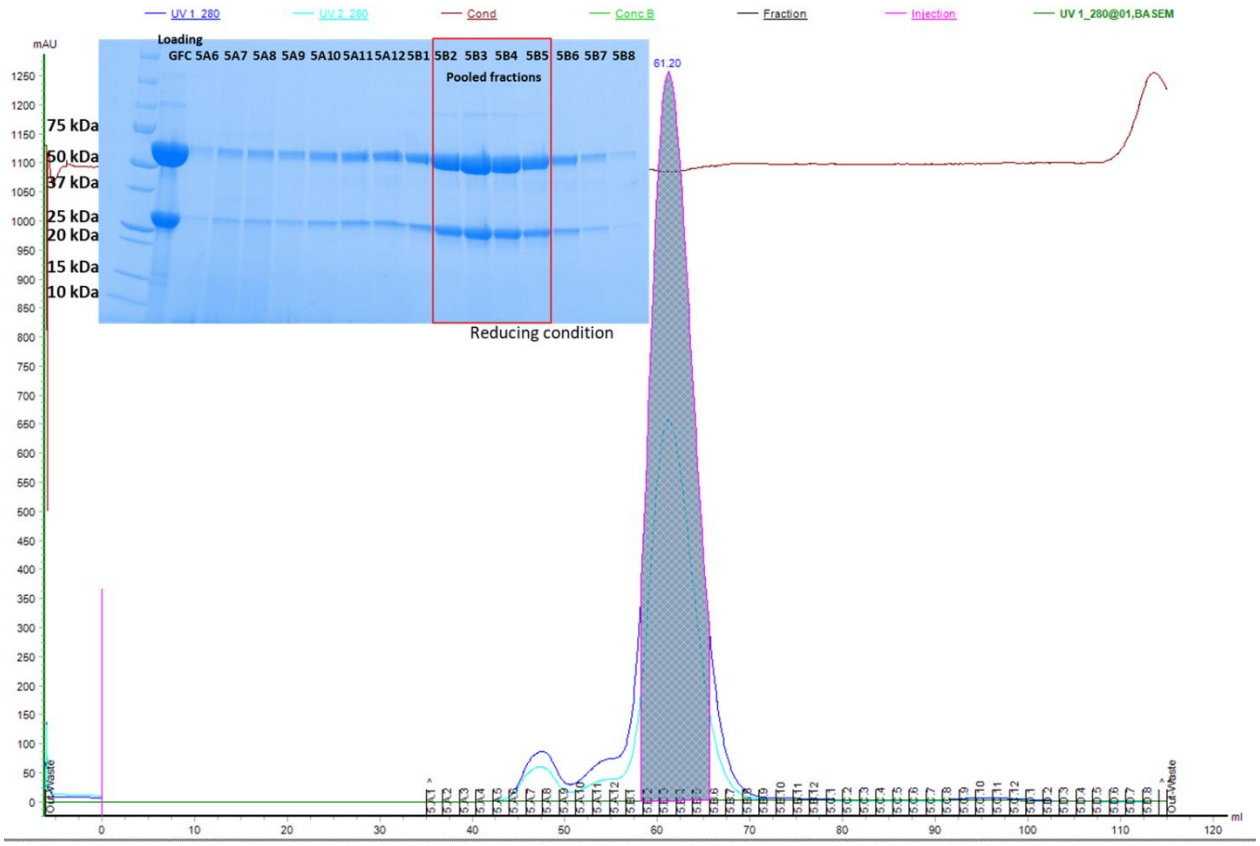

Figure 89. Chromatographic profile and relative SDS-page analysis obtained after the final polishing step of recombinant IgG anti-INFγ-N-term-Cfa antibody by GFC. The fractions underline in blue on chromatogram and by the red rectangle onto SDS-page gel was pooled as final sample.

In summary, at the end of the downstream process described above, we obtained a recombinant IgG anti-INFγ-N-term-Cfa antibody with an excellent degree of purity. We performed only a few antibody productions starting from 30 mL to 250 mL of cell culture supernant and found a final mean production relative to the purified antibody of approximately 60-70 mg/L of cell culture (data not shown). At this level we were more interested in exploring the ability of Cfa split-intein to perform a site-specific biotinylation of a recombinant IgG antibody and to evaluate the immunoreactivity of the related product but less in the overall yield of the purification process, as we were beginning to explore this new technique.

CFA SPLIT INTEIN REACTION TEST USING THE RECOMBINANT IgG anti-IFN γ N-TERM-CFA

We performed the protein trans splicing by Cfa split-intein mixing the purified recombinant IgG anti- IFN γ-N-term-Cfa with the synthetic C-term-Cfa-biotin peptide in order to obtain the site-specific biotinylation on the heavy chains of this antibody, in particular at the C-terminal of its polypeptide sequence. As reported in literature [1] and as seen in the previous paragraph for the C33 antigen, also in this case, we didn't expect the complete conversion of the initial reagents into the main product (reaction efficiency less than 100%). For this reason we considered the possibility to have the secondary products in addition to the recombinant IgG-anti-IFNγ-biotin (main product) at the end of the reaction. The scheme of the reaction with the expected products (main and secondary) is shown in the figure 90.

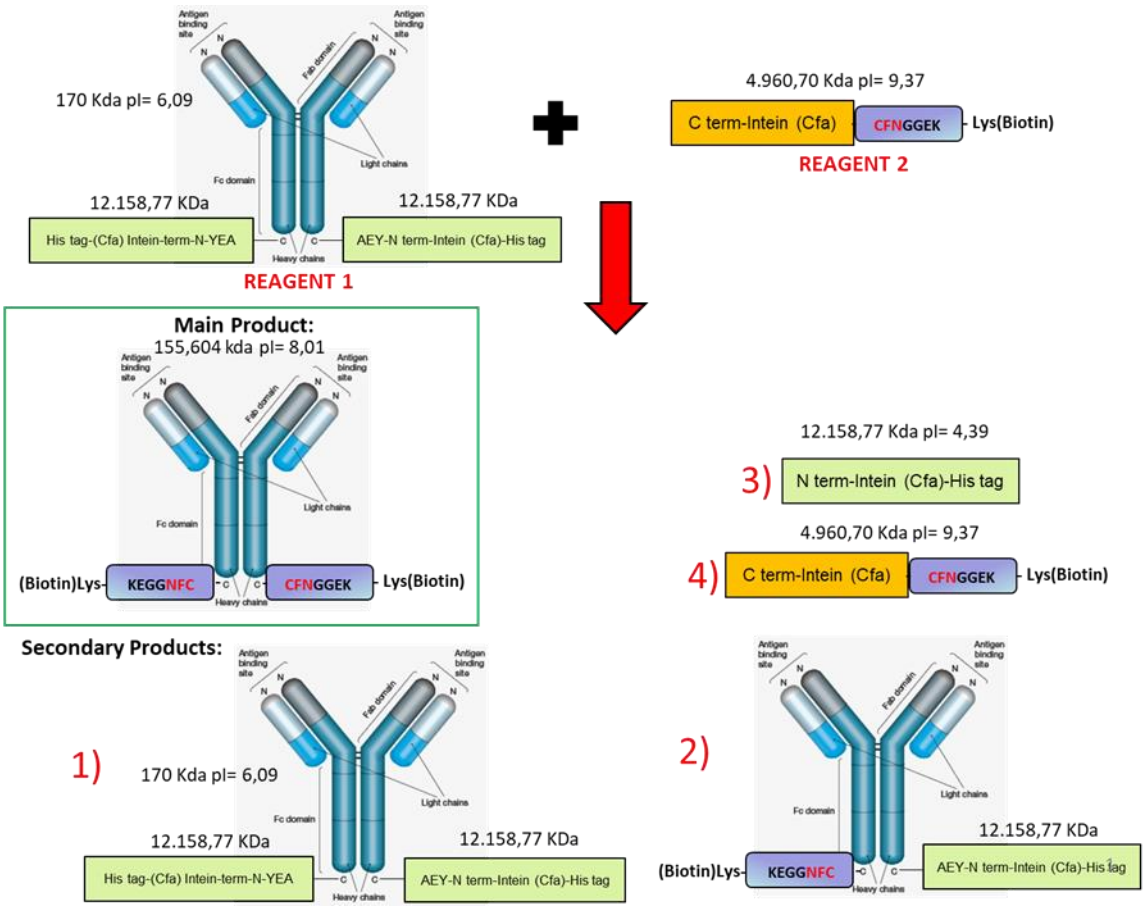

Figure 90. Cfa split-intein reaction scheme between recombinant IgG anti-IFNγ-N-term-Cfa and C-term-Cfa-Biotin with the characteristics of all the species involved in the reaction.

Also in this case, we explored some Cfa split-intein reaction conditions to understand the best one in which to perform the site-specific biotinylation of the recombinant IgG anti-IFN γ antibody by protein trans splicing technology. Based on the literature data and on the previous Cfa split-intein experiments carried out for the production on the NHis-C33-biotin we decided to test the conditions showed in the table below.

Test	Constructs	Concentration (mg/ml) Molarity (µM)	Molar ratio C-term-Cfa/ N-term-Cfa	Temperature	Buffer
A	Rec.IgG anti-IFNγ-N-term-Cfa	2,55 mg/ml 15 µM	10X	+25°C	Splicing Buffer
	C-term-Cfa-Biotin	0,75 mg/ml 150 µM			
B	Rec.IgG anti-IFNγ-N-term-Cfa	2,55 mg/ml 15 µM	20X	+25°C	Splicing Buffer
	C-term-Cfa-Biotin	1,5 mg/ml 300 µM			
C	Rec.IgG anti-IFNγ-N-term-Cfa	2,55 mg/ml 15 µM	10X	+25°C	Splicing Buffer + 2M UREA
	C-term-Cfa-Biotin	0,75 mg/ml 150 µM			

Splicing Buffer*:* Phosphate dibasic dihydrate ($Na_2HPO_42H_2O$) 100 mM, NaCl 150 mM, EDTA 1 mM, 2 mM TCEP, pH 7.2

Splicing Buffer 2M UREA*:* Phosphate dibasic dihydrate ($Na_2HPO_42H_2O$) 100 mM, NaCl 150 mM, EDTA 1 mM, 2 mM TCEP, 2M UREA, pH 7.2

Table 29. Conditions selected in which to perform the Cfa split-intein reaction between recombinant IgG anti-IFNγ-N-term-Cfa and C-term-Cfa-biotin

The SDS-page analysis about the kinetics of Cfa split intein reactions (Figure 91) showed that the conversion yield in recombinant IgG anti-IFNγ-biotin was slightly higher when we used the C-term-Cfa-biotin at the concentration of 0,75 mg/ml (test A) than the condition in which we used the same reagent at 1,5 mg/ml (Test B). For this reason, we decided to use the low concentration of C-term-Cfa-biotin (condition A) for the second Cfa- split intein reaction test. During this new experiment, we compared the condition A with another condition (C) in which we used the splicing buffer with 2 M UREA to relax the proteins structure and so to try to potentially improve the conversion yield of the trans-splicing reaction from initial reagents to the main product.

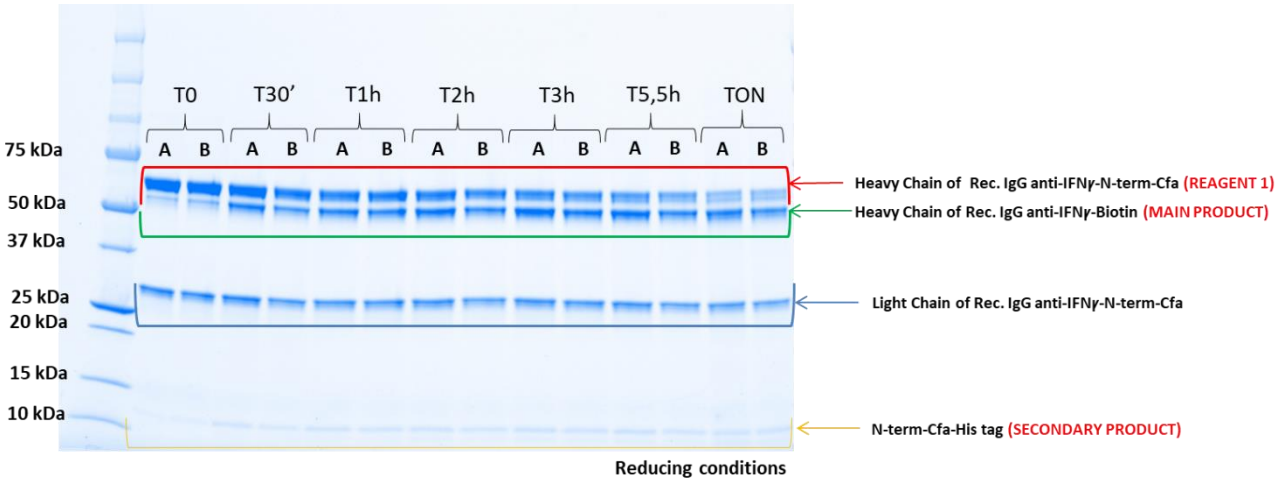

Figure 91. Kinetics of the Cfa split-intein reaction test performed between recombinant IgG anti-IFNγ antibody and C-term-Cfa-biotin using two different concentration of C-term-Cfa-Biotin (A= 0,75 mg/ml and B= 1,5 mg/ml).

The SDS-page analysis of the second Cfa split-intein reaction test (Figure 92) showed that in both the conditions that were tested (A and C), we achieved 70% of conversion yield in the final product (recombinant IgG a-IFNγ-biotin). For this reason, we chose to perform the split intein reaction with the splicing buffer without UREA to preserve the antibody integrity.

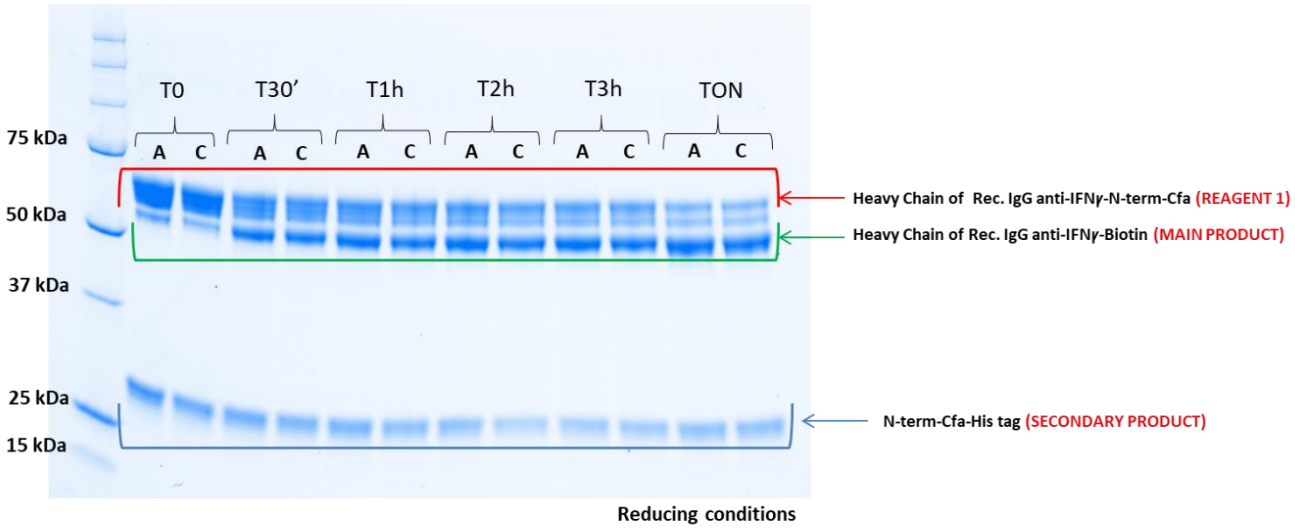

Figure 92. Kinetics of the second Cfa split-intein reaction test performed between recombinant IgG anti-IFNγ-N-term-Cfa antibody and C-term-Cfa-biotin using two different splicing buffers (with or without UREA).

All the explored conditions underlined that the protein trans splicing reaction was very fast: from T0 we observed the conversion of recombinant IgG anti-IFNγ-N-term-Cfa antibody into the main product and we noticed the completion of the reaction after 2h.

PURIFICATION OF RECOMBINANT IgG anti- IFNγ-BIOTIN

After these results, we performed the Cfa split-intein reaction exploiting the best reaction conditions selected from previous tests (condition A); summarizing this condition was based on the use of a molar excess 10X of C-term-Cfa-biotin than the recombinant IgG anti-IFNγ-N-term-Cfa and it was performed in the splicing buffer without UREA, at +25°C with stirring for two hours. After the reaction, we needed to purify the main product from the other undesired species and therefore we thought to a purification method based on two chromatographic steps: a first step represented by an IMAC followed by a second GFC polishing step. Our recombinant IgG anti-IFNγ antibody biotinylated on both of its heavy chains will not have the His tag and so in the first IMAC step will not interact with the resin and therefore it will be collected in the flow through with the C-term Cfa-Biotin; the other secondary products (recombinat IgG anti-IFNγ antibody non biotinylated or recombinat IgG anti-IFNγ antibody biotinylated on only one heavy chian and the N-term-Cfa) that instead own the His tag, will be able to bind the resin and they will be remove from the product of interest. (For a better comprehension, see the scheme of the reaction shown in figure 90).

After that, the flow through will be loaded on a gel filtration column in order to separate the main product from the C-term-Cfa-Biotin thanks to their different molecular weights.

In the future, we will try to apply this purification process in order to separate the main product from the other reaction products but, due to the lack of time and the need to test as soon as possible the immunoreactivity of the recombinant IgG anti-IFNγ biotinylated in a site-specific way, we decided to carry out only the gel filtration step, which does not require particular optimizations.

Through this chromatographic technique we separated the molecules of recombinant antibodies non-biotinylated or biotinylated on one or both heavy chains, characterized by a similar molecular weight (Rec.IgG anti- IFNγ-N-term-Cfa and Rec.IgG anti- IFNγ-biotin) from the other proteins involved in the split intein reaction having a low molecular weight (N-term-Cfa-HisTag and C-term-Cfa-biotin).

As will be fully explained in the next paragraph, the choice to carry out only the GFC step and not to separate the biotinylated from the non-biotinylated forms of the antibody does not invalidate the immunochemical assay.

The chromatographic profile and relative SDS-page analysis (Figure 93), show the results of the GFC purification through which we purified the mix of biotinylated and non-biotinylated recombinant IgG anti- IFNγ antibodies. For more details about the chromatographic conditions see materials and methods section.

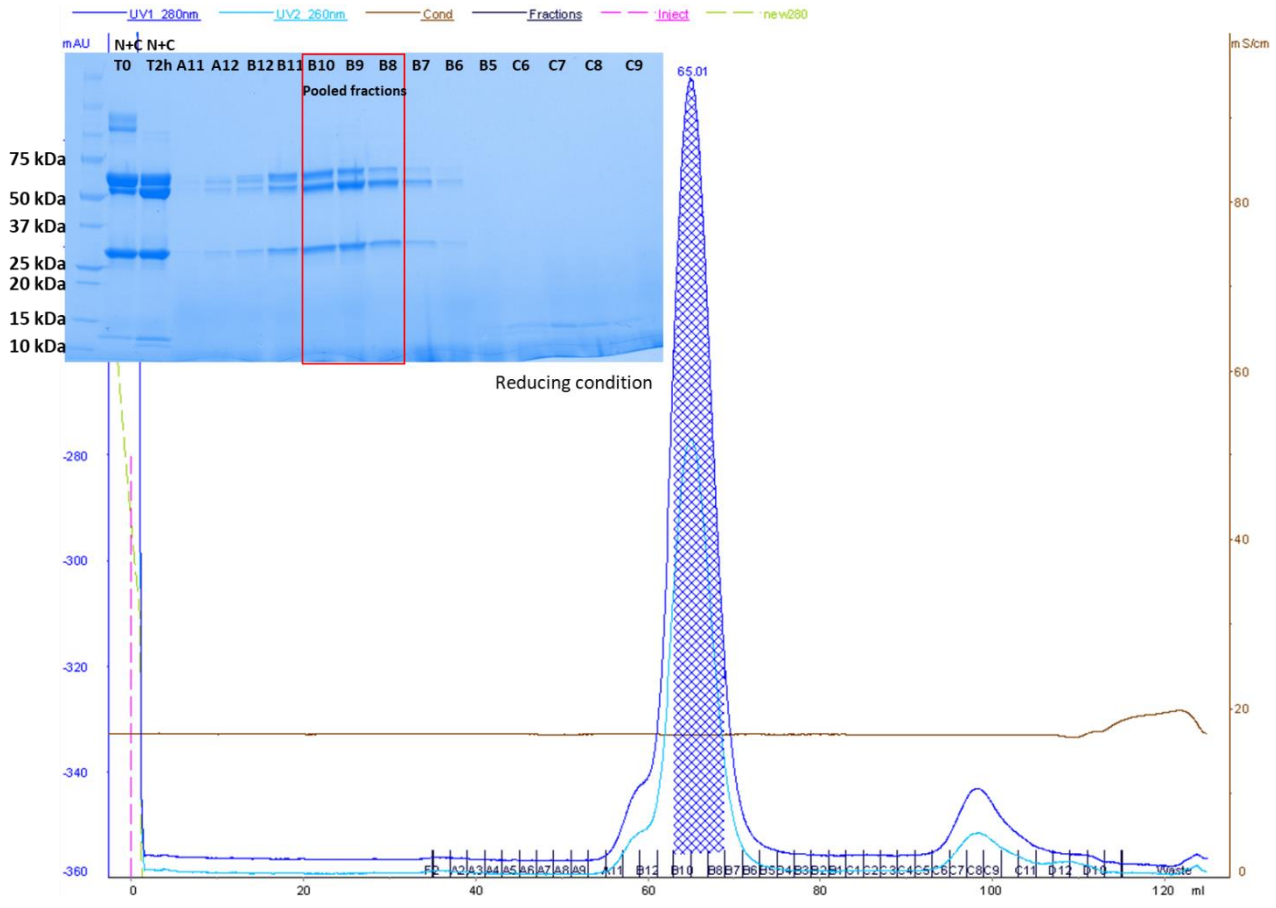

Figure 93. GFC profile and relative SDS-page analysis obtained after the loading onto column of the solution containing the Cfa split intein reaction products. The pooled fractions were highlight in blue in the chromatogram and by the red rectangle onto SDS-page gel.

IMMUNOREACTIVITY TEST OF REC.IgG anti- IFNγ-BIOTIN

The aim of this last part of my project was to demonstrate that the site-specific biotinylation of a recombinant IgG led to greater immunoreactivity than the classic biotinylation of the same antibody, when they were tested in the same immunoassay.

Specifically, we wanted to compare the immunoreactivity of our recombinant IgG anti-IFNγ biotin characterized by a site-specific biotinylation obtained through the Cfa split intein reaction to that of the same recombinant IgG anti-IFNγ antibody, which was biotinylated on the amine group of the lysine residues by an NHS-PEG-biotin reagent (standard random biotinylation).

In the immunoassay prototype for the detection of IFNγ, the recombinant IgG anti- IFNγ-biotin, which has been previously coated at the paramagnetic beads conjugated with streptavidin (solid phase), link the IFNγ present in samples, calibrators or controls. The IFNγ is then recognized by a second anti-IFNγ conjugated with a fluorescent dye called Alexa fluor. Finally, the complex is detected through an anti-Alex fluor antibody, functionalized with the ABEI chemiluminescent molecule that emitted a light signal expressed in RLU by the instrument (Figure 94). Two antibodies are used as tracers because this system allowed a signal amplification resulting in an increased sensitivity of the INFγ immunoassay prototype.

As mentioned before, even though the recombinat IgG anti- IFNγ antibody in the final GFC sample contained a mix of biotinylated and non- biotinylated antibodies, this fact does not invalidate the immunochemical assay. In fact, during the assay manufacturing, this reagent is coated on the paramagnetic beads functionalized with streptavidin to constitute the solid phase: non- biotinylated IgG anti-IFNγ antibodies, unable to link the streptavidin, are wash-out. For more details about the IFNγ immunoassay, see the materials and methods section.

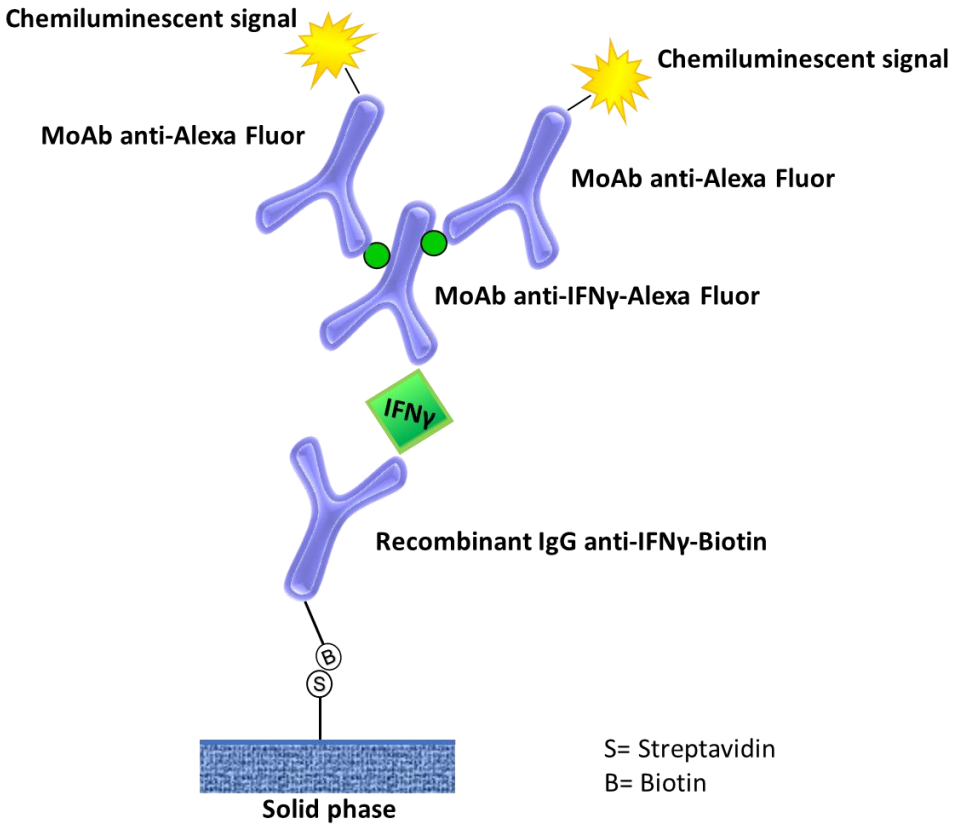

Figure 94. Scheme of the prototype of the IFNγ immunoassay.

In this assay, the two antibodies were tested on an IFNγ curve (axis X of the graphic below, Figure 95) at increasing concentrations.

The graphic showed the increase of the RLU signals obtained performing the IFNγ immunoassay with equal concentrations of both the two biotinylated anti- IFNγ antibodies (Figure 95).

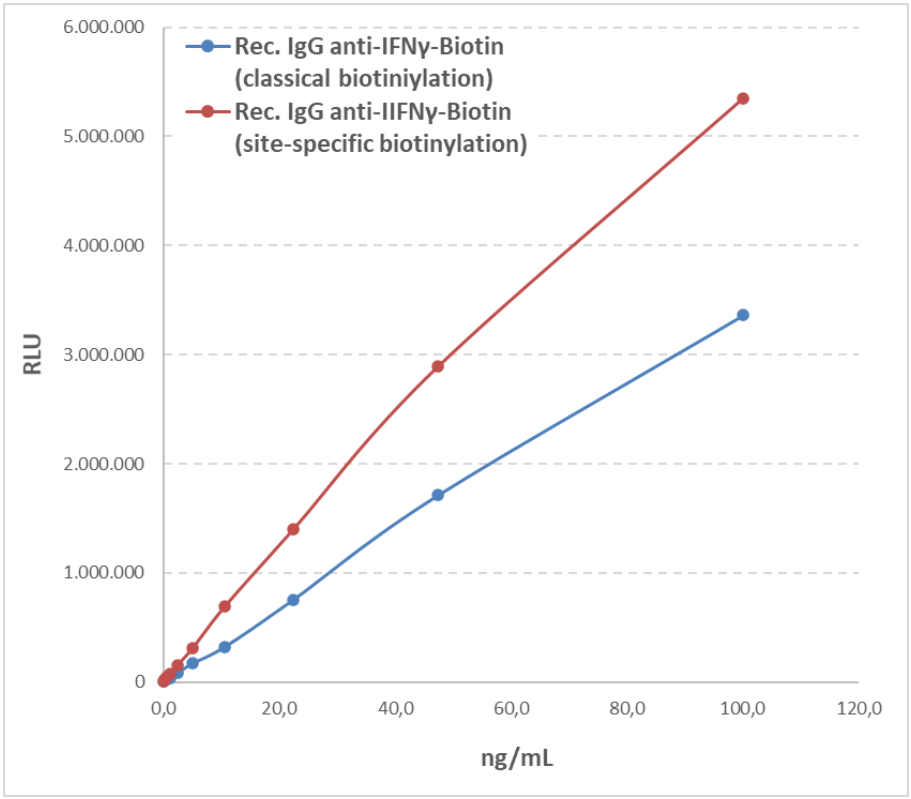

Figure 95. Graphic showing the comparison between the two Rec.IgG anti- IFNγ biotin antibodies in the prototype IFNγ immunoassay: the first was biotinylated with the traditional method (blue line) and the second in a site specific way through the PTS (red line).

From this experiment, we obtained a higher RLU signal in every curve dots using our recombinant IgG anti- IFNγ biotinylated in a site-specific way than the other one having a classical biotinylation. This result indicated that by the use of the site-specific biotinylated recombinant IgG anti-IFNγ antibody, we reached a better immunoreactivity in the prototype of IFNγ immunoassay.

To conclude, we managed to perform a site-specific biotinylation of a recombinant IgG anti-IFNγ antibody by protein trans splicing reaction and we also demonstrated its better immunoreactivity in a prototype of IFNγ immunoassay than the same antibody having a classical biotinylation.

DISCUSSION

In the last years, the immunodiagnostic sector carried out a lot of efforts in the development of new technologies and reagents in order to increase the spectrum of detected pathologies and to improve performances of the immunodiagnostic assays, in terms of sensitivity and specificity. In addition, there is the prominent necessity to obtain rapid and cost-effective procedures for the production of the key bio-reagents used in the immunodiagnostic kits. In particular, the downstream process of bio-reagents represents the most expensive step because requires many materials (i.e. chromatographic resins, buffered solutions, filters), costly instruments (i.e. chromatographers, centrifuges, liquid pumps, etc.) and of course also abundant manpower. Therefore, the streamline and optimization of the purification processes of bioreagents is a good strategy to significantly reduce time and costs required to obtain the desired products.

Another important research field in the immunodiagnostics sector is to increase the performance of bio-reagents in terms of immunoreactivity in the final assay products. This can be reached for example increasing the bio-reagent purities, increasing the bio-reagents storage stability exploring new additives to be added in the final buffer formulations and also, very important in the immunodiagnostic field, exploring new technologies on bioconjugation protocols. In fact, almost all immunodiagnostic assays require modified bio-reagents, called bioconjugates, where a biomolecule, often an antibody, protein, or oligonucleotide, is covalently linked to a specific molecule. These molecules are often substances like biotin, chemiluminescent molecules like ABEI (a luminol derivative), or enzymes (horseradish peroxidase (HRP), Alkaline Phosphatase (AP).

For all these reasons, we thought to develop innovative purification processes in order to improve the yield, production and productivity of different bioreagents and also to perform site-specific labelling of these reagents to verify if these new conjugation techniques could lead to a better performance in the immunodiagnostic assays.

In particular, during my PhD project I mainly focused on the improvement of the protocols for the purification and labelling of the Hepatitis C virus C33 antigen which includes the two first helicase domains of HCV NS3 antigen. The C33 is currently used in the Diasorin LIAISON® XL Murex HCV assay for the detection of human antibodies against the Hepatitis C Virus. The reason of this choice is that the sequence of C33 antigen results immunodominant and then with higher immunoreactivity than the entire NS3.

The purification process of the C33 antigen currently performed in Diasorin includes several chromatographic steps that require many days of work and in which, inevitably, there is a considerable loss of target protein. These drawbacks affect the yield, the production and productivity of the C33 antigen downstream process. Furthermore, since a biotinylated version of C33 protein, previously coated on the streptavidin beads (solid phase), is used in the current Liaison HCV IgG assay, it is necessary to perform the antigen biotinylation after the purification process.

The current biotinylation procedure of C33 antigen consists in the random conjugation of Maleimide-PEG-Biotin molecules on the side chain of Cysteine residues (reduced thiols) present in the antigen polypeptide sequence. This labeling process is characterized by a low efficiency, in fact significative fraction of the portion is still not labelled at the end of the protocol, and the conjugation is not controllable leading to conjugate heterogeneity. Moreover, it is performed after the purification process and then it entails other working days.

In order to solve these limitations, firstly, we tried to improve the C33 purification process developing a not conventional purification method easier and faster than that currently used and, especially, without chromatographic steps. Moreover, we thought to realize a site-specific biotinylation of our antigen directly linked to the purification process to optimize the experimental time (productivity), to have a controllable reaction and to increase the performance of the C33 antigen in the HCV immunodiagnostic assay.

To achieve these objectives, we explored the ELP-intein system as an alternative production method for the C33 antigen. This method is based on the combination of two technological tools, the ELP aggregation and solvation properties (physico-chemical tool) and the intein auto-cleavage activity (biochemical tool). ELPs are thermally responsive polypeptides that undergo an inverse temperature phase transition in response to thermal changes. The temperature-dependent, reversible self-aggregation of ELPs is exploited for proteins purification, in particular in a non-chromatographic protein purification method named Inverse Transition Cycling (ITC). ITC protein purification needs the use of ELPs as tag: in this way the target protein fused to an ELP sequence can be purified through repeated cycles of precipitation and re-solubilization in response to thermal and buffer salt concentration changes, exploiting the ELPs properties. The ELP-Intein system also relies on the self-cleaving properties of inteins: the insertion of an intein at the right position in the ELP fusion construct gives the opportunity to isolate the target protein from the ELP tag during the ITC process. In fact, modified inteins at only one position of the splincing junctions allow to perform a site-specific cleavage of target protein from the purification tag. Moreover, using the right reagents, this modified inteins also permit site-specific labelling of target protein.

Therefore, to apply this system, we created a fusion protein having at the C-terminal of the C33 a purification tag composed of the mutated *Mxe*GyrA N198A intein, directly fused to the antigen sequence, and then the ELP sequence at the C-terminal of the intein. In this way we had the possibility to obtain, in a single experimental protocol, a purified and site-specific biotinylated C33 antigen. First the intrinsic features of ELP during the ITC process were exploited to obtain a high purified C33 antigen and then *MxeGyrA* N198A intein permitted the simultaneous ELP-intein tag cleavage and the site-specific biotinylation at the C-terminus of the C33.

The use of the C-terminal mutated *Mxe*GyrA N198A intein in the fusion construct, allowed us to obtain a C33 antigen variant characterized by a C-terminal site specific biotinylation. In fact C33-thioester derivative, obtained through the thiols induced N-terminus cleavage activity of the mutated intein, was exploited in Expressed Protein Ligation technique (EPL), in which the reaction between the recombinant C33 antigen with a C-terminal thioester group and a synthetic peptide containing a thiol group at the N-terminus and a lysine-biotin at the C-terminus permitted to obtain a C-terminal site-specific biotinylation of target protein.

In detail, to obtain our purified and biotinylated C33, two ITC rounds were performed to obtain the fusion protein with a high purity degree. Then, the purification tag (intein-ELP) was cleaved by the 2-mercaptoethanesulfonic acid (MESNA) and the C33 antigen with a C-terminal thioester group was obtained. After that, we executed the third ITC cycles to separate the C33-thioester from the purification tag. Finally, we performed the site-specific biotinylation of C33 by reacting the C33-thioester with the appropriate peptide exploiting the EPL technique.

This new purification and labelling process of C33 was successful from several standpoints. We reached a high purity of the C33-thioester and for the first time in our laboratory we managed to get a purified antigen without chromatographic steps. After that, we verified the very high efficiency of site-specific biotinylation through the retardation assay, which was close to completion (almost 100%) and also, we demonstrated that our biotinylated C33 had an immunoreactivity comparable to the Diasorin C33-Biotin in the LIAISON Murex HCV Ab assay. This new purification protocol was characterized by a rather high production yield but the main advantage compared to the one currently used is the overall process time, which has been reduced to just 3 days. Finally, another very interesting result was that our site-specific biotinylated antigen could be use at a lower concentration than the current one in the HCV immunoassay maintaining the same performances.

These great results showed the many advantages of our new purification and labelling protocol and that this procedure could replace the current one to improve manufacturing of the biotinylated C33.

Encouraged by this results, our next aim was to further optimize the non-chromatographic purification process of C33 antigen described in the previous paragraphs; in particular we tried to improve the productivity of the purification method by further decreasing the working days needed to get the biotinylated C33. To achieve this goal, we developed a new purification process in which first we executed two rounds of ITC, as it was already done in our previous protocol, to drastically reduce the *E. coli* contaminants and therefore to obtain a C33-*MxeGyrA*-ELP target protein with a high purity degree. After that, we decided to perform the cleavage with MESNA and the site-specific biotinylation of C33 simultaneously. In this case, we were not able to separate the biotinylated C33 from the *MxeGyrA*-ELP tag

exploiting the ITC process and so we found-out that Hydrophobic Interaction Chromatography (HIC). was able to separate the two species.

By this purification process we were able to separate our target protein from the *MxeGyrA*-ELP and we obtained a biotinylated C33 target protein with a good purity in only two working days, although with an overall yield lower than the non-chromatographic purification method previously developed. Also in this case, the immunoreactivity of our antigen was comparable with the Diasorin-C33-Biotin in the LIAISON Murex HCV Ab assay. Therefore, we were able to purify from *E. coli* bacteria and label our target protein using a fast purification process (only two days) that allowed to obtain rapidly a biotinylated protein in a short experimental time.

After the optimization of the C33 purification and site-specific labelling protocol, we wanted to explore other technologies to perform the site-specific conjugation of reagents involved in immunodiagnostic assay. In particular, our interest was focused on the split intein technology.

In the general reaction mechanism of protein trans splicing by split inteins the N-terminal portion of the Intein is fused to the C-terminal end of the N-extein. Meantime, C-terminal portion of the Intein is located at the N-terminal of the C-extein. After assembly of the two intein fragments, a splicing reaction takes place, where the intein removes itself from the precursor protein and simultaneously ligates the exteins via a peptide bond.

As described in the introduction chapter, the use of the split-inteins has several biotechnological applications. The most relevant characteristics of the split intein concern the faster kinetics of the protein trans-splicing reactions than those with *cis*-inteins, and the possibility to execute the site-specific labeling or other modifications of proteins and antibodies.

In light of these features, we decided to exploit this new technology in order to obtain the site-specific biotinylation of C33 antigen. To perform our experiments, we chose the Cfa split intein because of its rapid protein trans-splicing rate, and unprecedented thermal and chaotropic stability.

Therefore, we created two constructs having respectively the N-terminal portion of the Cfa split intein and the C-terminal fragment of the Cfa split intein. In particular, the first construct was characterized by the fusion of the C33 sequence with the Cfa-N-terminal portion. At the N-terminal of C33 was present a His-Tag necessary for the purification of this first fusion protein. In the second construct, the C-terminal portion of Cfa was fused with the *MxeGyrA*-ELP tag; we exploited this tag to purify the C-terminal-Cfa-thioester and to perform its site-specific biotinylation, as previously described.

We purified them separately and then we set up the reaction between NHis-C33-N-terminal-Cfa (first reagent) and C-terminal-Cfa-Biotin (second reagent) to trigger the recognition of the two-intein portions and to promote the consequent protein trans-splicing mechanism. After several optimizations of the Cfa split intein reaction we obtained a good conversion yield of the NHis-C33-N-terminal-Cfa in the biotinylated NHis-C33 (final product). Furthermore, it was also necessary to develop a purification process of this biotinylated antigen to remove unreacted starting reagents, and the secondary reaction products from our final product. Also in this case, the objective was achieved, since we managed to purify successfully the biotinylated NHis-C33 by an Anion Exchange Chromatography (AEC) and subsequent Immobilized Metal Affinity Chromatography (IMAC). Moreover, we verified the very high biotinylation efficiency of NHis-C33 occurred by Cfa split-intein reaction. which was also in this case close to completion (almost 100%).Finally, we can state that the site-specific biotinylation of C33 antigen by protein trans splicing was a reliable and controllable process that led to a biotinylated protein with a good immunoreactivity in LIAISON XL Murex HCV Ab assay.

In light of the wide potentiality of the PTS by the use of Cfa split-intein, in the last part of my PhD project, we decided to exploit this system to perform a site-specific biotinylation of another target protein, in particular a recombinant IgG anti-interferon-γ (IFNγ) antibody. Our aim was to verify whether the site-specific biotinylation of the antibody could led to an improved immunoreactivity with respect to conventional, random biotinylation on the amine groups of Lysine residues. To this purpose, a recombinant IgG anti-IFNγ antibody was produced in CHO cells, having the N-term-Cfa-His tag sequence fused at the C-terminal of its heavy chains. In this way, we exploited the N-term-Cfa sequence fused at the C-terminus of the anti-IFNγ antibody to perform a trans splicing reaction with a second reagent represented by C-term-Cfa-Biotin (the same used for the site specific biotinylation of C33 antigen). As result of the protein trans splicing reaction we obtained the recombinant IgG anti-IFNγ antibody site-specific biotinylated at the C-terminus position.

At this point, we comparted the immunoreactivity of our site specific biotinylated recombinant IgG anti-IFNγ antibody with the same antibody biotinylated through classical random biotinylation using a prototype immunoassay for quantification of IFNγ.

In this assay, the recombinant IgG anti- IFNγ-Biotin, previously immobilized on a streptavidin-coated paramagnetic beads (solid phase), binds the IFNγ present in samples, calibrators or controls. The IFNγ is then recognized by a second anti-IFNγ conjugated with a fluorescent dye called Alexa fluor. Finally, the complex is detected through an anti-Alex fluor antibody, labelled with the ABEI chemiluminescent molecule that emitted a light signal expressed in RLU by the instrument.

The results obtained from this comparison showed that the site-specific biotinylated recombinant IgG anti-IFNγ antibody, had an improved immunoreactivity in the prototype IFNγ immunoassay. The explanation of that could be that the site-specific biotinylation on the heavy chains of the antibody lead to an optimal orientation of the antibody on the solid phase resulting in a better exposition of its antigen binding site, necessary for the interaction with IFNγ epitopes.

Performing the experiments of PTS by Cfa split intein we demonstrate that this system can be widely used to obtain the site-specific labeling of several target proteins. In particular, we could set up the Cfa split-intein reaction between different fusion proteins carrying the N-terminal-Cfa sequence and the C-term-Cfa sequence linked to a desire probe as a common building block.

In conclusion, we have demonstrated that the site-specific labeling of proteins and antibodies used in immunoassays can improve their functional sensitivities and therefore the relevant methods could be of interest for the development of critical bioreagents for immunodiagnostic applications.

REFERENCES

1. Farci P. Choo QL, Kuo G, Weiner AJ, Overby LR, Bradley DW, Houghton M. Isolation of a cDNA clone derived from a blood-borne non-A, non-B viral hepatitis genome [Science 1989;244:359–362]. Journal of Hepatology. 2002 May;36(5).

2. Kamal SM. Acute Hepatitis C: A Systematic Review. The American Journal of Gastroenterology. 2008 May;103(5).

3. Global Burden of Disease (GBD) for Hepatitis C. The Journal of Clinical Pharmacology. 2004 Jan;44(1).

4. Miller RH, Purcell RH. Hepatitis C virus shares amino acid sequence similarity with pestiviruses and flaviviruses as well as members of two plant virus supergroups. Proceedings of the National Academy of Sciences. 1990 Mar 1;87(6).

5. Tellinghuisen TL, Evans MJ, von Hahn T, You S, Rice CM. Studying Hepatitis C Virus: Making the Best of a Bad Virus. Journal of Virology. 2007 Sep 1;81(17).

6. Dubuisson J, Cosset F-L. Virology and cell biology of the hepatitis C virus life cycle – An update. Journal of Hepatology. 2014 Nov;61(1).

7. Kaito M, Ishida S, Tanaka H, Horiike S, Fujita N, Adachi Y, et al. Morphology of hepatitis C and hepatitis B virus particles as detected by immunogold electron microscopy. Medical Molecular Morphology. 2006 Jul 4;39(2).

8. op de Beeck A, Dubuisson J. Topology of hepatitis C virus envelope glycoproteins. Reviews in Medical Virology. 2003 Jul;13(4).

9. Elgharably A, Gomaa AI, Crossey MME, Norsworthy PJ, Waked I, Taylor-Robinson SD. Hepatitis C in Egypt – past, present, and future. International Journal of General Medicine. 2016 Dec;Volume 10.

10. Cristofari G. The hepatitis C virus Core protein is a potent nucleic acid chaperone that directs dimerization of the viral (+) strand RNA in vitro. Nucleic Acids Research. 2004 Apr 28;32(8).

11. Ivanyi-Nagy R, Kanevsky I, Gabus C, Lavergne J-P, Ficheux D, Penin F, et al. Analysis of hepatitis C virus RNA dimerization and core-RNA interactions. Nucleic Acids Research. 2006 May 17;34(9).

12. Kopp M, Murray CL, Jones CT, Rice CM. Genetic Analysis of the Carboxy-Terminal Region of the Hepatitis C Virus Core Protein. Journal of Virology. 2010 Feb 15;84(4).

13. Okamoto K, Mori Y, Komoda Y, Okamoto T, Okochi M, Takeda M, et al. Intramembrane Processing by Signal Peptide Peptidase Regulates the Membrane

Localization of Hepatitis C Virus Core Protein and Viral Propagation. Journal of Virology. 2008 Sep 1;82(17).

14. Hüssy P, Langen H, Mous J, Jacobsen H. Hepatitis C Virus Core Protein: Carboxy-Terminal Boundaries of Two Processed Species Suggest Cleavage by a Signal Peptide Peptidase. Virology. 1996 Oct;224(1).

15. Cristina J, Moreno M del P, Moratorio G. Hepatitis C virus genetic variability in patients undergoing antiviral therapy. Virus Research. 2007 Aug;127(2).

16. Bartosch B, Dubuisson J. Recent Advances in Hepatitis C Virus Cell Entry. Viruses. 2010 Mar 8;2(3).

17. Montserret R, Saint N, Vanbelle C, Salvay AG, Simorre J-P, Ebel C, et al. NMR Structure and Ion Channel Activity of the p7 Protein from Hepatitis C Virus. Journal of Biological Chemistry. 2010 Oct 8;285(41).

18. Chew CF, Vijayan R, Chang J, Zitzmann N, Biggin PC. Determination of Pore-Lining Residues in the Hepatitis C Virus p7 Protein. Biophysical Journal. 2009 Jan;96(2).

19. Erdtmann L, Franck N, Lerat H, le Seyec J, Gilot D, Cannie I, et al. The Hepatitis C Virus NS2 Protein Is an Inhibitor of CIDE-B-induced Apoptosis. Journal of Biological Chemistry. 2003 May 16;278(20).

20. Yang X-J, Liu J, Ye L, Liao Q-J, Wu J-G, Gao J-R, et al. HCV NS2 protein inhibits cell proliferation and induces cell cycle arrest in the S-phase in mammalian cells through down-regulation of cyclin A expression. Virus Research. 2006 Nov;121(2).

21. Kim KM, Kwon S-N, Kang J-I, Lee SH, Jang SK, Ahn B-Y, et al. Hepatitis C virus NS2 protein activates cellular cyclic AMP-dependent pathways. Biochemical and Biophysical Research Communications. 2007 May;356(4).

22. Oem J-K, Jackel-Cram C, Li Y-P, Kang H-N, Zhou Y, Babiuk LA, et al. Hepatitis C virus non-structural protein-2 activates CXCL-8 transcription through NF-κB. Archives of Virology. 2008 Feb 13;153(2).

23. Oem J-K, Jackel-Cram C, Li Y-P, Zhou Y, Zhong J, Shimano H, et al. Activation of sterol regulatory element-binding protein 1c and fatty acid synthase transcription by hepatitis C virus non-structural protein 2. Journal of General Virology. 2008 May 1;89(5).

24. Thibeault D, Maurice R, Pilote L, Lamarre D, Pause A. *In Vitro* Characterization of a Purified NS2/3 Protease Variant of Hepatitis C Virus. Journal of Biological Chemistry. 2001 Dec 7;276(49).

25. Kim JL, Morgenstern KA, Lin C, Fox T, Dwyer MD, Landro JA, et al. Crystal Structure of the Hepatitis C Virus NS3 Protease Domain Complexed with a Synthetic NS4A Cofactor Peptide. Cell. 1996 Oct;87(2).

26. Moving beyond interferon alfa: investigational drugs for hepatitis C virus infection.

27. Rehman S, Ashfaq UA, Javed T. Antiviral drugs against hepatitis C virus. Genetic Vaccines and Therapy. 2011;9(1).

28. Wölk B, Sansonno D, Kräusslich H-G, Dammacco F, Rice CM, Blum HE, et al. Subcellular Localization, Stability, andtrans-Cleavage Competence of the Hepatitis C Virus NS3-NS4A Complex Expressed in Tetracycline-Regulated Cell Lines. Journal of Virology. 2000 Mar 1;74(5).

29. Asabe SI, Tanji Y, Satoh S, Kaneko T, Kimura K, Shimotohno K. The N-terminal region of hepatitis C virus-encoded NS5A is important for NS4A-dependent phosphorylation. Journal of virology. 1997;71(1).

30. Gouttenoire J, Penin F, Moradpour D. Hepatitis C virus nonstructural protein 4B: a journey into unexplored territory. Reviews in Medical Virology. 2010 Mar;20(2).

31. Moradpour D, Kary P, Rice CM, Blum HE. Continuous human cell lines inducibly expressing hepatitis C virus structural and nonstructural proteins. Hepatology. 1998 Jul;28(1).

32. Pockros PJ. Review: New direct-acting antivirals in the development for hepatitis C virus infection. Therapeutic Advances in Gastroenterology. 2010 May 26;3(3).

33. Miller RH, Purcell RH. Hepatitis C virus shares amino acid sequence similarity with pestiviruses and flaviviruses as well as members of two plant virus supergroups. Proceedings of the National Academy of Sciences. 1990 Mar 1;87(6).

34. Doublié S, Tabor S, Long AM, Richardson CC, Ellenberger T. Crystal structure of a bacteriophage T7 DNA replication complex at 2.2 Å resolution. Nature. 1998 Jan;391(6664).

35. Kolykhalov AA, Mihalik K, Feinstone SM, Rice CM. Hepatitis C Virus-Encoded Enzymatic Activities and Conserved RNA Elements in the 3' Nontranslated Region Are Essential for Virus Replication In Vivo. Journal of Virology. 2000 Feb 15;74(4).

36. Sarrazin C, Zeuzem S. Resistance to Direct Antiviral Agents in Patients With Hepatitis C Virus Infection. Gastroenterology. 2010 Feb;138(2).

37. Kieffer TL, Sarrazin C, Miller JS, Welker MW, Forestier N, Reesink HW, et al. Telaprevir and pegylated interferon-alpha-2a inhibit wild-type and resistant genotype 1 hepatitis C virus replication in patients. Hepatology. 2007 Sep;46(3).

38. ZEUZEM S. Peginterferon alfa-2b plus ribavirin for treatment of chronic hepatitis C in previously untreated patients infected with HCV genotypes 2 or 3*1, *2. Journal of Hepatology. 2004 Jun;40(6).

39. Farnik H, Lange CM, Sarrazin C, Kronenberger B, Zeuzem S, Herrmann E. Meta-analysis Shows Extended Therapy Improves Response of Patients With Chronic Hepatitis C Virus Genotype 1 Infection. Clinical Gastroenterology and Hepatology. 2010 Oct;8(10).

40. Sarrazin C, Zeuzem S. Resistance to Direct Antiviral Agents in Patients With Hepatitis C Virus Infection. Gastroenterology. 2010 Feb;138(2).

41. Lauer GM, Walker BD. Hepatitis C Virus Infection. New England Journal of Medicine. 2001 Jul 5;345(1).

42. Kamili S, Drobeniuc J, Araujo AC, Hayden TM. Laboratory Diagnostics for Hepatitis C Virus Infection. Clinical Infectious Diseases. 2012 Jul 15;55(suppl_1).

43. Bajpai M, Gupta E, Choudhary A. Hepatitis C virus: Screening, diagnosis, and interpretation of laboratory assays. Asian Journal of Transfusion Science. 2014;8(1).

44. Goel A, Bhadauria DS, Aggarwal R. Hepatitis C virus infection and chronic renal disease: A review. Indian Journal of Gastroenterology. 2018 Nov 18;37(6).

45. Freiman JM, Tran TM, Schumacher SG, White LF, Ongarello S, Cohn J, et al. Hepatitis C Core Antigen Testing for Diagnosis of Hepatitis C Virus Infection. Annals of Internal Medicine. 2016 Sep 6;165(5).

46. Kuo G, Choo Q, Alter H, Gitnick G, Redeker A, Purcell R, et al. An assay for circulating antibodies to a major etiologic virus of human non-A, non-B hepatitis. Science. 1989 Apr 21;244(4902).

47. Gretch DR. Diagnostic tests for hepatitis C. Hepatology. 1997 Dec;26(S3).

48. Alter HJ. New kit on the block: Evaluation of second-generation assays for detection of antibody to the hepatitis C virus. Hepatology. 1992 Feb;15(2).

49. Aach RD, Stevens CE, Hollinger FB, Mosley JW, Peterson DA, Taylor PE, et al. Hepatitis C Virus Infection in Post-Transfusion Hepatitis. New England Journal of Medicine. 1991 Nov 7;325(19).

50. Kleinman S, Alter H, Busch M, Holland P, Tegtmeier G, Nelles M, et al. Increased detection of hepatitis C virus (HCV)-infected blood donors by a multiple-antigen HCV enzyme immunoassay. Transfusion. 1992 Nov;32(9).

51. Abdel-Hamid M, El-Daly M, El-Kafrawy S, Mikhail N, Strickland GT, Fix AD. Comparison of Second- and Third-Generation Enzyme Immunoassays for Detecting Antibodies to Hepatitis C Virus. Journal of Clinical Microbiology. 2002 May 1;40(5).

52. Colin C, Lanoir D, Touzet S, Meyaud-Kraemer L, Bailly F, Trepo C. Sensitivity and specificity of third-generation hepatitis C virus antibody detection assays: an analysis of the literature. Journal of Viral Hepatitis. 2001 Mar;8(2).

53. Glynn SA, Wright DJ, Kleinman SH, Hirschkorn D, Tu Y, Heldebrant C, et al. Dynamics of viremia in early hepatitis C virus infection. Transfusion. 2005 Jun;45(6).

54. Recommendations for prevention and control of hepatitis C virus (HCV) infection and HCV-related chronic disease. Centers for Disease Control and Prevention.

55. Miriam J Alter 1 WLKLFC for DC and P 2003. Guidelines for laboratory testing and result reporting of antibody to hepatitis C virus. Centers for Disease Control and Prevention.

56. Dufour DR, Talastas M, Fernandez MDA, Harris B. Chemiluminescence Assay Improves Specificity of Hepatitis C Antibody Detection. Clinical Chemistry. 2003 Jun 1;49(6).

57. Ismail N, Fish GE, Smith MB. Laboratory Evaluation of a Fully Automated Chemiluminescence Immunoassay for Rapid Detection of HBsAg, Antibodies to HBsAg, and Antibodies to Hepatitis C Virus. Journal of Clinical Microbiology. 2004 Feb 1;42(2).

58. Kent SBH. Novel protein science enabled by total chemical synthesis. Protein Science. 2019 Feb 18;28(2).

59. Fersht AR, Winter GP. Redesigning Enzymes by Site-Directed Mutagenesis. In 2008.

60. Xiao H, Schultz PG. At the Interface of Chemical and Biological Synthesis: An Expanded Genetic Code. Cold Spring Harbor Perspectives in Biology. 2016 Sep;8(9).

61. Dawson PE, Kent SBH. Synthesis of Native Proteins by Chemical Ligation. Annual Review of Biochemistry. 2000 Jun;69(1).

62. Muir TW, Sondhi D, Cole PA. Expressed protein ligation: A general method for protein engineering. Proceedings of the National Academy of Sciences. 1998 Jun 9;95(12).

63. Kane P, Yamashiro C, Wolczyk D, Neff N, Goebl M, Stevens T. Protein splicing converts the yeast TFP1 gene product to the 69-kD subunit of the vacuolar H(+)-adenosine triphosphatase. Science. 1990 Nov 2;250(4981).

64. Perler FB. InBase: the Intein Database. Nucleic Acids Research. 2002 Jan 1;30(1).

65. Perler FB, Davis EO, Dean GE, Gimble FS, Jack WE, Neff N, et al. Protein splicing elements: inteins and exteins — a definition of terms and recommended nomenclature. Nucleic Acids Research. 1994;22(7).

66. Doolittle RF. The comings and goings of homing endonucleases and mobile introns. Proceedings of the National Academy of Sciences. 1993 Jun 15;90(12).

67. Pietrokovski S. Conserved sequence features of inteins (protein introns) and their use in identifying new inteins and related proteins. Protein Science. 1994 Dec;3(12).

68. Perler F. Compilation and analysis of intein sequences. Nucleic Acids Research. 1997 Mar 15;25(6).

69. Derbyshire V, Wood DW, Wu W, Dansereau JT, Dalgaard JZ, Belfort M. Genetic definition of a protein-splicing domain: Functional mini-inteins support structure predictions and a model for intein evolution. Proceedings of the National Academy of Sciences. 1997 Oct 14;94(21).

70. Gogarten JP, Hilario E. Inteins, introns, and homing endonucleases: recent revelations about the life cycle of parasitic genetic elements. BMC Evolutionary Biology. 2006;6(1).

71. Brown S, Perrino T, Lombard J, Wang K, Toro M, Rundek T, et al. Health Disparities in the Relationship of Neighborhood Greenness to Mental Health Outcomes in 249,405 U.S. Medicare Beneficiaries. International Journal of Environmental Research and Public Health. 2018 Mar 1;15(3).

72. Galburt EA, Stoddard BL. Catalytic Mechanisms of Restriction and Homing Endonucleases. Biochemistry. 2002 Nov;41(47).

73. Duan X, Gimble FS, Quiocho FA. Crystal Structure of PI-SceI, a Homing Endonuclease with Protein Splicing Activity. Cell. 1997 May;89(4).

74. Sorci M, Dassa B, Liu H, Anand G, Dutta AK, Pietrokovski S, et al. Oriented Covalent Immobilization of Antibodies for Measurement of Intermolecular Binding Forces

between Zipper-Like Contact Surfaces of Split Inteins. Analytical Chemistry. 2013 Jun 18;85(12).

75. Wu H, Hu Z, Liu X-Q. Protein *trans* -splicing by a split intein encoded in a split DnaE gene of *Synechocystis* sp. PCC6803. Proceedings of the National Academy of Sciences. 1998 Aug 4;95(16).

76. Guan D, Ramirez M, Chen Z. Split intein mediated ultra-rapid purification of tagless protein (SIRP). Biotechnology and Bioengineering. 2013 Sep 22;110(9).

77. Lin Y, Li M, Song H, Xu L, Meng Q, Liu X-Q. Protein Trans-Splicing of Multiple Atypical Split Inteins Engineered from Natural Inteins. PLoS ONE. 2013 Apr 8;8(4).

78. Paulus H. Inteins as Enzyme. Bioorganic Chemistry. 2001 Jun;29(3).

79. Mills K v., Johnson MA, Perler FB. Protein Splicing: How Inteins Escape from Precursor Proteins. Journal of Biological Chemistry. 2014 May 23;289(21).

80. Southworth MW. An alternative protein splicing mechanism for inteins lacking an N-terminal nucleophile. The EMBO Journal. 2000 Sep 15;19(18).

81. Yamamoto K, Low B, Rutherford SA, Rajagopalan M, Madiraju MVVS. The Mycobacterium avium-intracellulare Complex dnaB Locus and Protein Intein Splicing. Biochemical and Biophysical Research Communications. 2001 Jan;280(3).

82. Tori K, Dassa B, Johnson MA, Southworth MW, Brace LE, Ishino Y, et al. Splicing of the Mycobacteriophage Bethlehem DnaB Intein. Journal of Biological Chemistry. 2010 Jan 22;285(4).

83. Tori K, Perler FB. Expanding the Definition of Class 3 Inteins and Their Proposed Phage Origin. Journal of Bacteriology. 2011 Apr 15;193(8).

84. Brace LE, Southworth MW, Tori K, Cushing ML, Perler F. The *Deinococcus radiodurans* Snf2 intein caught in the act: Detection of the Class 3 intein signature Block F branched intermediate. Protein Science. 2010 Aug;19(8).

85. Chong S, Mersha FB, Comb DG, Scott ME, Landry D, Vence LM, et al. Single-column purification of free recombinant proteins using a self-cleavable affinity tag derived from a protein splicing element. Gene. 1997 Jun;192(2).

86. Bentz WK, Davis A. Perceptions of emotional disorders among children as viewed by leaders, teachers, and the general public. American Journal of Public Health. 1975 Feb;65(2).

87. Evans TC, Benner J, Xu M-Q. The Cyclization and Polymerization of Bacterially Expressed Proteins Using Modified Self-splicing Inteins. Journal of Biological Chemistry. 1999 Jun 25;274(26).

88. Seyedsayamdost MR, Yee CS, Stubbe J. Site-specific incorporation of fluorotyrosines into the R2 subunit of E. coli ribonucleotide reductase by expressed protein ligation. Nature Protocols. 2007 May 10;2(5).

89. Otomo T, Teruya K, Uegaki K, Yamazaki T, Kyogoku Y. Improved segmental isotope labeling of proteins and application to a larger protein. Journal of Biomolecular NMR. 1999;14(2).

90. Cowburn D, Muir TW. Segmental Isotopic Labeling Using Expressed Protein Ligation. In 2001.

91. Topilina NI, Mills K v. Recent advances in in vivo applications of intein-mediated protein splicing. Mobile DNA. 2014;5(1).

92. Shah NH, Muir TW. Inteins: nature's gift to protein chemists. Chem Sci. 2014;5(2).

93. Wood DW, Camarero JA. Intein Applications: From Protein Purification and Labeling to Metabolic Control Methods. Journal of Biological Chemistry. 2014 May 23;289(21).

94. Hafez M, Hausner G. Homing endonucleases: DNA scissors on a mission. Genome. 2012 Aug;55(8).

95. Belfort M, Bonocora RP. Homing Endonucleases: From Genetic Anomalies to Programmable Genomic Clippers. In 2014.

96. Ozawa T, Sako Y, Sato M, Kitamura T, Umezawa Y. A genetic approach to identifying mitochondrial proteins. Nature Biotechnology. 2003 Mar 10;21(3).

97. Ozawa T. A high-throughput screening of genes that encode proteins transported into the endoplasmic reticulum in mammalian cells. Nucleic Acids Research. 2005 Feb 23;33(4).

98. Cui R, Han J, Zhao S, Su K, Wu F, Du X, et al. Functional conservation and diversification of class E floral homeotic genes in rice (*Oryza sativa*). The Plant Journal. 2010 Mar;61(5).

99. Telenti A, Southworth M, Alcaide F, Daugelat S, Jacobs WR, Perler FB. The Mycobacterium xenopi GyrA protein splicing element: characterization of a minimal intein. Journal of bacteriology. 1997;179(20).

100. Klabunde T, Sharma S, Telenti A, Jacobs WR, Sacchettini JC. Crystal structure of GyrA intein from Mycobacterium xenopi reveals structural basis of protein splicing. Nature Structural Biology. 1998 Jan;5(1).

101. Chong S, Mersha FB, Comb DG, Scott ME, Landry D, Vence LM, et al. Single-column purification of free recombinant proteins using a self-cleavable affinity tag derived from a protein splicing element. Gene. 1997 Jun;192(2).

102. Chong S, Montello GE, Zhang A, Cantor EJ, Liao W, Xu M-Q, et al. Utilizing the C-terminal cleavage activity of a protein splicing element to purify recombinant proteins in a single chromatographic step. Nucleic Acids Research. 1998 Nov 1;26(22).

103. Evans TC, Benner J, Xu M-Q. Semisynthesis of cytotoxic proteins using a modified protein splicing element. Protein Science. 1998 Nov;7(11).

104. Watanabe T, Ito Y, Yamada T, Hashimoto M, Sekine S, Tanaka H. The roles of the C-terminal domain and type III domains of chitinase A1 from Bacillus circulans WL-12 in chitin degradation. Journal of Bacteriology. 1994;176(15).

105. Muir TW, Sondhi D, Cole PA. Expressed protein ligation: A general method for protein engineering. Proceedings of the National Academy of Sciences. 1998 Jun 9;95(12).

106. Uhlén M, Forsberg G, Moks T, Hartmanis M, Nilsson B. Fusion proteins in biotechnology. Current Opinion in Biotechnology. 1992 Aug;3(4).

107. Uhlén M, Moks T. [12] Gene fusions for purpose of expression: An introduction. In 1990.

108. Maina C v., Riggs PD, Grandea AG, Slatko BE, Moran LS, Tagliamonte JA, et al. An Escherichia coli vector to express and purify foreign proteins by fusion to and separation from maltose-binding protein. Gene. 1988 Dec;74(2).

109. Smith DB, Johnson KS. Single-step purification of polypeptides expressed in Escherichia coli as fusions with glutathione S-transferase. Gene. 1988 Jul;67(1).

110. Tsao K-L, Debarbieri B, Michel H, Waugh DS. A versatile plasmid expression vector for the production of biotinylated proteins by site-specific, enzymatic modification in Escherichia coli. Gene. 1996 Feb;169(1).

111. Smith PA, Tripp BC, DiBlasio-Smith EA, Lu Z, LaVallie ER, McCoy JM. A plasmid expression system for quantitative in vivo biotinylation of thioredoxin fusion proteins in Escherichia coli. Nucleic Acids Research. 1998 Mar 1;26(6).

112. LaVallie ER, DiBlasio EA, Kovacic S, Grant KL, Schendel PF, McCoy JM. A Thioredoxin Gene Fusion Expression System That Circumvents Inclusion Body Formation in the E. coli Cytoplasm. Nature Biotechnology. 1993 Feb 1;11(2).

113. Kim J-S, Raines RT. Ribonuclease S-peptide as a carrier in fusion proteins. Protein Science. 2008 Dec 31;2(3).

114. Urry DW. Entropic elastic processes in protein mechanisms. I. Elastic structure due to an inverse temperature transition and elasticity due to internal chain dynamics. Journal of Protein Chemistry. 1988 Feb;7(1).

115. Urry DW, Luan CH, Parker TM, Gowda DC, Prasad KU, Reid MC, et al. Temperature of polypeptide inverse temperature transition depends on mean residue hydrophobicity. Journal of the American Chemical Society. 1991 May;113(11).

116. Urry DW, Trapane TL, Prasad KU. Phase-structure transitions of the elastin polypentapeptide-water system within the framework of composition-temperature studies. Biopolymers. 1985 Dec;24(12).

117. Ge X, Yang DSC, Trabbic-Carlson K, Kim B, Chilkoti A, Filipe CDM. Self-Cleavable Stimulus Responsive Tags for Protein Purification without Chromatography. Journal of the American Chemical Society. 2005 Aug;127(32).

118. Cole MA, Voelcker NH, Thissen H, Griesser HJ. Stimuli-responsive interfaces and systems for the control of protein–surface and cell–surface interactions. Biomaterials. 2009 Mar;30(9).

119. Chilkoti A, Dreher MR, Meyer DE. Design of thermally responsive, recombinant polypeptide carriers for targeted drug delivery. Advanced Drug Delivery Reviews. 2002 Oct;54(8).

120. Bidwell GL, Davis AN, Fokt I, Priebe W, Raucher D. A thermally targeted elastin-like polypeptide-doxorubicin conjugate overcomes drug resistance. Investigational New Drugs. 2007 Aug 5;25(4).

121. Urry DW, Parker TM, Reid MC, Gowda DC. Biocompatibility of the Bioelastic Materials, Poly(GVGVP) and Its γ-Irradiation Cross-Linked Matrix: Summary of Generic Biological Test Results. Journal of Bioactive and Compatible Polymers. 1991 Jul 26;6(3).

122. Meyer DE, Chilkoti A. Purification of recombinant proteins by fusion with thermally-responsive polypeptides. Nature Biotechnology. 1999 Nov;17(11).

123. MacEwan SR, Hassouneh W, Chilkoti A. Non-chromatographic Purification of Recombinant Elastin-like Polypeptides and their Fusions with Peptides and

Proteins from Escherichia coli Journal of Visualized Experiments. 2014 Jun 9;(88).

124. Meyer DE, Trabbic-Carlson K, Chilkoti A. Protein Purification by Fusion with an Environmentally Responsive Elastin-Like Polypeptide: Effect of Polypeptide Length on the Purification of Thioredoxin. Biotechnology Progress. 2001 Aug 3;17(4).

125. Hermodson M. Current protocols in protein science, edited by J.E. Coligan, B.M. Dunn, H.L. Ploegh, D.W. Speicher, and P.T. Wingfield. New York: Wiley, 1995, 864 pages (core) + 576 pages (4 supplements)/year (updated looseleaf), print and CD-ROM. Proteins: Structure, Function, and Genetics. 1996 Mar;24(3).

126. Diamandis EP, Yousef GM, Soosaipillai AR, Grass L, Porter A, Little S, et al. Immunofluorometric assay of human kallikrein 6 (zyme/protease M/neurosin) and preliminary clinical applications. Clinical Biochemistry. 2000 Jul;33(5).

127. Bahniuk MS, Alshememry AK, Unsworth LD. High-yield recombinant expression and purification of marginally soluble, short elastin-like polypeptides. BioTechniques. 2016 Dec 1;61(6).

128. Paulus H. Protein Splicing and Related Forms of Protein Autoprocessing. Annual Review of Biochemistry. 2000 Jun;69(1).

129. Perler F. Protein Splicing Mechanisms and Applications. IUBMB Life (International Union of Biochemistry and Molecular Biology: Life). 2005 Jul 1;57(7).

130. Shah NH, Muir TW. Split Inteins: Nature's Protein Ligases. Israel Journal of Chemistry. 2011 Nov;51(8–9).

131. Muralidharan V, Muir TW. Protein ligation: an enabling technology for the biophysical analysis of proteins. Nature Methods. 2006 Jun 23;3(6).

132. Perler FB, Adam E. Protein splicing and its applications. Current Opinion in Biotechnology. 2000 Aug;11(4).

133. Vila-Perelló M, Muir TW. Biological Applications of Protein Splicing. Cell. 2010 Oct;143(2).

134. Ludwig C, Pfeiff M, Linne U, Mootz HD. Ligation of a Synthetic Peptide to the N Terminus of a Recombinant Protein Using Semisynthetic Proteintrans-Splicing. Angewandte Chemie International Edition. 2006 Aug 4;45(31).

135. Kurpiers T, Mootz HD. Regioselective Cysteine Bioconjugation by Appending a Labeled Cystein Tag to a Protein by Using Protein Splicing intrans. Angewandte Chemie International Edition. 2007 Jul 2;46(27).

136. Tyszkiewicz AB, Muir TW. Activation of protein splicing with light in yeast. Nature Methods. 2008 Apr 13;5(4).

137. Buchinger E, Aachmann FL, Aranko AS, Valla S, Skjåk-BraeK G, Iwaï H, et al. Use of protein trans-splicing to produce active and segmentally ^{2} H, ^{15} N labeled mannuronan C5-epimerase AlgE4. Protein Science. 2010 Aug;19(8).

138. Binschik J, Zettler J, Mootz HD. Photocontrol of Protein Activity Mediated by the Cleavage Reaction of a Split Intein. Angewandte Chemie International Edition. 2011 Mar 28;50(14).

139. Ramirez M, Valdes N, Guan D, Chen Z. Engineering split intein DnaE from Nostoc punctiforme for rapid protein purification. Protein Engineering Design and Selection. 2013 Mar 1;26(3).

140. Ramirez M, Guan D, Ugaz V, Chen Z. Intein-Triggered Artificial Protein Hydrogels That Support the Immobilization of Bioactive Proteins. Journal of the American Chemical Society. 2013 Apr 10;135(14).

141. Nichols NM, Evans TC. Mutational Analysis of Protein Splicing, Cleavage, and Self-Association Reactions Mediated by the Naturally Split *Ssp* DnaE Intein. Biochemistry. 2004 Aug;43(31).

142. Nichols NM, Benner JS, Martin DD, Evans TC. Zinc Ion Effects on Individual *Ssp* DnaE Intein Splicing Steps: Regulating Pathway Progression. Biochemistry. 2003 May;42(18).

143. Han L, Zong H, Zhou Y, Pan Z, Chen J, Ding K, et al. Naturally split intein Npu DnaE mediated rapid generation of bispecific IgG antibodies. Methods. 2019 Feb;154.

144. Kane P, Yamashiro C, Wolczyk D, Neff N, Goebl M, Stevens T. Protein splicing converts the yeast TFP1 gene product to the 69-kD subunit of the vacuolar H(+)-adenosine triphosphatase. Science. 1990 Nov 2;250(4981).

145. Perler FB, Davis EO, Dean GE, Gimble FS, Jack WE, Neff N, et al. Protein splicing elements: inteins and exteins — a definition of terms and recommended nomenclature. Nucleic Acids Research. 1994;22(7).

146. Tavassoli A, Benkovic SJ. Split-intein mediated circular ligation used in the synthesis of cyclic peptide libraries in E. coli. Nature Protocols. 2007 May 3;2(5).

147. Shah NH, Dann GP, Vila-Perelló M, Liu Z, Muir TW. Ultrafast Protein Splicing is Common among Cyanobacterial Split Inteins: Implications for Protein Engineering. Journal of the American Chemical Society. 2012 Jul 18;134(28).

148. Schreiber G, Fersht AR. Rapid, electrostatically assisted association of proteins. Nature Structural Biology. 1996 May;3(5).

149. Schreiber G, Selzer T, Albeck S. Rational design of faster associating and tighter binding protein complexes. Nature Structural Biology. 2000 Jul 1;7(7).

150. Graddis TJ, Myszka DG, Chaiken IM. Controlled formation of model homo- and heterodimer coiled coil polypeptides. Biochemistry. 1993 Nov;32(47).

151. O'Shea EK, Lumb KJ, Kim PS. Peptide 'Velcro': Design of a heterodimeric coiled coil. Current Biology. 1993 Oct;3(10).

152. Gunasekaran K, Pentony M, Shen M, Garrett L, Forte C, Woodward A, et al. Enhancing Antibody Fc Heterodimer Formation through Electrostatic Steering Effects. Journal of Biological Chemistry. 2010 Jun 18;285(25).

153. Shi J, Muir TW. Development of a Tandem Protein Trans-Splicing System Based on Native and Engineered Split Inteins. Journal of the American Chemical Society. 2005 May;127(17).

154. Dassa B, Amitai G, Caspi J, Schueler-Furman O, Pietrokovski S. Trans Protein Splicing of Cyanobacterial Split Inteins in Endogenous and Exogenous Combinations. Biochemistry. 2007 Jan;46(1).

155. Oeemig JS, Aranko AS, Djupsjöbacka J, Heinämäki K, Iwaï H. Solution structure of DnaE intein from *Nostoc punctiforme* : Structural basis for the design of a new split intein suitable for site-specific chemical modification. FEBS Letters. 2009 May 6;583(9).

156. Shah NH, Vila-Perelló M, Muir TW. Kinetic Control of One-Pot Trans-Splicing Reactions by Using a Wild-Type and Designed Split Intein. Angewandte Chemie International Edition. 2011 Jul 11;50(29).

157. Volkmann G, Iwaï H. Protein trans-splicing and its use in structural biology: opportunities and limitations. Molecular BioSystems. 2010;6(11).

158. Al-Ali H, Ragan TJ, Gao X, Harris TK. Reconstitution of Modular PDK1 Functions on Trans-Splicing of the Regulatory PH and Catalytic Kinase Domains. Bioconjugate Chemistry. 2007 Jul;18(4).

159. Shi J, Muir TW. Development of a Tandem Protein Trans-Splicing System Based on Native and Engineered Split Inteins. Journal of the American Chemical Society. 2005 May;127(17).

160. Ozawa T, Umezawa Y. Detection of protein–protein interactions in vivo based on protein splicing. Current Opinion in Chemical Biology. 2001 Oct;5(5).

161. Ozawa T, Umezawa Y. Identification of Proteins Targeted Into the Endoplasmic Reticulum by cDNA Library Screening. In: Protein Targeting Protocols. Totowa, NJ: Humana Press; 2007.

162. Kim SB, Ozawa T, Watanabe S, Umezawa Y. High-throughput sensing and noninvasive imaging of protein nuclear transport by using reconstitution of split Renilla luciferase. Proceedings of the National Academy of Sciences. 2004 Aug 10;101(32).

163. Evans TC, Xu M-Q, Pradhan S. PROTEIN SPLICING ELEMENTS AND PLANTS: From Transgene Containment to Protein Purification. Annual Review of Plant Biology. 2005 Jun;56(1).

164. Li J, Sun W, Wang B, Xiao X, Liu X-Q. Protein *Trans* -Splicing as a Means for Viral Vector-Mediated *In Vivo* Gene Therapy. Human Gene Therapy. 2008 Sep;19(9).

165. Brenzel S, Cebi M, Reiß P, Koert U, Mootz HD. Expanding the Scope of Protein *Trans* -Splicing to Fragment Ligation of an Integral Membrane Protein: Towards Modulation of Porin-Based Ion Channels by Chemical Modification. ChemBioChem. 2009 Apr 17;10(6).

166. Scott CP, Abel-Santos E, Wall M, Wahnon DC, Benkovic SJ. Production of cyclic peptides and proteins in vivo. Proceedings of the National Academy of Sciences. 1999 Nov 23;96(24).

167. Guan D, Chen Z. Affinity Purification of Proteins in Tag-Free Form: Split Intein-Mediated Ultrarapid Purification (SIRP). In 2017.

168. Cooper MA, Taris JE, Shi C, Wood DW. A Convenient Split-Intein Tag Method for the Purification of Tagless Target Proteins. Current Protocols in Protein Science. 2018 Jan 21;91(1).

169. Shi C, Meng Q, Wood DW. A dual ELP-tagged split intein system for non-chromatographic recombinant protein purification. Applied Microbiology and Biotechnology. 2013 Jan 5;97(2).

170. Sarmiento C, Camarero JA. Biotechnological Applications of Protein Splicing. Current Protein & Peptide Science. 2019 Mar 27;20(5).

171. Han L, Zong H, Zhou Y, Pan Z, Chen J, Ding K, et al. Naturally split intein Npu DnaE mediated rapid generation of bispecific IgG antibodies. Methods. 2019 Feb;154.

172. Han L, Chen J, Ding K, Zong H, Xie Y, Jiang H, et al. Efficient generation of bispecific IgG antibodies by split intein mediated protein trans-splicing system. Scientific Reports. 2017 Dec 21;7(1).

173. Wu H, Hu Z, Liu X-Q. Protein *trans* -splicing by a split intein encoded in a split DnaE gene of *Synechocystis* sp. PCC6803. Proceedings of the National Academy of Sciences. 1998 Aug 4;95(16).

174. Iwai H, Züger S, Jin J, Tam P-H. Highly efficient protein *trans* -splicing by a naturally split DnaE intein from *Nostoc punctiforme*. FEBS Letters. 2006 Mar 20;580(7).

175. Cheriyan M, Pedamallu CS, Tori K, Perler F. Faster Protein Splicing with the *Nostoc punctiforme* DnaE Intein Using Non-native Extein Residues. Journal of Biological Chemistry. 2013 Mar 1;288(9).

176. Kim DR, McHenry CS. Identification of the β-binding Domain of the α Subunit of *Escherichia coli* Polymerase III Holoenzyme. Journal of Biological Chemistry. 1996 Aug 23;271(34).

177. Zettler J, Schütz V, Mootz HD. The naturally split *Npu* DnaE intein exhibits an extraordinarily high rate in the protein *trans* -splicing reaction. FEBS Letters. 2009 Mar 4;583(5).

178. Martin DD, Xu M-Q, Evans TC. Characterization of a Naturally Occurring Trans-Splicing Intein from *Synechocystis* sp. PCC6803. Biochemistry. 2001 Feb;40(5).

179. Nichols NM, Benner JS, Martin DD, Evans TC. Zinc Ion Effects on Individual *Ssp* DnaE Intein Splicing Steps: Regulating Pathway Progression. Biochemistry. 2003 May;42(18).

180. Shi J, Muir TW. Development of a Tandem Protein Trans-Splicing System Based on Native and Engineered Split Inteins. Journal of the American Chemical Society. 2005 May;127(17).

181. Wu Q, Gao Z, Wei Y, Ma G, Zheng Y, Dong Y, et al. Conserved residues that modulate protein trans-splicing of Npu DnaE split intein. Biochemical Journal. 2014 Jul 15;461(2).

182. Chen L, Benner J, Perler FB. Protein Splicing in the Absence of an Intein Penultimate Histidine. Journal of Biological Chemistry. 2000 Jul 7;275(27).

183. Iwai H, Züger S, Jin J, Tam P-H. Highly efficient protein *trans* -splicing by a naturally split DnaE intein from *Nostoc punctiforme*. FEBS Letters. 2006 Mar 20;580(7).

184. Dassa B, Amitai G, Caspi J, Schueler-Furman O, Pietrokovski S. Trans Protein Splicing of Cyanobacterial Split Inteins in Endogenous and Exogenous Combinations. Biochemistry. 2007 Jan;46(1).

185. Stevens AJ, Brown ZZ, Shah NH, Sekar G, Cowburn D, Muir TW. Design of a Split Intein with Exceptional Protein Splicing Activity. Journal of the American Chemical Society. 2016 Feb 24;138(7).

186. Iwai H, Züger S, Jin J, Tam P-H. Highly efficient protein *trans* -splicing by a naturally split DnaE intein from *Nostoc punctiforme*. FEBS Letters. 2006 Mar 20;580(7).

187. Lehmann M, Kostrewa D, Wyss M, Brugger R, D'Arcy A, Pasamontes L, et al. From DNA sequence to improved functionality: using protein sequence comparisons to rapidly design a thermostable consensus phytase. Protein Engineering, Design and Selection. 2000 Jan;13(1).

188. Steipe B. Consensus-Based Engineering of Protein Stability: From Intrabodies to Thermostable Enzymes. In 2004.

189. Shah NH, Muir TW. Inteins: nature's gift to protein chemists. Chem Sci. 2014;5(2).

190. Shah NH, Dann GP, Vila-Perelló M, Liu Z, Muir TW. Ultrafast Protein Splicing is Common among Cyanobacterial Split Inteins: Implications for Protein Engineering. Journal of the American Chemical Society. 2012 Jul 18;134(28).

191. Shah NH, Eryilmaz E, Cowburn D, Muir TW. Naturally Split Inteins Assemble through a "Capture and Collapse" Mechanism. Journal of the American Chemical Society. 2013 Dec 11;135(49).

192. Hayashi N, Kipriyanov S, Fuchs P, Welschof M, Dörsam H, Little M. A single expression system for the display, purification and conjugation of single-chain antibodies. Gene. 1995 Jul;160(1).

193. Schneider P. Production of Recombinant TRAIL and TRAIL Receptor: Fc Chimeric Proteins. In 2000.

194. Junutula JR, Bhakta S, Raab H, Ervin KE, Eigenbrot C, Vandlen R, et al. Rapid identification of reactive cysteine residues for site-specific labeling of antibody-Fabs. Journal of Immunological Methods. 2008 Mar;332(1–2).

195. Liu W, Brock A, Chen S, Chen S, Schultz PG. Genetic incorporation of unnatural amino acids into proteins in mammalian cells. Nature Methods. 2007 Mar 25;4(3).

196. Rodwell JD, Alvarez VL, Lee C, Lopes AD, Goers JW, King HD, et al. Site-specific covalent modification of monoclonal antibodies: in vitro and in vivo evaluations. Proceedings of the National Academy of Sciences. 1986 Apr 1;83(8).

197. Chang I-Nan, Lin J-Nan, Andrade JD, Herron JN. Photoaffinity Labeling of Antibodies for Applications in Homogeneous fluoroimmunoassays. Analytical Chemistry. 1995 Mar;67(5).

198. Doronina SO, Toki BE, Torgov MY, Mendelsohn BA, Cerveny CG, Chace DF, et al. Development of potent monoclonal antibody auristatin conjugates for cancer therapy. Nature Biotechnology. 2003 Jul 1;21(7).

199. Trail P, Willner D, Lasch S, Henderson A, Hofstead S, Casazza A, et al. Cure of xenografted human carcinomas by BR96-doxorubicin immunoconjugates. Science. 1993 Jul 9;261(5118).

200. Pishesha N, Ingram JR, Ploegh HL. Sortase A: A Model for Transpeptidation and Its Biological Applications. Annual Review of Cell and Developmental Biology. 2018 Oct 6;34(1).

201. Satiaputra J, Shearwin KE, Booker GW, Polyak SW. Mechanisms of biotin-regulated gene expression in microbes. Synthetic and Systems Biotechnology. 2016 Mar;1(1).

202. Gray PW, Goeddel D v. Structure of the human immune interferon gene. Nature. 1982 Aug;298(5877).

203. Wheelock EF. Interferon-Like Virus-Inhibitor Induced in Human Leukocytes by Phytohemagglutinin. Science. 1965 Jul 16;149(3681).

204. Green JA, Cooperband SR, Kibrick S. Immune Specific Induction of Interferon Production in Cultures of Human Blood Lymphocytes. Science. 1969 Jun 20;164(3886).

205. Schoenborn JR, Wilson CB. Regulation of Interferon-γ During Innate and Adaptive Immune Responses. In 2007.

206. Artis D, Spits H. The biology of innate lymphoid cells. Nature. 2015 Jan 14;517(7534).